

**“Legacy Soil Contamination by Crude Oil from the First
Gulf War: Geochemical Characteristics, Spatial Pattern and
Environmental Risk”**



Hamad Almebayedh

Ph.D. Academic Year: 2019 - 2020

Supervisors
Prof. Chuxia Lin
Dr. Wayne Wang

ABSTRACT

The first Gulf War resulted in large-scale oil spills in Kuwait. Selection of appropriate soil remediation methods needs to be informed by accurate soil characterization and this knowledge is currently lacking. The aim of this PhD study was to obtain insights into the geochemical characteristics of the aged contaminated soils and, using this knowledge, to develop 3-D predictive models for spatial distribution of the contaminated soils and remediation strategies based on site-specific environmental risk assessment.

The soil-borne petroleum hydrocarbons were spatially variable. Most of lighter petroleum hydrocarbons in the oil lake area has already been emitted to atmosphere. Under desert climate conditions, downward migration of the spilled oil was limited due to a lack of rainfall. The downward movement of long-chain hydrocarbons tended to be slow because of their low mobility. The contamination depth was generally very shallow in the oil sludge pit due to the presence of a liner. The application of geostatistical interpolation techniques to the development of 3-D predictive models for the investigated sites suggests that this approach is appropriate for 3-D mapping of the soil-borne petroleum hydrocarbons.

There was no evidence to show that groundwater was contaminated in the investigated area. Long-chain aliphatic hydrocarbons dominated the hydrocarbons in both the oil sludges and the contaminated soils. The pre-dominant presence of less toxic long-chain aliphatic hydrocarbons means that the hazardousness of the contaminated soils is likely to be much lower than what was thought.

The findings obtained from this study have implications for developing cost-effective remediation strategies for the clean-up of the crude oil-contaminated soils. Multiple management and remediation strategies need to be developed and implemented in an integrated way. It may not be necessary to intensively treat the hydrocarbon fractions of insignificant toxicity in order to achieve cost-effective remediation goals.

ACNOWLEDGEMENT

I would like to express my sincerely thanks to my Two supervisors for their help and assistance during my PhD project. My genuine gratitude to my advisor Prof. Chuxia Lin, Chair in Environmental Science at the School of (environmental and life sciences) at university of salford for the continuous support of my PhD study and related research, for his patience, motivation, and immense knowledge. His guidance helped me in all the time of research and writing of this thesis. I could not have imagined having a better advisor and mentor for my PhD study. Similarly, Dr. Yu Wang my second supervisor from the School of (Computing, Science and Engineering) who has been influential in providing valuable technical support, particularly his support in the 3D mapping technology development, computing, software and programme development. Furthermore, to Dr. Ian Podmore for his valuable contribution, and the University of Salford which provided me with all the necessary resources, facilities, training courses and laboratories which have enabled me to carry out my research. Special thanks for Kuwait Oil Company for their strong in-kind support specially KOC soil remediation Group for data sharing, and close collaboration on both SEED and KERP projects. Also, My special thanks to Kuwait Petroleum corporations for their continuous support.

DEDICATION

I dedicate this PhD thesis to my late father (Abdul Latif Abdul Malik Al-Saleh Al-Mebayedh) who has always been my source of inspiration and strength day and night.

LIST OF FIGURES

Page

Figure 2.1 Summary of petroleum product types and TPH analytical methods with respect to approximate carbon number and boiling point ranges. (Association of American Railroads BP Oil Company, 1998).....	10
Figure 2.2 Structures of commonly occurring compounds in TPH, (1) Benzene, (2) Toluene, (3) Ethylbenzene, (4) Dimethyl benzene, (5) Naphthalene, (6) Phenanthrene, (7) Pyrene (8) Benzo[a]pyrene, (9) Coronene, (10) Dibenz[a,h]anthracene (Adapted from Khan et al., 2018).....	11
Figure 2.3 Example chemical structures for the major classes of heavy hydrocarbons (Adapted from Brown et al., 2017).	13
Figure 2.4 The fate of oil in the marine environment (Adapted from National Research Council, 2002).....	22
Figure 2.5 A conceptual model of heavy hydrocarbon fate and transport in the environment. Heavy hydrocarbons are typically released together with lighter hydrocarbon fractions that are found in most crude oils. This modifies the physical and chemical properties that significantly affect the transport on soils and in the subsurface. Releases of viscous refined bitumen or extremely heavy crude oils (APIo < 12) are unlikely to travel any significant distance in the soil or subsurface. (Adapted from Brown et al., 2017).....	23
Figure 2.6 Soil texture triangle based on USDA particle-size classification (after U.S. Soil Conservation Service.)	25
Figure 2.7 A flow chart showing the effectiveness of technologies dependency (ETD) (Adapted from Al-Mebayedh, 2014).....	31
Figure 2.8 Components of environmental risk assessment	33
Figure 2.9 Potential routes of pathogen exposure from land application of biosolids (Adapted from Gerba, 2015).....	34
Figure 2.10 Implementation of risk-based TPH analysis within a 3-tiered RBCA framework (Adapted from Environment Agency R&D Technical Report, 2003).....	41
Figure 2.11 An overview of spatial interpolation methods (Adapted from Chen et al., 2016).....	43
Figure 2.12 Graphs showing various Variogram models	45
Figure 2.13 3-D map showing the use of Kriging for interpolation application (Courtesy: ESRI)	46
Figure 2.14 Example graph showing application of PointInterp (Courtesy: ESRI) ...	47
Figure 2.15 Example graph showing the application of Trend (Courtsey: ESRI).....	47
Figure 2.16 Example graph showing the application of Topo to Raster (Courtesy: ESRI)	48
Figure 2.17 Example graph showing the application IDW Interpolation (Courtesy: QGIS)	50
Figure 2.18 Example graph showing the application of IDW Interpolated Surface (Courtesy: ESRI).....	50
Figure 2.19 An example showing A radius is generated around each grid node from which data points are selected to be used in the calculation (Figure 2.19). Options to control the use of IDW include power, search radius, fixed search radius, variable search radius and barrier.	51
Figure 2.20 Example graph showing the application of Natural IDW (Courtesy: ESRI)	52
Figure 2.21 Example graph showing the application of Spline (Courtesy: ESRI)	53

Figure 2.22 A map showing the application of Spline Method.....	53
Figure 2.23 Photographs showing (a) a burning oil well, and (b) an oil lake	68
Figure 3.1 Map showing the Rawdhatain oil field in the northern Kuwait and Burgan oil field in the southern Kuwait.....	78
Figure 3.2 Map showing the soil sampling locations in the Rawdhatain oil lake area	79
Figure 3.3 Map showing the 16 sampling locations in the Oil Sludge Pit EPE4	80
Figure 3.4 Map showing the study area of Project SPB1	87
Figure 3.5 Image showing Sludge Pit SPB1 with sampling locations	87
Figure 3.6 An example of the in-house tool using IDW interpolation method	88
Figure 3.7 The developed inverse distance weighting interpolation code using MATLAB for SPB1 (A - each sampling point has a single value)	90
Figure 3.8 The developed inverse distance weighting interpolation code using MATLAB for SPB1 (B - each sampling point has multi-values)	90
Figure 3.9 The developed inverse distance weighting interpolation code using MATLAB for SPB1 (C- each sampling point has multi-values).....	90
Figure 3.10 Graph showing Cont Z3 mapping	91
Figure 3.11 A graph showing TPH (HEM) 3-D mapping	92
Figure 3.12 A graph showing thickness mapping	92
Figure 3.13 a graph showing 3-D elevation mapping	93
Figure 3.14 Comparison of the Kriging and IDW on a smooth curve	95
Figure 3.15 Comparison of the Kriging and IDW on a curve of steep variation.....	96
Figure 3.16 Comparison of the Kriging and IDW on random sampling points	97
Figure 3.17 The mass increase in the volume = mass flow in - mass flow out + mass generated in the volume.....	99
Figure 3.18 Images showing soil profiles at Sampling Locations (a) 4 and (b) 5	99
Figure 3.19 Fick's First Law for the contaminated profile in depth.....	100
Figure 3.20 Graphs showing vertical variation in TPH along the soils profiles using 1-D modeling	100
Figure 4.1 Photograph showing the morphology of Soil Profile TP-04.....	104
Figure 4.2 Photograph showing the morphology of Soil Profile TP-05.....	105
Figure 4.3 Photograph showing the morphology of Soil Profile TP-06.....	106
Figure 4.4 Photograph showing the morphology of Soil Profile TP-07.....	107
Figure 4.5 Photograph showing the morphology of Soil Profile TP-08.....	107
Figure 4.6 Photograph showing the morphology of Soil Profile TP-09.....	108
Figure 4.7 Photograph showing the morphology of Soil Profile TP-010.....	109
Figure 4.8 Photograph showing the morphology of Soil Profile TP-011.....	110
Figure 4.9 Photograph showing the morphology of Soil Profile TP-012.....	111
Figure 4.10 Photograph showing the morphology of Soil Profile TP-013.....	112
Figure 4.11 Photograph showing the morphology of Soil Profile TP-014.....	113
Figure 4.12 Photograph showing the morphology of Soil Profile TP-015.....	114
Figure 4.13 Photograph showing the morphology of Soil Profile TP-016.....	115
Figure 4.14 Photograph showing the morphology of Soil Profile TP-017.....	116
Figure 4.15 Photograph showing the morphology of Soil Profile TP-018.....	117
Figure 4.16 Photograph showing the morphology of Soil Profile TP-019.....	118
Figure 4.17 Photograph showing the morphology of Soil Profile TP-020.....	119
Figure 4.18 Horizontal and vertical variation in total aliphatic hydrocarbon for (a) the soils with contamination depth <50 cm, and (b) the soils with contamination depth >50 cm	122
Figure 4.19 Distribution patterns of different aliphatic hydrocarbon fractions for the soil	

profiles with a contamination depth <50 cm	123
Figure 4.20 Distribution patterns of different aliphatic hydrocarbon fractions for the soil profiles with a contamination depth <50 cm	124
Figure 4.21 Relationship in pH between the adjacent soil layers. (a) the 0-10 cm layer vs the 10-20 cm layer, and (b) the 30-40 cm layer vs the 40-50 cm layer	128
Figure 4.22 Relationship in EC between the adjacent soil layers. (a) the 0-10 cm layer vs the 10-20 cm layer, and (b) the 30-40 cm layer vs the 40-50 cm layer.....	130
Figure 4.23 Concentration of sulfate in the two selected soil profiles. (a) Profile 10 and (b) Profile 19	133
Figure 4.24 Soil grain size distribution patterns for the different soil layers in Soil Profile. (a) the 0-10 cm layer, (b) the 10-20 cm layer, (c) the 20-30 cm layer, (d) the 30-40 cm layer, and (e) the 40-50 cm layer.	134
Figure 4.25 Soil grain size distribution patterns for the different soil layers in Soil Profile. (a) the 0-20 cm layer, (b) the 20-40 cm layer, (c) the 40-60 cm layer, (d) the 60-80 cm layer, and (e) the 80-100 cm layer.	135
Figure 4.26 Relationship between the total sulfur and the sulfate-sulfur for Profile 19	137
Figure 4.27 Relationship between pH and EC for the investigated soils	138
Figure 5.1 TPH in the oil sludges at the 16 sampling locations.....	146
Figure 5.2 TPH in the surface soil layer for the 16 sampling locations	149
Figure 5.3 Distribution of various (a) aliphatic hydrocarbon fractions and (b) aromatic hydrocarbon fractions in the contaminated soils.....	150
Figure 5.4 Changes in various (a) aliphatic hydrocarbon fractions and (b) aromatic hydrocarbon fractions along Soil Profile 1	151
Figure 5.5 Changes in various (a) aliphatic hydrocarbon fractions and (b) aromatic hydrocarbon fractions along Soil Profile 12	152
Figure 5.6 Relationship in TPH between the sludge and the underlying surface soil layer	154
Figure 5.7 Relationship between the total aliphatic hydrocarbon and the total aromatic hydrocarbon	155
Figure 5.8 Relationship in aliphatic fraction (a) C16-C21, (b) C21-C35, and (c) C35-C40 between the sludge and the surface soil	156
Figure 5.9 Relationship in aromatic fraction (a) C12-16, (b) C16-C21, and (c) C21-C35 between the sludge and the surface soil	157
Figure 6.1 3-D distribution of TPH within the investigated area. (A) 0-50 cm consisting of 5 soil layers; 0-10, 10-20, 20-30, 30-40 and 40-50 cm, and (B) 50-90 cm consisting of 4 soil layers: 50-60, 60-70, 70-80 and 80-90cm.....	162
Figure 6.2 3-D distribution of BTEX within the investigated area. (A) 0-50 cm consisting of 5 soil layers; 0-10, 10-20, 20-30, 30-40 and 40-50 cm, and (B) 50-90 cm consisting of 4 soil layers: 50-60, 60-70, 70-80 and 80-90 cm.	164
Figure 6.3 3-D distribution of aliphatics within the investigated area. (A) 0-50 cm consisting of.....	167
Figure 6.4 3-D distribution of aromatics within the investigated area. (A) 0-50 cm consisting of 5 soil layers; 0-10, 10-20, 20-30, 30-40 and 40-50 cm, and (B) 50-90 cm consisting of 4 soil layers: 50-60, 60-70, 70-80 and 80-90 cm.	169
Figure 6.5 Spatial distribution of total PAH in the top 10 cm of soil within the investigated area.....	170
Figure 6.6 Graph showing the interface between the soil (upper part) with TPH > 10000 mg/kg (1%) and the soil (lower part) with TPH <10000 mg/kg (1%). The estimated	

total volume of soil above the interface is 112,730 m³, which accounts for 11.8% of the total volume of soil for the 90 cm thick soil layer in the investigated area.171

Figure 6.7 Distribution of TPH in the sludge materials within the investigated area.173

Figure 6.8 Distribution of the total aliphatic hydrocarbon in the sludge materials within the investigated area174

Figure 6.9 Distribution of the aliphatic hydrocarbon fraction C16-C21 in the sludge materials within the investigated area.175

Figure 6.10 Distribution of the aliphatic hydrocarbon fraction C21-C35 in the sludge materials within the investigated area.176

Figure 6.11 Distribution of the aliphatic hydrocarbon fraction C35-C40 in the sludge materials within the investigated area.177

Figure 6.12 Distribution of the total aromatic hydrocarbon in the sludge materials within the investigated area.178

Figure 6.13 Distribution of the aromatic hydrocarbon fraction C12-C16 in the sludge materials within the investigated area.179

Figure 6.14 Distribution of the aromatic hydrocarbon fraction C16-C21 in the sludge materials within the investigated area.180

Figure 6.15 Distribution of the aromatic hydrocarbon fraction C21-C35 in the sludge materials within the investigated area.181

Figure 6.16 Distribution of total PAH in the sludge materials within the investigated area.182

Figure 6.17 3-D distribution of TPH within the investigated area.....183

Figure 6.18 3-D distribution of aliphatics within the investigated area.185

Figure 6.19 3-D distribution of aromatics within the investigated area.186

Figure 6.20 Spatial distribution of total PAH in the top 10 cm of soil within the investigated area.....187

Figure 6.21 Comparison between the Kriging and IDW for one set of the observation data.188

Figure 6.22 Quality of Kriging is quite sensitive to the distribution of sample data. 189

Figure 6.23 Cross-validation for assessing the performance of spatial interpolation methods for 2-B Section of the Raudhatain Area.....190

Figure 6.24 The use of 7 samples from the 15 locations.192

Figure 6.25 The use of 6 samples from the 15 locations.193

Figure 6.26 The use of 8 samples from the 15 locations.194

LIST OF TABLES

Page

Table 2.1 Example phytotoxicity of PHCs (after Khan et al., 2018)	17
Table 2.2 Toxicity of PHCs to soil invertebrates and microorganisms (after Khan et al., 2018).....	18
Table 2.3 Treatment technologies for PHC-contaminated soils (Friend, 1996)	32
Table 2.4 A summary of approaches developed by the organizations in some developed countries for environmental risk assessment (Turczynowicz & Robinsn, 2008).....	39
Table 2.5 Statistics of petroleum hydrocarbon-contaminated soils within the State of Kuwait (Kuwait Environment Public Authority, 2011).....	69
Table 4.1 TPH (mg/kg) in the soils for the soil profiles with the depth of contamination limited to the top 50 cm.....	120
Table 4.2 TPH (mg/kg) in the soils for the soil profiles with the depth of contamination extending beyond 50 cm.....	120
Table 4.3 BTEX ($\mu\text{g}/\text{kg}$) in the soils for the Soil Profiles 11, 18, 19 and 20.....	121
Table 4.4 Aromatic petroleum hydrocarbons in the investigated soil profiles	125
Table 4.5 Polycyclic aromatic hydrocarbons (PAHs) in the surface soils	126
Table 4.6 pH in the investigated soils collected from northern part of the study area	127
Table 4.7 pH in the investigated soils collected from the southern part of the study area	128
Table 4.8 EC (mS/m) in the investigated soils collected from northern part of the study area	129
Table 4.9 Electrical conductivity (mS/m) in the investigated soils collected from southern part of the study area	130
Table 4.10 Chemical composition of the soil collected from Location 10.....	131
Table 4.11 Chemical composition of the soil collected from Location 19	132
Table 4.12 A comparison of major soil properties (profile average) between Profile 10 and Profile 19.....	136
Table 5.1 Soil profile characteristics at the 16 sampling locations.	144
Table 5.2 Concentration (mg/kg) of aliphatic hydrocarbons in the oil sludges.....	146
Table 5.3 Concentration (mg/kg) of aromatic hydrocarbons in the oil sludges.....	148
Table 5.4 Concentration (mg/kg) of PAHs in the oil sludges	148

LIST OF EQUATIONS

Page

1-	$Z(X) = M(X) + \Delta(X)$	44
2-	$E[M(X) - M(X + h)] = 0$	44
3-	$E \left[(Z(X) - Z(X + h))^2 \right] = E \left[(\Delta(X) - \Delta(X + h))^2 \right] = 2\gamma(h)$	44
4-	$\gamma(h) \approx \frac{1}{2n} \sum_{i=1}^n (Z(X_i) - Z(X_i + h))^2$	44
5-	$Z(X) = M(X) + \gamma(h)$	38
6-	$Z(X) = \sum_{i=1}^n w_i Z(X_i)$	45
7-	$\sum_{i=1}^n w_i Z(X_i) = M(X) + \gamma(h)$	45
8-	$M(X) = \beta_0 + \sum_{i=1}^n \beta_i X_i$	45
9-	$w_i = \frac{\frac{1}{(X-X_i)^p}}{\sum_{j=1}^n \frac{1}{(X-X_j)^p}}$	49
10-	$CV \% = \frac{\text{Standard Deviation}}{\text{Mean}} \times 100$	65
11-	$SD = \sqrt{\frac{\sum (x_n - \bar{x})^2}{n-1}}$ <p style="margin-left: 20px;">where: \bar{x} = mean (average) of the QC values $\sum (x_n - \bar{x})^2$ = the sum of the squares of differences between individual QC values and the mean n = the number of values in the data set</p>	65
12-	$J_x = -D \frac{dC}{dx}$	98
13-	$\frac{\partial C}{\partial t} = \frac{\partial}{\partial x} \left(D \frac{\partial C}{\partial x} \right)$	99
14-	$\frac{\partial C}{\partial t} = \frac{\partial}{\partial x} \left(D \frac{\partial C}{\partial x} \right) + \dot{R}$	101

ABBREVIATIONS

(3-D)	Three-dimensional
(TPH)	Total Petroleum Hydrocarbon
(GIS)	Geographic Information System
(IDW)	Inverse Distance Weighted
(NNIDW)	Natural Neighbour Inverse Distance Weighted
(RBF)	Radial Basis Functions
(SOC)	Soil Organic Carbon
(GPS)	Global Positioning System
(LPI)	Polynomial Interpolation
(OK)	Ordinary Kriging
(RMSE)	Determination (R ²) and Root Mean Square Error
(SEED)	Sustainable Environmental Economic Development
(UNCC)	United Nation Compensation Commission
(KNFP)	Kuwait National Focal Point
(KISR)	Kuwait Institute for Scientific Research
(CV)	Coefficient of Variation
(PHCs)	Petroleum hydrocarbons
(PAHs)	Polycyclic aromatic hydrocarbons
(KOC)	Kuwait Oil Company
(KERP)	Kuwait Environmental Remediation Program (KERP)
(EPA)	Environmental Protection Agency

TABLE OF CONTENTS

ABSTRACT	ii
ACKNOWLEDGEMENTS.....	iii
DEDICATION.....	iv
LIST OF FIGURES	v
LIST OF TABLES	ix
LIST OF EQUATIONS	x
ABBREVIATIONS	xi
Chapter 1 Introduction.....	1
1.1 Background and Significance	1
1.2 Research Aim and Objectives.....	4
1.3 Thesis Structure	6
Chapter 2 Literature Review.....	8
2.1 Introduction	8
2.2 Petroleum Hydrocarbon in Relation to Environments.....	8
2.2.1 Petroleum hydrocarbons.....	9
2.2.2 Quantification of petroleum hydrocarbons.....	13
2.2.3 Toxicity of petroleum hydrocarbons	15
2.2.4 Petroleum spills and their environmental, economic and social impacts	19
2.2.5 Fate and transport of petroleum hydrocarbons	21
2.3 Soil Contamination	24
2.3.1 Soils and soil properties.....	24
2.3.2 Formation of soils	27
2.3.3 Sources and fate of soil contaminants	27
2.3.4 Remediation of contaminated soils	28
2.3.5 Soil Contamination by Petroleum Hydrocarbons	29
2.4 Environmental Risk Assessment	32
2.4.1 Environmental hazard identification and characterisation	33
2.4.2 Exposure assessment	34
2.4.3 Environmental risk characterization.....	35
2.4.4 Major environmental risk assessment systems	35
2.4.5 Environmental Risk Assessment Tools for PHC-Contaminated Soils	41
2.5 Spatial Interpolation and 3-D Soil Mapping.....	42
2.5.1 Geostatistical interpolation (Kriging).....	43
2.5.2 Inverse Distance Weighting (IDW).....	49
2.5.3 Comparison of the Interpolation Methods on Digital Terrain	53

2.5.4	The use of interpolation methods in environmental projects.....	57
2.5.5	Applications of Spatial Interpolation to Soil Mapping.....	58
2.5.6	Spatial interpolation evaluation and comparison techniques.....	60
2.5.7	Assessment measures for assessing the performance of spatial interpolation methods.....	64
2.5.8	Factors affecting the performance of the spatial interpolation methods.....	66
2.6	Petroleum Hydrocarbon contamination in Kuwait	66
2.6.1	Kuwait Environmental Background.....	67
2.6.2	Kuwaiti Oil Fires and the Resulting Environmental Contamination during the First Gulf War	67
2.6.3	PHC-contaminated soils in Kuwait.....	70
2.7	Conclusions.....	72
Chapter 3	METHODS AND MATERIALS.....	76
3.1	Introduction	76
3.2	Selection of the Study Sites	77
3.2.1	Regional settings	77
3.2.2	Study site in the oil lake area	78
3.2.3	Study site in the oil extraction area	79
3.3	Field methods	80
3.3.1	Sampling method used in the Rawdhatain oil lake area.....	80
3.3.2	Sampling method used in the Oil Sludge Pit EPE4	81
3.4	Laboratory methods.....	82
3.4.1	Soil pH and electrical conductivity (EC).....	82
3.4.2	Particle size analysis.....	83
3.4.3	Element analysis	83
3.4.4	Benzene, toluene, ethylbenzene and xylene (BTEX).....	84
3.4.5	Petroleum hydrocarbon fractions	84
3.4.6	Polycyclic aromatic hydrocarbons (PAHs).....	85
3.4.7	QC/QA and statistical analysis.....	85
3.5	Geostatistical methods used for 3-D model development	86
3.5.1	Selection of interpolation methods.....	86
3.5.2	Method validation	94
3.5.3	Novel theory development for hydrocarbon-contaminated soil	97
3.6	Conclusions.....	101
Chapter 4	Geochemical Characteristics and Environmental Risk of the Crude Oil-Contaminated Soils in the Raudhatain Oil Lake.....	102
4.1	Introduction	102
4.2	Materials and Methods	103
4.3	Results	103
4.3.1	Soil morphology.....	103
4.3.2	Petroleum Hydrocarbons	119
4.3.3	Other soil parameters.....	127

4.4 Discussion	136
4.5 Conclusions.....	142
Chapter 5 Geochemical Characteristics and Environmental Risk of the Crude Oil-Contaminated Soils in a Constructed Sludge Pit.....	143
5.1 Introduction	143
5.2 Methodology.....	144
5.3 Results	144
5.3.1 Soil profile characteristics	144
5.3.2 Characteristics of the oil sludges	145
5.3.3 The contaminated soils	149
5.4 Discussion	153
5.5 Conclusions.....	158
Chapter 6 3-D Model Development for Predicting Spatial Variation of Crude Oil-Contaminated Soil.....	159
6.1 Introduction	159
6.2 Research methods	160
6.3 Data analysis and 3D mapping technology for 2-B Section of the Raudhatain Area.....	160
6.3.1 Total petroleum hydrocarbon.....	161
6.3.2 BTEX.....	163
6.3.3 Aliphatic petroleum hydrocarbons	165
6.3.4 Aromatic petroleum hydrocarbons.....	168
6.3.5 Polycyclic aromatic hydrocarbons	170
6.3.6 Estimation of Total Contaminated Soil Volume.....	171
6.3.7 Summary.....	172
6.4 Model development for the Sludge Pit EPE4.....	172
6.4.1 Oil sludge.....	172
6.4.2 The Contaminated Soils.....	182
6.4.3 Concluding Discussion.....	188
Chapter 7 Conclusions and Recommendations	199
7.1 Conclusions.....	199
7.2 Implications of the research findings	200
7.3 Limitations	203
7.4 Recommendations for future study	204
References.....	205
Appendix1.....	220

Chapter 1

Introduction

1.1 Background and Significance

Kuwait has faced an unprecedented environmental disaster in human history after the First Gulf War in 1991. The oil fire during the war resulted in widespread oil spill, leading to the formation of approximately 115 km² of oil lakes. There are nearly 50 million m³ of petroleum hydrocarbon-contaminated soils across the country. This in combination with the construction of oil trenches by the Iraqi military force and the soil bunds built by the rescue team to contain the spilled oil, led to widespread contamination of soils by the petroleum hydrocarbons. The widely distributed petroleum hydrocarbon-contaminated soils in Kuwait represent a serious threat to human health and ecosystems. Therefore, there is an urgent need for clean-up of these contaminated lands to minimize their adverse environmental impacts.

To assist in the clean-up of the crude oil contamination caused by the first Gulf War, the United Nation Compensation Commission has awarded to the State of Kuwait a war compensation grant of US\$3.6 billion (UNCC decision 258). Off these US\$3.6 billion, approximately US\$2.2 billion was allocated to the remediation of oil lakes and the associated soil contamination. This allows an environmental remediation plan, collectively called “Kuwait Environmental Remediation Program” (KERP) being initiated. The KERP is being administered by the Kuwait Oil Company (KOC), overseen by the Kuwait National Focal Point (KNFP) and the United Nation Compensation Commission (UNCC). The major challenges related to this program are (a) no precedence in terms of international law to address this level of environmental damages, (b) a lack of baseline data or pristine information, (c) not possible to understand the extent of environmental damages without the conduction of detailed M&A studies, and (d) full understanding of the soil characterization and the hydrocarbon contaminated soil required (Asem et al., 2014).

Research studies carried out by Kuwait Institute for Scientific Research (KISR) and others since 1992, including the UNCC supported Monitoring and Assessment Program (2001 – 2006), which revealed that the native vegetation cover has been totally

destroyed or severely impacted by the oil lakes, and contamination of the soil by oil originating from contaminated piles and seepage to deeper layers. The fresh groundwater lens in the Umm Al-Aish area in North Kuwait has also been heavily impacted by contamination originating from overlying wet and dry oil lakes and oil-contaminated piles. Remediation of the contamination in this area is of high priority since the fresh groundwater in Kuwait is considered to be an important strategic drinking water resource for the State of Kuwait. The fresh groundwater lens in the Raudhatain area in the north Kuwait is threatened by the wet and dry oil lakes, oil-contaminated piles on the surface in adjacent areas. Considering the potential long-term impacts of the contaminated soils on the ecosystems and human health, the removal of the oil-contaminated materials, including those in the wellhead pits and tarcrete in the area of the fresh groundwater catchment, has a high priority during the implementation of the remediation projects (Revised Project Plan for Remediation of Damage Project Claim KERP, 2013).

Another study conducted by Kuwait Institute for Scientific Research in 2004 for quantification of the size of the contamination used remote sensing as a main tool for estimating the area and extent of contamination requiring remediation. The volume was calculated by multiplying the remote sensed surface area by the average oil penetration depth from preliminary field surveys (0.6 m). This has been increased by a 20% contingency to account for sand drift and subsequent flow of oil due to heavy rains. The study concluded that since there have been no detailed field investigations to determine the actual depth of oil penetration under the different types of oil contamination, the accuracy of this estimate is unknown. Most of these estimates have been conducted with little or no ground truth information to support the remote sensed interpretations, so the reliability of the estimates is unknown (KISER, 2004). The same study presented statement of limitations with two caveats. One is that the estimates of oil-contaminated soil volume and area have some associated sampling errors that are not known. Two is that the volume estimates produced by this study are the potential total volumes of oil-contaminated soil that need rehabilitation. The actual volume of soil that needs to be rehabilitated may be different from this, and will be a decision based on cost-benefit analysis involving the risk assessment of human and ecological health associated with levels and distribution patterns of oil contamination.

Selection of appropriate soil remediation methods and techniques needs to be informed by accurate soil characterization and reliable estimates. Currently soil investigation into petroleum hydrocarbon-contaminated soil in oil lake areas involves grid sampling with a high horizontal sampling density. However, vertical variation in petroleum hydrocarbon concentration along the soil profile is not sufficiently considered. This approach could lead to substantial costs due to intensive horizontal sampling on one hand and inaccurate estimation of the contaminated soil volume that need to be treated on the other hand (Almebayedh et al., 2016).

Geostatistical interpolation techniques have been used to estimate the value of the investigated soil parameter in unsampled locations by a weighted average of the nearby observations (Veronesi et al., 2014). This allows a predictive model being established to assist in soil mapping for a large area without the need to conduct intensive soil sampling, and therefore significantly reduces capital and labor inputs. Interpolation methods are widely used for 2-D soil mapping. However, until now, there have been limited applications of geostatistical interpolation techniques to 3-D mapping of soil properties.

To develop predictive models that can be used for 3-D soil mapping, a combination of 2-D interpolation with soil profile depth function is required (Veronesi et al., 2012). The accuracy of 3-D distribution of soil parameters heavily depends on the reliability of soil dataset obtained from soil survey. To obtain highly reliable datasets, soil sampling design needs to be optimized for geostatistics. This represents a major challenge for developing sensible 3-D soil mapping technologies.

Investigation of soil properties by applying conventional chemical methods is always expensive and requires time, manpower and budget, especially when large regions are concerned (Nanni & Demattê, 2016). Providing accurate and continuous spatial data can remarkably be supportive for decision making in environmental management (Li & Heap, 2011). Utilizing advanced interpolation methods give rise to better understand spatial and temporal changes of soil properties. In addition, these methods minimize cost and time required for soil sampling (Simakova et al., 2011). As such, interpolation methods attracted the interest of decision makers due to their beneficial and low-cost prediction of un-sampled locations within the last two decades

(Robinson & Metternicht, 2006; Krasilnikov et al., 2014; Yao et al., 2013; Bijanzadeh et al., 2014).

There have been a few pieces of research work on 3D mapping of soil organic carbon and soil texture (Adhikari et al., 2013; Lacoste et al., 2014; Veronesi et al., 2014; Chen et al., 2015). However, no systematic research work has so far been done to develop 3-D predictive models for spatial distribution of oil-contaminated soils. The spatial variation of a given soil property is determined by many factors. To optimize soil sampling design, it is important to understand the biogeochemical processes governing the soil formation. Soil contamination by petroleum hydrocarbons is a complex process, so far most research on petroleum hydrocarbon-contaminated soils was conducted in small areas with light petroleum hydrocarbons being the major contaminants entering the soil systems. There has not been sufficient understanding on geochemical processes related to contamination of soils by crude oil, especially for those experiencing long-term weathering in desert areas such as the oil lakes in Kuwait. This does not allow optimization of soil sampling design for the development of reliable predictive models for 3-D mapping of various petroleum hydrocarbons with varying degrees of environmental hazardousness.

Modern mapping and interpolation methods are addressed as new and advanced techniques (Cruz-Cárdenas et al., 2014; Mehrabian et al., 2011) that attain soil information through estimating spatial variation of soil characteristics based on field measurements, environmental information and application of various spatial interpolation methods (Shi et al., 2012). To achieve cost-effective goals for remediation of the oil-contaminated soils, it is necessary to develop innovative predictive models that can be used to guide 3-D mapping of the key soil parameters for characterization of the contaminated soils in order to inform environmental risk assessment, development of remediation strategies, and selection of appropriate soil treatment methods and technologies. There has been so far no research on 3-D predictive models for large-scale aged crude oil-contaminated soil such as those encountered in the Kuwaiti oil lake areas.

1.2 Research Aim and Objectives

The overall aim of this PhD study was to obtain insights into the geochemical

characteristics of the aged crude oil-contaminated soils, and using this knowledge, to develop 3-D predictive models for spatial distribution of the contaminated soils and remediation strategies based on site-specific environmental risk assessment. As an industrially funded project (Kuwait Petroleum Corporation Scholarship program) with the PhD candidate being a senior engineer working in the Kuwait Oil Company Soil Remediation team, this PhD project had a practical goal to develop a set of cost-effective technologies for direct applications to the UN-funded KERP.

The main focus of this research is to develop innovative technologies that can be used to cost-effectively estimate/predict 3D distribution of key soil characteristics in oil lake and sludge pits area, which can be used to assist in selection of soil remediation methods and procedures. The following specific research objectives are set to achieve the research aim:

Objective 1. To characterize the crude oil-contaminated soils in the selected Kuwaiti oil lake areas. (Chapter 4)

Objective 2. To characterize the oil sludges and the underlying soils in a selected oil sludge pit constructed to store petroleum wastes from Kuwait Oil Company's production operations (Chapter 5)

Objective3. To compare the characteristics of the petroleum hydrocarbon-contaminated soils between the oil lake and the sludge pit (Chapters 4 and 5).

Objective 4. To establish the fate and transport of the spilled crude oil derived from the First Gulf War (Chapter 4)

Objective 5. To assess the environmental risk from the petroleum hydrocarbon-contaminated soils in the oil lake and the sludge pit (Chapters 4 and 5)

Objective 6. To develop 3-D predictive models for 3-D soil mapping using geostatistical interpolation methods (Chapter 6).

Objective 7. To develop remediation strategies for the petroleum hydrocarbon-contaminated soils in both oil lake areas and oil sludge pits (Chapter 7).

1.3 Thesis Structure

This thesis consists of seven chapters (a) Introduction, (b) Literature Review, (c) Materials and Methods, (d) Geochemical Characteristics and Risk Assessment in the Selected Oil Lake, (e) Geochemical Characteristics and Risk Assessment in the Selected Sludge Pit, (f) 3-D Model Development and Soil Mapping, and (g) Conclusions and Recommendations

Chapter 1 (this chapter) provides general background information on the selected research and highlights the significance of the proposed study. The research aim is stated based on the identified research gaps and a series of specific research objectives are set to achieve the research aim. It focuses on the justification of the research topic selection and the scientific novelty of the expected research outcomes. Detailed background information on the oil contamination caused by the First Gulf War is not provided in this chapter but in the literature review chapter.

Chapter 2 provides a general review of available literature on the key issues related to the selected research topic. It covers petroleum hydrocarbon chemistry, analytical methods for determination of petroleum hydrocarbon, toxicology of petroleum hydrocarbons, fate and transport of petroleum hydrocarbon in environments, environmental impacts of petroleum hydrocarbon contamination, environmental risk assessment for petroleum hydrocarbon contamination, soil and soil contamination, remediation technologies for soil contamination, the application of geospatial interpolation for 3-D soil mapping, and physiographic settings of Kuwait and environmental legacy of the Kuwait fire caused during the First Gulf War.

Chapter 3 Describes and justifies the research approach and the selected methods for field sampling, laboratory soil analysis, and computer-assisted model development for soil mapping.

Chapter 4 presents soil investigation results obtained from the selected oil lake study site in the northern Kuwait (2-B Section of the Raudhatain Area). It covers a range of soil geochemical parameters and the petroleum hydrocarbon contamination status, which allows an understanding of the fate and transport of the spilled oil in the oil lake areas and provides a basis for assessing the environmental risk from the soil-borne petroleum hydrocarbons.

Chapter 5 presents the investigation results obtained from a selected oil sludge within the Kuwait Oil Company's operation area in the southern Kuwait. Apart from the contaminated soils, the oil sludges overlying the contaminated soils were also characterized. This chapter allows comparison of soil geochemical characteristics and environmental risk being made between the oil lakes and the purpose-built oil waste storage facility.

Chapter 6 develops 3-D predictive models using the soil data obtained from Chapters 4 and 5. Geostatistical methods were used for model development and 3-D mapping of various petroleum hydrocarbon fractions. In this chapter we have had evaluated available interpolation methods, namely Kriging and IDW performance to establish predictive models for 3-D mapping of the petroleum hydrocarbon-contaminated soils. Series of case studies are presented. One in Northern Kuwait, and another in South Kuwait which will lead to the establishment of the predictive models for 3-D mapping of the petroleum hydrocarbon-contaminated soils. Secondary data previously collected by the Kuwait Oil Company associated to SEED project "Hydrocarbon soil contamination related to KOC operational areas" project SPB1 have been incorporated with cross validation errors technics for interpolating to IDW and OK to investigate the most accurate interpolating method and technics to generate prediction maps. Modelling was conducted on two theoretical mathematical functions of a single variable to evaluate the influence of the sampling number and distribution, during this case study further improvement and development of new methods for sampling and software for 3-D mapping was achieved and corroborated with cross-validation.

Chapter 7 summarizes the key findings obtained from this PhD project and highlight their implications for developing cost-effective remediation strategies for the petroleum hydrocarbon-contaminated sites in Kuwait, including the oil lakes formed due to widespread oil spill during the First Gulf War (KERP Program) and the oil sludge pits constructed to store petroleum wastes during oil production operations. It also identifies the limitation of the study and make recommendations for future work.

Chapter 2

Literature Review

2.1 Introduction

As stated in Chapter 1, the overall aim of this PhD study was to obtain insights into the geochemical characteristics of the aged crude oil-contaminated soils and, using this knowledge, to understand the fate and transport of the spilled oil and develop sound remediation strategies for clean-up of the oil-contaminated soils. This chapter provides a review on aspects related to the selected research topic in this PhD study. It covers (a) petroleum hydrocarbons and their environmental issues, (b) soils and soil contamination, (c) environmental risk assessment, (d) application of geostatistical technologies for 3-D soil mapping, and (e) an overview of environmental issues resulted from the first Gulf War and the environmental remediation efforts made so far in Kuwait.

2.2 Petroleum Hydrocarbon in Relation to Environments

Crude oil is a mixture of petroleum hydrocarbons with different structure and molecular weight (Potter & Simmons, 1998). Apart from carbon and hydrogen, crude oil usually contains trace amounts of other elements such as nitrogen, oxygen, sulfur, phosphorus and various metals (Balba et al., 1998). Based on the chemical structure, the petroleum hydrocarbon contained in crude oil can be divided into aliphatic that consist of straight carbon chains and aromatics that contain aromatic rings. Within each category, further fractionation can be done according to the number of carbons contained in a petroleum hydrocarbon molecule. Long-chain hydrocarbons tend to be less soluble and less mobile, as compared to their short-chain counterparts. Also, it is generally believed that aromatic hydrocarbons, especially polycyclic aromatic hydrocarbons, are more toxic to biota, relative to aliphatic hydrocarbons. Within the same category, the longer the carbon chain, the weaker the toxicity is (Trapp et al., 2001; Chen et al., 2008).

Worldwide oil spills cause contamination of soils by petroleum hydrocarbons. The downward movement of the spilled oil is affected by many factors such as rainfall

regime, soil texture, landform etc. (Williams et al., 2006). The presence of petroleum hydrocarbons in soils could affect growth of soil microbes and plants (Bundy et al., 2002; Reynoso-Cuevas et al., 2008). Ingestion of petroleum hydrocarbon-contaminated soils may also cause health problems to animals and human being (Aguilera et al., 2010). To minimize the environmental impacts of petroleum hydrocarbon-contaminated soils, appropriate remedial actions need to be taken.

2.2.1 Petroleum hydrocarbons

Petroleum hydrocarbons (PHCs) are chemical substances present in geological formations. They are formed from transformation of biomass contained in sedimentary rocks under high temperature and pressure (CCME, 2008). PHCs encountered in the Earth surface environments are derived from crude oil that is extracted from underground oil reserves. Crude oil can be processed to produce various products, including fuels, lubricants, asphalt (refined bitumen) and various petrochemicals.

The major petroleum fuel products include diesel, petrol (gasoline), kerosene, liquefied petroleum gas etc. Diesel fuels are produced from fractional distillation of crude oil under a temperature range of 180-380°C. The carbon number of petroleum hydrocarbons contained in diesel ranges from 11 to 25. Petrol is produced under a temperature range of 30-200°C and therefore contains more volatile petroleum hydrocarbons with a carbon number between 4 and 12. Kerosene has a narrow range of carbon number (C11-C12) and is mainly used as aviation fuels (Ahmed & Fakhruddin, 2018). Liquefied petroleum gas mainly contains propane (C₃H₈) or/and butane (C₄H₁₀).

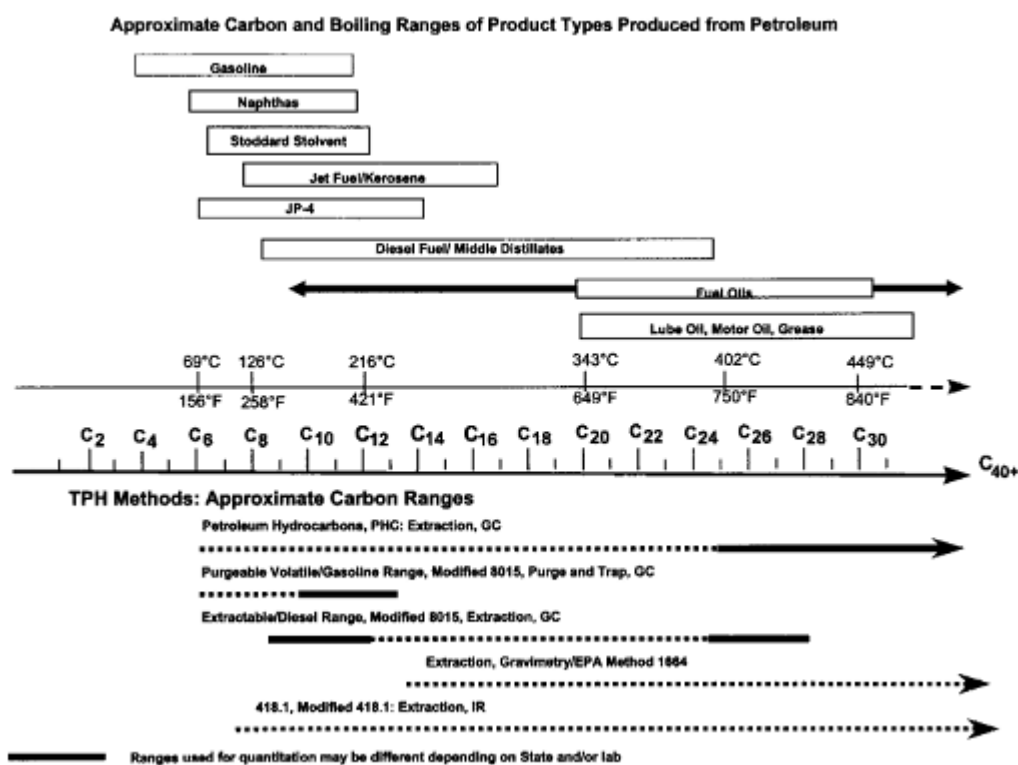


Figure 2.1 Summary of petroleum product types and TPH analytical methods with respect to approximate carbon number and boiling point ranges. (Association of American Railroads BP Oil Company, 1998).

Petroleum-based lubricating oil (mineral oil) is a liquid by-product of crude oil fractional distillation after extraction of petroleum fuel products. Mineral oil consists mainly of higher-molecular-weight petroleum hydrocarbons, as compared to those in diesel, petrol and kerosene. Ethylene, propylene, butadiene, benzene, toluene and xylene are the six most basic petrochemicals, which can then be used to produce a wide range of secondary petrochemical products such as plastics, pesticides etc. Asphalt can be obtained from the residue of crude oil fractional distillation. It consists of high-molecular-weight petroleum hydrocarbons and appears as highly viscous liquid or semi-solid. Asphalt is mainly used for road construction.

Crude oil and oil products are a mixture of organic molecules with varying number of hydrogen and carbon (Potter & Simmons, 1998). Sometimes, they may also contain other elements such as oxygen, sulfur, and nitrogen as impurities (Balba et al., 1998). PHCs can be divided into different categories based on chemical structure and size of the molecules. In terms of chemical structure, PHCs can be classified into aromatic petroleum hydrocarbons and non-aromatic petroleum hydrocarbons. Aromatic PHCs are compounds that contain at least one aromatic ring i.e. cyclic hydrocarbons

with alternating double and single bonds. Non-aromatic PHCs are also called aliphatic PHCs, which include alkanes, alkenes, alkynes and cycloalkanes that contain carbon and hydrogen arranged in straight chains, branched chains or non-aromatic rings (Wittcoff et al., 1996).

Alkanes (also called paraffins) are saturated hydrocarbons with all the carbon being fully saturated by hydrogen. They are the most important constituents in most crude oil and petroleum products. Alkanes arranged in straight chains and branched chains have an empirical formula of C_nH_{2n+2} . Cycloalkanes have the carbon atoms arranged in a circle with an empirical formula of C_nH_{2n} . In literature, alkanes with a straight chain are called normal paraffins, normal alkanes, or n-alkanes while those with branched chains are called isoparaffins or isoalkanes. Cycloalkanes are sometimes called alkyl cycloalkanes. Alkenes are also called olefins, which are usually not present in crude oil. However, much of alkene can be produced during oil refining and therefore, substantial amounts of alkenes may be found in petroleum products. Unlike alkanes, the carbon in alkenes are not saturated by hydrogen (Kostecki et al., 2005).

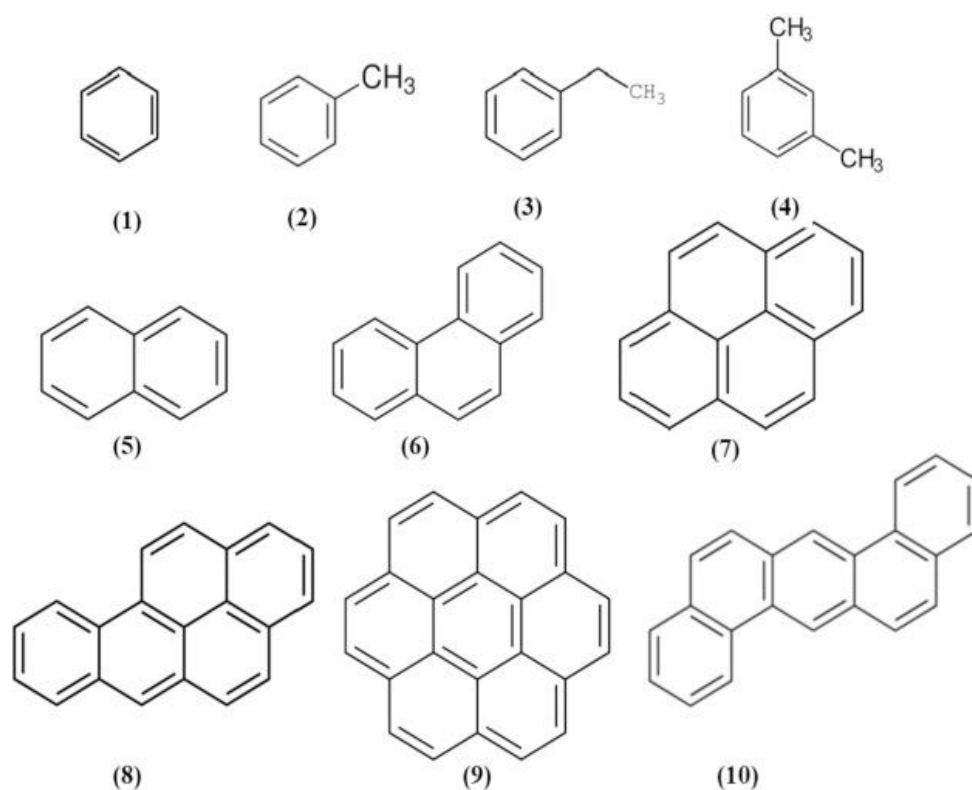


Figure 2.2 Structures of commonly occurring compounds in TPH, (1) Benzene, (2)

Toluene, (3) Ethylbenzene, (4) Dimethyl benzene, (5) Naphthalene, (6) Phenanthrene, (7) Pyrene (8) Benzo[a]pyrene, (9) Coronene, (10) Dibenz[a,h]anthracene (Adapted from Khan et al., 2018).

Because crude oil and oil products may contain hundreds of different hydrocarbon species, it is not practical to identify all individual hydrocarbons contained in a sample. To characterize a sample of crude oil or oil product, PHCs contained in the sample can be operationally divided into various fractions based on their number of Carbon. The carbon number of PHCs ranges from 1 to 90 with the molecular weight varying from 16 g/mole for methane (CH₄) to >1000 g/mole for asphaltenes (Mullins, 2007). PHCs with a small number of Carbon are called light or low-molecular-weight PHCs while PHCs with a great number of carbons are called heavy or high-molecular-weight PHCs. Low-molecular-weight PHCs tend to be more water-soluble and volatile, as compared to high-molecular-weight PHCs. Benzene, toluene, ethyl-benzene and xylene are common low-molecular-weight PHCs that are collectively called BTEX. Other commonly occurring low-molecular-weight PHCs include, dimethyl benzene, naphthalene, phenanthrene, pyrene, benzo[a]pyrene, coronene, dibenz[a,h]anthracene etc. The structure of the common low-molecular-weight PHCs is shown in Fig. 2.2. Heavy PHCs can be defined as the residues after distillation of crude oil (McMillen et al., 2001). The content of heavy PHCs in a given crude oil varies from source to source and can range from 0 to 70% (Coleman et al., 1978). Heavy petroleum hydrocarbons tend to have more complex chemical structures (Fig. 2.3).

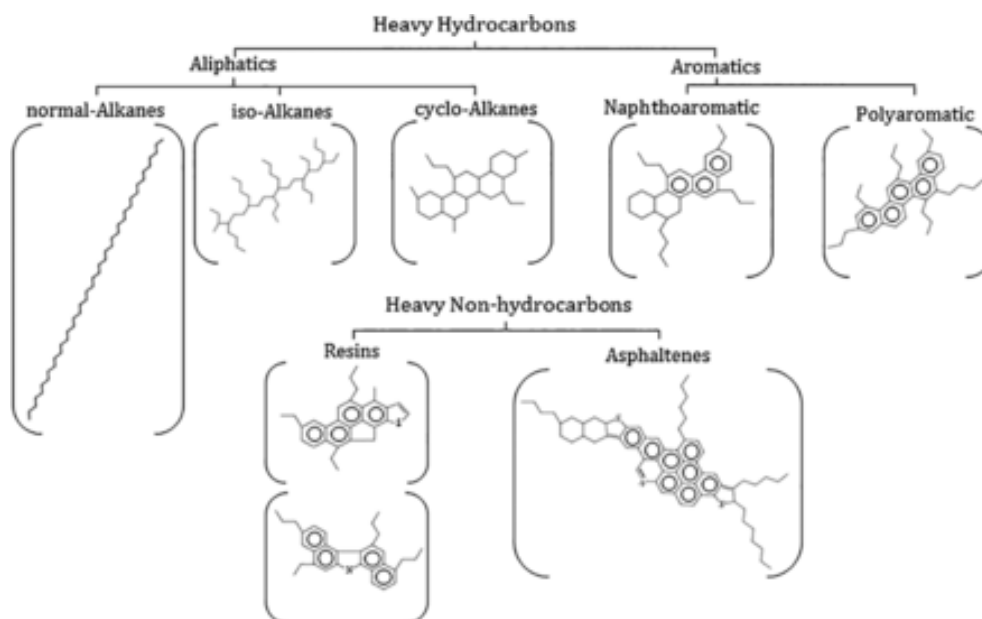


Figure 2.3 Example chemical structures for the major classes of heavy hydrocarbons (Adapted from Brown et al., 2017).

2.2.2 Quantification of petroleum hydrocarbons

Total petroleum hydrocarbons (TPH) is a normally used gross parameter for quantifying environmental contamination originated from various PHC products such as fuels, oils, lubricants, waxes, and others (Environmental Sciences Division, 1993). Measuring the total concentration of petroleum hydrocarbons (TPH) in soil does not give an useful basis for the evaluation of the potential risks to man and the environment (TPHCWG, 1998a). The available petroleum fraction methods are GC-based and are thus sensitive to a broad range of hydrocarbons (Environmental Sciences Division, 1993). Identification and quantification of aliphatic and aromatic fractions allows one to identify petroleum products and evaluate the extent of product weathering (TPHCWG, 1998a). These fraction data can also be used in risk assessment (Association of American Railroads BP Oil Company, 1998). Petroleum group type methods separate and quantify different categories of hydrocarbons (Environmental Sciences Division, 1993). Concentration data for individual petroleum constituents can be used to evaluate human health risk. Individual constituent methods quantify concentrations of specific compounds that might be present in petroleum-contaminated samples, such as benzene, ethylbenzene, toluene, and xylenes (BTEX), and polycyclic

aromatic hydrocarbons (PAHs) (Environmental Sciences Division, 1993).

2.2.2.1 Total petroleum hydrocarbon (TPH)

TPH is the parameter used to account for the total amount of PHCs contained in an environmental sample. EPA Method 418.1 (USEPA, 1979a) for total recoverable petroleum hydrocarbons (TRPH) is the frequently used method for estimation of TPH in water and soil samples. This method was developed based on EPA Method 413.1 (USEPA 1979b) and EPA Method 413.2 (USEPA 1979c) for determining total recoverable oil and grease (TOG) in wastewater sample. Silica gel is used to remove non-PHCs and then TPH is measured by infrared spectrometry.

For determination of TPH in soil samples, n-hexane is used as a solvent to extract oil and grease in the soils (EPA Method 1664). The extracted petroleum hydrocarbons can then be determined by either gravimetric method or gas chromatography with flame ionization detection (GC/FID) (EPA Method 8015) or mass spectrometry (GC/MS) (EPA Methods 8270 and 625). TPH determined by gravimetric method is called TPH (HEM).

In addition to the above lab-based methods, field methods such as immunoassays (IMA) (EPA Methods 4030 and 4035), fluorescence spectroscopy, portable gas chromatograph/mass spectrometry (GC/MS), Raman spectroscopy and visible and near-infrared (vis-NIR) spectroscopy are also used.

2.2.2.2 Petroleum hydrocarbon species or fractions

Determination of individual PHC is limited to highly toxic aromatic species such as benzene, toluene, ethylbenzene and xylenes (Kheirmand et al., 2014; ASTM, 2015). The methods developed for determination of common polycyclic aromatic hydrocarbons (PAHs) in environmental samples are also frequently used to determine PAHs in petroleum hydrocarbon-contaminated environments, including naphthalene, acenaphthene, fluorene, phenanthrene, anthracene, fluoranthene, pyrene, benzo[a]anthracene, chrysene, benzo [a] pyrene, benzo[g,h,i]perylene, dibenz [a,h] anthracene and indeno [1,2,3-cd] pyrene (Law & Biscaya, 1994; El Harrak et al., 1996; Daniel et al., 2008).

For other PHCs, fractionation methods are used to measure both volatile and extractable hydrocarbons. The first PHC fractionation method was developed by Massachusetts Department of Environmental Protection (MADEP) and is frequently referred to as MADEP EPH/VPH Method (MADEP, 1994). This method is good for determine PHC fractions with a carbon number >6 and <28 . For PHCs with a carbon number <6 or >28 , the recovery rate is lower. Lighter and heavier hydrocarbons may have lower recoveries, but their detection is possible and may be enhanced by method modification. TPHCWG (1997a) further developed the fractionation method by dividing the petroleum hydrocarbons into 13 fractions with similar physicochemical properties and consequently fate and transport characteristics (Table 2.1). Different fractions of aliphatic hydrocarbons and aromatic hydrocarbons are separately measured by gas chromatography with a flame ionization detector (FID) or mass spectrometry (MS).

2.2.3 Toxicity of petroleum hydrocarbons

Petroleum hydrocarbons are toxic to biota (Trapp et al., 2001; Chen et al., 2008). The toxicity of petroleum hydrocarbons to a given receptor varies from species to species, and the toxicity of each petroleum hydrocarbon varies from receptor to receptor. In general, aromatic petroleum hydrocarbons tend to be more toxic, as compared to their aliphatic counterparts (on a carbon number basis); short-chain hydrocarbons tend to be more toxic than long-chain hydrocarbons for the same type of petroleum hydrocarbons (Trapp et al., 2001; Chen et al., 2008).

2.2.3.1 Toxic effects on human health

The toxic effects of petroleum hydrocarbons on human health depend on the types of PHC species, the way and duration of exposure, and the amount of PHCs in contact etc., When exposed to the same PHC at the same dose in the same way during the same period of time, the toxic effects tend to be more severe for people who are more sensitive e.g. babies/young children. Toxicity data for some PHCs are available on the major toxicity database provided by government agencies such as Agency for Toxic Substances and Disease Registry (ATSDR), USEPA etc. However, very little is known about the toxicity of many petroleum hydrocarbons and the available data are largely limited to a few highly toxic species such as BTEX (benzene, toluene,

ethylbenzene and xylenes) and other low-molecular-weight polycyclic petroleum hydrocarbons such as naphthalene (Hutcheson et al., 1996). There is a lack of toxicity data for most of individual petroleum hydrocarbons. Assessment of petroleum hydrocarbon toxicity has been mainly based on operationally defined petroleum hydrocarbon fractions or oil products (U.S. Environmental Protection Agency, 2009). The approach to assess the toxicity of petroleum hydrocarbons on the basis of PHC fractions with similar physical and chemical properties was first developed by Massachusetts Department of Environmental Protection (MADEP) in 1990's (MADEP, 1994; Hutcheson et al., 1996). MADEP then revised the toxicity values of different petroleum hydrocarbon fraction for a few times (MADEP, 1996; 1997; 2001; 2002; 2003). Total Petroleum Hydrocarbon Criteria Working Group (TPHCWG) used a similar approach for assessing the toxicity of various aliphatic and aromatic petroleum hydrocarbon fractions (TPHCWG, 1997a; 1997b; 1998a; 1998b; 1999).

2.2.3.2 Ecotoxicity of petroleum hydrocarbons

Petroleum hydrocarbons have toxic effects on microorganisms, plants and invertebrates (Chaineau et al., 1997; Hentati et al., 2013; Khan et al., 2018). In PHC-contaminated soils, plant uptake of water and nutrients could be inhibited (Kirk et al., 2005). Low-molecular-weight hydrocarbons taken by plants might block stomata and intercellular spaces, reducing plant transpiration rate and damaging cell membrane (Baker, 1970). Tables 1 and 2 show some examples of PHC phytotoxicity and toxicity to soil invertebrates and microorganisms (Khan et al., 2018).

Table 2.1 Examples phytotoxicity of PHCs (Khan et al., 2018)

Product	Endpoint	Endpoint value	Indicator/Comment	Reference
Diesel	LC50 for seed germination	25,000 mg kg ⁻¹ in sand	9 grass species	Adam and Duncan, 1999
Diesel	LC50 for seed germination	50,000 mg kg ⁻¹ in sand	22 grass species, legumes and commercial crops	
Fuel oil	LC50 for seed germination	3000–70000 mg kg ⁻¹ in sand	7 crops (most sensitive lettuce, least sunflower)	Chaineau et al., 1997
Fuel oil (light)	LC50 for seed germination	3000 mg kg ⁻¹ in sand	Maize	
Fuel oil (heavy)	LC50 for seed germination	60,000 mg kg ⁻¹ in sand	Maize	
Crude oil (light)	20–70% growth reduction	4200–26,600 mg kg ⁻¹ TPH	Wheat and oats; More sensitive but more variable than seed germination	Salanitro et al., 1997
TPH	LC50 for seed germination	3.04%	Maize	Salanitro et al., 1997, Tang et al., 2011
	LC50 for root elongation	2.86%	Wheat	
		1.11%	Maize	
		1.64%	Wheat	
Diesel	LC50 for seed germination	<1.25%	Cabbage, clover, lettuce and oat	Balseiro-Romero and Monterroso, 2014
		3.5%	Maize	
		5.4%	Pea	
Gasoline	LC50 for seed germination	5–10%	The most tolerant species are Pea and Maize	
Gasoline	LOEL for root elongation	2.5%	Maize	
Diesel		1.25%		
Gasoline	LOEL for shoot biomass	2.5%	Oat	
Diesel		1.25%		

LOEL: Lowest observed effect level; LC: Lethal concentration.

Table 2.2 Toxicity of PHCs to soil invertebrates and microorganisms (Khan et al., 2018)

Candidate	TPH source	Product	Endpoint	Endpoint Value	Comment	Source	
Invertebrates	<i>Eisenia fetida</i>	Artificially Weathered soil	Crude oil (light)	LC ₅₀ for survivability	42–96 mg kg ⁻¹	Depended on the soil's organic content	Salanitro et al., 1997
	<i>E. fetida</i>	Weathered soil	Crude oil	NOEC for survivability	1000 mg kg ⁻¹	Generally non-toxic above 4000 mg kg ⁻¹	Saterbak et al., 1999
	<i>E. fetida</i> and <i>Onychiuris folsomi</i>	Freshly contaminated soil	Fraction C ₁₀ -C ₁₆	EC ₅₀ on the 25th percentile	200 mg kg ⁻¹	Artificial soil was spiked; hydrocarbon fraction was obtained from the distilled Federated crude oil	Stephenson, 2000
	<i>E. fetida</i>			EC ₅₀ on 63 days of incubation of juveniles	160 mg kg ⁻¹		
				LC ₅₀ on 14 days of incubation	170 mg kg ⁻¹		
	<i>E. fetida</i> and <i>O. folsomi</i>	Weathered soil	Fraction C ₆ -C ₁₀	EC ₅₀ on the 25th percentile;	75 mg kg ⁻¹	Field soil was spiked; hydrocarbon fraction was obtained from the light-end distilled Mogas oil.	
	<i>E. fetida</i>			EC ₅₀ on 14 days of incubation	56 mg kg ⁻¹	Mogas spiked on sandy loam field soil	
	<i>O. folsomi</i>			LC ₅₀ on 35 days of incubation for juveniles production;	320 mg kg ⁻¹	Mogas spiked on sandy loam artificial soil	
					500 mg kg ⁻¹	Mogas spiked on sandy loam field soil	
	<i>E. fetida</i>			TPH	LD ₅₀	1.37%	
	<i>Lumbricus terrestris</i> and <i>E. fetida</i>	TPH	–	–	Survivability of <i>Lumbricus terrestris</i> reduced >40% at 1.5% oil content at day 7; No effect at 0.5% oil loading. No <i>E. fetida</i> survived on 10 days at 2.5% TPH.	Shakir Hanna and Weaver, 2002	
	<i>E. fetida</i>	Weathered soil	TPH	–	–	At 0.5% TPH, 100% and 90% of <i>E. fetida</i> survived for 10 days and 15 days, respectively; All died at 2.5% TPH	
	<i>E. andrei</i>	–	TPH	EC ₅₀ at 14 days	644 mg kg ⁻¹	67% of the earthworm died after 14 days at 1000 mg kg ⁻¹	Hentati et al., 2013
<i>E. fetida</i>	–	Motor oil	LC ₅₀ after 4 weeks	40,330 and 3880 mg kg ⁻¹ for fresh and used oil, respectively	Motor oil was more toxic than fresh oil; 100% mortality by 50,000 mg kg ⁻¹ motor oil in soil, while 6200 mg kg ⁻¹ fresh oil in soil	(Ramadass et al., 2015)	
Bacteria	<i>Photobacterium phosphoreum</i>	Freshly contaminated	Crude oil (light)	LC ₅₀	10,000–27,000 mg kg ⁻¹ in sand	Toxicity depended on the soil organic matter	Dorn et al., 1998
			Crude oil (light)	LC ₅₀	>2000 mg kg ⁻¹ TPH	Soil was diluted 0.1 g mL ⁻¹ of Microtox diluent	Salanitro et al., 1997
			TPH	EC ₅₀	0.47% for luminescent bacteria	0.5% TPH content affected the activity of luminescent bacteria (<i>P. phosphoreum</i>)	Tang et al., 2011
Bacterial community	Weathered (low-high concentration, 0.25–4% as initial concentration)	TPH	–	–	Bacterial community significantly altered with hydrocarbon concentration.	Khan et al., 2018	
Fungi	<i>Glomus mosseae</i>	–	TPH	–	Reduction: (i) 11% for spore germination and (ii) 40% of hyphal length	–	Steliga et al., 2015
	<i>Scutellospora heterogama</i>			–	Reduction: (i) 12.5% for spore germination and (ii) 27% of hyphal length	This arbuscular mycorrhizia fungi was in the rhizosphere of <i>Citrus aurantium</i>	
	<i>G. ambisporum</i>			–	Reduction: (i) 30% for spore germination and (ii) 44% of hyphal length	This arbuscular mycorrhizia fungi was in the rhizosphere of <i>C. aurantium</i> and <i>Echinochloa polystachya</i>	
Microalgae	<i>Chlorococcum</i> sp.; <i>Scenedesmus</i> sp.	Weathered	Diesel	NOEC for biomass and enzyme activity	<2120 mg kg ⁻¹	The C ₉ -C ₁₄ fraction had <31 mg kg ⁻¹ ; <C ₉ was not present	Megharaj et al., 2000

NOEC: No observed effect concentration; EC: Effective concentration; LC: Lethal concentration; LD: Lethal dose.

The soluble low-molecular-weight aromatic hydrocarbons are acutely toxic to various marine organisms (Incardona, et al., 2004; Saiz et al., 2009; Almeda et al., 2013).

2.2.4 Petroleum spills and their environmental, economic and social impacts

Petroleum spills cause contamination of environments and consequently could damage ecosystems and reduce its capacity to provide services. It could also form a threat to the health of people who are exposed to the spilled petroleum, and result in financial loss and mental stress for people who are liable to the spills. Large-scale oil spills could even create social conflicts and threaten political stability. Large-scale oil spills are amongst the most threatening environmental disasters in human history. In the past decades, there were several major oil spills taking place around the world, which are highlighted below (John, 2010).

2.2.4.1 The Amoco Cadiz Oil Spill (1978)

Approximately 69 million gallons of light crude oil were released into the English Channel after the oil tanker Amoco Cadiz ran aground on shallow rocks off the coast of Brittany, France. This caused contamination of about 300 km of French coast with the oil slick, which killed millions of invertebrates and an estimated 20,000 birds, and contaminated oyster beds in the region. Amoco Corporation, the owners of the Cadiz, agreed to pay \$120 million to French claimants, along with an additional \$35 million to Royal Dutch Shell, which had owned the lost oil.

2.2.4.2 The Atlantic Empress Oil Spill (1979)

An estimated 90 million gallons of crude oil were released into the Atlantic Ocean off the islands of Trinidad and Tobago due to collision between the VLCCs Atlantic Empress and Aegean Captain, causing oil fire that resulted in emission of toxic gases. 27 sailors died during the accident.

2.2.4.3 The Ixtoc 1 Oil Spill (1979)

Approximately 140 million gallons of crude oil were released into the Bay of Campeche due to the explosion aboard the Ixtoc 1 drilling platform due to maloperation. Some of the spill contaminated the beaches from the western Yucatan Peninsula to

southern Texas, which resulted in hundreds of millions of dollars in lost tourism revenue and reduced commercial fishing in the region for as many as five years afterward.

2.2.4.4 The Castillo de Bellver Oil Spill (1983)

About 79 million gallons of crude oil were released into the South Atlantic Ocean roughly 70 miles from Cape Town, South Africa due to an oil tanker fire.

2.2.4.5 The Incidents at the Nowruz Oil Field (1983)

Roughly 80 million gallons of crude oil were released into the Persian Gulf in two incidences due to oil well leak from the Iranian oil platforms struck by an oil tanker and attacked by an Iraqi helicopter.

2.2.4.6 The First Gulf War Oil Spill (1991)

The most disastrous oil spill in the human history, causing the formation of 115 km² oil lakes and discharge of between 380 million and 520 million gallons of crude oil into the Persian Gulf. This is the subject of this PhD study and details will be presented here.

2.2.4.7 The Mingbulak (or Fergana Valley) Oil Spill (1992)

An estimated amount of 88 million gallons of crude oil were released due to oil well maloperation in Uzbekistan, causing oil fire.

2.2.4.8 The Kolva River Spill (1994)

Some 84 million gallons of oil were released into the Kolva River, Russia due to a breach in a corroded oil pipeline, causing contamination of 186 km² of tundra and wetlands by oil.

2.2.4.9 BP's Deepwater Horizon Oil Spill (2010)

Approximately 134 million gallons of oil were released into the Gulf of Mexico due to a blast in the oil platform, causing contamination of about 2,100 km of the U.S. Gulf Coast and killing 11 workers and injuring 17. BP was liable to a compensation payment of \$65 billion.

2.2.5 Fate and transport of petroleum hydrocarbons

Upon a petroleum hydrocarbon spill, the spilled hydrocarbons spread out and cause contamination of environment. The volatile constituents tend to be translocated to atmosphere (Cappello et al., 2004). Depending on the nature of environmental media, the fate and transport of the spilled petroleum hydrocarbons are different.

2.2.5.1 Water environments

When the spill takes place in surface water environments, some petroleum constituents with high water solubility dissolve in the water and enter into the water column. However, most of the spilled PHCs float on the water surface because they are less dense than water. Transport of the spilled PHCs is driven by water current and wind. Some of the PHCs may be adsorbed onto suspended particulate materials and removed from the water by sedimentation. Over time, the spilled petroleum hydrocarbons experience abiotic and biotic decomposition, including photochemical oxidation, microbial degradation and ingestion by aquatic organisms (Alloway & Ayres, 1993; Hassanshahian & Cappello, 2013). A conceptual model for the fate of spilled crude oil in marine environments was developed by National Research Council (2002).

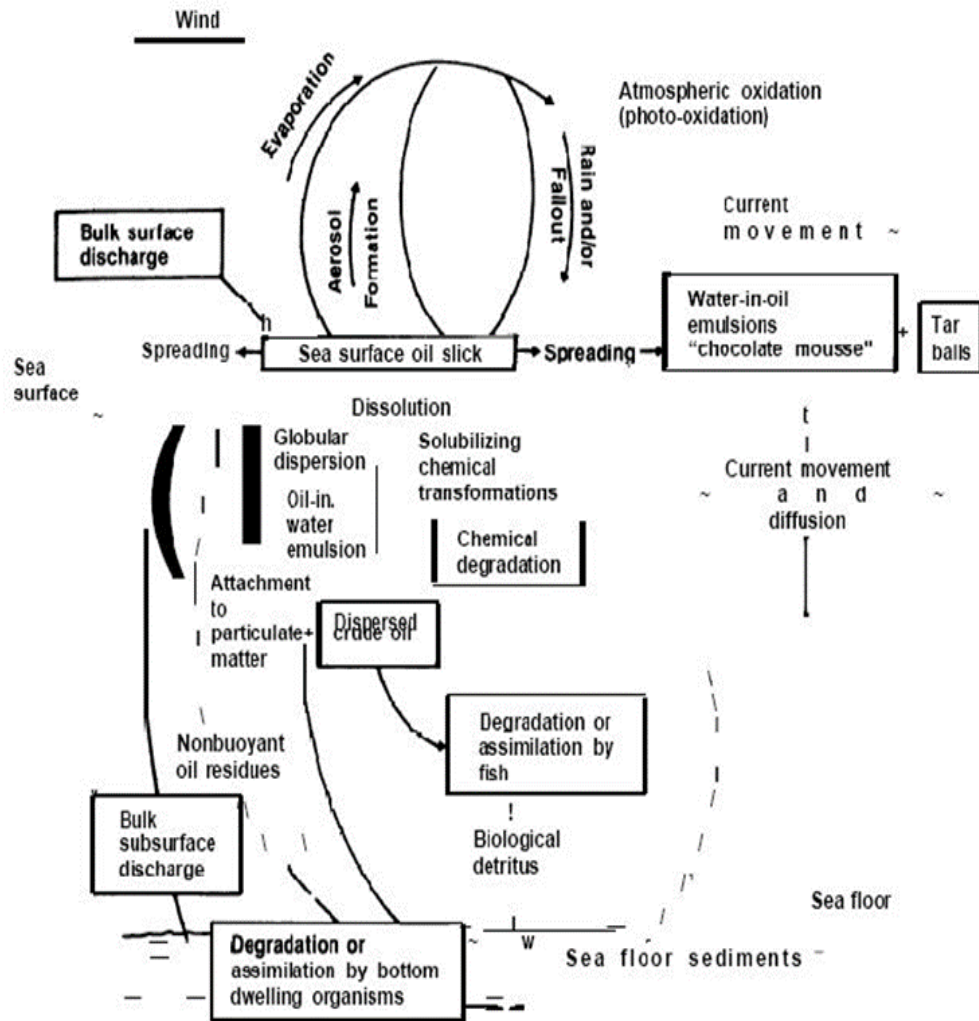


Figure 2.4 The fate of oil in the marine environment (National Research Council, 2002).

2.2.5.2 Terrestrial environments

Land-based oil spills cause contamination of soils. Following a spill, the spilled PHCs can move laterally and vertically through the soils, as driven by capillary and gravity forces. Small soil pores act as traps for the PHC molecules and retain a certain amount of PHCs in the soils the spilled PHCs flow through. In-soil migration of the petroleum hydrocarbon will stop when all the flowing PHCs are held by the soils. For small-scale petroleum spills, the downwardly moved PHCs may never reach aquifers. However, if there are sufficient amounts of spilled PHCs, the contaminant plume could reach the aquifers and cause contamination of groundwater (Brown et al., 2017) developed a conceptual model for fate and transport of spilled crude oil in land

environments (Fig. 2.5).

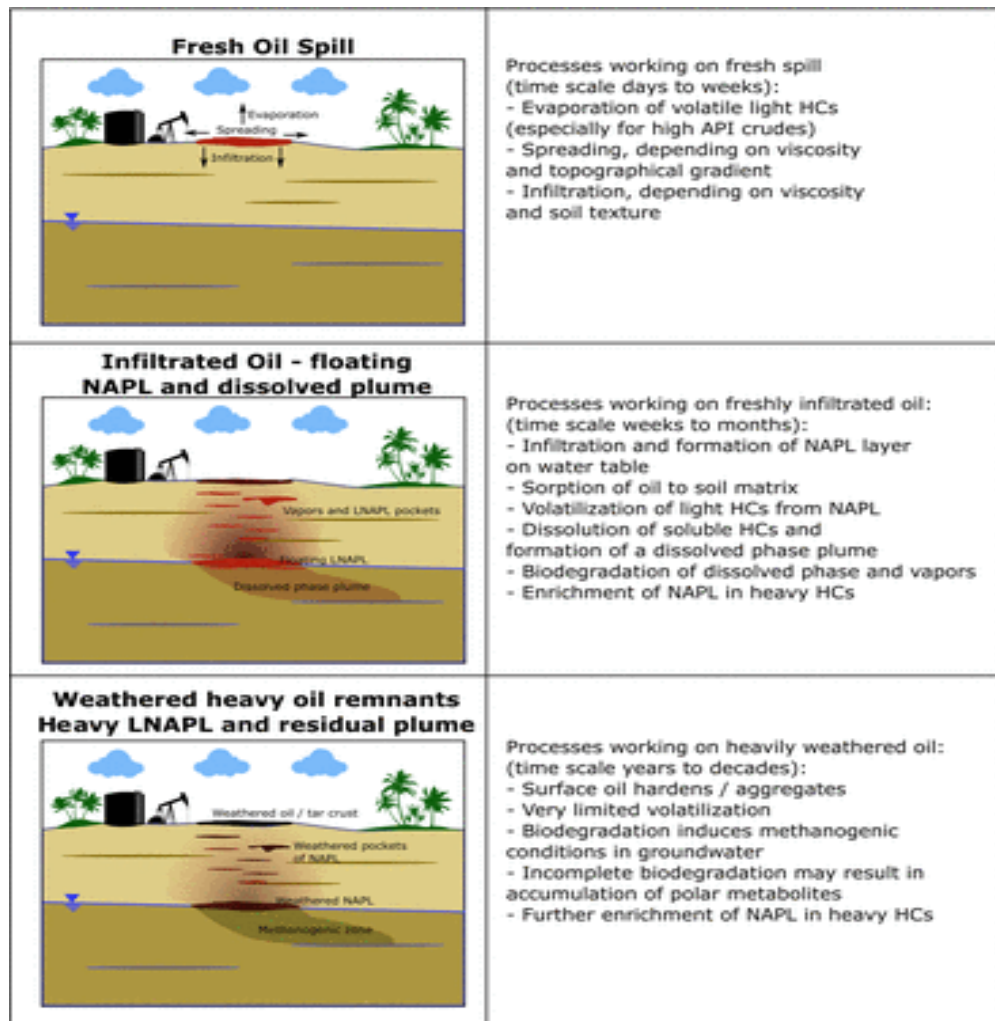


Figure 2.5 A conceptual model of heavy hydrocarbon fate and transport in the environment. Heavy hydrocarbons are typically released together with lighter hydrocarbon fractions that are found in most crude oils. This modifies the physical and chemical properties that significantly affect the transport soils and in the subsurface. Releases of viscous refined bitumen or extremely heavy crude oils (API_o < 12) are unlikely to travel any significant distance in the soil or subsurface. (Brown et al., 2017).

In this conceptual model, three stages are identified for a petroleum hydrocarbon spill incidence: (1) initial surface release of crude oil and infiltration into the unsaturated zone; (2) partitioning of a non-aqueous-phase liquid (NAPL) body near the water table; and (3) attenuation of oil resulting in progressive increase in proportion of heavy hydrocarbons and mass subsequent removal of heavy hydrocarbons by biodegradation.

If there are sufficient amounts of spilled oil, the non-aqueous-phase liquid (NAPL) could move downwards due to the force of gravity. However, the rate of infiltration will be determined by the viscosity of the oil and permeability of the soils (API, 1972; Brost & DeVaul, 2000; Keller & Simmons, 2005). If the NAPL is highly viscous and the soil permeability low, its infiltration in the unsaturated zone is expected to be limited. Downward movement of the spilled oil to reach groundwater can only take place when both the conditions are favourable. When the infiltrating NAPL arrives at the water table, only soluble low-molecular-weight constituents will dissolve in the water to form the contaminant plume. Any heavier constituents will float on the water table. In humid areas, the infiltrating rainwater could accelerate the downward movement of soluble PHCs and cause contamination of groundwater in a much quick manner (National Academies of Sciences, 2003).

2.3 Soil Contamination

Soil contamination is a process through which potentially toxic substances (contaminants) are introduced into a given soil due to human activities. The soils receiving the contaminants are called contaminated soils and the areas where the contaminated soils occur are known as contaminated lands. Common soil contaminants include heavy metals, pesticides, radionuclides, petroleum hydrocarbons and other organic contaminants of non-petroleum sources (Patin et al., 2004).

2.3.1 Soils and soil properties

The definition of “soil” varies depending on the purpose of its uses. For civil engineering projects, soils are defined as any unconsolidated loose materials no matter whether they support plant growth (British Society of Soil Science, 2018). However, from an ecological perspective, soil is a mixture of inorganic and organic particles with pores being filled by air and water, which allows the growth of plants (The Environmental Literacy Council, 2015). The inorganic solid particles with varying sizes are derived from weathering of rocks and consist mainly of primary and secondary minerals such as quartz, feldspars, kaolinite, smectite, goethite, hematite and gibbsite etc. Depending on biological conditions, soils also contain a certain amount of organic

matter at different stage of decomposition.

2.3.1.1 Soil texture and soil structure

Soil texture is about the distribution of soil particle size fractions in a soil. There are different classification systems for soil texture around the world. But it seems that the soil texture classification system developed by the U.S. Department of Agriculture (USDA) has been more frequently used. In this system, soil particles in a soil sample are divided into 3 particle fractions named as sand (0.05-2 mm), silt (0.002-0.05 mm) and clay (<0.002 mm). The soil texture can then be determined by the proportion of each soil particle fractions using the specially designed soil texture triangle (Figure 2.6).

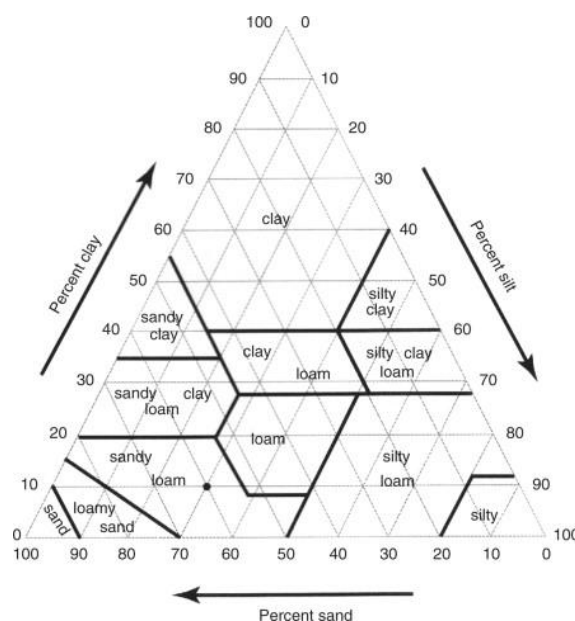


Figure 2.6 Soil texture triangle based on USDA particle-size classification (U.S. Soil Conservation Service.)

Soil structure describes the way through which the soil particles are arranged (Marshall & Holmes, 1979). Soil texture, together with other factors such as humic substances, secondary minerals, soil, climatic conditions and agricultural practices affects soil structure, which determines soil pore size and connectivity of pores and consequently the capacity of a soil to hold water. Fine soil texture tends to have small soil pores and poor connectivity of pores. This does not allow soil solution to move easily within the soil and consequently the soil pores may be largely occupied by soil water, making insufficient space for soil air. Therefore, soil texture and soil structure

could significantly affect plant growth and movement of soil constituents, including contaminants.

2.3.1.2 Humic substances and mineral clays

Humic substances are complex organic molecules formed from biodegradation of organic debris. They are relatively stable and can exist in soils for a long period of time. Humic substances can be divided into humic acid, fulvic acid and humin. Clay minerals are secondary minerals formed from chemical weathering of primary minerals. Humic substances and clay minerals form a complex colloid system in soils and play very important roles in sorption of ions including various contaminants.

2.3.1.3 Soil pH

Soil pH is a parameter used to indicate the activity of hydronium ions (H^+) in a soil solution. It gives an estimate of soil acidity or basicity. Soil pH affects many soil biogeochemical processes that affect microbial activities, plant nutrient supply, and mobility of contaminants in soils.

2.3.1.4 Soil salinity

Soil salinity reflects the level of soluble salts, as indicated by the sum of soluble sodium, potassium, magnesium and calcium. Salinity can be indicated by measuring electrical conductivity (EC) of a soil solution but, under strongly acidic conditions, EC also include contribution from acidic cations such as Al, Mn, Fe and various heavy metals. High soil salinity could adversely affect microbial activities and plant growth.

2.3.1.5 Trace elements

The term “trace element” has different meanings when being used in different disciplines. In geochemistry, it is referred to as an element with a low concentration in the Earth’s crust (White, 2007) whilst in biochemistry, it is referred to as an element that is needed in a trace amount for the proper growth, development, and physiology of biota (Bowen, 1966). Trace elements could become toxic to organisms when concentration exceed the threshold level. The common trace elements that have a high level of toxicity include some heavy metals and metalloids such as arsenic (As), cadmium (Cd), cobalt (Co), chromium (Cr), copper (Cu), mercury (Hg), nickel (Ni),

lead (Pb) and zinc (Zn).

2.3.2 Formation of soils

Soils are formed via weathering of rocks. There are three different types of weathering: (a) physical weathering, (b) chemical weathering, and (c) biological weathering (Energy and resources institute, 2017).

Physical weathering is the process leading to disintegration of rock into smaller and smaller fragments, as driven by exfoliation and frost action due to change in temperature of the rock surfaces.

Chemical weathering is the process leading to decomposition of rocks, as driven predominantly by carbonic acid formed when carbon dioxide dissolves in water. To a lesser extent, chemical weathering can take place due to oxidation of sulphide minerals by oxygen and the sulfuric acid produced from acid sulfate weathering can act as a strong agent to accelerate decomposition of silicate carbonate rocks. Acid precipitation can also cause rapid chemical weathering of soil minerals. Chemical weathering results in leaching of soluble salts and the formation of clay minerals.

Biological weathering describes soil forming processes associated with biological activities. For example, growing plant roots can exert pressure on rock and cause disintegration of the rock; organic acids released from plant roots can decompose minerals.

The intensity of weathering varies from place to place due to different physiographic conditions and human impacts. The soil formation is mainly controlled by five most important factors: climate, rock type, geomorphology/hydrology, vegetation and time (Ahluwalia, 2017). Climate has an overriding control on chemical and biological weathering. Hot and humid climate favours chemical weathering, allowing deep soil profiles being developed and leaching of soluble constituents from the soils. In contrast, chemical and biological weathering are weak in desert areas where physical weathering prevails (Ahluwalia, 2017).

2.3.3 Sources and fate of soil contaminants

Contaminants enter into soils via various pathways, including atmospheric

deposition, surface runoff (irrigation or flooding), waste disposal and application of contaminant-containing soil conditioners (Muhammad Ashraf et al., 2013). Due to the presence of clays and humic substances, soils have the strong capacity to retain contaminants and act as a sink of the contaminants (Bhabananda et al., 2018). Depending on the physico-chemical characteristics of soils, contaminated soils can act as a source of contaminants for other environmental compartments. For example, volatilization of contaminants from soils to atmosphere, leaching of contaminants to surface water and shallow aquifers, uptake of contaminants by plants.

2.3.4 Remediation of contaminated soils

There have been great efforts made to manage and remediate contaminated lands (European Environmental Agency, 2017). Basic approaches for minimizing the environmental impacts of contaminated lands include: (a) isolation, (b) containment, and (c) direct treatment.

Isolation involves setting up an exclusion zone to restrict access to the contaminated land in order to minimize human exposure to the contaminated soils.

Containment involves treatments that prevent direct contacts between the humans/protected organisms and the contaminated soils. These include in-situ treatment such as soil capping and ex-situ treatments such as landfilling.

Direct treatment involves the use of physical, chemical or biological methods to remove the contaminants from the soils. For heavy metal-contaminated soils, heavy metals can be removed from the contaminated soils by soil flushing (in-situ treatment), soil washing (ex-situ treatment), chemical fixation to reduce metal mobility and bioavailability (in-situ treatment), and phytoextraction (in-situ treatment). For volatile contaminants, they can be removed from soils by various thermal treatments but these are at the expense of translocating the contaminants from soils to atmosphere. For non-volatile organic contaminants, they can be removed from soils by incineration, soil washing, microbially mediated degradation and chemical oxidation.

2.3.5 Soil Contamination by Petroleum Hydrocarbons

Soil contamination by petroleum hydrocarbons takes place during the process of production, storage and distribution of the petroleum products. Terrestrial lands that are subject to PHC contamination include oilfields, oil pipeline routes, roadsides, and the areas surrounding oil refiners, oil tanks, petrol stations. The widespread uses of crude oil for production of fuel and petroleum products have resulted in environmental contamination (Bennett et al., 1993; Obuekwe et al., 2000).

2.3.5.1 Environmental Policy and Regulation Related to Soil Contamination by Petroleum Hydrocarbons

To understand the main factor influencing the environmental policies and the related regulation, either by the way how to implement them or the way in how this policies and regulation been developed, we have to understand the definition of risk. The United States Environmental Protection Agency (USEPA) considers risk to be “the chance of harmful effects to human health or to ecological system resulting from exposure to environmental stressor” (USEPA, 2019). Environmental risk assessment is the tool to be used to characterize the nature and magnitude of risk to human health and ecological receptors from chemical contaminants and another stressor that may be present in the environment (USEPA, 2019).

Damages caused by pollution incidents can be extensive enough to cause financial collapse for an unprotected business (Crawford et al., 2019). In the effort of protecting the environment from contamination that harms or might harms human or ecological system and reducing the costs associated with the clean-up of the contaminated environments, most countries around the world have established their environmental policies and regulations. These rules and policies have huge effects and impacts on the organizations and oil companies operating around the world. For example in USA, over the past five decades, the US Congress has enacted or amended several key environmental statutes which are further interpreted and enforced through regulations by federal agencies including the US Department of the Interior, US Environmental Protection Agency (EPA) and the US Army Corps of Engineers (David et al., 2017). The government regulators set rules for financial obligations towards organizations and business causing environmental threats (Crawford et al., 2019).

Changes in environmental legislation have had a major impact on how the long-term impacts of oil and chemical spills are evaluated and controlled and remediation of contaminated land and groundwater in the UK is governed by Part IIA of the Environmental Protection Act (Lenn et al., 2006), which came into force in England on 01 April 2000 (Environment Agency, 2016). Part 2A of the Environmental Protection Act 1990 (EPA 1990) requires the Environment Agency to prepare a report on The State of Contaminated Land "from time to time, or at the request of the Secretary of State". The framework of England's contaminated land regime ("CLR") was set out in Part IIA of the Environmental Protection Act 1990 (Penny et al., 2019). The regime sets out the local authority's duty to inspect their area for, and for regulators to identify and investigate, potential "contaminated land" and determine those responsible for its remediation. They then have the power to issue remediation notices on those responsible or to undertake the remediation and recover the costs from the responsible parties, if they are not satisfied that the remediation will be undertaken voluntarily (Penny et al., 2019).

The degree of remediation required at a contaminated site should generally be determined using a risk-based approach to underpin decision-making and regulatory approval (Lenn et al., 2006). The main objectives of the Government's policy on contaminated land and the Part 2A regime are to:

- (a) identify and remove unacceptable risks to human health and the environment.
- (b) seek to ensure that contaminated land is made suitable for its current use.
- (c) ensure that the burdens faced by individuals, companies and society as a whole are proportionate, manageable and compatible with the principles of sustainable development

Regulatory regimes aimed at preventing land from becoming contaminated include the Environmental Permitting (England and Wales) Regulations 2010 and the Environmental Damage (Prevention and Remediation) Regulations 2009 (Environment Agency, 2016).

2.3.5.2 Remediation of Petroleum Hydrocarbon-contaminated Soils

Hamad Almebayedh (2014) pointed out that the effectiveness of remediation technologies for clean-up of the crude oil-contaminated soils is dependent on a few factors, including contaminant and site characteristics, regulatory requirements, and cost limitations (Fig. 2.7). There is a range of remediation technologies, which have been developed or proposed for treating petroleum hydrocarbon-contaminated soils (King et al., 1998; Khan et al., 2004; Beyke and Fleming, 2005; Jadidi et al., 2014; Madadian et al., 2014; Huguenot et al., 2015). These can be divided into physical, chemical and biological methods. The physical methods frequently used for treating petroleum hydrocarbons include thermal removal, soil washing, landfilling and capping. Chemical method involves the use of strong oxidants such as free radicals to destroy hydrocarbon molecules. Bioremediation allows petroleum hydrocarbon being degraded by microorganisms.

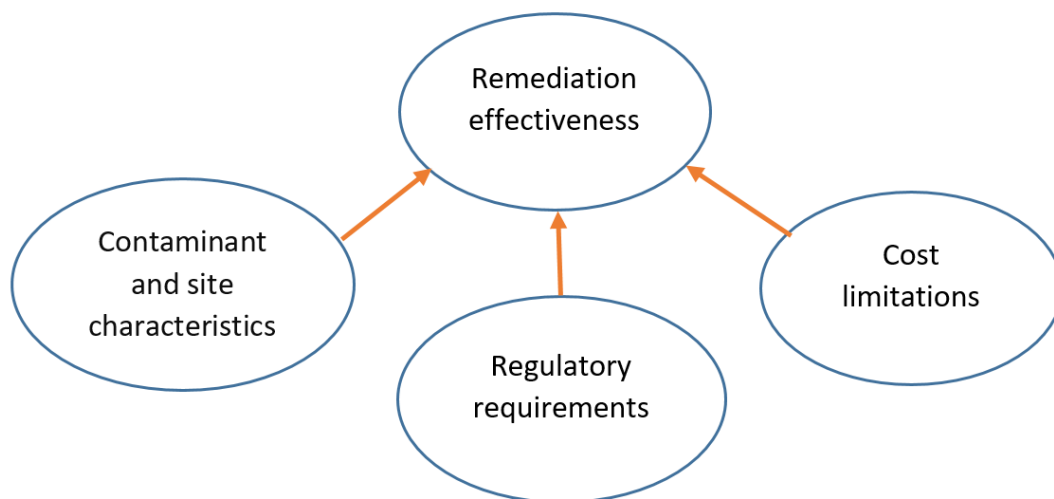


Figure 2.7 A flow chart showing the effectiveness of technologies dependency (ETD) (Adapted from Al-Mebayedh, 2014)

The available PHC-contaminated soil remediation technologies can be divided into two categories: in-situ treatments and ex-situ treatments.

In-situ treatment is referred to as treating the contaminated soils at the location where they occur. Ex-situ treatment is referred to as the situation where the contaminated soils are removed from their original locations and cleaned off-site.

Based on the treatment agents used, both in-situ and ex-situ methods can be

further divided into the following categories (Friend, 1996):

- Physical treatment,
- Chemical treatment,
- Biological treatment,
- Thermal treatment, and
- Containment

Details on the classification of remediation technologies are given in Table 2.3.

Table 2.3 Treatment technologies for PHC-contaminated soils (Friend, 1996)

General Category	Type of Process	Technology applied in-Situ	Technology Applied Ex-Situ
Treatment	Biological	<ul style="list-style-type: none"> • Passive biodegradation • Bioventing • In-Situ Biodegradation 	<ul style="list-style-type: none"> • Biopiles • Land treatment or landfarming • Slurry biodegradation • Composting
	Physical	<ul style="list-style-type: none"> • Soil Venting - Conventional - Hot air or steam stripping • Soil flushing 	<ul style="list-style-type: none"> • Soil washing • Coal tar agglomeration
	Chemical	<ul style="list-style-type: none"> • Chemical Oxidation/reduction 	<ul style="list-style-type: none"> • Chemical Oxidation/reduction • Solvent extraction
	Thermal	<ul style="list-style-type: none"> • Radio frequency (RF) heating • Vitrification 	<ul style="list-style-type: none"> • Thermal desorption by: <ul style="list-style-type: none"> -Low and high temperature. -Thermal strippers - Hot-mix asphalt plants • Vitrification
Containment	Other	<ul style="list-style-type: none"> • Solidification/stabilization • Capping 	<ul style="list-style-type: none"> • Solidification/stabilization • Microcontaminated by cold-mix asphalt • Capping or re-use • Land disposal or Land filling

2.4 Environmental Risk Assessment

Environmental risk is about the likelihood of harmful effects on human health and ecosystems as a result of environmental contamination. The process used to evaluate environmental risk is called environmental risk assessment (ERA), which has two components: human health risk assessment and ecological risk assessment. However, applied industrial risk assessment is sometimes included under the umbrella of ERA (Fig. 2.8). The level of environmental risk is determined by the severity of environmental hazards and the probability of exposure (Iyyanki et al., 2017). ERA usually involves the following steps: hazard identification, hazard characterisation,

exposure assessment, and risk characterization. The purpose of ERA is to inform risk management.

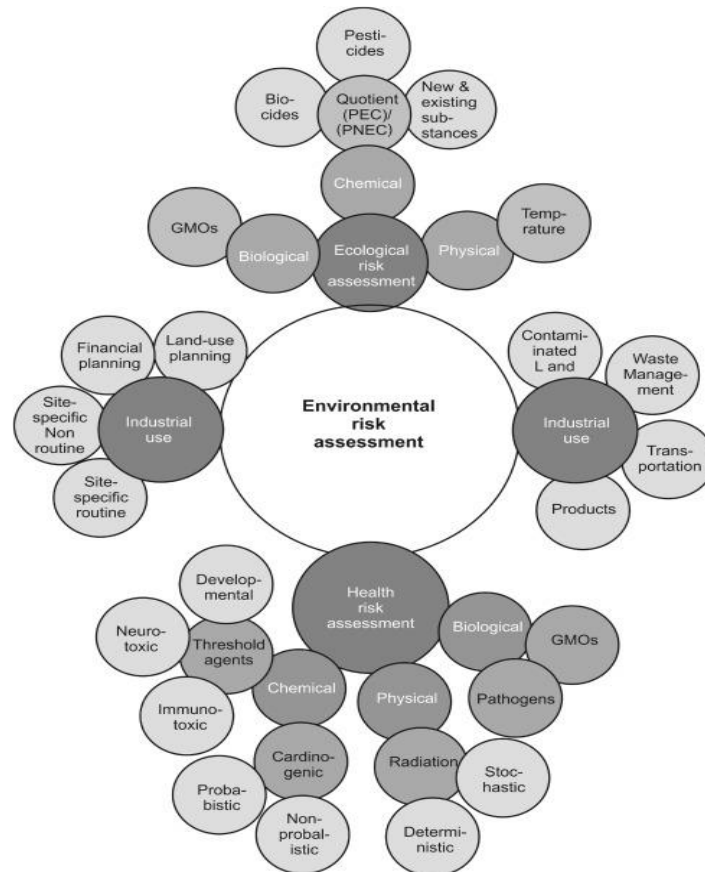


Figure 2.8 Components of environmental risk assessment (Iyyanki et al., 2017)

2.4.1 Environmental hazard identification and characterisation

An environmental hazard is a substance that has an adverse effect on human health or ecosystems in certain circumstances. Environmental hazards likely to be caused by a specific environmental contaminant can be estimated by dose-response experiments (Ishaque & Aighewi, 2008). This process is known as hazard characterisation (Chartres et al., 2019). Hazard characterisation allows quantitative assessment of the toxic response by a given species of biota receiving varying doses of a given contaminant and the establishment of a dose-response curve that shows the relationship between the two variables.

In reality, co-existence of different environmental contaminants is common and therefore, the environmental hazard is the combined effects of multiple contaminants. The environmental conditions such as temperatures, pH etc. could markedly affect the severity of the hazard (EnHealth et al., 2012).

2.4.2 Exposure assessment

Exposure assessment is the process of characterizing, estimating, measuring, and modelling the magnitude, frequency, and duration of contact with an agent as well as the number and characteristics of the population exposed (Vallero, 2014).

The major pathways through which biota are exposed to contaminants are inhalation, ingestion and absorption by skin upon dermal contacts. To quantify the exposure, three sets of factors need to be considered (Gerba, 2004):

- i) concentrations of contaminants in the media
- ii) exposure magnitude, frequency and duration
- iii) quantified biological characteristics of receptor

An example conceptual model showing the exposure pathways is given in Fig. 2.9 (Gerba, 2015)

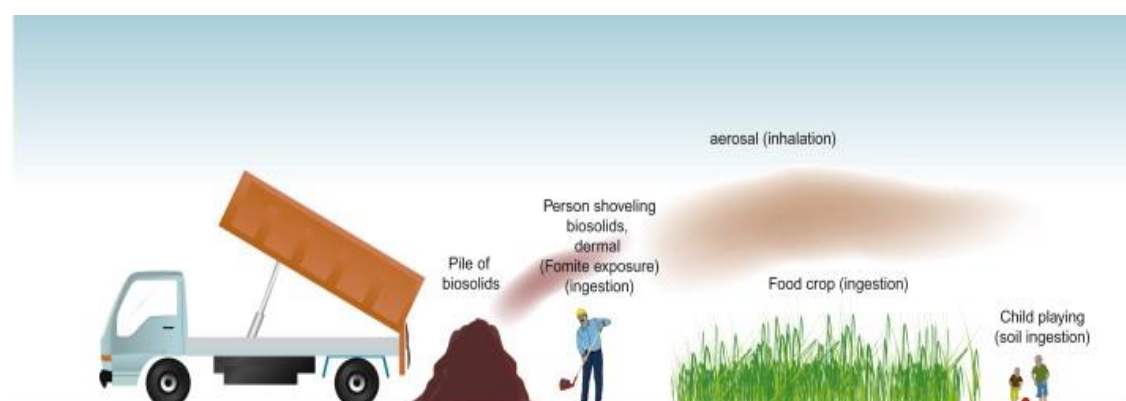


Figure 2.9 Potential routes of pathogen exposure from land application of biosolids (Adapted from Gerba, 2015).

2.4.3 Environmental risk characterization

Risk characterization is the qualitative and/or quantitative prediction of the adverse effects of contaminants on biological receptors based on hazard identification, hazard characterization and exposure assessment (Voysey et al., 2002; Bleam, 2017). Various intake equations describing each potential exposure route have been developed to estimate the potential dose and hazard quotient. Using the outcomes from risk characterization, screening levels for each contaminant the exposure routes can be established. In many countries, the standards for environmental enforcement are largely based on risk-based screening levels obtained from risk characterization.

2.4.4 Major environmental risk assessment systems

The environmental risk assessment typically falls in to one of two areas: (a) human health, and (b) ecological system. The risk assessment is an evaluation tool that estimates and evaluates the effects and the harm caused by the contact of human and other biota such as animal, plants, fish with the contamination now and in the future (USEPA, 2019).

Environmental risk assessment processes typically begin by collecting data that allows the characterization of the chemical contamination in the environment, as well as information needed to predict how the contaminants could behave in the long-term and short-term future. A number of international organizations have adopted approaches for risk assessment systems for petroleum hydrocarbon-contaminated sites, and for setting soil assessment criteria for soil contamination by petroleum hydrocarbons.

The use of petroleum fractions and indicator compounds criteria together with exposure models developed from risk-based approaches as the criteria are toxicologically focused. Here the emphasis is on identifying the key indicator compounds and/or petroleum fractions presenting risks for human at a hydrocarbon-contaminated site, by indicating their environmental behavior and toxicology. It could be considered as a 'tiered' approach as commonly started with simple preliminary assessments (DETR et al, 2000).

2.4.4.1 USA risk assessment systems

2.4.4.1.1. American Society for Testing and Materials (ASTM) Approach

The American Society for Testing and Materials (ASTM) established risk-based indicator standards E1739-95 and E2081-00 (ASTM, 1995, 2000). The standard for petroleum- and chemically-contaminated sites concluded Risk-Based Corrective Action (RBCA) in three-tier approaches; each tier has the objective of compliance with an acceptable level of risk; the tiers become less generic and less conservative. This relies on reviews of toxicology and environmental fate and exposure for site-specific target levels (SSTLs) for assessing risks from contaminated soil and risk-based soil screening levels (RBSLs). The ASTM standard has been widely used in USA and Europe. In this three-tier risk-based corrective action (RBCA) the polycyclic aromatic hydrocarbons (PAHs) are most important for the sites contaminated with fuel oils and kerosene. For the sites contaminated by gasolines, the usually selected chemicals of concern are BTEX.

2.4.4.1.2 The Massachusetts Department of Environmental Protection Approach

This approach depends on the use of representative petroleum fractions for assessing the risk associated with the soil contamination (MaDEP, 1994, 1997, 2002a and 2002b). The MaDEP approach is the precursor of the now widely used TPHCWG approach, which is presented in the next section.

2.4.4.1.3 Total Petroleum Hydrocarbons Criteria Working Group Approach

This approach focuses on the type of petroleum contamination at a contaminated site. A hybrid method that employs petroleum hydrocarbon fractions and carcinogenic indicator compounds is used for evaluating human health risk from the potential exposures to petroleum contamination (TPHCWG, 1999b). The TPHCWG determines petroleum hydrocarbon fractions based on equivalent carbon numbers (EC) for environmental risk assessment (TPHCWG, 1997a). TPHCWG identified 13 aromatic and aliphatic fractions with the petroleum hydrocarbons with each fraction being similar in terms of physicochemical characteristics (TPHCWG, 1999b).

2.4.4.1.4 US Agency for Toxic Substances and Disease Registry (ATSDR) Approach

The TPHCWG and the MaDEP approaches has been reviewed and recommended as the preferred approaches by US Agency for Toxic Substances Disease Registry. The ATSDR implemented a precautionary approach to indicate the toxicity of the entire fraction by using the most toxic representative mixture.

2.4.4.2 The Canada-Wide Standard (CWS) for Petroleum Hydrocarbons in Soils

The CWS approach uses broader bands of petroleum hydrocarbon fractions, as compared to the TPHCWG fractions. Only four petroleum hydrocarbon fractions are used for the assessment of the toxic threshold effects. This eliminates the need for an aromatic/aliphatic split and the four fractions are as follows:

- Fraction 1: nC6-C10;
- Fraction 2: >nC10-C16;
- Fraction 3: >nC16-C34; and
- Fraction 4: >nC34.

The CSW approach was endorsed by the Canadian Council of Ministers of the Environment (CCME) in 2001 (CCME, 2000; 2001a; 2001b). The scientific rationale behind the CWS approach is algorithms used for the calculation.

2.4.4.3 EU risk assessment systems

To support scientific cooperation between European countries, the Concerted Action on Risk Assessment for Contaminated Sites (CARACAS) was initiated in February 1996 in order to tackle the problem of contaminated land. This initiative was funded by the EC Environment and Climate R&D Program. It brought together the combined knowledge of academics, government representatives and other experts from all EU Member States plus Norway and Switzerland to develop risk assessment methods for the contaminated lands across the EU.

2.4.4.3.1 The Dutch National Institute for Public Health and the Environment Approach

The Dutch National Institute for Public Health and the Environment (RIVM) have chosen the TPHCWG approach with slight adjustments, by allocating maximum permissible risk (MPR) levels to seven petroleum fractions (Vermeire, 1993; Janssen et al, 1995).

2.4.4.4 New Zealand

TPHCWG approach has been adopted for petroleum hydrocarbon-contaminated site in New Zealand (Ministry for the Environment, 1999) with Tier 1 soil and groundwater acceptance criteria being developed on the basis of the following fractions:

- C7 to C9;
- C10 to C14; and
- C15 to C36

The TPH fractions were not differentiated between aromatic and aliphatic compounds but BTEX and PAHs are used separately for risk assessment.

2.4.4.5 UK risk assessment systems system

The UK adopted TPHCWG approach for evaluating human health risks from petroleum hydrocarbon-contaminated soil, which has been published recently by the Environment Agency. Environment Agency proposed to add three further fractions into TPHCWG scheme. The UK approach also considers the combined toxicological effects of all the fractions.

Environmental Agency sets the framework for evaluating human health risks from petroleum hydrocarbons as follows

- be scientifically authoritative and based on the principles of toxicology, exposure and risk;
- be based on a state-of-the-art understanding of petroleum in the environment;

- be able to be implemented by the full range of practitioners and disciplines involved in the contaminated site assessment and management processes;
- be proportionate to the risks posed; and
- enable decision-makers to arrive at practical, sound management decisions that are protective of human health.

Table 2.4 A summary of approaches developed by the organizations in some developed countries for environmental risk assessment (Turczynowicz & Robinsn, 2008)

	United States ATSDR	International TPHCWG	Canada PHC CWS	The Netherlands RIVM	New Zealand Ministry for the Environment	United Kingdom Environment Agency
Indicator substances	Indicator compounds include most toxic compounds only.	Indicator compounds include most toxic compounds only.	Indicator compounds include most toxic compounds (target compounds) and others frequently tested for.	Indicator compounds include most toxic compounds and others frequently tested for.	Specific indicator chemicals cited: BTEX, naphthalene, pyrene, benzo[a]pyrene.	Individual compounds identified.
Fractions Number and basis	Similar to TPHCWG. Minor modification to aromatic groups to include all BTEX compounds in same fraction. EC numbers as per TPHCWG	13 analytical fractions (6 aliphatic and 7 aromatic) using 7 toxicity values (3 aliphatic and 4 aromatic). Fractions based on EC number, driven by fraction transport properties and subsequently summed to produce toxicity fractions.	4 fractions based on 13 developed by TPHCWG. Separate evaluation of aromatic/aliphatic compounds not required. EC numbers, as per TPHCWG.	7 fractions based on toxicity values (3 aliphatic and 4 aromatic). EC numbers as per TPHCWG.	3 aliphatic fractions only. Not clear on whether EC or C numbers presented. No reference to TPHCWG EC numbers.	16 petroleum hydrocarbon fractions: 7 aliphatic 8 aromatic 1 combined fraction TPHCWG plus API fractions

	United States ATSDR	International TPHCWG	Canada PHC CWS	The Netherlands RIVM	New Zealand Ministry for the Environment	United Kingdom Environment Agency
Basis of toxicity and transport properties	Most toxic compound/mixture in fraction generally used as surrogate for toxicity values.	Toxicity values based on surrogates and fresh product compositions. Transport properties based on entire fraction.	Use of TPHCWG toxicity and transport data.	Toxicity values based on surrogates. Transport properties based on entire fraction (as per TPHCWG).	Use of adjusted TPHCWG toxicity and transport data. Method of adjustment not presented.	TPHCWG/API toxicity and transport data with review.
Toxicodynamics of concurrent exposure	Precautionary approach, developing 'index of concern', based on addition of hazard quotients across fractions for compounds affecting same target organs or systems.	Precautionary approach, based on addition of hazard quotients across fractions.	Not advised due to different toxicological endpoints and exposure pathways of different fractions.	Precautionary approach, based on addition of hazard quotients across fractions.	Additive effects considered when using acceptance criteria. Precautionary approach adopted.	Additive effects of concurrent exposure across fractions considered.

	United States ATSDR	International TPHCWG	Canada PHC CWS	The Netherlands RIVM	New Zealand Ministry for the Environment	United Kingdom Environment Agency
Application of approach	As for TPHCWG	Use of RBCA 3-tiered approach. Look up tables for Tier 1 and increasing use of site-specific information in Tiers 2 and 3.	Use of RBCA 3-tiered approach. Look up tables for Tier 1 and increasing use of site-specific information in Tiers 2 and 3.	Use of a tiered approach, moving from generic guidelines to less conservative values by using site-specific data.	Use of a 3-tiered approach, moving from generic guidelines to less conservative values by using site-specific data.	Subject to current development.
Recommended analysis	As for TPHCWG	Direct method. Indicator compounds not reported.	2-step analytical method developed and benchmarked across laboratories in Canada. Indicator compounds not reported.	Single analytical method (NEN 5733) recommended. Indicator compounds not reported.	Based on American Petroleum Institute <i>Method for Characterisation of Petroleum Hydrocarbons in Soil</i> . Chemicals of concern not reported.	Direct method (AEHS 2000) with extension and review suggested. Indicator compounds not reported.
Other comments			Aesthetic issues, such as odour, identified as a need for further research.		Aesthetic issues, such as odour, identified as requiring site-specific assessment.	Based on extensive public consultation and expert workshop discussions.

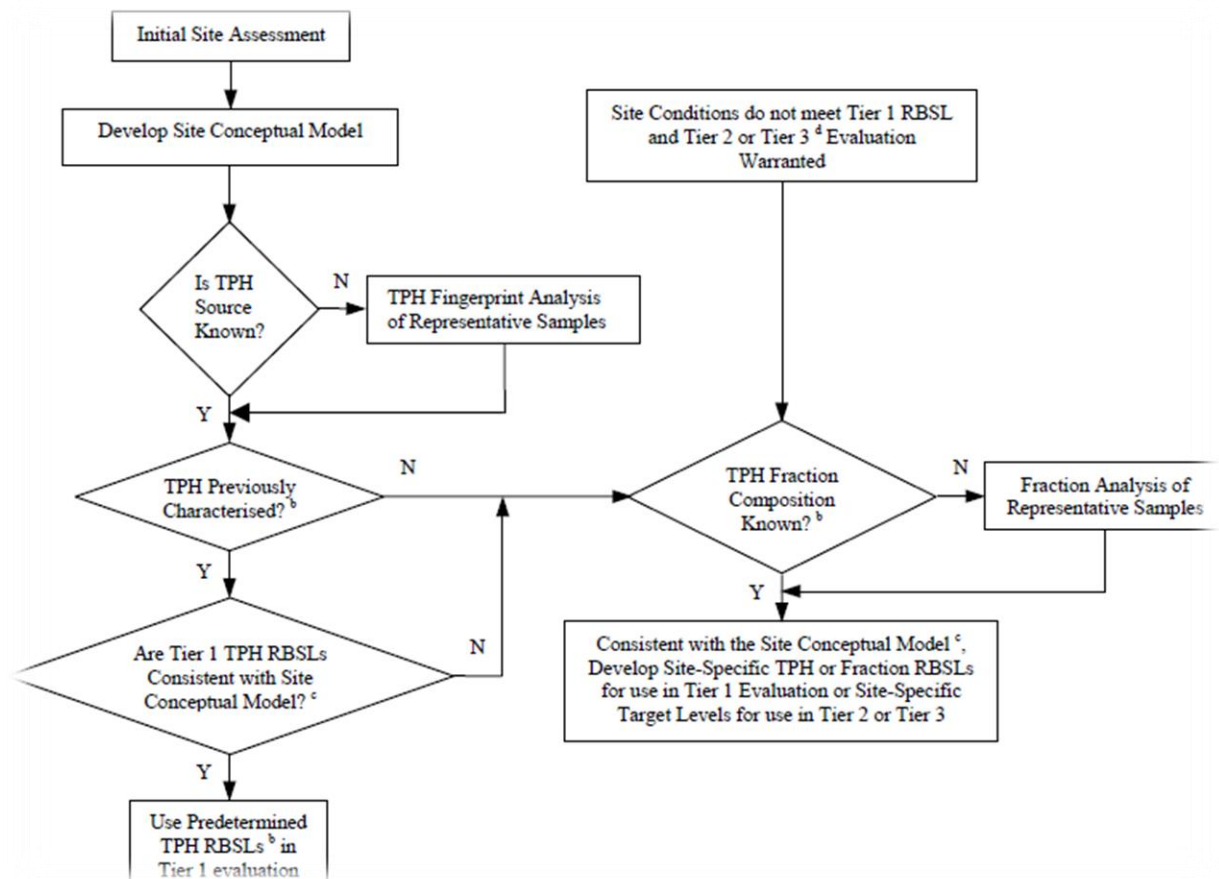


Figure 2.10 Implementation of risk-based TPH analysis within a 3-tiered RBCA framework (Adapted from Environment Agency R&D Technical Report, 2003)

2.4.5 Environmental Risk Assessment Tools for PHC-Contaminated Soils

Iononutu (2010) concluded that the qualitative and quantitative assessment of the environmental risk for hydrocarbon-contaminated site such as industrial sites for drilling and gas oil separation are complex and require a range of data. The methodology they developed was based on several research studies for the environmental risk assessment of soil pollution from accidental crude oil spills. For these reasons, their environmental risk assessment methodology for soil structured in modules and steps. Their environment risk assessment for contamination with hydrocarbons from crude oil comprises five interrelated modules, including hazard assessment, hazard identification, risk estimation by the award of “grades” for the frequency and severity of consequences environmental risk assessment based on risk criteria (ALARP) and environmental risk management. The modules required several data to be obtained; technical data for the equipment in the upstream industrial activities, extraction and gas-oil separation, physico-chemical analysis for the soil contaminants,

soil properties that may influence the severity and consequences of the default risk, charts, mathematical equations and matrix assessment of environmental risk intensity. In the methodology are established the steps needed to calculate the alert threshold and intervention and additional studies needed such as (geotechnical study, pedological and chemical study).

Diana et al. (2017) developed an assessment of human health risk caused by exposure to carcinogenic PAHs, MAHs, and heavy metals existing in a soil contaminated as a consequence of crude oil pollution with a risk analysis software package (RECOLAND v1.0), which show an effective method for decreasing, or even eliminating the impact of the contaminated site on human and environmental health by using this risk-based approach. The results specified that it is necessary to find an optimal solution for decontaminating the investigated soil to minimize the health risks.

Chen et al. (1998) developed a hybrid HSSM-FPA model, which was applied to a case study for a petroleum-contaminated site in western Canada, where soil and groundwater was contaminated by industrial wastes containing benzene, toluene, ethylbenzene and xylenes (BTEXs). The results suggest that the HSSM-FRA can provide insight into the potential risk to the receptor of concern downward the aquifer and can serve as a basis for further remediation-related decision analysis.

2.5 Spatial Interpolation and 3-D Soil Mapping

Spatial distributions of geo-physical properties, such as elevations, land uses, soil properties, soil moisture contents etc. can be approximated using the functions of locations. Spatial interpolation refers to the process estimating the unknown property values at specific locations in terms of the measured/observed data at other locations, the sampling points. Many interpolation and approximation methods have been developed, which have been successfully used to predict values of spatial phenomena and the data transformations between different discrete and continuous representations of spatial and spatiotemporal fields.

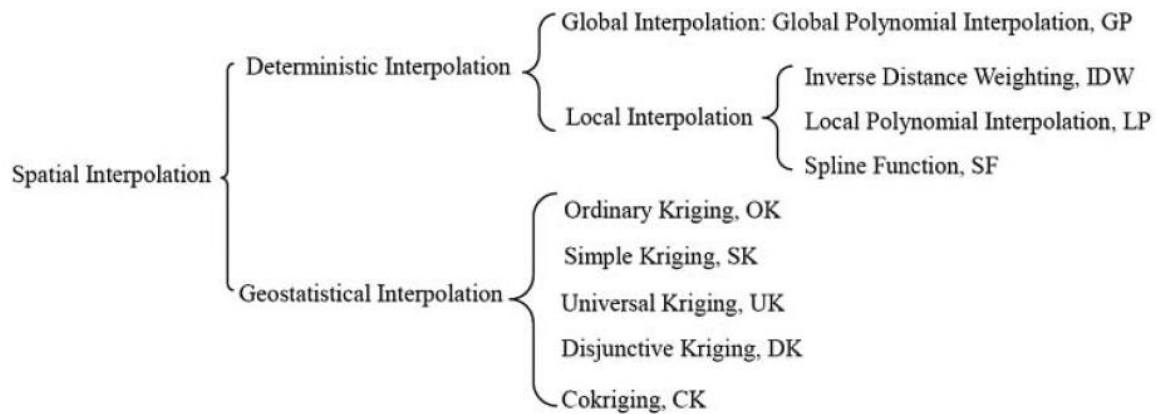


Figure 2.11 An overview of spatial interpolation methods (Adapted from Chen et al., 2016)

These methods are summarized by Fig. 2.11. They can be grouped into of two categories: (a) the deterministic interpolation, and (b) geostatistical interpolations in which the Inverse Distance Weighting (IDW) in the first group and the Kriging methods in the second group are the two of the most popularity. Meanwhile, previous research has confirmed that the Kriging methods performance better than IDW particularly for the cases of a complex terrain (Yao et al., 2013). As a result, this research decides to adopt the Kriging method for the characterization of soil contamination while a comparison with the IWD method has also been investigated.

2.5.1 Geostatistical interpolation (Kriging)

The principles of geostatistical interpolation have been described in a large body of literature. Kriging refers in general to all such geostatistical interpolation methods, which predicts the value at an unobserved location taking a linear combination of the values at surrounding locations, using weights according to a model that describes the spatial correlation (Knotters et al. 2010). In other words, seeing that the special variation of any continuous attributes is general too complicated to be represented using a simple, smooth deterministic mathematical function, Kriging instead is based on a concept using a random function to represent the geo-parameters/geo-properties, which have a certain spatial covariance. For example, for a spatially continuous geo-property, $Z(X)$, where X indicates the spatial coordinates, we may find a deterministic spatial function, $M(X)$, to model it. As a result, the geo-property can be expressed in terms of the modelling function as:

$$Z(X) = M(X) + \Delta(X) \quad (1)$$

Where Δ is a stochastic spatial residual function. There are two assumptions. Firstly, it is assumed that the mean value of the $M(X)$ over a certain spatial region is the same as that within the whole area, $X+h$, where h is the assemble of all the distances of all the location X to all the regional points, and this can be expressed using a mean function E as below:

$$E[M(X) - M(X + h)] = 0 \quad (2)$$

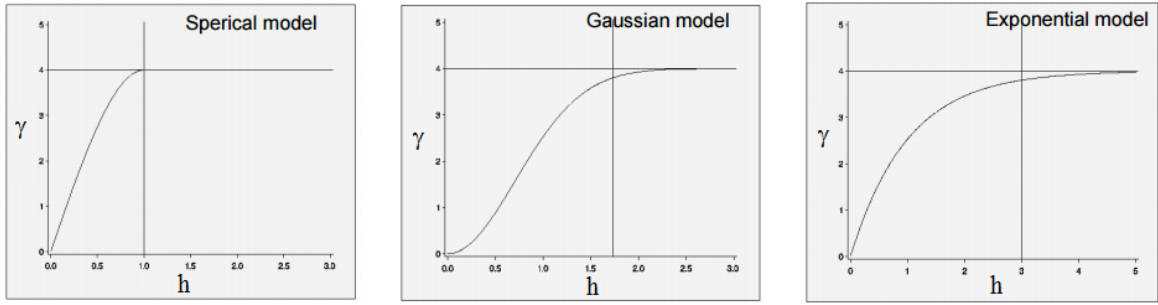
Secondly, it is also assumed that the variance the geo-property over the spatial area is auto-correlated to the distance, i.e., points closer to each other have more similar values, and this can expressed using a variance function of the distance as the Eq. 3 below:

$$E[(Z(X) - Z(X + h))^2] = E[(\Delta(X) - \Delta(X + h))^2] = 2\gamma(h) \quad (3)$$

Where $\gamma(h)$ is called the semi-variance of the variance of the geo-property referring to the distance, which can be estimated in terms of the sampling data taking the following formula:

$$\gamma(h) \approx \frac{1}{2n} \sum_{i=1}^n (Z(X_i) - Z(X_i + h))^2 \quad (4)$$

where i indicates the individual sampling points and n is the total sampling points. The Eq. 4 forms the fundamental principle for the Kriging interpolation technique. To implement the interpolation based on the Eq. 4, the semi-variance function needs to be defined with a mathematical function, for which different models have been proposed and investigated. There are Three typical models in common use, they are spherical, Guassian and exponential, respectively, as shown in the Figure 2.12.



$$\gamma(h) = \begin{cases} c_0 \left[\frac{3}{2} \frac{h}{a_0} - \frac{1}{2} \left(\frac{h}{a_0} \right)^3 \right], & \text{for } h \leq a_0 \\ c_0, & \text{for } h > a_0 \end{cases} \quad \gamma(h) = c_0 \left[1 - \exp \left(-\frac{h^2}{a_0^2} \right) \right] \quad \gamma(h) = c_0 \left[1 - \exp \left(-\frac{h}{a_0} \right) \right]$$

Figure 2.12 Graphs showing various Variogram models

With these two assumptions and using the semi variance function to represent the stochastic spatial residual function $\Delta(X)$, the Eq. (1) can be rewritten as:

$$Z(X) = M(X) + \gamma(h) \quad (5)$$

Finally, in term of the interpolation principle, the data value of a geo-property at a point can be estimated by giving weights to the sampling points and taking a general formula as:

$$Z(X) = \sum_{i=1}^n w_i Z(X_i) \quad (6)$$

According to the Eqs. (5) and (6), we have:

$$\sum_{i=1}^n w_i Z(X_i) = M(X) + \gamma(h) \quad (7)$$

Using a linear regression function for the modelling function, i.e.:

$$M(X) = \beta_0 + \sum_{i=1}^n \beta_i X_i \quad (8)$$

We can work out the w_i , the weighting value for each sampling points, by solving the produced equation system.

Kriging is a geostatistical interpolation technique that considers both the distance and the degree of variation between known data points when estimating values in unknown areas. A kriged estimate is a weighted linear combination of the known sample values around the point to be estimated (Child, 2004).

Kriging procedure that generates an estimated surface from a scattered set of points with z-values. Kriging assumes that the distance or direction between sample points reflects a spatial correlation that can be used to explain variation in the surface

(Fig. 2.13). The Kriging tool fits a mathematical function to a specified number of points, or all points within a specified radius, to determine the output value for each location. Kriging is a multistep process; it includes exploratory statistical analysis of the data, variogram modeling, creating the surface, and (optionally) exploring a variance surface. Kriging is most appropriate when you know there is a spatially correlated distance or directional bias in the data. It is often used in soil science and geology (GIS Resources, 2015).

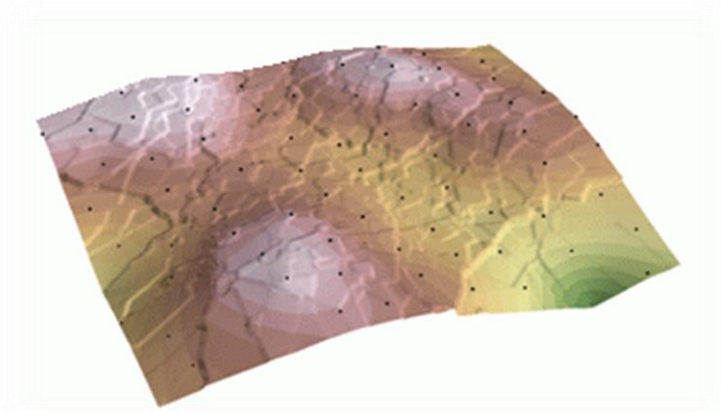


Figure 2.13 3-D map showing the use of Kriging for interpolation application
(Courtesy: ESRI)

The predicted values are derived from the measure of relationship in samples using sophisticated weighted average technique. It uses a search radius that can be fixed or variable. The generated cell values can exceed value range of samples, and the surface does not pass through samples.

2.5.1.1 PointInterp

PointInterp function allows more control over the sampling neighborhood (Fig. 2.14). The influence of a particular sample on the interpolated grid cell value depends on whether the sample point is in the cell's neighborhood and how far from the cell being interpolated it is located. Points outside the neighborhood have no influence (GIS Resources, 2015).

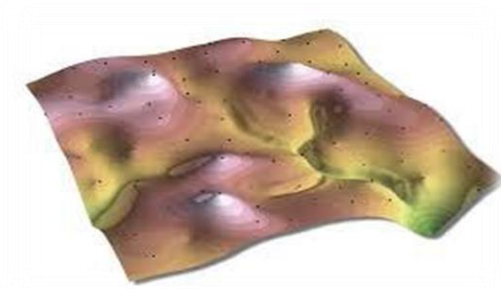


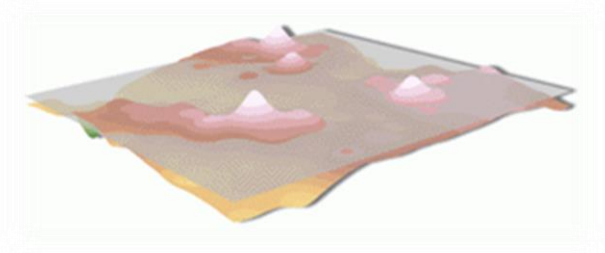
Figure 2.14 Example graph showing application of PointInterp (Courtesy: ESRI)

The weighted value of points inside the neighborhood is calculated using an inverse distance weighted interpolation or inverse exponential distance interpolation. This method interpolates a raster using point features but allows for different types of neighborhoods. Neighborhoods can have shapes such as circles, rectangles, irregular polygons, annuluses, or wedges (Child, 2004).

2.5.1.2 Trend

Trend is a statistical method that finds the surface that fits the sample points using a least-square regression fit. It fits one polynomial equation to the entire surface. This results in a surface that minimizes surface variance in relation to the input values. The surface is constructed so that for every input point, the total of the differences between the actual values and the estimated values (i.e., the variance) will be as small as possible (Child, 2004).

Figure 2.15 Example graph showing the application of Trend (Courtesy: ESRI)



It is an inexact interpolator, and the resulting surface rarely passes through the input points. However, this method detects trends in the sample data and is similar to natural phenomena that typically vary smoothly (Fig. 2.15).

2.5.1.3 Topo to Raster

By interpolating elevation values for a raster, the Topo to Raster method imposes constraints that ensure a hydrologically correct digital elevation model that contains a connected drainage structure and correctly represents ridges and streams from input contour data. It uses an iterative finite difference interpolation technique that optimizes the computational efficiency of local interpolation without losing the surface continuity of global interpolation. It was specifically designed to work intelligently with contour inputs (GIS Resources, 2015).

Below is an example of a surface interpolated from elevation points, contour lines, stream lines, and lake polygons using Topo to Raster interpolation (Figure 2.16).

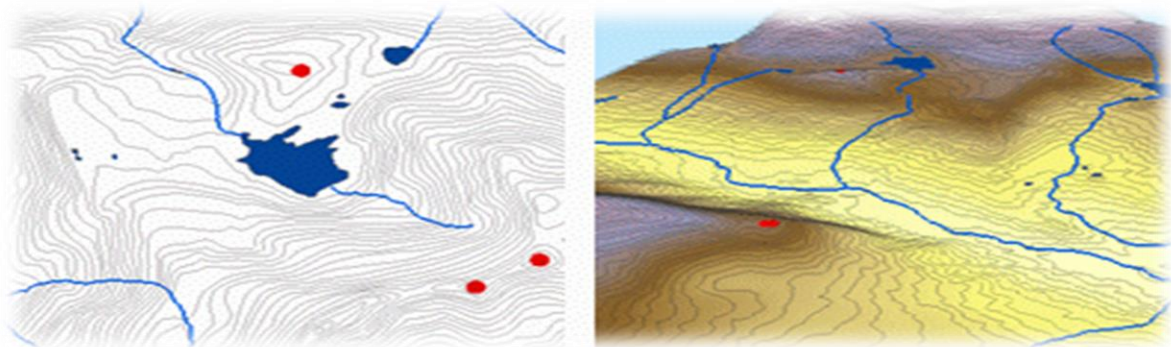


Figure 2.16 Example graph showing the application of Topo to Raster (Courtesy: ESRI)

Topo to Raster is a specialized tool for creating hydrologically correct raster surfaces from vector data of terrain components such as elevation points, contour lines, stream lines, lake polygons, sink points, and study area boundary polygons (GIS Resources, 2015).

2.5.1.4 Radial Basis Functions (RBF)

RBF is a family of five deterministic exact interpolation techniques: thin-plate spline, spline with tension, completely regularized spline, multi-quadratic function and inverse multi-quadratic function. An exact interpolator is that one which predicts values identical with those measured at the same point. RBF methods predict values that can vary above the maximum or below the minimum of the measured values. For all RBF methods, there is a parameter that controls the smoothness of the resulting surface. The

estimated values of the methods are based on a mathematical function that minimizes overall surface curvature, generating quite smooth surfaces (ArcGIS 9.2 Desktop help, 2007).

In this section we concluded the fact that the most appropriate method will depend on the distribution of sample point and the phenomenon benign studied (Arc-User, 2004).

2.5.2 Inverse Distance Weighting (IDW)

Inverse distance weighting is a simple interpolation method popular in practice. It assumes that the value of a geo-property at a spatial position relates to the data at other the points in a surrounding neighbourhood, and their relation can be approximated in terms of their distance. The interpolation takes the weights on a given set of sampling data according, which are inversely proportional to a power of the distance between the interpolation position and the sampling positions. The user has the control over the order of the power function and the size of the neighborhood (expressed as a radius or a number of points). The basic principle takes the Eq. (6) above, with the weighting function is defined as:

$$w_i = \frac{\frac{1}{(X-X_i)^p}}{\sum_{j=1}^n \frac{1}{(X-X_j)^p}} \quad (9)$$

where $X - X_i/j$ indicates the distance between interpolation position and the sampling points, n is the total number of the sampling points in the selected neighborhood, p is the order of the power, for which $p = 2$ is the most popular order selected.

The Inverse Distance Weighting interpolator assumes that each input point has a local influence that diminishes with distance (Figure 2.17). It weights the points closer to the processing cell greater than those further away. A specified number of points or all points within a specified radius can be used to determine the output value of each location. Use of this method assumes the variable being mapped decreases in influence with distance from its sampled location (GIS Resources, 2015).

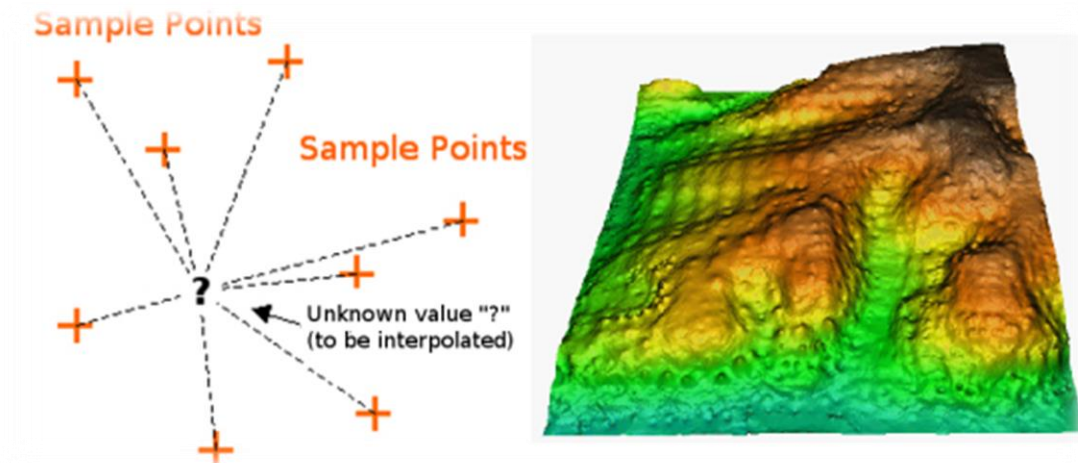


Figure 2.17 Example graph showing the application IDW Interpolation (Courtesy: QGIS)

The Inverse Distance Weighting (IDW) algorithm effectively is a moving average interpolator that is usually applied to highly variable data (Figure 2.18). For certain data types it is possible to return to the collection site and record a new value that is statistically different from the original reading but within the general trend for the area. The interpolated surface, estimated using a moving average technique, is less than the local maximum value and greater than the local minimum value (GIS Resources, 2015).

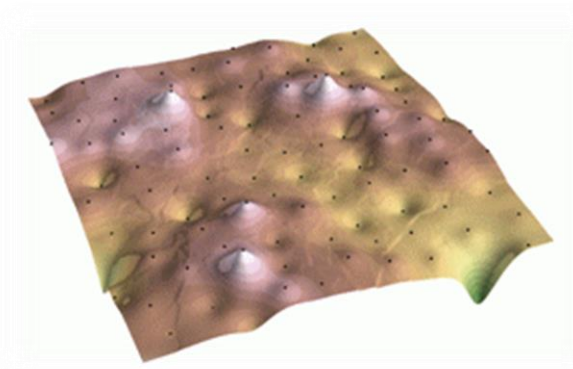


Figure 2.18 Example graph showing the application of IDW Interpolated Surface (Courtesy: ESRI)

IDW interpolation explicitly relies on the First Law of Geography. To predict a value for any unmeasured location, IDW will use the measured values surrounding the prediction IDW interpolation explicitly implements the assumption that things that are close to one another are more alike than those that are farther apart. To predict a value

for any unmeasured location, IDW will use the measured values surrounding the prediction location. Those measured values closest to the prediction location will have more influence on the predicted value than those farther away (GIS Resources, 2015). Thus, IDW assumes that each measured point has a local influence that diminishes with distance. The IDW function should be used when the set of points is dense enough to capture the extent of local surface variation needed for analysis. IDW determines cell values using a linear-weighted combination set of sample points. It weights the points closer to the prediction location greater than those farther away, hence the name inverse distance weighted (GIS Resources, 2015).

The IDW technique calculates a value for each grid node by examining surrounding data points that lie within a user-defined search radius. Some or all of the data points can be used in the interpolation process. The node value is calculated by averaging the weighted sum of all the points. Data points that lie progressively farther from the node influence the computed value far less than those lying closer to the node (GIS Resources, 2015).

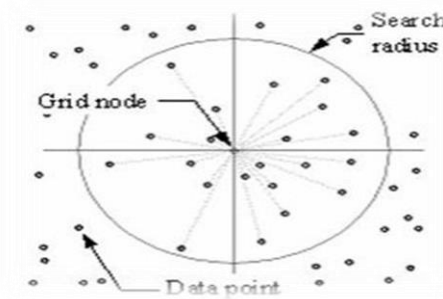


Figure 2.19 An example showing A radius is generated around each grid node from which data points are selected to be used in the calculation (Figure 2.19). Options to control the use of IDW include power, search radius, fixed search radius, variable search radius and barrier.

2.5.2.1 Natural Neighbour Inverse Distance Weighted (NNIDW)

Natural neighbor interpolation has many positive features, can be used for both interpolation and extrapolation, and generally works well with clustered scatter points (Figure 2.20). The basic equation used in natural neighbor interpolation is identical to the one used in IDW interpolation. This method can efficiently handle large input point datasets. When using the Natural Neighbor method, local coordinates define the amount

of influence any scatter point will have on output cells. The Natural Neighbors method is a geometric estimation technique that uses natural neighborhood regions generated around each point in the data set (GIS Resources, 2015). Like IDW, this interpolation method is a weighted-average interpolation method. However, instead of finding an interpolated point's value using all of the input points weighted by their distance, Natural Neighbors interpolation creates a Delaunay Triangulation of the input points and selects the closest nodes that form a convex hull around the interpolation point, then weights their values by proportionate area. This method is most appropriate where sample data points are distributed with uneven density. It is a good general-purpose interpolation technique and has the advantage that you do not have to specify parameters such as radius, number of neighbors or weights (GIS Resources, 2015).

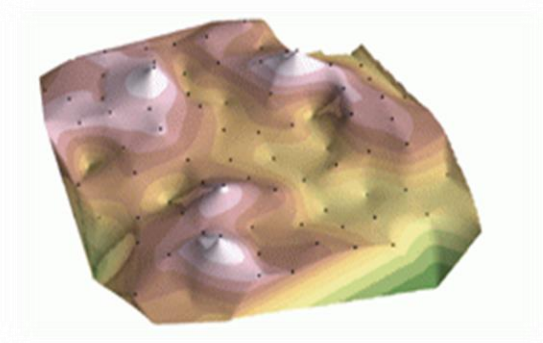


Figure 2.20 Example graph showing the application of Natural IDW (Courtesy: ESRI)

This technique is designed to honour local minimum and maximum values in the point file and can be set to limit overshoots of local high values and undershoots of local low values. The method thereby allows the creation of accurate surface models from data sets that are very sparsely distributed or very linear in spatial distribution.

2.5.2.2 Spline

Spline (Figure 2.21) estimates values using a mathematical function that minimizes overall surface curvature, resulting in a smooth surface that passes exactly through the input points (Child, 2004).

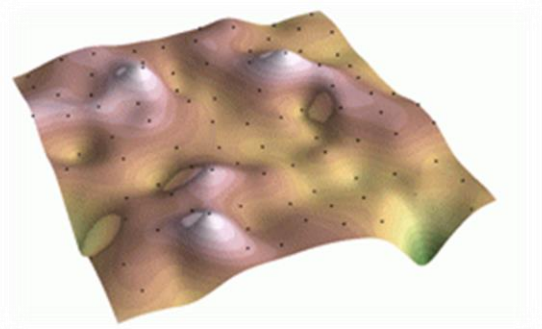
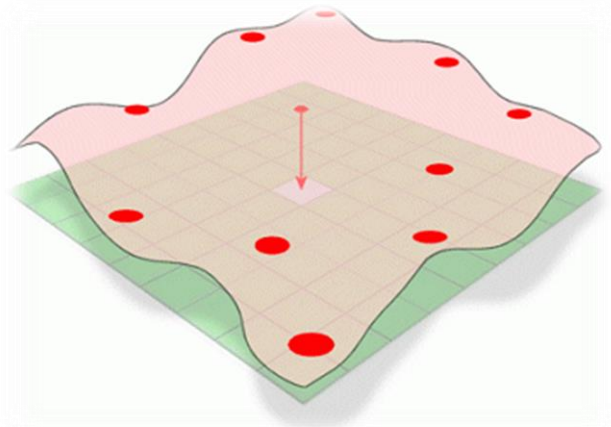


Figure 2.21 Example graph showing the application of Spline (Courtesy: ESRI)

Conceptually, it is analogous to bending a sheet of rubber to pass through known points while minimizing the total curvature of the surface. It fits a mathematical function to a specified number of nearest input points while passing through the sample points. This method is best for gently varying surfaces, such as elevation, water table heights, or pollution concentrations (Child, 2004).

Figure 2.22 A map showing the application of Spline Method



The Spline method of interpolation estimates unknown values by bending a surface through known values (Fig. 2.22).

2.5.3 Comparison of the Interpolation Methods on Digital Terrain

The ecological, economical, and agricultural benefits of accurate interpolation of spatial distribution patterns of soil organic carbon (SOC) are well recognized on a study done by (Bhunia et al., 2016). They analyzed and compared different interpolation techniques in a geographical information system (GIS) environment for estimating the spatial variation of SOC at three different soil depths (0–20cm, 20–40

cm and 40–100 cm) in Medinipur Block, West Bengal, India. Stratified random samples of total 98 soils were collected from different land use sites including agriculture, scrubland, forest, grassland, and fallow land of the study area.

A portable global positioning system (GPS) was used to collect coordinates of each sample site. Five interpolation methods such as inverse distance weighting (IDW), local polynomial interpolation (LPI), radial basis function (RBF), ordinary kriging (OK) and Empirical Bayes kriging (EBK) are used to generate spatial distribution of SOC. SOC is concentrated in forest land and less SOC is observed in bare land. The cross validation is applied to evaluate the accuracy of interpolation methods through coefficient of determination (R^2) and root mean square error (RMSE). The results indicate that OK is superior method with the least RMSE and highest R^2 value for interpolation of SOC spatial distribution (Bhunia et al., 2016).

Sarkari et al. (2010) carried out an interpretation and analysis of spatial variability of soil properties using ordinary kriging and inverse distance weighting (IDW) methods to generate continuous sample for site-specific management. A total of 535 soil samples (0-25 cm) were collected at an interval of 2 km grid in Dhalai district of Tripura, India. The data were interpolated by ordinary kriging and IDW with power 2. All the selected soil chemical parameters were strongly spatially dependent, but the range of spatial dependence was found to vary within soil parameters. Available potassium had the shortest range of spatial dependence (6.9 km) whereas pH had the longest range (23.7 km). The study shows that prediction of spatial variability for different soil parameters (except available nitrogen) may be better understood by ordinary kriging than by IDW method.

Karydas et al. (2009) evaluated prediction maps created with interpolation for five common topsoil properties, namely organic matter, total CaCO_3 , electric conductivity, Fe content, and clay content in a Mediterranean agricultural system. The work conducted on a 25 ha block of fields cultivated with grape vines and olive trees in the island of Crete was targeted as a study site. 106 topsoil samples were collected on a 50×50 m² grid and then analyzed in the laboratory. Three well-known spatial interpolation techniques, namely Ordinary Kriging (OK), Inverse Distance Weighting (IDW), and Radial Basis Functions (RBF) were applied for generating the prediction

maps, which then were assessed for their accuracy and effectiveness with a new, independent set of samples. This time the samples were collected randomly.

The results obtained by Karydas et al. (2009) indicated that there was not a method clearly more accurate than the other methods for any of the tested properties. The Goodness of prediction (G) had positive values for Fe content and total CaCO₃ for all interpolation techniques and positive values for Organic Matter only for IDW. Among G values, only the value for total CaCO₃ was big enough for all techniques, indicating that only this specific property counted for mapping. It is believed that the topography, crop alteration and farming practices significantly affected the results in the specific landscape. Karydas et al. (2009) recommended that future research to be focus on taking account of between-field variations that are due to different crops or farming practices, incorporating segmentation techniques on cadastral data and satellite imagery.

Gotway et al. (1994) found that the IDW method generated more accurate results than Kriging for mapping soil organic matter and soil NO₃ levels. Wollenhaupt et al. (1994) compared these two interpolation techniques and concluded that IDW was more accurate for mapping P and K levels of soil.

Mueller et al. (2004) observed that for the optimal parameters of the method, the accuracy of IDW interpolation generally equaled or exceeded the accuracy of Kriging at all scales of measurement. On the other hand, other researchers observed that Kriging was more accurate for the interpolation of several soil attributes.

Leenaers et al. (1990) assessed the Kriging interpolation method as more accurate compared to IDW, for mapping soil Zn content. Kravchenko (2003) evaluated the effect of data variability and the strength of spatial correlation in the data on the performance of the grid soil sampling of different sampling density and two interpolation procedures, ordinary point Kriging and optimal Inverse Distance Weighting (IDW). Kriging with known variogram parameters performed significantly better than the IDW for most of the studied cases. Many other studies also compared Kriging, IDW, and RBF in soil science.

Indicatively, Schloeder et al. (2001) observed that Ordinary Kriging (OK) and

IDW were similarly accurate and effective methods, while thin-plate smoothing spline with tensions was not. Weller et al. (2002) concluded that even in cases where the assumptions for Kriging were not fulfilled the Kriging approach was as good as any other radial base function interpolation. Summarizing the above, the accuracy of each method depends on the assumptions and subjective judgments that are made, such as the application of smoothness of the results or not and linearity of interpolation functions or not. Apart from research studies to judge the quality of a technique's performance, validation or accuracy assessment of a method is rarely done in operational applications because of its high cost (Karydas et al., 2009).

Zandi et al. (2011) evaluated spatial interpolation techniques for Soil pH. Soil pH has a major effect on plant nutrient availability by controlling the chemical structure of the nutrient.

Adjusting soil acidity or alkalinity improves soil nutrition without adding extra fertilizers. Soil nutrients needed by plants in the largest amount are referred to as macronutrients. In addition to macronutrients, plants also need trace nutrients and both macro and trace nutrient availability is controlled by soil pH. Understanding of spatial variability of soil properties is important in site-specific management. Analysis of spatial variation of soil properties is fundamental to sustainable agricultural and rural development (Zandi et al., 2011).

The special variability of soil property is often measured using various interpolation methods resulting in map generation. Selecting a proper spatial interpolation method is crucial in surface analysis, since different methods of interpolation can lead to different surface results. Among statistical methods, geo statistical kriging-based techniques have been frequently used for spatial analysis and surface mapping. In Zandi et al. (2011)'s work, three common interpolation methods are used to study the spatial distributions of soil pH in a vineyard. Interpolation techniques were used to estimate the pH measurement in unsampled points and create a continuous dataset that could be represented over a map of the entire study area. The method investigated includes; Inverse Distance Weighting (IDW), Radial base Function (RBF) and Ordinary.

Kriging (OK). The performance of conventional statistics showed that soil pH had a low variation in this study. The performances of interpolation methods were evaluated and compared using the cross-validation. The results showed that RBF method performed better than IDW and OK for prediction of the spatial distribution of topsoil (Zandi et al., 2011)

Many researchers have compared IDW and kriging. In some cases, the performance of kriging was generally better than IDW (Hosseini et al., 1994; Dalthorp et al., 1999; Kravchenko et al., 1999; Kravchenko, 2003; Reinstorf et al., 2005). Warrick (1998) also reported kriging to be better than IDW for mapping potato yield and soil properties. In other studies, IDW generally out-performed kriging (Nalder et al., 1998). Gotway et al. (1996) observed the best results in mapping soil organic matter contents and soil N03' levels when IDW was used as the interpolation technique. The results, however, have often been mixed (Schloeder et al., 2001; Mueller et al., 2001; Lapen et al., 2003). Kriging performance can be significantly affected by variability and spatial structure of the data (Leenaers et al., 1990) and by the choice of variogram model, search radius and number of the closest neighboring points used for estimation. As might be expected, the performance of kriging improved relative to IDW when spatial structure was known. The objectives of this study were (i) to determine the spatial variability of selected soil nutrients, such as pH, organic carbon content, available nitrogen and available potassium with geostatistical analysis and (ii) to describe and predict the relative performance of ordinary kriging and IDW (Reza et al., 2010).

2.5.4 The use of interpolation methods in environmental projects.

The spatial interpolation methods have been useful to many disciplines such as environmental sciences (Burrough & McDonnell, 1998; Goovaerts, 1997; Webster & Oliver, 2001) and mining engineering (Journel & Huijbregts, 1978). On the basis of a bibliographic research (Zhou et al., 2007), it was found that the top 10 fields that employ geostatistics are: 1) water resources, 2) geosciences, 3) agriculture or soil sciences, 4) mathematics, 5) environmental sciences, 6) statistics and probability, 7) civil engineering, 8) petroleum engineering and 9) limnology 10) ecology (Australian government). Our concentration in this review is on environmental sciences, including: water resources, meteorology, ecology, agriculture, and marine environmental science

with more attention on soil science. Examples of the application of different spatial interpolation methods in each of these disciplines are provided in brief in this chapter with more focus in soil as it our main concern in this research. The focus is further narrowed down on relative studies that compared the performance of the spatial interpolation methods and technics to end up with clear conclusions and recommendation which will support our research methodology and target the objectives set for the development of our novel 3D mapping technology for hydrocarbon contaminated soils.

2.5.5 Applications of Spatial Interpolation to Soil Mapping

Analysis and interpretation of spatial variability of soils properties is a keystone in site-specific management. A study demonstration by Shiraz University in evaluation and comparison of ordinary kriging and Inverse distance weighting methods for prediction of spatial variability of some soil Chemical parameters, the objective of this study was to determine degree of spatial variability of soil chemical properties with Ordinary Kriging (OK) and Inverse Distance Weighting (IDW) methods. Spatial distributions for 6 soil chemical properties were examined in a fallow land in Bajgah, Fars province, Iran. Soil samples were collected at approximately 60×60 m grids at 0-30 cm depth and coordinates of each of the 100 points were recorded with GPS (Yasrebi et al., 2009).

Kriging and inverse-distance weighting are two commonly used techniques for characterizing this spatial variability and interpolating between sampled points. Data were interpolated with OK and IDW with powers of 1-5. All studied soil chemical parameters were strongly spatially dependent, but the range of spatial dependence was found to vary within the soil parameters. Phosphorous had the shortest range of spatial dependence (49.50 m) and pH had the longest (109.50 m).

The accuracy of OK predictions was generally unaffected by the coefficient of variation. We concluded, for all soil chemical properties, OK performed much better than the five IDW procedures in this study (Yasrebi et al., 2009).

On the study of “Improving the Prediction Accuracy of Soil Mapping through Geostatistics” Omran et al. (2012), applied a technique based on fundamental theorems

of surfaces, to interpolate the spatial pattern of soil properties. The intent of this study was to provide quantitative information on soil properties and mapping methods that are in common use by the commercial sector.

Omran et al. (2012) case study showed that the OK method is more accurate for predicting the spatial patterns of soil (EC, pH, CaCO₃) properties than the other methods, namely OK, IDW and Splines. It is also the most accurate method when we avoid the outlier effects in assessing the performance of all methods.

The generally superior performance of OK is due to less prediction errors. OK obtains the soil property surfaces without oscillation problems and Bull's eyes. Therefore, UK can be considered as an accurate method for interpolating soil (EC, pH, CaCO₃) properties (Omran et al., 2012).

These results may help GIS specialists to select the best method for the generation of soil properties. A technique should be chosen not only for its performance on a specific soil type and data density, but also for its applicability to a wide range of spatial scales.

Veronesi et al. (2012) concluded that high resolution 3-D mapping technology can be used to estimate soil properties achieving a reasonable accuracy even with relatively poor data support, thus minimizing the cost of the survey, and which can practically be applied over large areas.

In the first stage the primary objective was the development of a new method for accurately mapping soil properties in 3-D; a method that was easier to use than 3-D geostatistics and sufficiently flexible to be used with less dense datasets. The method was extensively tested, validated and compared to the established method of 3-D ordinary kriging.

This study developed novel methods with high level Quality Assurance and Quality control QA/QC in mapping soil compaction, performing much better than 3-D ordinary kriging. This method is much easier to use compared to 3-D geostatistics, because it relies on bi-dimensional interpolation; it is also flexible as it can be used with much less analytical data losing only a fraction of its accuracy (Veronesi et al., 2012).

A study conducted by (Ghobakhlou et al., 2011) Auckland University of Technology, Auckland, New Zealand, 2011, evaluated the performance of three commonly used interpolation methods for soil pH. OK, RBF and IDW techniques were used to characterize the spatial variability and interpolating between sampled points.

These spatial interpolation methods had various decision parameters. Both IDW and RBF interpolation method needed to adjust the power parameter and the search radius to improve accuracy. The processes of analyzing the global trends, generating semivariograms and choice of search neighborhoods required much time and effort. Overall, the results obtained from the comparison of the three applied interpolation methods indicated that RBF was the most suitable methods for prediction and mapping the spatial distribution of soil pH in this study and produced good results for such gently varying surface. The results also showed that OK and IDW had almost the same precisions. Results also revealed that although the IDW is relatively simple and easy to use, but in this case study it was less accurate than OK. S. (Ghobakhlou et al., 2011) concluded in this study that is reasonable to conduct further experiments on soil pH obtained from two other depths in order to validate the results from this study. It is desirable to compare these results with soil pH measured in laboratory.

2.5.6 Spatial interpolation evaluation and comparison techniques

Geostatistics techniques have been increasingly applied in the assessment of spatial variability of parameters of interest for agrarian sciences, thus allowing for mapping, quantification and modeling of continuous phenomena through interpolation of sampled points in space (Goovaerts, 1999). However, challenges still exist in determining the best method of interpolation for that purpose (de Moura Guerreiro et al., 2017; Piccini et al., 2014; Reza et al., 2010).

The concern about their accuracy and precision is because they were developed either for specific disciplines or even for specific variables based on the data properties modeled and each method has its own specific assumptions and features (global versus local, exact versus inexact, deterministic versus stochastic, and gradual versus abrupt) (Li and Heap, 2008). Rather than assume one interpolation method is better than another, we should try different interpolation methods and compare the results to determine the

best interpolation method for a given project (Gisresources, 2014). Therefore, several error measurement methods have been used to assess the accuracy and precision of the interpolation methods (Li & Heap, 2008; 2011).

Many interpolation methods may be tested to select the appropriate interpolation approach for an area (Attaeian et al., 2016). Commonly used assessment measures are summarized in relation to: (1) the performance of variogram models, (2) the performance of the spatial interpolation methods, and (3) the performance of a spatial interpolation method for datasets with different sample sizes.

Chin, et al. (2004) compared 12 different interpolation methods by using 5 meters DTM (digital terrain model), For each method, applicability, algorithm, efficiency and advantage been analysed. In this study they concluded that there is no absolutely best method but only the optimal choice under certain circumstances. Furthermore, we should first review the characteristic and theorem of each method as well as the property and spatial analysis of data before we can successfully select a spatial interpolation method which is relatively best in certain situation (Chin, et al., 2004).

Ghobakhlou et al. (2011) evaluated and made a comparison on the performance of three commonly used interpolation methods for soil pH. OK, RBF and IDW. A cross-validation used to find the best model. The performance of each interpolation technique, in terms of the accuracy of predictions, was assessed by comparing the deviation of estimates from the measured data by performing a cross-validation technique over the entire dataset. In a cross-validation procedure, each data point is removed from the data set, one at a time, and predicted value is return by performing interpolation algorithm on the rest of dataset. This yield a list of estimated values of variable data paired to the test data. The comparison of performance between interpolation techniques was achieved by using the Mean Error (ME) and Root Mean Square Error (RMSE).

A study conducted by Hassan et al. (2018) to compare spatial prediction methods namely (RBF), (IDW), (OK), (UK), and (SK) for the production of the groundwater level map. Cross-validation was used to compare and evaluate the accuracy of each model, as it was an effective tool in comparison and assessment that

allowed access to the most accurate model to represent the groundwater level with the least time and effort. The study reveals that comparing the spatial interpolation models and evaluating their accuracy, through some statistical indicators and cross-validation is the best way to choose the optimal model for the representation of data entered in any site.

The performance of the interpolation technique Radial Basis Functions (RBF) in term of the accuracy of prediction was assessed by Sarmadian et al (2014) to investigate the spatial pattern of SOC in the Kouhin watershed in Qazvin province, Iran. The performance of the interpolation technique, in term of the accuracy of prediction, was assessed by comparing the deviation of estimates from the measured data by performing a cross-validation technique over the validation dataset (20% data) by using the Root Mean Square Error (RMSE).

A portable global positioning system (GPS) was used to collect coordinates of each sample site. Five interpolation methods such as inverse distance weighting (IDW), local polynomial interpolation (LPI), radial basis function (RBF), ordinary kriging (OK) and Empirical Bayes kriging (EBK) are used to generate spatial distribution of SOC. SOC is concentrated in forest land and less SOC is observed in bare land. The cross validation is applied to evaluate the accuracy of interpolation methods through coefficient of determination (R^2) and root mean square error (RMSE). The results indicate that OK is superior method with the least RMSE and highest R^2 value for interpolation of SOC spatial distribution (Bhunia et al., 2016).

After an exhaustive testing done by Robinson et al. (2005) for the performance of spatial interpolation techniques for mapping soil properties on ordinary kriging, lognormal ordinary kriging, inverse distance weighting (IDW) and splines for interpolating seasonally stable soil properties (pH, electric conductivity and organic matter) they concluded that many parameters would be better identified from the RMSE statistic obtained from cross-validation.

A comprehensive research study done by Taha Gorji et al. (2017) to compare the performance of Local Polynomial Interpolation (LPI) and Radial Basis Functions (RBF) as two different interpolation approaches for mapping spatial variation of soil

characteristics including soil organic matter, phosphorus, lime and boron in the Tuz Lake Basin of Turkey by using soil samples collected in the field. a surface area of 1500 km² a total number of 312 soil samples had been collected and analysed in which 50 samples that were homogeneously distributed selected as validation samples for checking the accuracy and performance of each interpolation method; whereas, the remaining 262 samples were reserved for generating the prediction maps by utilizing the two interpolation methods for organic matter, phosphorus, lime and boron. the study concluded that RBF indicates slightly better performance for estimating lime and boron compared to LPI; whereas, considerably better performance is obtained for organic matter. However, LPI illustrates remarkably better performance than RBF approach to create prediction map of phosphorus. In this study, Root Mean Square Error (RMSE) and R-squared (R²) are used as the two common statistical measures for interpreting the performance of results. R² indicates the degree of closeness of the predicted data to the measured validation points. The closer to the R² value to 1, the higher the prediction accuracy. RMSE is utilized for measuring the error of estimation. The lowest RMSE value indicates the most accurate estimation.

A study done by Jose et al. (2017) to analyze the spatial variability of hydrogen potential (pH) and electric conductivity (EC) within an agricultural region in Cuamba district of Mozambique. Soil samples were collected at random locations scattered through the study region, and were later analyzed in water and soil laboratory. These point data were then used to produce interpolated surfaces of soil chemical properties. Efficiency of spatial interpolation methods was assessed based on prediction errors' statistics derived from cross-validation. The Efficiency of a deterministic and a stochastic interpolator were compared, namely Inverse Distance Weighting (IDW) and Ordinary kriging. The results show that ordinary kriging was more accurate than IDW at samples' locations.

Hailu et al. (2017) used Cross-validation method to analyzed the performance of frequently used spatial interpolation techniques (OK, RBF and IDW) for predicting topsoil pH, soil organic carbon (SOC), available phosphorus (AP) and texture, and to determine the optimum spatial interpolation method for mapping of selected soil properties in agricultural watershed. The study area was divided into a 100m by 100m

18 grids and approximately at the center of each grid, topsoil (10-15cm) samples were collected over 75 locations across the entire study area. This study considered 5 to 25 neighboring points for each interpolation method. Meanwhile, the five kernel functions and a power of 1, 2, and 3 were tested for RBF and IDW, respectively. The best kernel function for RBF was found to be completely regularized spline, while the best weighting parameter for IDW was found to be a power of two. The Nash-Sutcliffe efficiency (E) for each soil property except silt showed a positive value of ($E \geq 0.17$). The surface maps for the selected soil properties indicated that values of R² range from 0.00 to 0.51. The highest value of R², E and d (0.51, 0.51, and 0.83, respectively) resulted from the spatial interpolation of AP using RBF. Therefore, Cross-validation was used in this case study to get the best agreement between the observed data and the predicted values of selected spatial interpolation methods. The performance of each interpolation method was assessed quantitatively in terms of mean error (ME), mean squared error (MSE), root mean squared error (RMSE), Nash-Sutcliffe efficiency (E), coefficient of determination (R²) and index of agreement (d). The methodology used in this study was adequate for spatial interpolation and evaluation of measured soil properties and can serve as a general method for surface map generation in future studies of similar regions.

2.5.7 Assessment measures for assessing the performance of spatial interpolation methods.

The assessment measures for assessing the performance of spatial interpolation method are very important tools to validate and compare interpolation methods, as each interpolation method and technics need to be tested to know the accuracy level, as it been stated above each method have different effect depending on the model of evaluation that been studied or examine, especially in our case we are reviewing the available methods which can be the best for developing 3D mapping technology for hydrocarbon contaminated soils.

2.5.7.1 Cross-validation for assessing the Performance of Spatial Interpolation Methods.

Cross Validation is one of the most important concepts in any type of data modeling. It simply says, try to leave a sample on which you do not train the model and

test the model on this sample before finalizing the model (Tavish, 2016). It removes one data location then predicts the associated data using the data at the rest of the locations. The main use for this tool is to associate the predicted value to the observed value, in order to obtain useful information about some of model parameters (ArcGIS, 2016).

2.5.7.2 Coefficient of Variation (CV)

The coefficient of variation (CV) is the most discerning aspect as it is a useful statistic for comparing the degree of variation from one data series to another, even if the means are drastically different from each other (Wei et al., 2008). According to the soil variability guidelines provided by Wilding (1985), the property shows low variability when CV is less than or equals to 0.15, moderate variability when the CV is between 0.15 to 0.35, and the most variability when the CV is greater than 0.35.

The coefficient of variation is the ratio of the standard deviation to the mean. Express CV as a percentage. Variability of soil properties can be described by the minimum and maximum values, standard deviation (SD) Eq. (11), and coefficient of variation (CV) Eq. (10).

The following formula is used to calculate the CV:

$$CV \% = \frac{\text{Standard Deviation}}{\text{Mean}} \times 100 \quad (10)$$

2.5.7.3 Standard Deviation (SD)

This formula is used to calculate the standard deviation:

$$SD = \sqrt{\frac{\sum (x_n - \bar{x})^2}{n - 1}}$$

where:

- \bar{x} = mean (average) of the QC values
- $\sum (x_n - \bar{x})^2$ = the sum of the squares of differences between individual QC values and the mean
- n = the number of values in the data set

(11)

2.5.8 Factors affecting the performance of the spatial interpolation methods

With the wide and increasing applications of the spatial interpolation methods, there is also a growing concern about their accuracy and precision (Hartkamp et al., 1999). As any other statistical modeling techniques, the spatial interpolation methods also produce a certain degree of errors associated with the estimation

Several factors that affect the performance of the spatial interpolation methods including sampling design, sample spatial distribution, data quality, correlation between the primary and secondary variables, and interaction among various factors. The impacts of sample density, variation in the data, sampling design and stratification on the estimations of the spatial interpolation methods are quantified by (Jin & Andrew, 2008) using data from 77 cases in 17 reviewed comparative studies. The results show that variation within the data is a dominant factor and has tremendous impacts on the performance of the spatial interpolators. As the variation increases, the accuracy of all methods decreases. Irregular-spaced sampling design and stratification would improve the accuracy of estimation. There is no evidence of the effects of sampling density on the performance of the spatial interpolation methods in this comprehensive comparative study (Australian government, 2008). In this section, we will review the most important factors affecting the performance of the spatial interpolation methods.

2.6 Petroleum Hydrocarbon contamination in Kuwait

The environmental catastrophe in Kuwait was considered as the worst environmental disaster in the world. Oil producing wells were set burning and damage allowed crude oil to flow freely onto the desert soil surface, forming networks of oil rivers and oil lakes that accumulated around oil wells. The Kuwait desert environment was polluted by the formation of oil lakes, and oil-contaminated surfaces from the damage of the oil infrastructure, by the retreating Iraqi troops. Soot from the burning oil was deposited over large distances across the surrounding land surface. Near the burning wells, oil mist and soot combined to form tar mats (KISER, 2004).

It has been 29 years since this disaster occurred and the remediation projects will now start. The affects and the magnitude of the damages particularly to the contaminated soil, and groundwater is currently unknown. They require advanced

technology to quality, time, and cost, to effectively estimate the hydrocarbon contaminated sites before the remediation efforts is initiated.

2.6.1 Kuwait Environmental Background

Kuwait is characteristic of extremely dry climate with mean daily maximum humidity ranging from 31 to 36% during the hot season. The average daily maximum temperature is 45C for July and 18C for January. The evaporation rates are very high and temporally variable with a daily mean of 16.6 mm in July and 5.2 mm in January (KISER, 2004). Desertification is a serious problem in Kuwait. It results primarily from the combined effects of climatological (scarcity and irregularity of rainfall, prevalence of long drought periods, prevalence of strong northwesterly winds, occurrence of strong intensive rain and extended summer) and geological processes (increasing amounts of aeolian deposits and widespread desert landforms), with intensive human activities accelerating these processes. (KISER, 2004).

Kuwait's desert soils can be categorized as arid soils with sandy soil texture and poorly developed soil profiles. The calcareous hardpan (gatch) occurs at varying depths and locations (KISER, 2004). These hardpan layers consisted predominantly of calcium carbonate and quartz. The desert soils contain limited amounts of organic matter and nitrogen. Although the total concentration of phosphorous in soils is relatively high, its bioavailability is low due to formation of practically insoluble calcium phosphate (KISER, 2004).

2.6.2 Kuwaiti Oil Fires and the Resulting Environmental Contamination during the First Gulf War

During the first Gulf War from late 1990 to early 1991, Iraq embarked on a systematic destruction of Kuwait's oil industry by setting fire to 720 individual Kuwaiti oil wells (Whitaker, 2000). This resulted in emission of toxic gases and particulate matters into atmosphere (Browning et al., 1991) that caused acid rain and smog. Figure 1a shows a burning oil well with black smoke. The oil fires also caused widespread oil spills with the spewed crude oil flowing into Persian Gulf or the low-lying desert areas to form so-called oil lakes (Figure 221b). The amount of oil lost due to both the fires

and oil flows was calculated to be approximately 1.0-1.5 billion barrels (Petroleum Economist, 1992). An estimated two million barrels of oil escaped from the damaged wells daily (PAAC, 1999). Oil mist and soot covered an additional 1772 km² of the land surface of Kuwait (Al-Ajmi et al., 1994; El-Baz et al., 1994; Kwarteng, 1998).

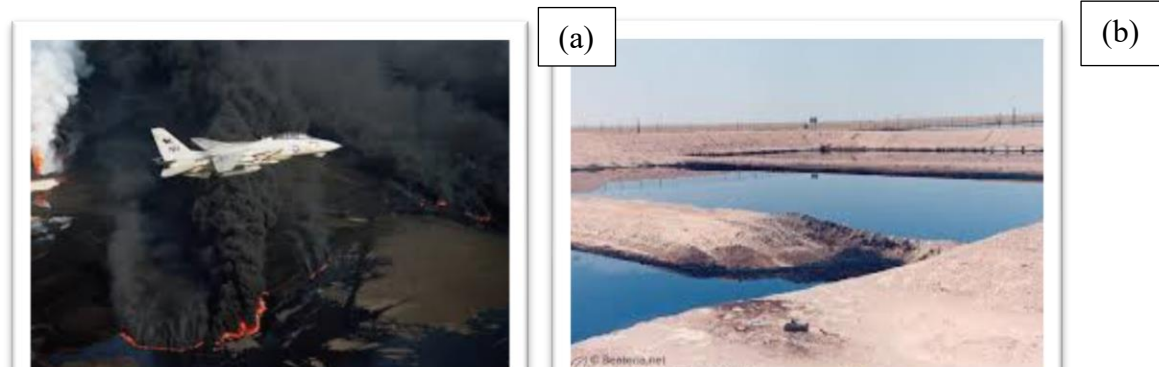


Figure 2.23 Photographs showing (a) a burning oil well, and (b) an oil lake

The oil released into the Gulf produced devastating consequences on the marine wildlife of the area, including the endangered Hawksbill and green turtles. Thousands of cormorants (a marine bird) died as a result of exposure to oil or polluted water.

It is estimated that approximately 300 oil lakes of various sizes covered more than 110 km² of surface area (Salam, 1996; Kuwait Oil Company, 2012). Following weathering for over two decades, most of volatile petroleum hydrocarbon component from the oil lakes has been emitted into atmosphere, causing continuous air pollution. The soils beneath and oil lakes were contaminated by the spilled oil. According to Kuwait Environment Public Authority (2011), there are nearly 50 million m³ of petroleum hydrocarbon-contaminated soils across the country, which are distributed in oil lake areas (both dry and wet oil lakes), oil contaminated piles and areas used to construct the oil trenches and place the pipelines (see Table 2.5).

Table 2.5 Statistics of petroleum hydrocarbon-contaminated soils within the State of Kuwait (Kuwait Environment Public Authority, 2011)

	Contamination Depth (cm)	Area (km ²)	Estimated Volume of Contaminated Soils (m ³)
Dry Oil Lake	25	98.38	24,500,000
Wet Oil Lake	64	7.19	4,600,000
Oil-contaminated Piles	173	8.59	14,800,000
Oil Trenches and Pipeline Spills	351	1.63	5,700,000
Total		115.79	49,600,000

At some locations where seawater was used to put out the oil fire, the light components of the crude oil could penetrate to reach shallow aquifers, threatening the precious groundwater resources (Al-Sulaimi et al., 1993; Al-Awadi et al., 2009).

To assist Kuwait to remediate the damaged environment caused by the oil fires during the first Gulf War, The United Nation Compensation Commission has awarded the State of Kuwait a grant of US\$3.6 billion (UNCC decision 258) in December 2005 (Asem, 2014). Approximately US\$2.2 billion was allocated to remediation of oil lakes and the associated soil contamination. This allows an environmental remediation program, collectively called “Kuwait environmental remediation plan” (KERP) being initiated. The major challenges related to this project are (a) no precedence in terms of international law to address environmental damages, (b) a lack of base data or pristine information, (c) not possible to understand the extend of environmental damages without the conduction of detailed M&A studies, and (d) full understanding of the soil characterization, and the hydrocarbon contaminated soil required (Asem, 2014).

Kuwait National Focal Point (KNFP), The United Nation Compensation Commission (UNCC), and Kuwait Oil Company (KOC) co-operated in this joint project to undertake comprehensive efforts to remediate the approximate 26 million cubic meters of heavily contaminated soils, with the persistence of extremely highly weathered oil and TPH levels (Al-Gharabally & Al-Barood, 2015).

Research work carried out by KISR and others since 1992, including the UNCC supported Monitoring and Assessment (M&A) Program (2001–2006) revealed that remediation of the contamination in this area is of high priority since the fresh water in

the north part of the country is considered to be an important strategic drinking water source for the State of Kuwait. Similarly, the fresh groundwater lens in the Raudhatain area in the north Kuwait is also threatened by the wet and dry oil lakes, oil-contaminated piles on the surface in adjacent areas, although significant contamination in this lens has not yet been observed. Considering the potential impact in the long-term, the removal of the oil-contaminated materials, including those in the wellhead pits and tarcrete in the area of the fresh groundwater catchment, has high priority during the implementation of the remediation projects (KISER,2004)

Based on the recent soil survey for the State of Kuwait, Omar et al. (1999) recommended to make modifications to the current soil taxonomy keys (Soil Survey Staff, 1994) in order to accommodate the human-induced soils that occur in Kuwait. In particular, soils with soot and fragments formed from the burning oil-wells as well as the soils contaminated by bombing and shelling to be re-classified to incorporate an “olic” material and possibly as “sootic” and “ordnance” material.

2.6.3 PHC-contaminated soils in Kuwait

The crude oil in these lakes in Kuwait has been exposed to harsh atmospheric conditions, resulting in the loss of volatile hydrocarbons, and has experienced other physical and chemical changes (KISR, 2004). With time, the lighter oil evaporated, oil mist hardened, and smaller and shallower oil lakes dried up and continue to disintegrate gradually (Kwarteng, 1999). Atmospheric deposition from the burning oil could have dispersed trace pollutants over a wide area, resulting in long-term impacts associated with the persistent presence of these pollutants in surface and subsurface soils (Omar et al.,1996). There is a possibility that contaminants have been transmitted to humans by entering the food chain through grazing animals and marine life (KISER, 2004).

The vertical distribution in petroleum hydrocarbons along the soil profile did not follow a predictable pattern. In some locations, oil penetration was limited to the top 50 cm and, in others, it could be visually seen at much deeper soil layers (Balba et al., 1998). TPH concentration decreased with increasing depth and reached insignificantly low levels at 60 to 80 cm depths (Balba et al., 1998).

Five types of PHC-contaminated lands have been identified and categorized (KISR, 2004). These are detailed as follows:

Soot areas: The main feature of this soil is a thin (0.2 cm), continuous or discontinuous soot layer in the upper soil horizon. In most areas, the soot layer has been covered by a thin veneer of sand or mixed into the upper soil layer. It is often very difficult to identify.

Tarcretes: tar mat layer that is 1 cm thick, black in color, composed of soil solidified by oil, and overlies clean sandy soil. The tar mat layer can be peeled off the underlying clean soil like a mat. These soils occur in all landscape positions. They have been formed by oil mist plastering the soil surface and mixing with the upper layer of soil.

Tar mats: The main feature of this soil is a thin (1 cm) oil crust over a 'clean' soil. The main problem for soil management and remediation is that the oil mat prevents vegetation growth; it also prevents water moving into the soil and increases runoff. Breaking the tar mat, allowing plant growth and water infiltration, may rehabilitate these problems.

Wet oil lakes: Consists of an oil layer 7 to 65 cm of black liquid or semisolid oil, over 6 to 80 cm (or more) of dark brown, sandy, oily soil, the main feature of this soil is liquid or semi-solid oil at the surface. The main problem for soil management and remediation is the liquid oil on the surface that prevents easy access; safety is also a concern as there is a risk of encountering unexploded ordnance hidden in the oil layer. Most of these units are now confined to linear drainage channels or enclosed by earth banks into ponds. There remains a large volume of oil-contaminated soil below the surface. This contamination category usually occurs in depressions or channels where the liquid oil has accumulated by flowing in.

Dry oil lakes: Consists of 3 to 90 cm (or more) of dark brown, oil-contaminated sandy soil, over a yellowish-brown sand that is not oil-contaminated. In some areas, there may be a tar mat 1 to 2 cm thick, black in color, with a moderately hard, dry consistency, the main feature of this soil is the oil contamination in the sandy soil that occurs to varying depths. The main problem for soil management is that the oil

concentration in the soil is high and will need to be rehabilitated prior to further land use. These soils were formed by liquid oil sitting on the surface for a period of time and then penetrating into the soil; therefore, all vegetation and fauna have been killed, and in some less contaminated areas, there may be reestablishment of vegetation.

2.7 Conclusions Literature Review

It has been 29 years since the biggest environmental disaster in the world occurred. More than 600 oil wells were burning, around 149 were badly damaged, 45 were overflowing, approximately 300 oil lakes of various sizes covered more than 49 km² of surface area of Kuwait. The total area 17,818 km², and 361 water lagoons of sizes of small lakes. The remediation projects will now start. The estimates of the damages particularly to the contaminated soil, and groundwater is currently unknown.

The literature review generalized and categorized the oil contamination in Kuwait as follows: soot areas, tarcrettes, tar mats, wet oil lakes, dry oil lakes. The effluent pit can be categorized into oil water treatment facilities and waste oil pits. We have concluded that the different types and categories of oil contaminations in Kuwait highly depends on the external and internal properties of crude oil and soil properties which changes the way they both form as end products. Dramatic changes happened to both related to the climates around them, including the time and the amount and type of crude oil.

In the literature sections 2.1.5 “Fate and transport of petroleum hydrocarbons” we observed that the factors influencing the characteristics of any crude oil contaminated soils are external and internal on any specific location, weathering, emulsification, dissolution, oxidation, biodegradation, evaporation, and leaching. These have extraordinary effects on how the soil becomes contaminated. We have learned that each type of oil has distinct physical and chemical properties such as light-weight components, medium-weight components, and heavy-weight components. Furthermore, the Literature review reveals the fact that the most important factor influencing the oil when it was spilled was evaporation. Evaporation generally causes the largest changes in mass balance after the spill and influences other parameters. Emulsification is the second-most important aspect. Oils that emulsify experience a

rapid increase in viscosity. Emulsification is dependent on oil composition. Some oils can lose sufficient aromatics by evaporation and then emulsify. We have observed that there are several factors influencing the properties of the soil in nature externally such as weathering, and internal physical and chemical properties of soil.

In the literature review we understand that soil hydrocarbon contamination might cause not only ecological and environmental harms, they may also have an adverse effect on the mechanical properties of soils and the geotechnical characteristics of crude oil-contaminated sands. Moreover, TPH data do not provide ideal information for investigating sites and establishing target cleanup criteria. Identification and quantification of aliphatic and aromatic fractions allows identification of petroleum products and evaluate the extent of product weathering. These fraction data can also be used in risk assessment.

In the literature review section 2.2.5.1, Environmental Policy and Regulation Related to Soil Contamination by Petroleum Hydrocarbons, we have concluded that the main factor influencing the environmental policies and the regulation related are the environmental risk associated, the Environmental protection agencies EPA consider risk to be “the chance of harmful effects to human health or to ecological system resulting from exposure to environmental impacted sites. the risk assessment systems and tools discussed in section 2.3.4, 2.3.5. reveal the facts that these tools and systems in place to measures the magnitude and the effects effort of the contamination that harms or might harms our human or ecological system around us. We have concluded that USEPA and UKEPA, including major international environmental organisation adopted (TPHCWG) Approach for evaluating human health risks from petroleum hydrocarbons contamination. We have reviewed the risk assessment tools available to investigate the magnitude and to estimate the risk in section 2.3.5.

We have concluded that the estimates for hydrocarbon contaminated soil completed to date in the world have been conducted with little or no ground truth information to support the remote sensed interpretations. Therefore, the reliability of the estimates is unknown. The estimates of oil-contaminated soil volume and area have associated sampling errors that are also unknown. In addition, the current approach used by the contractors for soil sampling and soil characterization lacks a rigid scientific

basis. The cost-effectiveness of estimating the volume of contaminated soils needed to be treated can be significantly improved by advanced 3-D modelling technologies, combined with an improved sampling procedure. In this literature review we have illuminated Spatial interpolation methods which play a significant role in planning, risk assessment, and decision making in environmental management, as they provide essential elements towards site characterization.

In reviewing the literature related to Spatial interpolation, we found that nothing has been done previously with concern to the area of hydrocarbon contaminated soil. This demonstrates the need for this research. In addition, we have found that time and the high cost required for soil samples collection has motivated researchers to develop methods for creating soil maps from sparse soil data. The keystone in site-specific management analysis is the interpretation of spatial variability of soils properties.

In this chapter, section 2.4.8, we concluded that the factors affecting the performance of the spatial interpolation methods are scale, secondary variables, spatial correlation, accuracy variance and range, data quality, sample size, sampling design, surface type sample density, and sample spatial distribution.

It was observed in the literature review that there are two main groupings of interpolation techniques for generating raster surfaces, deterministic and geostatistical techniques. The deterministic models use a mathematical function to predict unknown values. Furthermore, the two interpolation methods that can be automatically applied to certain data types such as soil chemistry and geology are the Inverse Distance Weighting, and the Kriging. The IDW considered a deterministic technique, and Kriging is considered a geostatistical technique. The most appropriate method will depend on the distribution of sample point benign studied--the choice of spatial interpolation techniques were project and user dependent. In our PhD research the phenomenon benign studied is 3-D soil characterization and mapping for hydrocarbon contaminated sites.

In section 2.4.7 of this chapter we reviewed the assessment measures for assessing the performance of spatial interpolation methods and we concluded that cross validation is one of the most important concepts in any type of data modelling.

In the next chapter, we will investigate the characteristics of the crude oil-contaminated soils, and select a range of petroleum hydrocarbon-contaminated sites in Kuwait as potential research projects and case studies towards achieving our aims and objectives of this research. This will lead to the development of more cost-effective set of methods that will be used to develop our 3-D soil characterization and mapping technology for hydrocarbon contaminated sites to guide the selection of remediation technologies in oil-contaminated sites. The review will conclude several aspects which will be reflected in the research structure, especially the methodologies adopted, i.e. sampling methodology and design, laboratory analysis, and 3-D mapping technology development. The chapter will end with clear conclusions and recommendations.

Chapter 3

Methods and Materials

3.1 Introduction

As stated in Introduction chapter, the overall aim of this PhD study was to obtain insights into the geochemical characteristics of the aged crude oil-contaminated soils, and using this knowledge, to develop 3-D predictive models for spatial distribution of the contaminated soils and remediation strategies based on site-specific environmental risk assessment. As an industrially funded project (Kuwait Petroleum Corporation Scholarship program) with the PhD candidate being a senior engineer working in the Kuwait Oil Company Soil Remediation team, this PhD project had a practical goal to develop a cost-effective technology (3-D soil mapping for characterization of crude oil-contaminated soils in the Kuwait oil lake areas) for direct applications to the UN-funded KERP.

To ensure that the research outcomes generated from this project will be directly applicable to the United Nations-fund KERP, specific requirements by KERP needed to be met when designing the project. The study area is an exclusion zone containing unexploded ordnance (UXO) from the First Gulf War. Strict approval procedures needed to be followed in order to get access to the study area. This posed some limitations to the development of the research plan, including but not limited to selection of the sampling sites and preparation of sampling schedule. KERP requires all soil analyses being performed in accredited laboratories. At the time when this PhD project commenced (in September 2015), there was no quarantine laboratory in University of Salford to allow import of soil samples from Kuwait. It was also impractical to obtain accreditation from the UK Accreditation Services (UKAS) for the analytical methods needed to collect soil data for a PhD project. Therefore, it was decided that the project would focus on the development of computer-assisted modelling for 3-D soil mapping plus characterization and environmental risk assessment of the contaminated soils using an accredited commercial laboratory for soil

sample analysis.

To achieve the set research objectives, a multi-method approach was adopted. This involved (a) reviewing the existing literature related to the research area, (b) collecting and reviewing secondary data from the Kuwait Oil Company, (c) conducting field and laboratory investigations to collect primary data that are required for characterization of soils at the selected study sites, and (d) developing computer-assisted 3-D predictive models to allow mapping of soil-borne petroleum hydrocarbons in the selected study areas. This chapter describes and justifies the selection of study sites and specific research methods.

3.2 Selection of the Study Sites

3.2.1 Regional settings

Kuwait is part of the Arabian plate and is located at the northwestern end of the Arabian Peninsula between latitudes 28°30' and 30°5' North and longitudes 46°33' and 48°30' East. It covers approximately 17,800 km² of desert land with no river and natural lake (State of Kuwait Environment Public Authority, 2012). The topography is characteristic of low to moderate relief. The geological materials exposed on the land surfaces are of early Miocene to Recent origins (Milton, 1967). Kuwait has a hyper arid desert climate with an average annual rainfall of 116 mm. In summer months, average daily high temperatures range from 42°C to 46°C, with the highest ever recorded temperature of 53.5°C (State of Kuwait Environment Public Authority, 2012).

The surface materials of the desert lands are dominated by gravel lag that stabilizes the surface, the desert floor and playa deposits that occur in areas of depressions (Khalaf and Al-Ajmi, 1993; Khalaf et al., 1980). Kuwait's desert soils are characteristic of arid soil, with poorly developed profiles and sandy texture. The calcareous hardpan (gatch) occurs at varying depths and locations. These hardpan layers consist predominantly of calcium carbonates and quartz. The desert soils only contain a limited amount of organic matter and nitrogen. Although the concentration of total phosphorous is relatively high, its bioavailability is low due to formation of practically insoluble Ca and Mg carbonates (KISR, 2004).

Apart from petroleum hydrocarbon-contaminated soils in the oil lake areas caused by the first Gulf War, there are also contaminated soils derived from the oil extraction operations by the Kuwait Oil Company. These two types of oil-contaminated soils may have different geochemical characteristics due to the pathways through which the soils were contaminated. In order to compare the geochemical characteristics of these two types of oil-contaminated soils, separate soil investigations were required.



Figure 3.1 Map showing the Rawdhatain oil field in the northern Kuwait and Burgan oil field in the southern Kuwait

3.2.2 Study site in the oil lake area

There are two major oil lake areas within Kuwait; Rawdhatain oilfield located in the northern Kuwait and Burgan oilfield in the southern Kuwait (Fig. 3.1). Due to the delay in research contract and permission to entering the exclusion zone in the Burgan oil lake area by the time of thesis submission, only results obtained from the Rawdhatain oilfield are reported here.

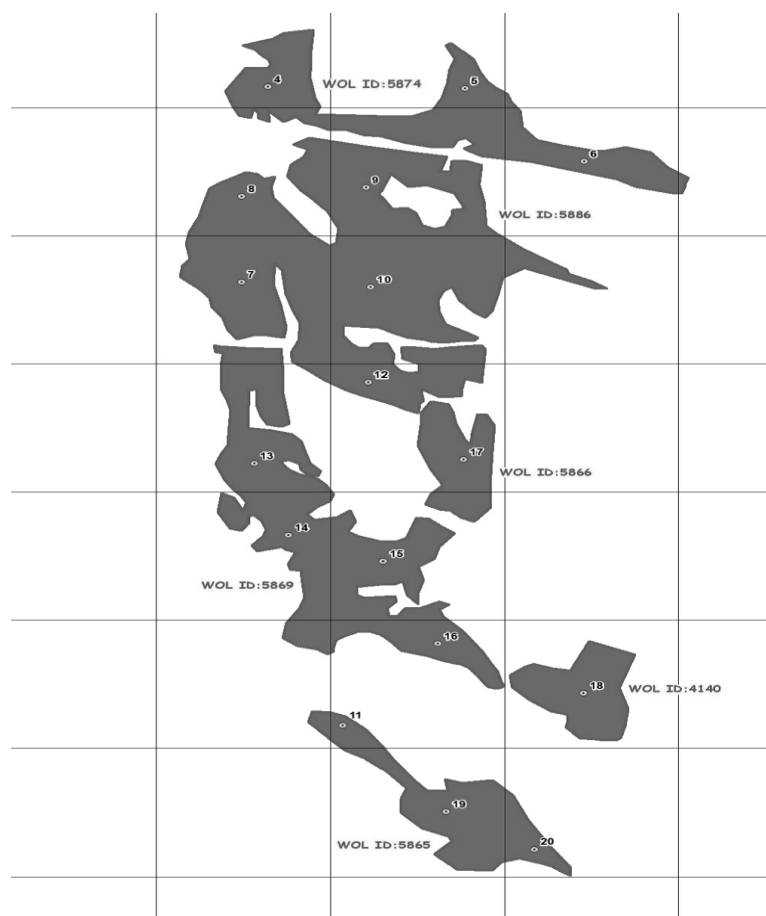


Figure 3.2 Map showing the soil sampling locations in the Rawdhatain oil lake area

There have been concerns about the possible contamination of groundwater by petroleum hydrocarbons in the Rawdhatain oil lake area (Viswanathan et al., 1997; KISR, 2004). Due to the limitations of resources, time and access to the area, only the central part of the oil lake (B Section of the Raudhatain Area) was selected for sample collection (Fig. 3.2).

3.2.3 Study site in the oil extraction area

A typical oil sludge pit (EPE4) within the KOC operation area in the southern Kuwait Burgan oilfields was selected for this study (Fig. 3.3). As KOC operations being obstructed at Burgan oilfield by the presence of oil lakes and oil-contaminated piles, particularly in certain priority areas in the south-east of the Burgan oil field. these areas instantly require removal and remediation of heavily contaminated materials and have

accordingly been included in the fast track projects initiating the KERP within the Claim No. 5000454.

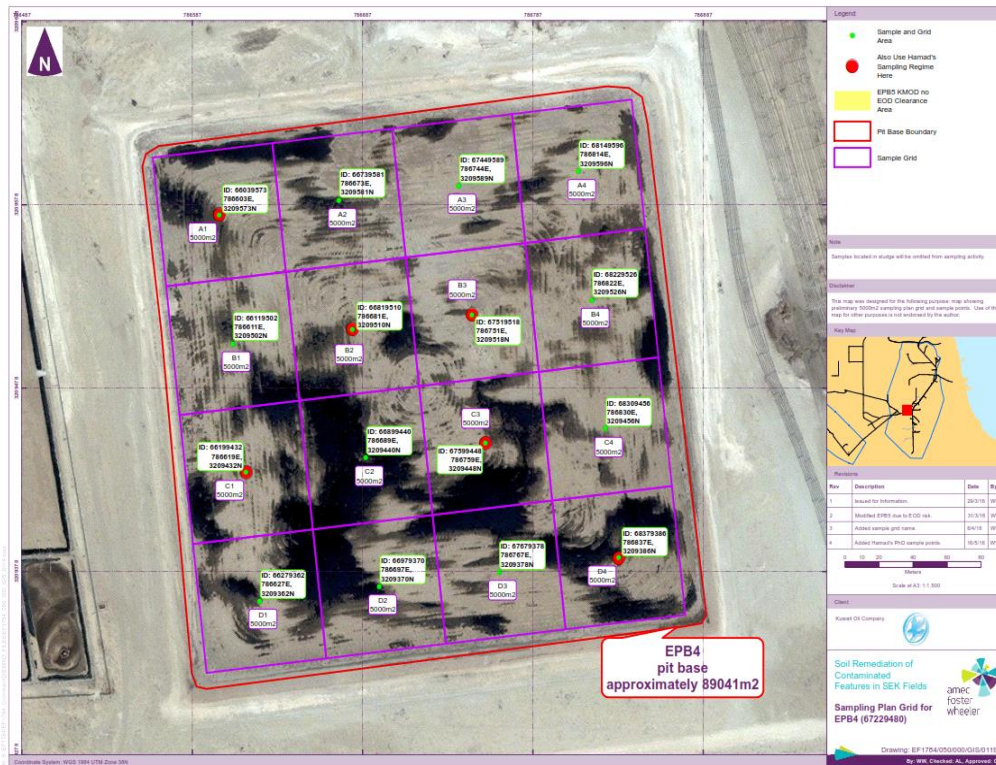


Figure 3.3 Map showing the 16 sampling locations in the Oil Sludge Pit EPE4

3.3 Field methods

Due to the difference in contamination depth, different sampling schemes were adopted for the two selected study sites.

3.3.1 Sampling method used in the Rawdhatain oil lake area

Samples were collected from 17 soil locations (Fig. 3.2) using a random grid sampling method. At each location, the soils samples were taken at set depths to account for vertical variation of petroleum hydrocarbons along the soil profile to enable easy comparison of results between profiles. Soil samples were collected at 10 cm interval for the soil profile with a depth of contamination less than 50 cm, and at 20 cm interval for the soils with a depth of contamination between 50 and 100 cm. For each soil profile at these 17 locations, the sampling location (UTM coordinates 34N WGS 1984) was

determined with a Garmin GPS unit and then 5 soil samples at different depths were collected. The soil samples were taken using a trowel wrapped with a plastic cover, which was changed after each sample was collected to avoid cross contamination. Each sampling location was assigned a location ID, which was composed by the last 4 digits of northern UTM and the last 4 digits of eastern UTM.

The soil samples were taken from lower layer up and the description and labelling were the opposite to this (in order from top to bottom of the pit). In addition, a photograph of each soil profile was taken with a measuring tape being placed in the sampling pit for depth reference. Soil attributes described in the field included horizon thickness and sequence, colour, texture, structure, consistence, presence of salt crystals, coarse fragments, mottles, and roots.

Composite sampling was used for the sample collection (IAEA-TECDOC-1415, 2004). This involved thoroughly mixing discrete samples from the same soil layer at the same location to obtain a representative soil sample for that location. Composite sampling is widely used for large-scale soil investigation to achieve cost-efficient goal. This was deemed appropriate for this study given that the accuracy of soil data from the composite samples was sufficient for this project while the costs can be minimized, which is the primary goal for any technologies to be used for soil remediation under the UN's KERP program.

After collection, each composite soil sample was split into 2 sub-samples and contained in two separate 170 mL glass jars that were packed into a plastic cooler with ice. The packed samples were then shipped from Kuwait to the Manchester laboratory.

3.3.2 Sampling method used in the Oil Sludge Pit EPE4

Samples were taken from 16 locations, as shown in Fig. 3.3. At each sampling location, the contaminated soil was sampled at 5 cm interval from the boundary between the sludge layer and the contaminated soil layer to the boundary between the contaminated soil layer and the non-contaminated soil. In addition to the contaminated soil samples, a sludge sample and a clean soil sample immediately below the contaminated soil were also collected. A total of 23 contaminated soil samples, together with 16 sludge samples and 16 non-contaminated soil samples were collected from 16

locations within the study area. After collection, each soil sample was split into 2 sub-samples and contained in two separate 170 mL glass jars that were packed into a plastic cooler with ice. The packed samples were then shipped from Kuwait to the Manchester laboratory for analysis of various petroleum hydrocarbon fractions (BTEX, aliphatic fractions, and aromatic fractions), and polycyclic aromatic hydrocarbons (PAHs). In addition, the soil profile morphology was observed and described in the field.

3.4 Laboratory methods

As mentioned above, the United Nations KERP soil remediation projects require analyses of all key soil parameters being conducted in accredited laboratories. There was also a requirement for a quarantine license to allow import of soil samples to UK from Kuwait. At the time when this PhD project commenced, University of Salford did not have a quarantine laboratory. It was also realized that it was not practical for an international student (limited available time for project under the UK immigration regulations) to obtain method accreditation by UKAS before the scheduled sampling campaigns. Therefore, the soil analysis needed for the completion of this PhD project was performed by a selected accredited commercial laboratory near Manchester (Concept Life Science Analytical Service). As a result, the candidate only performed selection of analytical parameters and methods and liaise sample shipment from Kuwait to Manchester but not laboratory analysis operations.

Concept Life Science Analytical Service (CLS) was an UKAS-accredited laboratory based in Manchester, which is convenient for this project. The analytical methods/procedures described below reflects the technical information provided by the analytical service supplier. The method statement provided by CLS is provided as Appendix 1.

3.4.1 Soil pH and electrical conductivity (EC)

1:5 (soil: water) extracts were prepared by shaking 5 g of the air-dried soil in 25 mL of deionized water in a rotary shaker for 1 hour. pH and electrical conductivity (EC) in the soil extracts were then measured by a calibrated pH (HI-2020 edge) meter and a Mettler Toledo EC meter, respectively.

3.4.2 Particle size analysis

Since no or only a trace amount of soil particles with a diameter less than 0.063 mm was present in the soil samples, particle size distribution was determined by sieving only. The entire soil sample was weighed and then passed through a series of sieves with mesh sizes of 2 mm, 0.6 mm, 0.355 mm, 0.125 mm and 0.063 mm using a Endecott test sieve shaker. The weight of various particle size fractions (> 2mm, 0.6-2 mm, 0.355-0.6 mm, 0.125-0.355 mm and 0.063-0.125 mm) was determined by weighing. The percentage of each particle size fraction was then obtained by calculation.

3.4.3 Element analysis

Various elements in the soils, including potassium, sodium, aluminum, arsenic, barium, beryllium, calcium, cadmium, cobalt, chromium, copper, iron, mercury, magnesium, manganese, molybdenum, nickel, phosphorous, lead, antimony, selenium, silica, tin, Sulphur, tellurium, thallium, vanadium, zinc were determined by inductively coupled plasma-optical emission spectrometry (Agilent 5110 ICP-OES) after aqua regia digestion 1 g of dried and ground soil (<0.425 mm) was weighed into a 50 mL Environmental Express Digestube. 10 mL of concentrated hydrochloric and 3.5 mL of concentrated nitric acid were added to the sample via a dispenser. Samples were digested in aqua regia at 110°C +/-5 °C for 90-100 min in a digiblock (hotblock). The following wavelengths were used for determining the various elements in the samples: Al (396.152 nm), As (188.98 nm), Ba (233.527 nm), Be (249.473 nm), Bi (223.061 nm), Ca (315.887 nm), Cd (228.802 nm), Co (230.786 nm), Cr (267.716 nm), Cu (217.895 nm), Fe (259.940 nm), Hg (184.887 nm), K (766.491 nm), Li (610.365 nm), Mg (279.078 nm), Mn (259.373 nm), Mo (202.032 nm), Na (589.592 nm), Ni (231.604 nm), P (213.618 nm), Pb (220.353 nm), S (181.972 nm), Sb (206.834 nm), Se (196.026 nm), Sn (189.925 nm), Sr (346.445 nm), Ti (334.941 nm), Tl (190.794 nm), V (311.070 nm) and Zn (213.857 nm).

Total sulfate concentration was obtained by calculation based on total sulfur concentration.

3.4.4 Benzene, toluene, ethylbenzene and xylene (BTEX)

BTEX in the soil samples was determined by headspace gas chromatography mass spectrometry (GC/MS). The GC-MS was an Agilent 7890A GC coupled to an Agilent 5975C MSD using a Gerstel headspace autosampler using Agilent Chemstation E.01.00 software. The column was a 30 m DB-624 with a 0.32 mm ID and a 1.8 μm film thickness. Stationary phase was 6% cyanopropylphenyl/94% dimethyl polysiloxane. The temperature profile was: initial temperature of 60 °C held for 2 minutes then ramped at 20 °C/min up to 280 °C and then held for 1 minute. System ran in constant flow mode with a 60:1 split. Autosampler was set to agitate for 15 minutes at 60 °C. Helium was used as the carrier gas and the inlet temperature was set at 250 °C. MSD was operated in scan mode between 40 and 450 Da and set to high resolution.

3.4.5 Petroleum hydrocarbon fractions

A TPH CWG method (Weisman, 1998) modified by the UKAS-accredited CLS was used to determine the petroleum hydrocarbon fractions in the soils. Various petroleum hydrocarbons contained in the soils were extracted by dichloromethane. Sodium sulfate and silica were used for solution clean-up. The aliphatic and aromatic fractions are separated using solid-phase extraction techniques. Additional clean-up for the extract was performed by passing the solution through a membrane filter. The filtrate was treated with 15 g of acid silica in a clean round bottom flask placed on a rotary evaporator with no heat for 30 min.

The short-chain aliphatic and aromatic fractions (C5-C10) in the solution was determined by headspace gas chromatography mass spectrometry (GC/MS), the same as the determination of BTEX described in 3.4.4.

Long-chain aliphatic and aromatic fractions (C10-C35) was determined using a capillary gas chromatography with flame ionization detection (GC/FID) method. The GC used was a Varian 3900 GC-FID with Varian Star software. The column was a 15 m select mineral oil with a 0.32 mm ID and a 0.1 μm phase thickness. Stationary phase is a polysiloxane based mixture. The temperature profile was: initial temperature of 45 °C, held for 1.5 min and then ramped at 40 °C/min up to 320 °C and held for 2.6 min. Instrument ran under constant flow 1.4 mL/min conditions splitless. Helium was used as the carrier gas. Inlet temperature was set at 250 °C. The sample was injected with a

pressure pulse of 10 psi for 0.5 min.

Fraction C35-C40 was obtained by the difference between total petroleum hydrocarbon and the sum of C5-C35 fractions. This resulted in the separation of the following 16 petroleum hydrocarbon fractions: TPH (C5-C6 aliphatic), TPH (C6-C8 aliphatic), TPH (C8-C10 aliphatic), TPH (C10-C12 aliphatic), TPH (C12-C16 aliphatic), TPH (C16-C21 aliphatic), TPH (C21-C35 aliphatic), TPH (C35-C40 aliphatic), TPH (C6-C7 aromatic), TPH (C7-C8 aromatic), TPH (C8-C10 aromatic), TPH (C10-C12 aromatic), TPH (C12-C16 aromatic), TPH (C16-C21 aromatic), TPH (C21-C35 aromatic) and TPH (C35-C40 aromatic).

3.4.6 Polycyclic aromatic hydrocarbons (PAHs)

16 common polycyclic aromatic hydrocarbon species including naphthalene, acenaphthylene, acenaphthene, fluorine, phenanthrene, anthracene, fluoranthene, pyrene, benzo(a)Anthracene, chrysene, benzo(b)fluoranthene, benzo(k)fluoranthene, benzo(a)Pyrene, indeno(123-cd)Pyrene, dibenzo(ah)Anthracene, and benzo(ghi)Perylene were determined by gas chromatography-mass spectrometry. The GC-MS was an Agilent 6890N GC attached to an Agilent 5973 MSD using Chemstation D.02.02 software. The column was a 30 m HP-5MS with a 0.25 mm ID and a 0.25 μ m film thickness. Stationary phase was 5% diphenyl/95% dimethyl polysiloxane. The initial temperature was set at 50 °C and held for 5 min. The temperature was then increased at a rate of 20 °C/min to 310 °C and then hold for 3 min. System ran ramped flow with a hold at 1 mL/min for 18 min and then increased to 1.5 mL/min and held for 3 min. 25:1 split injection was performed and inlet temperature was set at 280 °C with helium being used as the carrier gas. MSD was operated in SIM mode. Dwell time was set at 50 m/s utilizing SIM grouping.

3.4.7 QC/QA and statistical analysis

The analysis was performed in the UKAS-accredited commercial analytical laboratory (Concept Life Sciences Analytical & Development Services Limited). Analytical quality control was maintained by a number of measures:

- Multi-point calibration with authentic standards (with defined minimum performance characteristics).

- Analysis of control samples within each analytical batch, such as independent standards, matrix spikes or reference materials.
- Analysis of reagent / method blanks within each analytical batch.
- Ongoing quality assured by the use of control charts in conjunction with warning and action limits for the QC sample data.
- Participation in external proficiency testing and inter laboratory schemes such as LGC Standards CONTEST and AQUACHECK.

3.5 Geostatistical methods used for 3-D model development

It was observed from the literature review that there are two interpolation techniques can be automatically applied to certain data types such as soil chemical parameters: deterministic technique and geostatistical technique, namely Inverse Distance Weighting (IDW), and Ordinary Kriging (OK). These two common interpolation methods were evaluated for their possible uses in this project. The most appropriate method depended on the distribution of sample point. One of these methods or a combination of them could be used or integrated from each other to develop the best interpolation technics for the development of our 3-D mapping technology for hydrocarbon contaminated soil.

3.5.1 Selection of interpolation methods

The data were collected from Kuwait Oil Company (KOC) for oil lake/effluent pit Project SPB1. The selected case study used a total area of 13,000 m² (Fig. 3.4) and Figure 3.5 The soils underneath and adjacent to the oil lakes were heavily contaminated by petroleum hydrocarbons and therefore required remediation. The samples collected by contractors using different methods, and the sampling survey provided involved collection of soil samples at up to three depths/ layers (layer 1, contaminated surface; layer 2 subsurface contaminated layer; and layer 3 the layer below all visible contamination).

In the first phase of the research, an in-house inverse distance weighting (IDW) interpolation tool was developed using MATLAB, and SPB1 data provided by KOC concerning the contaminated soil samples (Figs. 3.4 and 3.5). Subsequent to that, an

interpolation tool with a novel sampling design has been improved and developed. Furthermore, both Kriging and MATLAB were used for a preliminary 3-D mapping of soil hydrocarbon contamination characterization for a specific area in a project EPE4. The purpose to develop our own in-house tool was to support the advanced development of new technologies. To validate the developed tool and compare the performance of the Kriging and IDW, modelling was conducted on two theoretical mathematical functions of a single variable.



Figure 3.4 Map showing the study area of Project SPB1

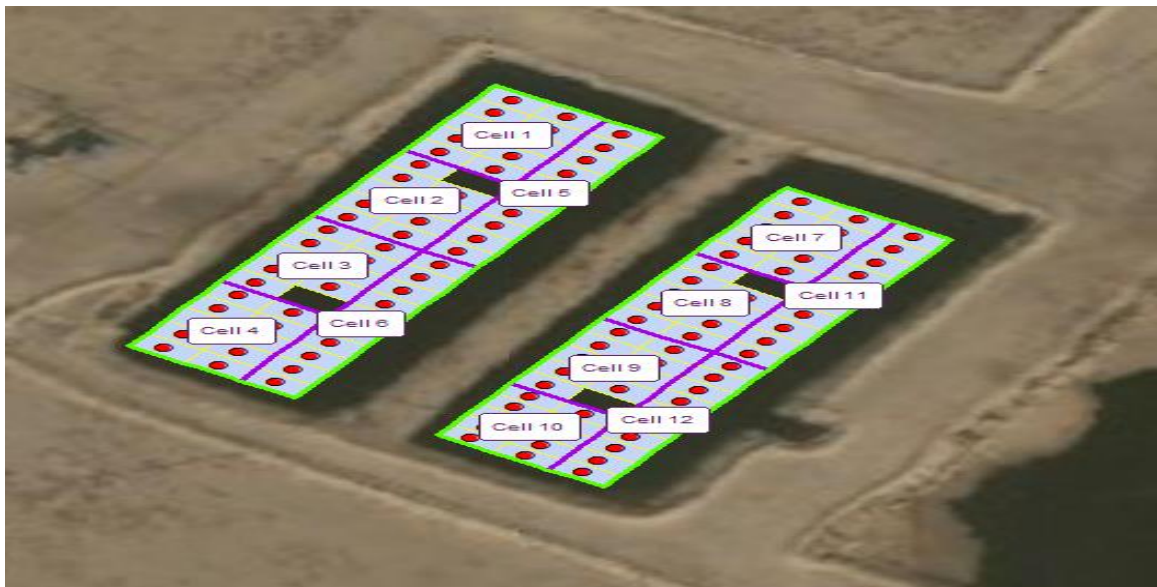


Figure 3.5 Image showing Sludge Pit SPB1 with sampling locations

The results show that IDW method works well (Figs. 3.6 – 3.9) except for the

surveyed quantity having more than one data at the same position. So it was necessary to edit the collected survey data before the interpolation to avoid the multi-data at the same position.

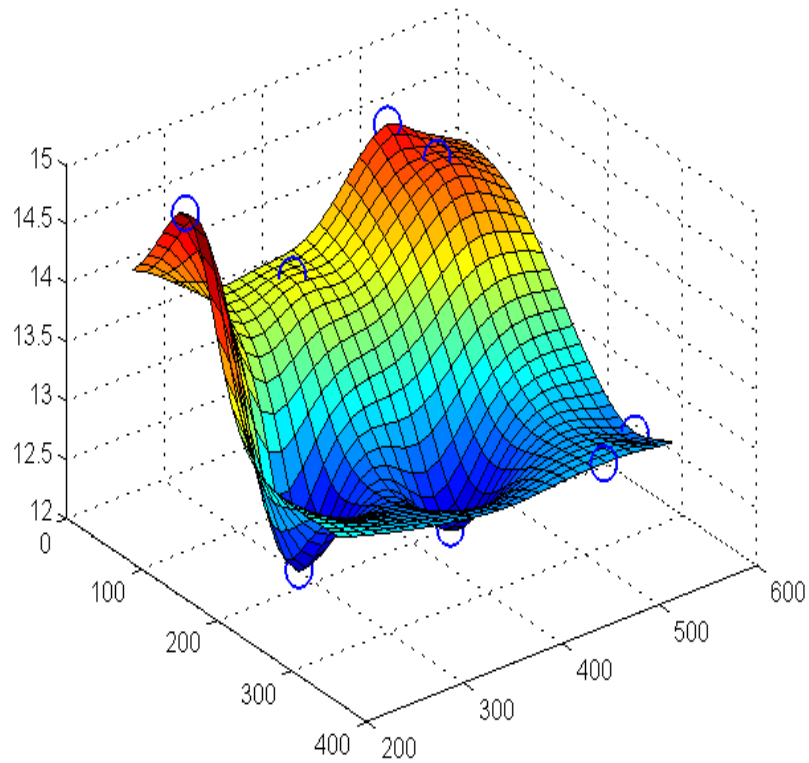


Figure 3.6 An example of the in-house tool using IDW interpolation method

Fig. 3.6 show an example using the IDW interpolation method for elevation map in terms of the 8 data in the Cell 1 in the Fig. 3.5. A smooth reconstruction for geographical surface in Cell 1 has obtained.

Elevation Mapping

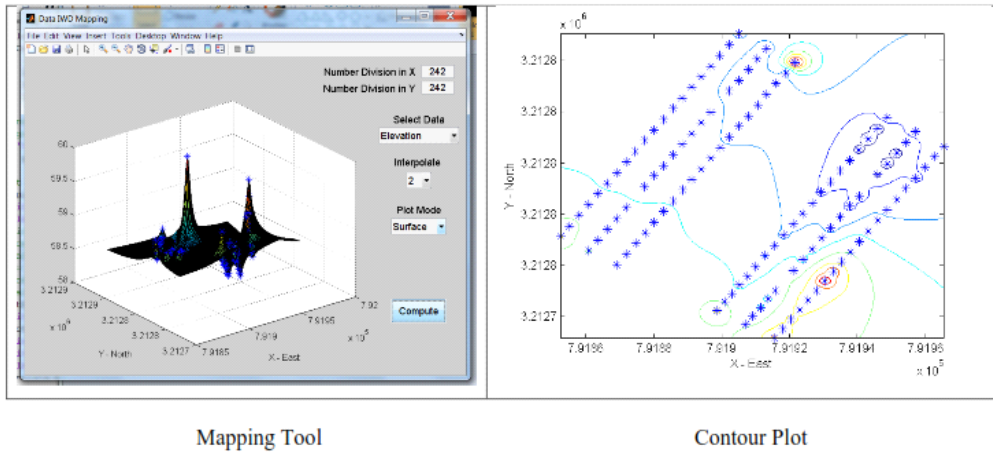
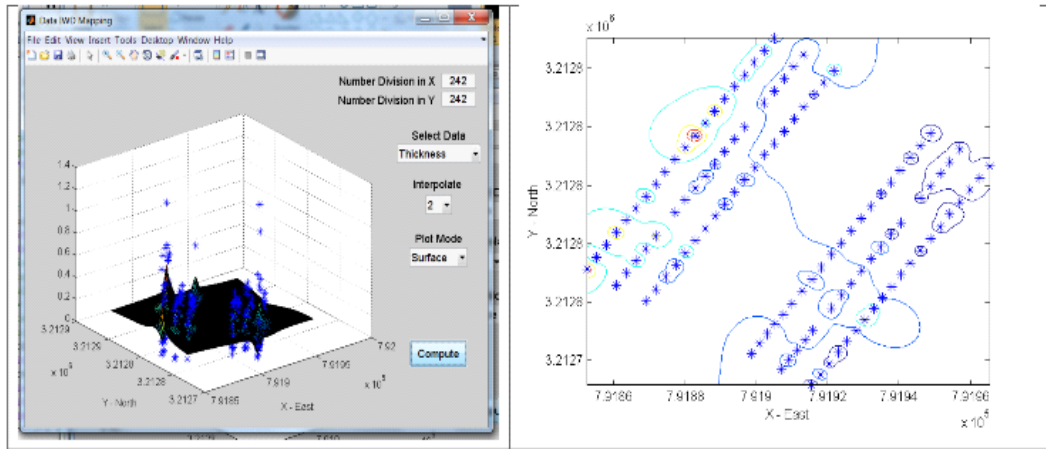


Figure 3.7 The developed inverse distance weighting interpolation code using MATLAB for SPB1 (A - each sampling point has a single value)

Fig. 3.7 shows the elevation map for the whole area of the SPB1 using the IDW interpolation method, which presents a sharp variation of the geo-surface particularly at the sampling points.

Thickness Mapping



Mapping Tool

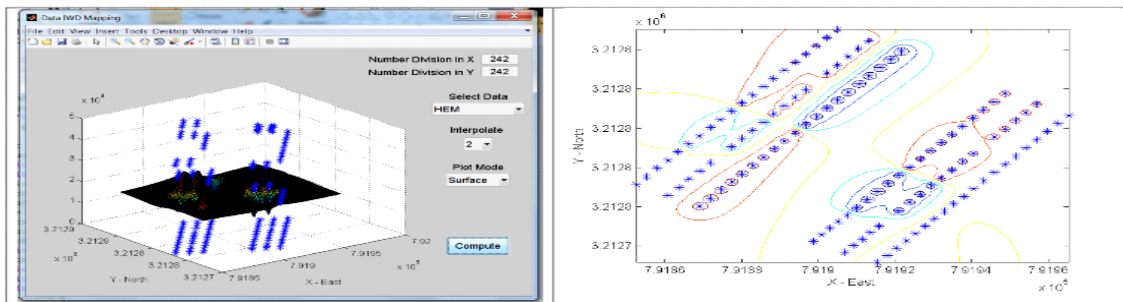
Contour Plot

There are more than one data at the same sampling position.

Figure 3.8 The developed inverse distance weighting interpolation code using MATLAB for SPB1 (B - each sampling point has multi-values)

Fig. 3.8 shows the interpolated map of the local contamination thickness in the whole area of the SPB1 using the IDW interpolation method. There is more than one data at some sampling points, for which only one was used. The mapping result again presents a sharp variation in the region near the sampling points.

HEM Mapping



Mapping Tool

Contour Plot

There are more than one data at the same sampling position.

Figure 3.9 The developed inverse distance weighting interpolation code using MATLAB for SPB1 (C- each sampling point has multi-values).

Fig. 3.9 shows the interpolated map of the HEM in the whole area of the SPB1 using the IDW interpolation method. Similar as that in Fig. 2.8, there are more than one

data at some sampling points, for which only one was used as well. The mapping result demonstrates again the IDW method presents a sharp local variation at the sampling points.

Figs. 3.10 - 3.13 show the mapping results for the four parameters investigated in the project. They are Cont Z, HEM, thickness and elevation. Based on the mapping results we can effectively estimate the total contamination volume and distribution.

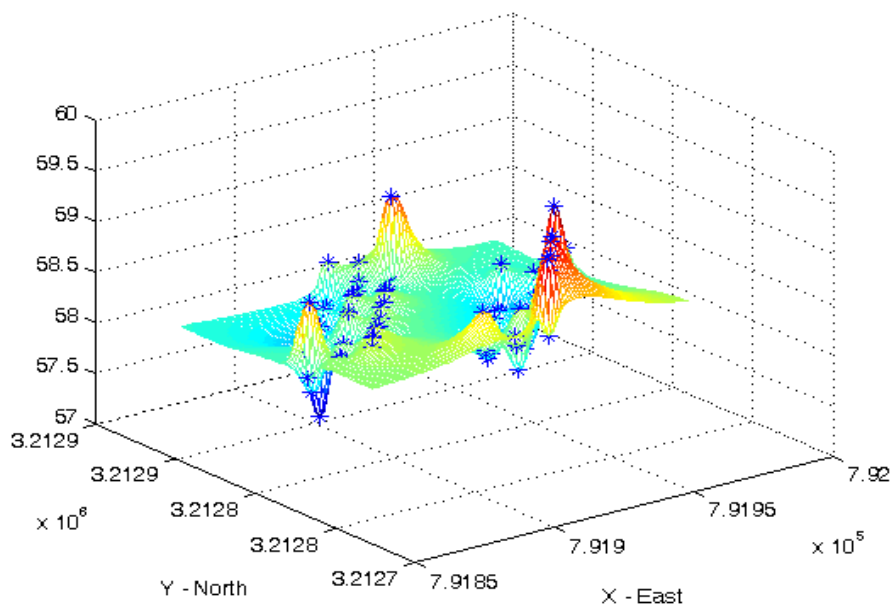


Figure 3.10 Graph showing Cont Z3 mapping

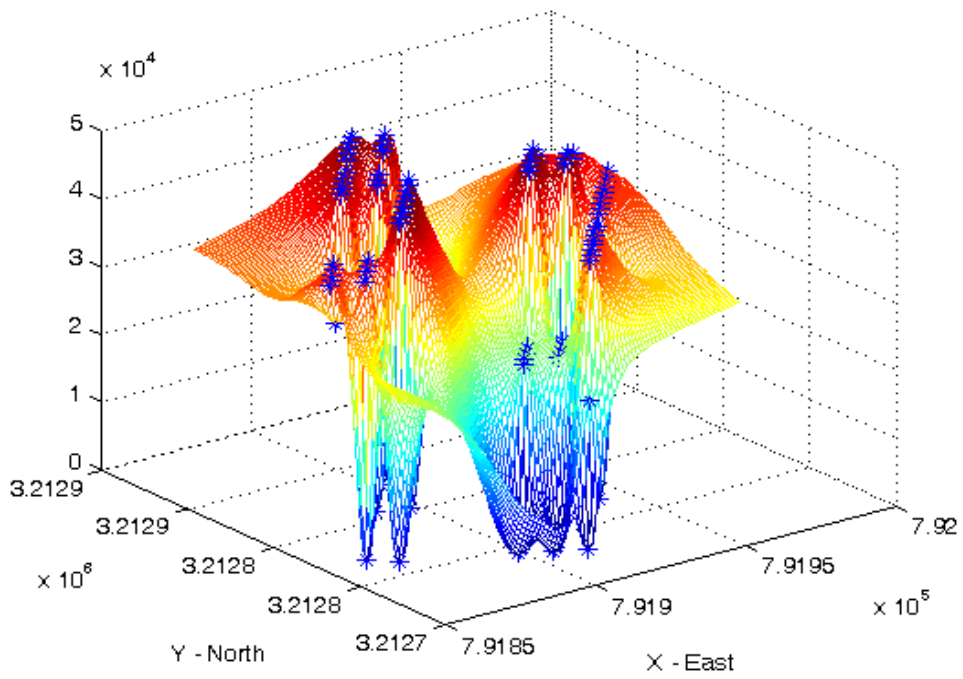


Figure 3.11 A graph showing TPH (HEM) 3-D mapping

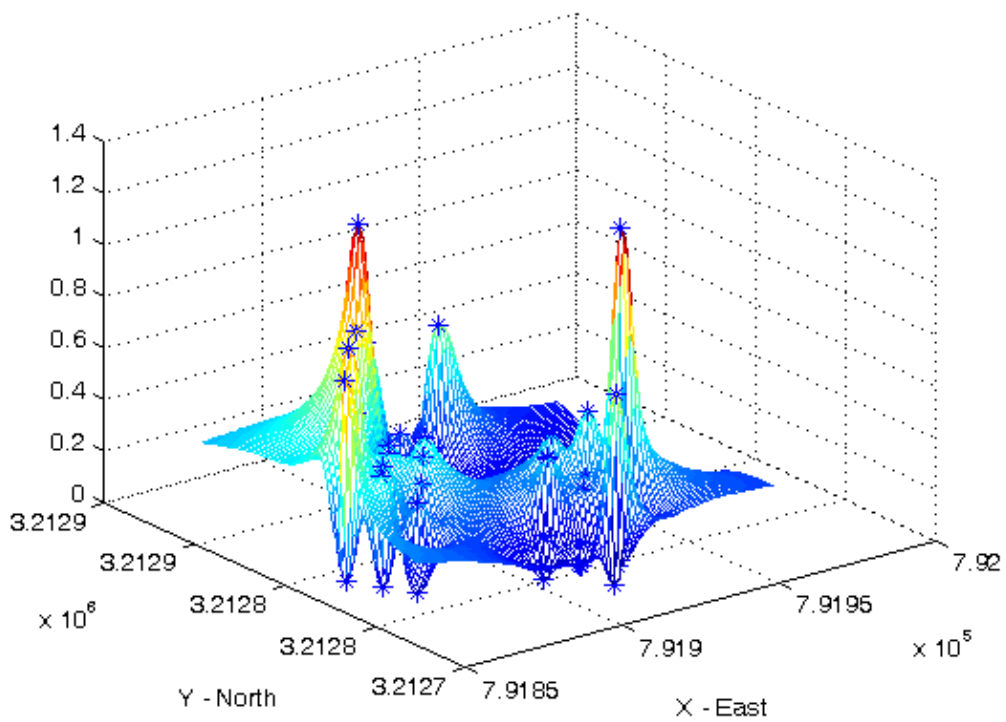


Figure 3.12 A graph showing thickness mapping

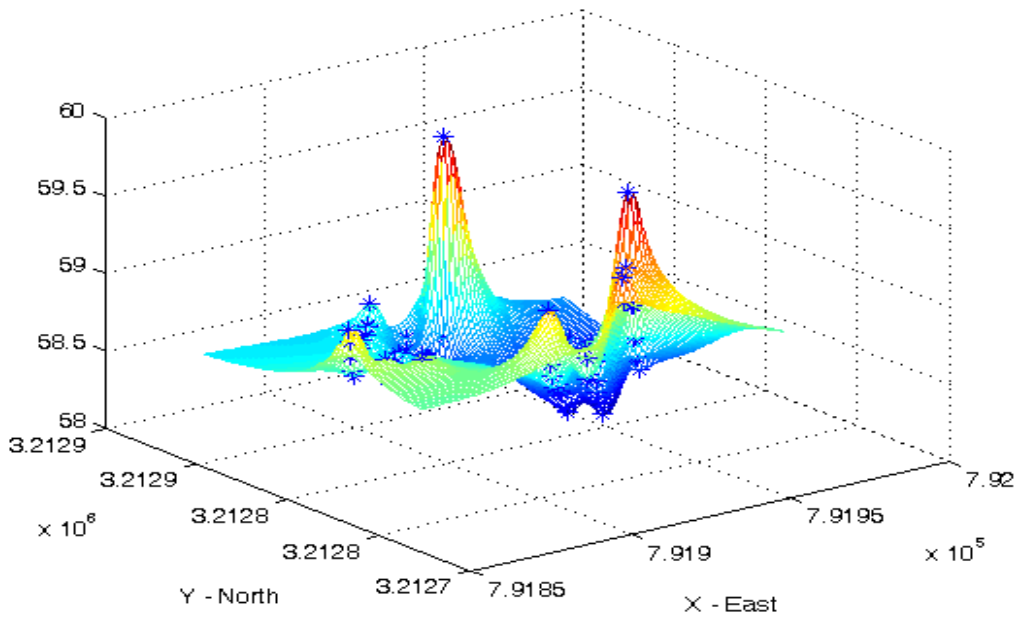


Figure 3.13 a graph showing 3-D elevation mapping

Figs. 3.10 to 3.13 replots all the interpolation of these parameters again respectively in single plots. These replots highlight the sharp variation of the mapping at the sampling points when using the IWD technique. For the reason, IWD method here has identified to be less effective for the specific problems that we are investigating.

It was observed in the SPB1 case study that currently soil investigation into petroleum hydrocarbon-contaminated soils in oil lake area involves grid sampling with a high horizontal sampling density. However, vertical variation in petroleum hydrocarbon concentration along the soil profile is not sufficiently considered. This approach could lead to substantial costs due to intensive horizontal sampling on one hand and inaccurate estimation of the volume of soils that need to be treated. It was observed that the sampling technics and methods been used by the KOC contractor didn't provide an easy way to manage and analyze data through interpolating methods.

It was concluded from the first case study that the existing approach and methods used were not able to provide sufficient information to cost-effectively guide development of remediation strategies and selection of appropriate technology. These

include:

- The existing soil sampling design and method does not take into account vertical variation in various petroleum hydrocarbons and therefore does not allow separation of soil layers with different levels of TPH (i.e. <0.5-5%, 5-7% and >7%). This information is necessary for selection of treatment procedure and calculate the treatment cost.
- The existing method heavily relies on the determination of total amount of petroleum hydrocarbons (TPH). This does not allow evaluation of the oil-contaminated soils based on their toxicity and environmental risk.
- The existing simple average method used to estimate the volume of contaminated soils does not consider both horizontal and vertical variation in petroleum hydrocarbon in the soils and could lead to significant overestimating or underestimating of the contaminated soil volume.

Inverse Distance Weighting (IDW) was selected as the platform for 3-D modelling. IDW is deterministic but the choice of which weight to assign is subjective. Nevertheless, as a first step to see how overall workflow behaved, IDW gave a look at the surface. In the second phase of the research, the software tool has been further developed to implement a more advanced interpolation method.

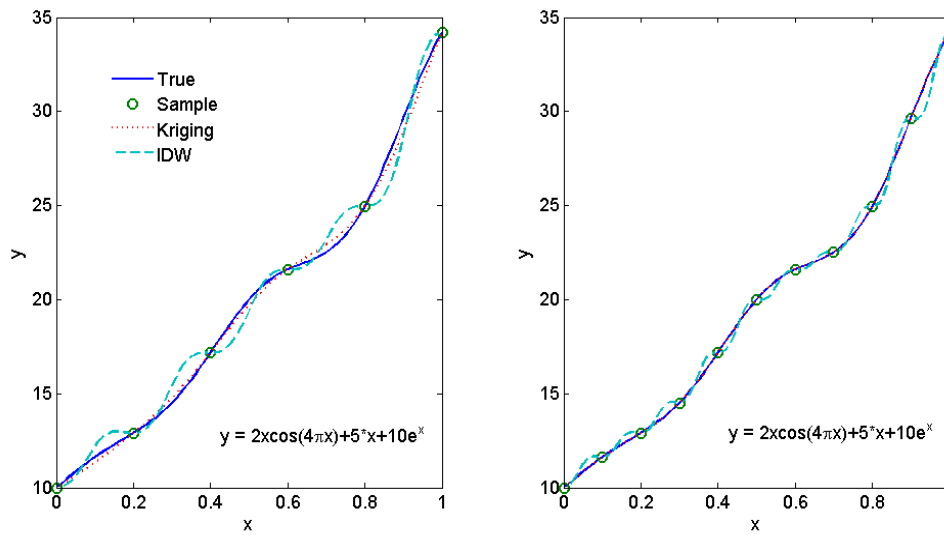
Kriging method was tested and investigated as there was a statistical basis for the weighting. With the developed interpolation approach, using our developed sampling design/method, and sampling analysis to characterize the soil contamination in case study 2-B Section of the Raudhatain Area for further improvements.

3.5.2 Method validation

To validate the developed tool and compare the performance of the Kriging and IDW, modeling was conducted on two theoretical mathematical functions of a single variable.

Figure 3.14 compares the modelling results of the two interpolation methods for a function based on different numbers of sampling points of B Section of the Raudhatain case study. It can be seen that Kriging presents much better results than IDW in the

closeness to the true curve. Kriging has also been less influenced by the number of the sampling points.



6 sampling points

(b) 11 sampling points

Figure 3.14 Comparison of the Kriging and IDW on a smooth curve

Figure 3.15 compares the two methods in the modelling of a function of a steep variation, i.e. where a similar result can be noticed. (as that of the Fig. 3.14 above) In this case, it can be clearly observed that Kriging has a certain advantage for the properties of a steep spatial variation.

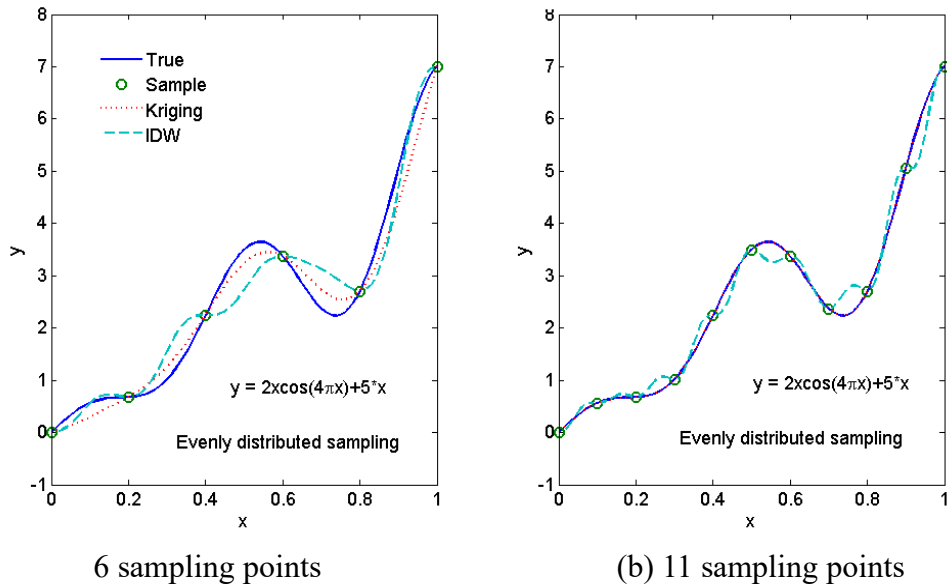


Figure 3.15 Comparison of the Kriging and IDW on a curve of steep variation

Figure 3.16 compares the modelling results of the two methods based on randomly distributed sampling points. Fig. 3.16(a) shows that both methods perform poorly when extrapolate the data based on the sampling points in a small region for a wide region. Fig. 3.16(b) shows that Kriging produced significant improvement if the random sampling points covered the whole interpolation range.

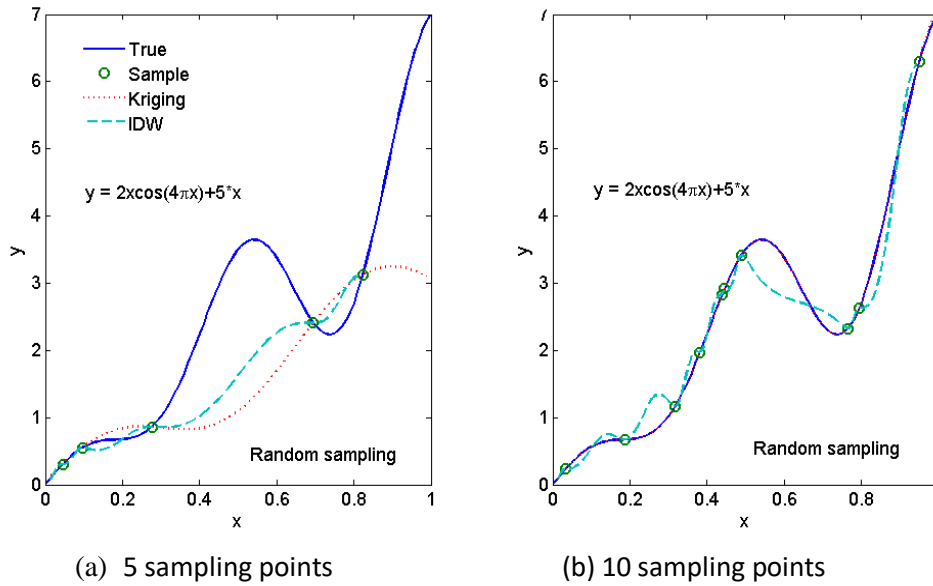


Figure 3.16 Comparison of the Kriging and IDW on random sampling points

From the three validation tests, it can be concluded that Kriging is a more accurate method than IDW. It produces a more reliable prediction for data interpolation rather than extrapolation. As a result, this study will use the Kriging method and interpolation approach presented below to characterize the soil field contamination.

3.5.3 Novel theory development for hydrocarbon-contaminated soil

The novel 3-D mapping for soil characterization characteristics include but not limited to:

- COST: less numbers of sampling
- TIME: Cover more distance and areas, with less sampling, 3-D mapping software easy to use to provides the required data and information.
- QUALITY: All samples analyzed in approved lap shipped from Kuwait, analyzed in developed program which make the deference;

From the above section, it is understood that both Kriging and IDW applied in this project produce predictions for the contamination profile in surface direction. For

the local contamination degree in depth direction, we noticed that both Kriging and IDW had poor performance, because they do not consider any physical mechanisms of the soil contamination process. One advantage of our novel investigation in this project is the consideration of the vertical infiltration mechanism and the corresponding vertical contamination profile modelling by using Fick's First Law, which has been proved to be more reasonable and accurate.

Fick's First Law relates the diffusive "to spread way out" flux to the concentration under the assumption of steady state. It hypothesizes that the flux goes from regions of high concentration to regions of low concentration across a concentration gradient (Atkins et al. 2006).

We assume contaminate ingress and transportation process for crude oil vertical contamination in soils downwards. The contaminating hydrocarbon components' concentration profile within the soil changes with time going on. The transportation process of the contaminating components in soil can be described using Fick's First Law (Eq. 12). We solved the parabolic problems using MATLAB PDE Tool to develop 1-D modeling as interpolation approach combined with Kriging method. In one spatial dimension the law can be written:

$$J_x = -D \frac{dC}{dx} \tag{12}$$

where J_x (mole/m²s) is the flux of the hydrocarbon through a cross section perpendicular to the flow direction x (m). D (m² /s) is called the diffusion coefficient, and C (mole/m³) is the concentration of crude oil at a specific position along x . the mass increase in the volume = mass flow in - mass flow out + mass generated in the volume figure (Fig. 3.17) below.

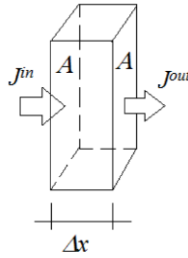


Figure 3.17 The mass increase in the volume = mass flow in - mass flow out + mass generated in the volume

Modelling crude ingress into soil in the environment. If we do not consider mass generated in the volume at this stage, i.e. there is no extra crude added in the ingress process the Eq. 13 can be rewritten as:

$$\frac{\partial C}{\partial t} = \frac{\partial}{\partial x} \left(D \frac{\partial C}{\partial x} \right) \quad (13)$$

We used MATLAB PDE tool to solve the above equation to model the crude ingress. We have investigated and applied our theory in Sampling Locations 4 and 5 of (Fig. 3-18 a and b) 2-B Section of the Raudhatain Area.

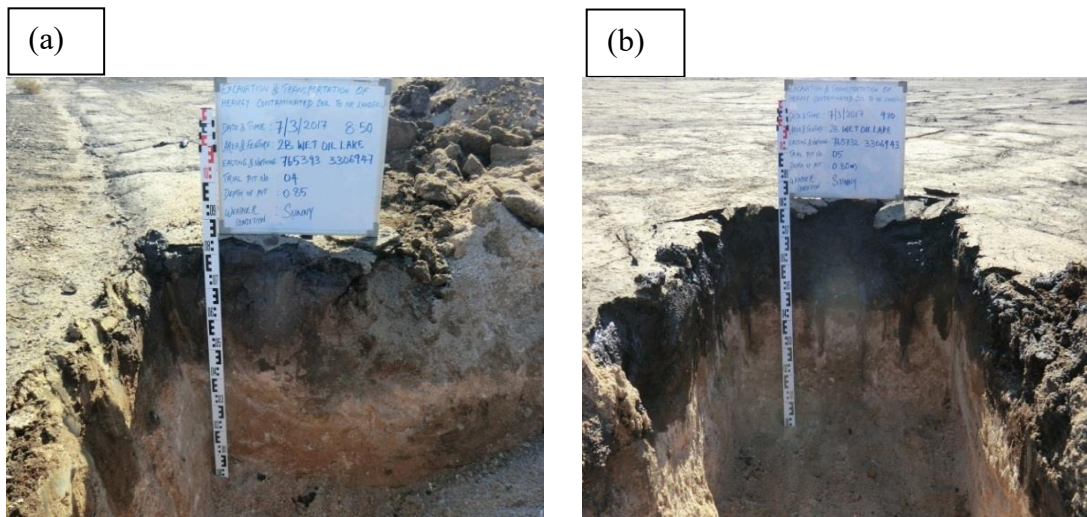


Figure 3.18 Images showing soil profiles at Sampling Locations (a) 4 and (b) 5

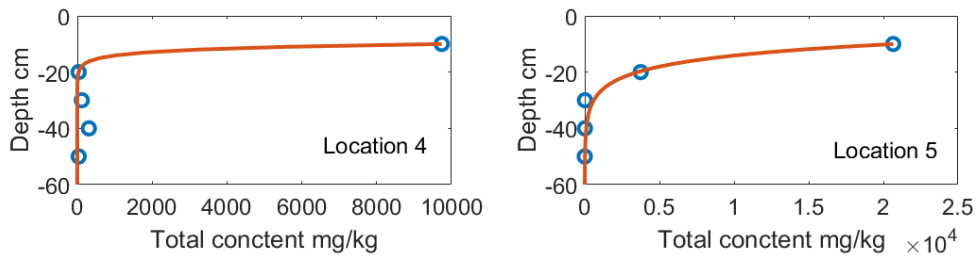


Figure 3.19 Fick's First Law for the contaminated profile in depth

Fig. 3.19 shows a predicted total contaminate concentration profile in depth direction using the infiltration model of the Eq. (13). Compared with the prediction using interpolation method showed in Fig. 3.20, it can be seen that the prediction based on physical mechanisms (Fig. 3.19) gives out a logic shape of a curve without oscillation, i.e. the contaminated degree consistently decreases with the increase of the depth. The novelty of this research is to develop a coupled methodology and technology for 3D mapping of hydrocarbon contaminated sites, which optimistically exploits the efficiency of the interpolation technology for the effect of horizontally orientation of geographical characteristics on large scale field hydrocarbon contamination and the physical process modelling technology for local point underground contamination driven by vertical infiltration mechanism.

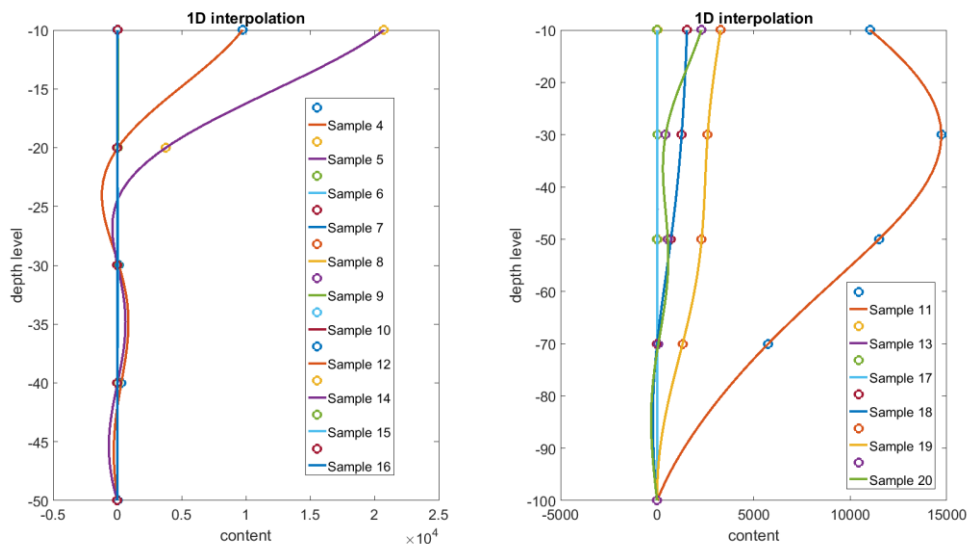


Figure 3.20 Graphs showing vertical variation in TPH along the soil's profiles using 1-D modeling

In our case, as the hydrocarbon soil contamination was old since 1990, we have

used the formula presented above Eq. 12. We considered no variables to have effects in the contaminated soil such as evaporation rate or weather, as this was done long time ago. For example, if the oil spill happened recently, several variable factors would be considered such as the evaporation rate, weather, time, etc. We could write a MATLAB programme which solve a nonlinear problem, in which we will take account of all the mechanisms, including the diffusion coefficient, D , and the local evaporation rate, R , for the following parabolic equation Eq. 14 governing crude oil transport in soil.

$$\frac{\partial C}{\partial t} = \frac{\partial}{\partial x} \left(D \frac{\partial C}{\partial x} \right) + \dot{R}$$

(14)

This could be considered as recommendation for further and future research study.

3.6 Conclusions

This chapter justifies the selection of the study sites and research methods used for collection of the required data for soil characterization, environmental risk assessment and 3-D predictive model development. Two study sites were selected, covering both oil lakes created during the First Gulf War and oil sludge pits produced during the oil extraction operations by KOC. Different soil sampling schemes were adopted for the two study sites. A range of analytical methods were selected to determine the petroleum hydrocarbons and other soil parameters in the investigated soils.

Chapter 4

Geochemical Characteristics and Environmental Risk of the Crude Oil-Contaminated Soils in the Raudhatain Oil Lake

4.1 Introduction

Soil characteristics are basic information required for many purposes. For agricultural activities, they provide information for evaluating the suitability for crop production; to geotechnical engineer, they are essential information for making engineering design of the structures; for environmental remediation purpose, they are needed for developing remediation strategies and guiding selection of treatment technologies. The geochemical characteristics also provide information for tracking environmental changes. Given the widespread contamination of soils by petroleum hydrocarbons, there has been increasing research into the characteristics of PHC-contaminated soils. However, so far much of the research has focused on geotechnical characteristics of the PHC-contaminated soils (Shin & Das, 2000; Khomehchiyan, 2007; Rahman et al., 2007; Rahman et al., 2010; Rahman, 2011; Ijimdiya, 2012; Akinwumi et al., 2014; Rasheed, 2014; Oluremi et al., 2015). Investigations into the PHC-contaminated soils with a focus on other aspects are relatively limited. Osuji and Nwoye (2007) investigated the impacts of petroleum hydrocarbons on soil fertility and found that PHC contamination caused a reduction in soil pH. However, Wang et al. (2013) found that crude oil contamination increased the pH and reduced the availability of phosphorus in marsh soils. Agbogidi et al. (2007) revealed that crude oil-contaminated soils affected the nutrient status of maize grown in these soils. Aislabie et al. (2004) investigated the properties of petroleum hydrocarbon-contaminated flare pit soils in British Columbia, Canada. There has been great research interest in the microbial characteristics in the PHC-contaminated soils due to the potential to use petroleum hydrocarbon-degrading microbes for remediating the PHC-contaminated soils (Pinholt et al., 1979; Das and Mukherjee, 2007; Greer et al., 2010).

The geochemical characteristics of oil-contaminated soil reflect the interactive effects of the original soil, the introduced petroleum hydrocarbons, the climatic conditions, the geomorphic feature and time. This knowledge can be used to explain

the fate, transformation and transport of the petroleum contaminants following the petroleum spills. It provides a basis for evaluating the environmental risk from the PHC-contaminated soils at the time of investigation, which will enable cost-effective remediation goals being achieved. Currently, systematic characterization of the oil lake soils is lacking. The set target for remediation of the oil-contaminated soils in the KERP program largely depends on the determination of total petroleum hydrocarbon (TPH) (Al-Gharabally & Al-Barood, 2015) that does not allow identification of environmental risk from the contaminating petroleum hydrocarbons with different levels of toxicity. The lack of a sensible risk-based approach is likely to result in unreliable evaluation of environmental risk from the oil-contaminated soils and lead to either under-treatment or over-treatment of the contaminated soils. There is therefore an urgent need to obtain sufficient understanding of the geochemical characteristics of the oil lake soils and their associated environmental risk in order to better guide the remedial action. This work aims to fill this knowledge gap.

4.2 Materials and Methods

The information on the study site and research methods used to collect soil data presented in this chapter can be seen in Chapter 3.

4.3 Results

4.3.1 Soil morphology

The soil morphology of the 17 investigated soil profiles Figure 4.1 is described below.

4.3.1.1 Profile TP-04

It is observed that there was a layer of black crust from 0 to 0.02 m, which could be considered as a tar mat layer. From 0.02 to 0.15 m was the black oily sludge. From 0.15 to 0.40 m, the soil was dark grayish brown with silty fine to medium sand and medium dense residual contamination, which could be considered as a soot layer. From 0.40 to 0.85m, the soil was light grayish brown with slightly gravelly fine to medium sand. In some areas, a layer of sandy soil over a layer of yellowish-brown sand. Soil moisture was medium (Fig. 4.3).



Figure 4.2 Photograph showing the morphology of Soil Profile TP-04.

4.3.1.2 Profile TP-05

It is observed that from 0-0.02 m, there was a layer of highly contaminated black crust with observation of tar mat. This was where the oil contamination was most likely to occur as oil penetrated from the surface downward into the soil. From 0.02 to 0.20 m, it was black oily sludge. From 0.20 to 0.34 m, the soil was dark grayish brown with silty fine to medium sand. From 0.34 to 0.80 m, it was a layer of light grayish brown with slightly gravelly fine to medium sand. The nearby area had sludge and crash and the depth of the sludge is varying (Fig. 4.4).



Figure 4.3 Photograph showing the morphology of Soil Profile TP-05.

4.3.1.3 Profile TP-06

A layer of black and a dark brown crust was observed from 0-0.03 m, which consisted of highly contaminated sandy soil with tar mat. From 0.03 to 0.19 m was black liquid or semi-solid oil, oily sludge. From 0.19 to 0.22 m, the soil had dark grayish brown colour with slightly gravelly fine to medium sand. From 0.22 to 0.75 m, the soil contained slightly gravelly fine to medium sand with light grayish, brown colour. A pipeline near the pit was observed (Fig. 4.5).



Figure 4.4 Photograph showing the morphology of Soil Profile TP-06.

4.3.1.4 Profile TP-07

The black crust layer with highly contaminated sandy soil occurred from 0 to 0.02 m. From 0.02 to 0.08 m, there was a layer of black oily sludge. From 0.08 to 0.26 m, the soil was dark grayish brown with slightly gravelly fine to medium sand. From 0.26 to 0.50 m the soil had grayish brown colour with slightly gravelly fine to medium sand. From 0.50 to 0.90 was light greyish brown soil with silty fine to medium sand. In some areas, there was appearances of tar mat with a thickness of 1 to 2 cm, which was black in color, with a moderately hard, dry consistency. They occurred in shallow depressions and flat areas, often around the edges of oil, which could be considered in general as oil lakes (Fig. 4.6).

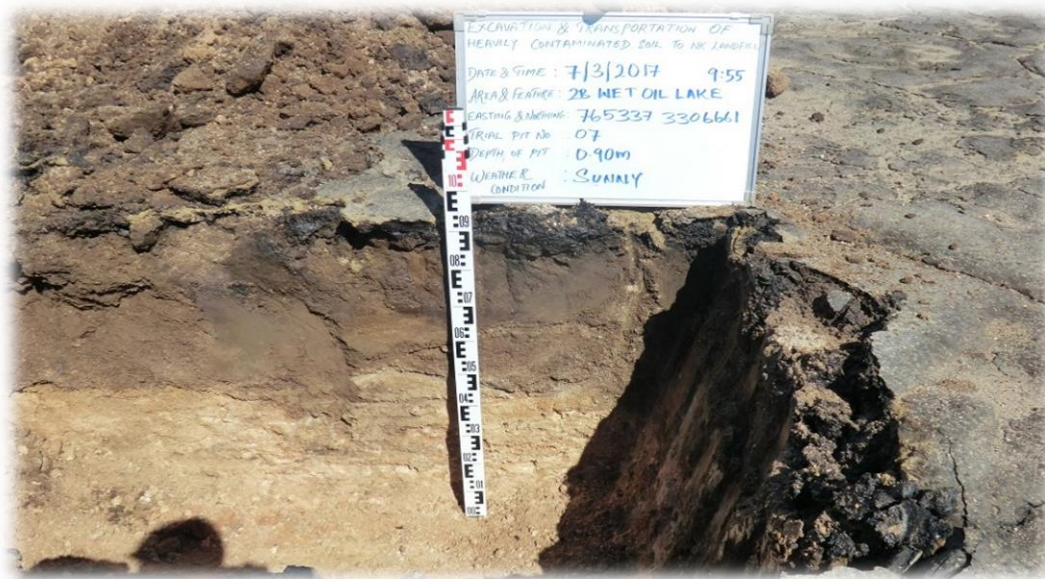


Figure 4.5 Photograph showing the morphology of Soil Profile TP-07.

4.3.1.5 Profile TP-08

It is observed that from 0- 0.02 m black crust, highly contaminated layer-1A covered with tarcreat. From 0.02 to 0.08m Black oily sludge, highly contaminated tar mat layer. From 0.08 to 0.33m the soil is dark grayish brown, fine to medium sand, residual contamination medium dense, layer- 2 soot layer occurs in the upper layer of the soil. From 0.33 to 0.90 m light grayish brown, slightly gravelly, fine to medium sand, Layer-3 (Fig. 4.7).



Figure 4.6 Photograph showing the morphology of Soil Profile TP-08.

4.3.1.6 Profile TP-09

It is observed from 0-0.03 m black crust with oily sludge, highly contaminated layer- 1 as provided on (Fig. 4.8). From 0.03 - 0.40m dark greyish brown, silty fine to medium sand, residual contamination moist, medium dense layer-2, sample taken 0.24-0.28 m. From 0.40 to 1.00 m the soil is light grayish brown, slightly gravelly, fine to medium sand, layer-3 clear soil, moist, medium dense.



Figure 4.7 Photograph showing the morphology of Soil Profile TP-09.

4.3.1.7 Profile TP-10

It is observed from 0-0.01 m black crust, highly contaminated layer-1A as provided on (Fig. 4.9) from 0.01 - 0.07 m Black oily sludge highly contaminated layer-1B. From 0.07-0.43m dark greyish brown, silty fine to medium sand, residual contamination moist, medium dense layer -2. From 0.43 to 0.90 m the soil is light grayish brown, slightly gravelly, fine to medium sand, layer-3 clear soil, moist, medium dense.



Figure 4.8 Photograph showing the morphology of Soil Profile TP-010.

4.3.1.8 Profile TP-11

It is observed in (Fig. 4.10) that from 0-0.01 m black crust, highly contaminated layer-1A tar mat. From 0.01 - 0.06 m Black oily sludge highly contaminated layer- 1B. From 0.06-0.32 m dark greyish brown, silty fine to medium sand, residual contamination moist, loose layer-2. From 0.32 to 1.08 m the soil is light grayish brown, slightly gravelly, fine to medium sand, layer-3 clear soil, moist, medium dense.



Figure 4.9 Photograph showing the morphology of Soil Profile TP-011.

4.3.1.9 Profile TP-12

It is observed in (Fig. 4.11) that from 0-0.03 m black crust, highly contaminated layer-1. From 0.03 - 0.34m dark greyish brown, silty fine to medium sand, residual contamination moist, loose layer- 2 area covered by tarcrete. From 0.34 to 0.96 m the soil is light grayish brown, slightly gravelly, fine to medium sand, layer-3 clear soil, moist, medium dense. No sludge observed in this pit, crust and sludge observed in the vicinity of the pit.

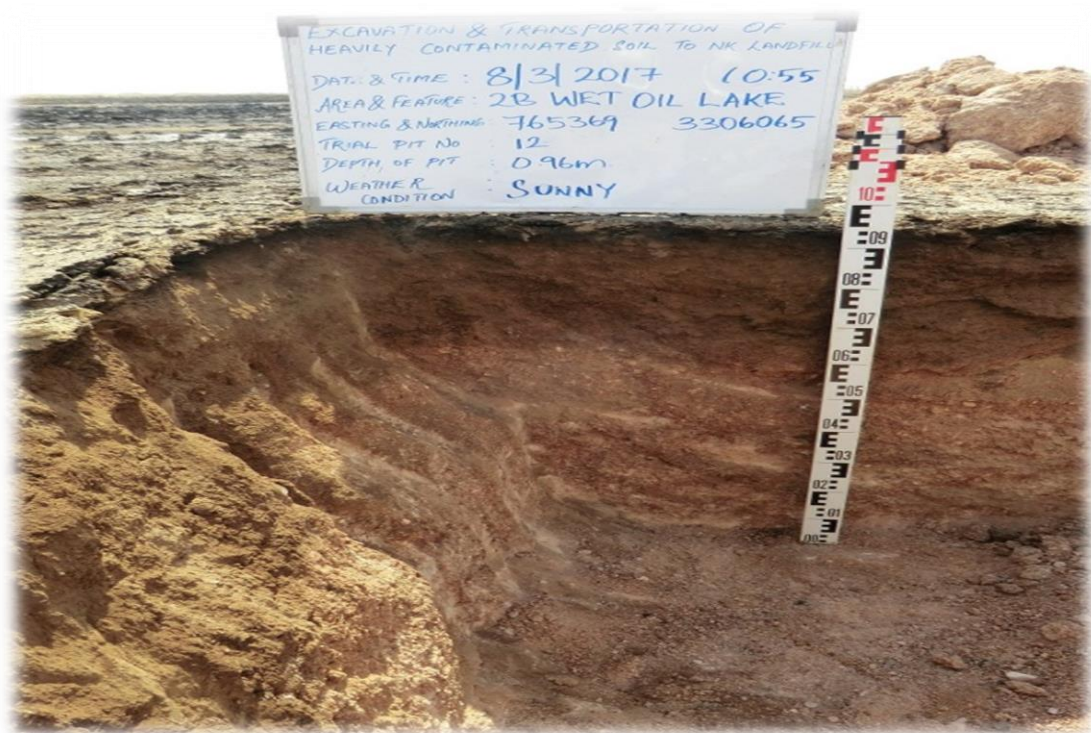


Figure 4.10 Photograph showing the morphology of Soil Profile TP-012.

4.3.1.10 Profile TP-13

It is observed that from 0-0.02 m black crust, highly contaminated layer-1A as provided on (Fig. 4.12). From 0.02 - 0.06 m Black oily sludge, Highly contaminated layer-1B. From 0.06-0.46 dark greyish brown, silty fine sand, residual contamination moist, loose layer- 2. From 0.46 to 1.10 m the soil is light grayish brown, slightly gravelly, fine sand, layer-3 clear soil, moist, medium dense. Contamination is varying in this pit. vehicles and truck wheel print around the area, which mix the layers as we can see some tar, soot and sludge mixed together.



Figure 4.11 Photograph showing the morphology of Soil Profile TP-013.

4.3.1.11 Profile TP-14

It is observed in (Fig. 4.13) that from 0-0.02 m black crust, highly contaminated layer-1A. From 0.02 - 0.09 m Black oily sludge, highly contaminated layer-1B. From 0.09-0.56 dark greyish brown, silty fine sand, residual contamination moist, medium dense layer-2. From 0.56 to 1.14 m the soil is light grayish brown, slightly gravelly, fine to medium sand, layer-3 clear soil, moist, medium dense. Contamination is varying in this pit. Actual coordinate was relocated due to pressure of dry oil lake.



Figure 4.12 Photograph showing the morphology of Soil Profile TP-014.

4.3.1.12 Profile TP-15

It is observed (Fig. 4.14) that from 0- 0.01 m black crust, highly contaminated layer-1A. From 0.01 - 0.04 m Black oily sludge, highly contaminated layer-1B. From 0.04-0.09 m dark greyish brown, silty fine sand, residual contamination moist, loose layer-2A. From 0.09 to 0.53 m the soil is light grayish brown, slightly gravelly, fine to medium sand, layer-2B residual, contamination oily smell, moist medium dense. From 0.53-1.10 m light reddish brown, silty, slightly gravelly, fine to medium sand, clear soil moist medium dense layer-3. It is observed that the contamination is varying in this pit.



Figure 4.13 Photograph showing the morphology of Soil Profile TP-015.

4.3.1.13 Profile TP-16

(Fig. 4.15) show that from 0-0.01 m black crust, highly contaminated layer-1 A tarcrete. From 0.01-0.05 m Black oily sludge, highly contaminated layer-1B. From 0.05-0.10 dark greyish brown, silty fine sand, residual contamination moist, loose layer-2A oil mat. From 0.10 to 0.45 m the soil is grayish brown, slightly gravelly, fine sand, layer-2B soot layer mixed with the upper soil layer residual contamination moist, loose. From 0.45-1.30 light reddish brown, silty, slightly gravelly, fine to medium sand, clear soil moist medium dense layer-3. Actual coordinate was relocated due to pressure of dry oil lake. It is observed that the surrounding area is having solidified crust and oily sludge.



Figure 4.14 Photograph showing the morphology of Soil Profile TP-016.

4.3.1.14 Profile TP-17

It is observed (Fig. 4.16) that from 0-0.02 m black crust, highly contaminated layer-1A the area covered by tarcrete. From 0.02 - 0.17 m Black oily sludge, highly contaminated layer-1B. From 0.17-0.82 dark greyish brown, silty fine sand, residual contamination moist, medium dense soot layer. Layer-2. From 0.82 to 1.35 m the soil is light grayish brown, slightly gravelly, fine to medium sand, layer-3 clear soil moist. It been observed that water was trapped between crust and oily sludge.



Figure 4.15 Photograph showing the morphology of Soil Profile TP-017.

4.3.1.15 Profile TP-18

It is observed in (Fig. 4.17) that from 0- 0.02 m black crust tarcrete, highly contaminated layer-1A a tar mat layer. From 0.02 - 0.19 m Black oily sludge, highly contaminated layer-1B with black fragments in the soil matrix could considered as soot layer. From 0.19- 1.09 dark greyish brown, silty fine sand, residual contamination moist, medium dense. layer-2. From 1.09 to 1.40 m the soil is light grayish brown, slightly gravelly, fine to medium sand, layer-3 clear soil moist.



Figure 4.16 Photograph showing the morphology of Soil Profile TP-018.

4.3.1.16 Profile TP-19

It is observed in (Fig. 4.18) that from 0- 0.08 m black crust, highly contaminated layer-1A. From 0.08 - 0.52 m Black oily sludge, highly contaminated layer-1B. From 0.52- 0.80 dark greyish brown, fine to medium sand, residual contamination moist, medium dense. layer-2. From 0.80 to 1.25 m the soil is light grayish brown, slightly gravelly, fine to medium sand, layer-3 clear soil moist, medium dense tar mat.



Figure 4.17 Photograph showing the morphology of Soil Profile TP-019.

4.3.1.17 Profile TP-20

It is observed in (Fig. 4.19) that from 0- 0.005 m black crust, highly contaminated layer. From 0.005-0.04 m, black oily sludge, highly contaminated layer-1B. From 0.04-0.79 m dark greyish brown, fine sand, residual contamination moist, medium loose layer-2. From 0.97 to 0.99 m the soil is grayish brown, silty, fine sand, layer-3A clear soil, moist, loose. From 0.99 to 1.70 m light reddish brown, slightly gravelly, fine to medium sand, layer-3B clear soil moist, medium dense.



Figure 4.18 Photograph showing the morphology of Soil Profile TP-020.

4.3.2 Petroleum Hydrocarbons

4.3.2.1 Total petroleum hydrocarbon (TPH)

The depth of contamination was limited to the top 50 cm of the soil profiles except in 4 Locations (11, 18, 19 and 20) Figure 4.19 where the depth of contamination extended to about 1 meter from the soil surface (Tables 4.1 and 4.2). TPH in the contaminated soils was highly variable both horizontally and vertically. For the 13 shallow soil profiles (Locations 4, 5, 6, 7, 8, 9, 10, 12, 13, 14, 15, 16 and 17), the mean \pm SD was 7717 \pm 6370, 2991 \pm 3300, 1636 \pm 2108, 710 \pm 1438 and 5 \pm 11 mg/kg for the 0-10 cm soil, 10-20 cm soil layer, 20-30 cm soil layer, 30-40 cm soil layer and 40-50 cm layer, respectively (Table 4.1). For the 4 deep soil profiles (Locations 11, 18, 19 and 20), the mean \pm SD was 32445 \pm 38146, 9415 \pm 4043, 10415 \pm 2391, 4255 \pm 4769 and 429 \pm 708 mg/kg for the 0-20 cm soil, 20-40 cm soil layer, 40-60 cm soil layer, 60-80 cm soil layer and 80-100 cm layer, respectively (Table 4.2). The lowest profile average of TPH (76 mg/kg) was recorded in Location 8 while the highest profile average of TPH (20604 mg/kg) was found in Location 11. The soils with a TPH concentration of over 10000 mg/kg (>1%) were only found at 9 out of 17 sampling locations (i.e. Locations 5, 7, 10, 11, 13, 15, 18, 19 and 20) and limited to the topsoil layer (0-10 cm) except for Soil Profiles 11, 18, 19 and 20, where a high level of TPH was detected to a depth of 60 cm (Table 4.2).

Table 4.1 TPH (mg/kg) in the soils for the soil profiles with the depth of contamination limited to the top 50 cm

Location	0-10 cm	10-20 cm	20-30 cm	30-40 cm	40-50 cm	Mean	SD
4	9740	36	120	309	37	2048	4301
5	20656	3744	13	8	0	4884	8964
6	0	316	0	782	0	220	343
7	13780	4860	3811	176	0	4525	5605
8	380	0	0	0	0	76	170
9	6111	4585	1438	1540	0	2735	2520
10	11940	10850	2741	0	0	5106	5862
12	1749	0	0	0	0	350	782
13	11700	5510	2630	563	13	4083	4773
14	3601	34	0	0	0	727	1607
15	11681	4228	6242	5253	14	5484	4199
16	21	0	18	584	0	125	257
17	8960	4720	4260	18	7	3593	3747
Mean	7717	2991	1636	710	5		
SD	6370	3300	2108	1438	11		

Different vertical variation patterns were observed. The most common pattern was that TPH decreased gradually with increasing depth (7 soil profiles). Other patterns included sudden decrease in TPH from the surface layer to the subsoil layer (4 soil profiles) and no marked decrease in TPH within the top 60 or 80 cm of the soil profiles (2 soil profiles). In addition, there were a few soil profiles that exhibited vertical TPH fluctuation along the soil profiles with greater TPH value in the soil layer underlying the upper layer(s) with lower TPH value (Tables 4.1 and 4.2).

Table 4.2 TPH (mg/kg) in the soils for the soil profiles with the depth of contamination extending beyond 50 cm

Location	0-20 cm	20-40 cm	40-60 cm	60-80 cm	80-100 cm	Mean	SD
11	89526	4209	8778	494	13	20604	38689
18	13679	13375	13896	14	163	8225	7430
19	10053	8384	10061	9686	52	7647	4301
20	16522	11693	8924	6824	1487	9090	5590
Mean	32445	9415	10415	4255	429		
SD	38146	4043	2391	4769	708		

4.3.2.2 Benzene, toluene, ethylbenzene and xylenes (BTEX)

BTEX were not detected for most of the locations except for profiles 11, 18, 19 and 20. The sum of BTEX in these 4 locations ranged from 0 to 14350 mg/kg with a

mean value of 686 mg/kg. Xylene (o-xylene and m/p-xylene) dominated BTEX (83%). BTEX tended to decrease with increasing depth within the soil profile but different vertical variation patterns were observed. However, for profile 11, the concentration of toluene, ethylbenzene and xylenes was lower in the surface layer (0-20 cm) than in the subsoil layer (20-60 cm). The distribution of BTEX in different soil layers more or less maintained the same patterns with soil profile 11 showing the following decreasing order: m/p xylene > o xylene > ethylbenzene > toluene while other soil profiles showing the trend of m/p xylene > o xylene > ethylbenzene > toluene (Table 4.3).

Table 4.3 BTEX ($\mu\text{g}/\text{kg}$) in the soils for the soil profiles 11, 18, 19 and 20

Location		0-20 cm	20-40 cm	40-60 cm	60-80 cm	80-100 cm	SD
11	Benzene	udl	udl	udl	udl	udl	0
	Toluene	520	450	630	220	udl	253
	EthylBenzene	1500	2000	1500	780	udl	779
	M/P Xylene	5000	6700	5200	2600	udl	2629
	O Xylene	3800	5200	3900	2000	udl	2018
18	Benzene	udl	udl	udl	18	18	10
	Toluene	8	5	<5	18	18	7
	EthylBenzene	100	82	42	18	18	37
	M/P Xylene	560	460	250	18	18	249
	O Xylene	810	670	390	18	18	364
19	Benzene	udl	udl	udl	udl	udl	0
	Toluene	12	udl	10	5	udl	6
	EthylBenzene	300	250	200	120	udl	118
	M/P Xylene	1100	830	660	370	udl	424
	O Xylene	1800	1500	1400	790	udl	715
20	Benzene	udl	udl	udl	udl	udl	0
	Toluene	10	3	2	udl	udl	4
	EthylBenzene	160	26	38	6	udl	66
	M/P Xylene	830	140	200	22	udl	341
	O Xylene	1200	250	290	37	udl	489

4.3.2.3 Aliphatic hydrocarbons

Like TPH, the sum of aliphatic hydrocarbons (total aliphatic hydrocarbon) was highly variable both horizontally and vertically (Fig. 4.20). For the soils with contamination depth <50 cm (Locations 4, 5, 6, 7, 8, 9, 10, 12, 13, 14, 15, 16 and 17),

the mean±SD was 7678±6347, 2965±3288, 1628±2103, 709±1434 and 5±11 mg/kg for the soil layers 0-10 cm, 10-20 cm, 20-30 cm, 30-40 cm and 40-50 cm, respectively (Fig. 4.20a). For the soils with contamination depth >50 cm, the mean±SD was 31441±37546, 8930±3780, 10090±2284, 3895±4357 and 412±675 mg/kg for the soil layers 0-20 cm, 20-40 cm, 40-60 cm, 60-80 cm and 80-100 cm, respectively (Fig. 4.20b).

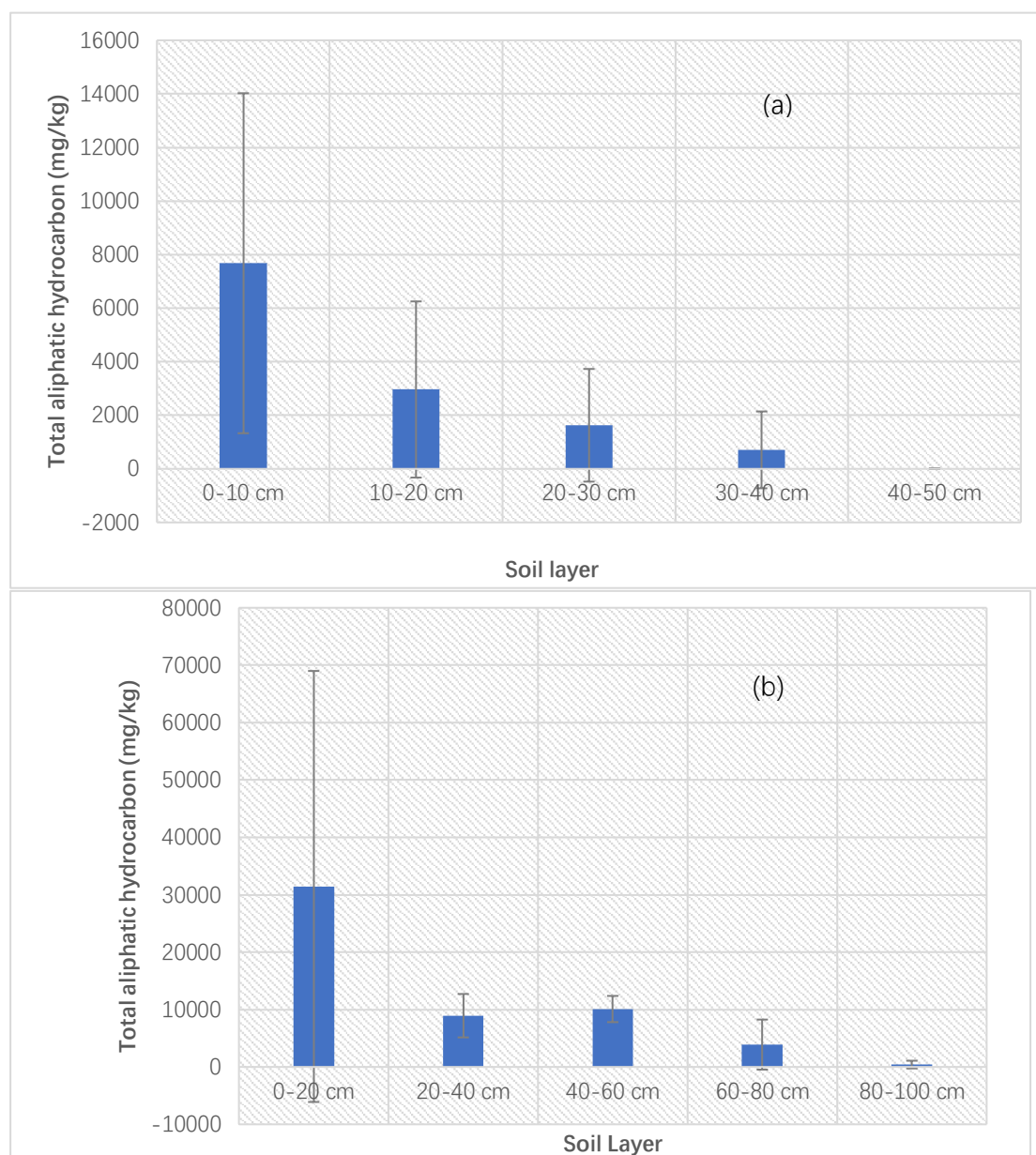


Figure 4.20 Horizontal and vertical variation in total aliphatic hydrocarbon for (a) the soils with contamination depth <50 cm, and (b) the soils with contamination depth >50 cm

In most situations, Fraction C16-C35 dominated the aliphatic hydrocarbons and in general, the following decreasing order was observed: C21-35 > C16-21 > C12-16 >

C35-40 > C10 -12. Fraction <C10 was only at trace amount or non-detectable (Figs. 4.21 and 4.22).

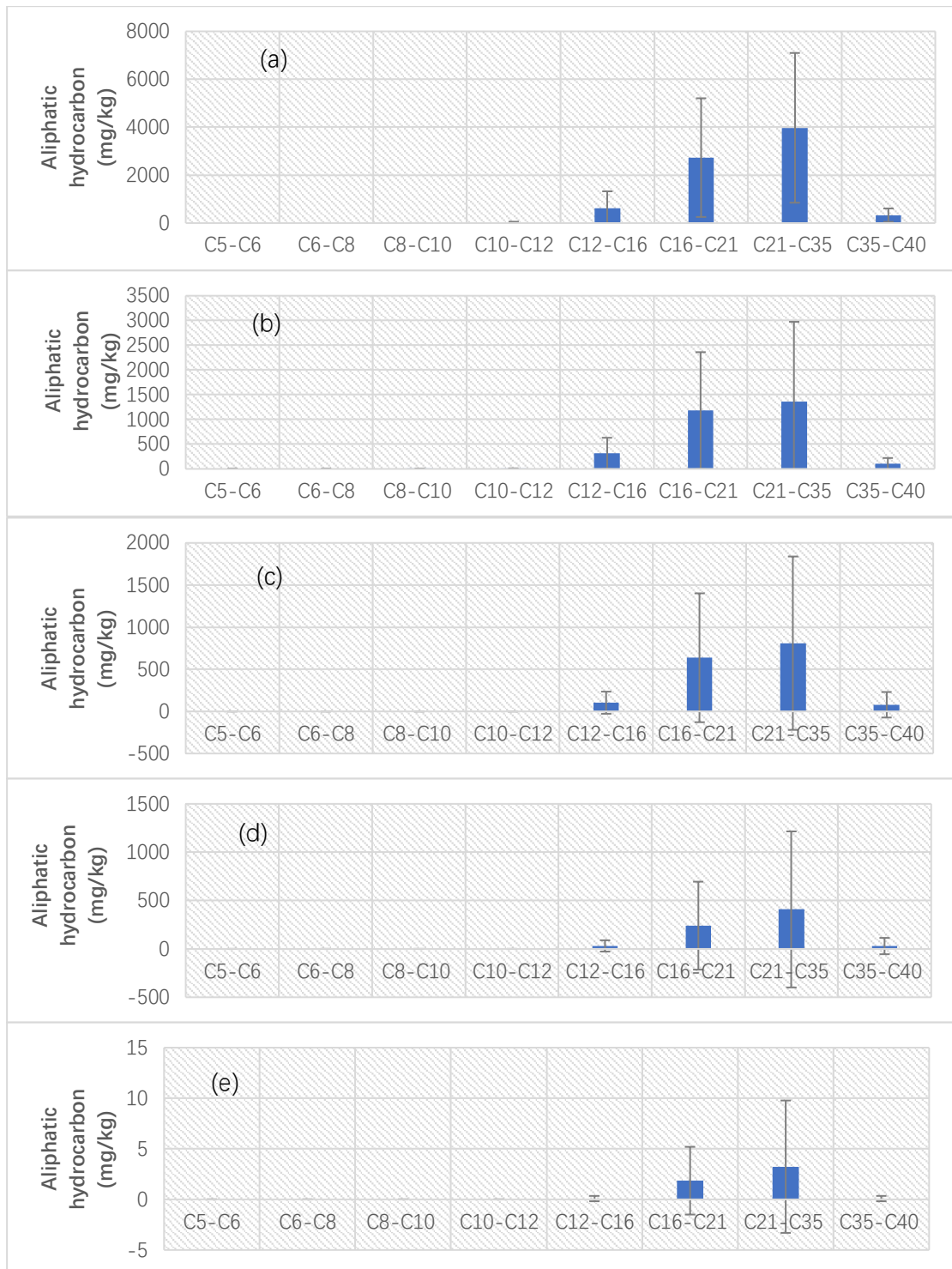


Figure 4.21 Distribution patterns of different aliphatic hydrocarbon fractions for the soil profiles with a contamination depth <50 cm

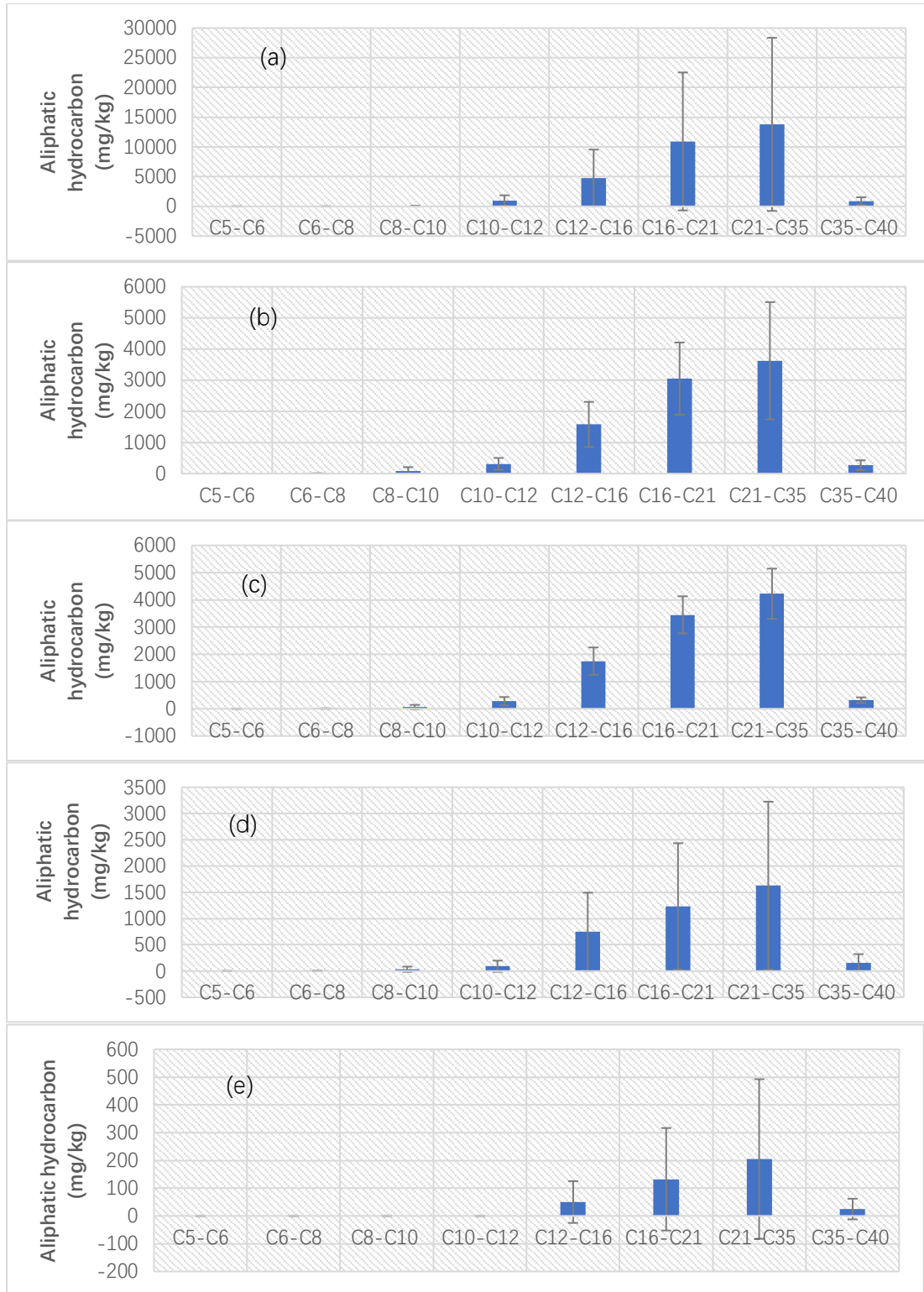


Figure 4.22 Distribution patterns of different aliphatic hydrocarbon fractions for the soil profiles with a contamination depth <50 cm

4.3.2.4 Aromatic petroleum hydrocarbons

No or only a small amount (<50 mg/kg) of aromatic hydrocarbons was detected in most of the investigated soil profiles (data not shown) except for Locations 5, 9, 11, 15, 18, 19 and 20. In most situations, Fraction C8-C16 dominated the aromatic hydrocarbons (Table 4.4).

Table 4.4 Aromatic petroleum hydrocarbons in the investigated soil profiles

Profile	Depth (cm)	C6-C7	C7-C8	C8-C10	C10-C12	C12-C16	C16-C21	C21-C35	C35-C40
5	0-10	udl	udl	1.4	43	68	udl	udl	udl
	10-20	udl	udl	0.34	13	udl	udl	udl	udl
	20-30	udl	udl	udl	udl	udl	udl	udl	udl
	30-40	udl	udl	udl	udl	udl	udl	udl	udl
	40-50	udl	udl	udl	udl	udl	udl	udl	udl
9	0-10	udl	udl	2.7	99	80	udl	udl	udl
	10-20	udl	udl	1.2	85	200	udl	udl	udl
	20-30	udl	udl	udl	20	48	udl	udl	udl
	30-40	udl	udl	udl	udl	udl	udl	udl	udl
	40-50	udl	udl	udl	udl	udl	udl	udl	udl
11	0-20	udl	0.52	50	1100	710	udl	udl	udl
	20-40	udl	0.45	81	52	udl	udl	udl	udl
	40-60	udl	0.63	44	170	udl	udl	udl	udl
	60-80	udl	0.22	28	4	udl	udl	udl	udl
	80-100	udl	udl	udl	udl	udl	udl	udl	udl
15	0-10	udl	udl	0.49	53	58	udl	udl	udl
	10-20	udl	udl	0.24	13	25	udl	udl	udl
	20-30	udl	udl	0.27	19	13	udl	udl	udl
	30-40	udl	udl	0.11	udl	13	udl	udl	udl
	40-50	udl	udl	udl	udl	2	udl	udl	udl
18	0-20	udl	udl	21	190	200	udl	udl	udl
	20-40	udl	udl	17	190	240	udl	udl	udl
	40-60	udl	udl	12	190	270	udl	udl	udl
	60-80	udl	udl	udl	udl	udl	udl	udl	udl
	80-100	udl	udl	udl	udl	udl	udl	udl	udl
19	0-20	udl	udl	28	140	100	udl	udl	udl
	20-40	udl	udl	19	110	110	udl	udl	udl
	40-60	udl	udl	20	150	170	udl	udl	udl
	60-80	udl	udl	18	120	630	72	udl	udl
	80-100	udl	udl	udl	udl	udl	udl	udl	udl
20	0-20	udl	udl	34	350	880	180	32	udl
	20-40	udl	udl	12	240	670	200	udl	udl
	40-60	udl	udl	11	110	640	86	udl	udl
	60-80	udl	udl	1.1	62	440	65	udl	udl
	80-100	udl	udl	udl	udl	52	18	udl	udl

udl: under detection limit

For the soil profiles with shallower contamination depth (Profiles 5, 9 and 15), the level of aromatic hydrocarbons was lower and limited to a thinner surface soil layer, as compared to the soil profiles with deeper contamination depth (Profiles 11, 18, 19 and 20). Soil profile 11 had the highest level of total aromatic hydrocarbon in the top 10 cm of the soil profile. Different soil profiles had different dominant fraction; Soil Profile had Fraction C10-C12 being the most important fraction while Fraction C12-C16 was more important than C10-C12 in Soil Profile 20 (Table 4.4).

4.3.2.5 Polycyclic aromatic hydrocarbons

Polycyclic aromatic hydrocarbons in the surface soils were only detected from 9 out of the 17 sampling locations. The sum of the 16 investigated PAHs was less than 16 mg/kg with the total PAH greater than 10 mg/kg only being found at locations 10, 13 and 20. The total PAH in the surface soils of various sampling locations was in the following decreasing order: Location 20 > Location 13 > Location 10 > Location 18 > Location 11 > Location 7 > Location 19 > Location 9 > Location 5 (Table 4.5).

Table 4.5 Polycyclic aromatic hydrocarbons (PAHs) in the surface soils

Sampling location	5	7	9	10	11	13	18	19	20
Naphthalene	udl	0.3	1.6	udl	2.6	udl	3.5	2.2	5.4
Acenaphthylene	udl	0.4	udl	udl	0.3	0.3	udl	0.2	0.5
Acenaphthene	udl	0.2	udl	udl	udl	0.2	udl	udl	0.3
Fluorene	udl	0.2	udl	udl	0.7	0.2	udl	0.6	0.5
Phenanthrene	3.7	3.9	2.4	4.1	2.5	5.1	3.6	1.9	3.4
Anthracene	udl	udl	udl	4.1	udl	5	udl	udl	3.4
Fluoranthene	udl	udl	udl	udl	0.1	0.1	udl	udl	0.1
Pyrene	udl	0.6	udl	udl	0.3	0.4	udl	udl	0.4
Benzo(a)Anthracene	udl	0.6	udl	1.6	0.3	0.8	0.1	udl	0.6
Chrysene	udl	0.3	udl	1.7	0.2	0.9	0.6	0.5	0.7
Benzo(b)fluoranthene	udl	udl	udl	udl	udl	0.1	udl	udl	0.1
Benzo(k)fluoranthene	udl	0.1							
Benzo(a)pyrene	udl	0.2							
Indeno(123-cd)pyrene	udl								
Dibenzo(ah)anthracene	udl								
Benzo(ghi)perylene	udl	0.1							
Coronene	udl								
PAH (Sum)	3.7	6.5	4	12	7	13	7.8	5.4	16

Major PAH species included naphthalene, phenanthrene and anthracene, depending on the sampling locations. Phenanthrene was found in all the soil profiles

listed in Table 10. Other more common PAH species included benzo(a)anthracene and chrysene. Soil Profile 20 contained 13 out of the 16 investigated PAH species.

4.3.3 Other soil parameters

4.3.3.1 Soil pH

The investigated soils all had alkaline pH (>7). The soils (profiles 4-10) collected from the northern part of the study area tended to have a lower pH, as compared to those collected from the southern part of the study area (Tables 4.6 and 4.7).

Table 4.6 pH in the investigated soils collected from northern part of the study area

Location	0-10 cm	10-20 cm	20-30 cm	30-40 cm	40-50 cm	Mean
4	7.29±0.46	7.78±0.59	7.64±0.32	7.55±0.08	7.11±0.51	7.47
5	7.51±0.11	7.73±0.37	7.39±0.08	7.46±0.11	6.48±1.47	7.31
6	7.67±0.10	7.62±0.24	7.72±0.18	7.54±0.28	7.67±0.08	7.64
7	7.60±0.01	7.52±0.03	7.39±0.12	7.33±0.06	7.36±0.09	7.44
8	7.64±0.01	7.85±0.17	8.19±0.26	8.10±0.43	7.95±0.59	7.94
9	7.81±0.10	7.58±0.19	7.64±0.03	7.55±0.21	7.41±0.23	7.60
10	7.70±0.03	7.76±0.22	7.74±0.25	7.80±0.35	7.86±0.32	7.77
13	7.82±0.27	8.02±0.10	7.78±0.16	7.73±0.17	7.76±0.07	7.82
15	8.07±0.00	8.02±0.20	8.05±0.25	7.79±0.14	7.83±0.22	8.06
16	8.22±0.50	8.38±0.34	8.47±0.53	8.41±0.56	8.27±0.28	8.13
17	8.14±0.78	8.29±0.64	8.46±0.78	8.45±0.60	8.96±0.36	7.95
Mean	7.77	7.84	7.83	7.69	7.56	
SD	0.29	0.26	0.33	0.26	0.44	

For most of the investigated soil profiles, there was no clear increasing or decreasing trend for soil pH along the soil profile. 9.01 was the maximum pH detected in the subsoil layer (20-30 cm) at sampling location 17 (Tables 4.6 and 4.7).

Table 4.7 pH in the investigated soils collected from the southern part of the study area

Location	0-20 cm	20-40 cm	40-60 cm	60-80 cm	80-100 cm	Mean
11	8.09±0.14	8.03±0.45	8.07±0.39	8.09±0.23	8.26±0.29	8.11
12	8.09±0.23	8.32±0.53	8.33±0.31	8.26±0.10	8.06±0.40	8.21
14	8.13±0.09	8.17±0.19	8.16±0.28	7.97±0.01	7.91±0.24	8.06
18	8.21±0.37	8.42±0.35	8.22±0.05	7.63±0.61	7.84±0.30	8.06
19	8.28±0.51	8.14±0.23	8.27±0.08	8.15±0.24	7.82±0.53	8.13
20	7.97±0.21	7.89±0.36	8.21±0.34	7.78±0.54	7.90±0.59	7.95
Mean	8.13	8.16	8.21	7.98	7.96	
SD	0.11	0.19	0.09	0.24	0.17	

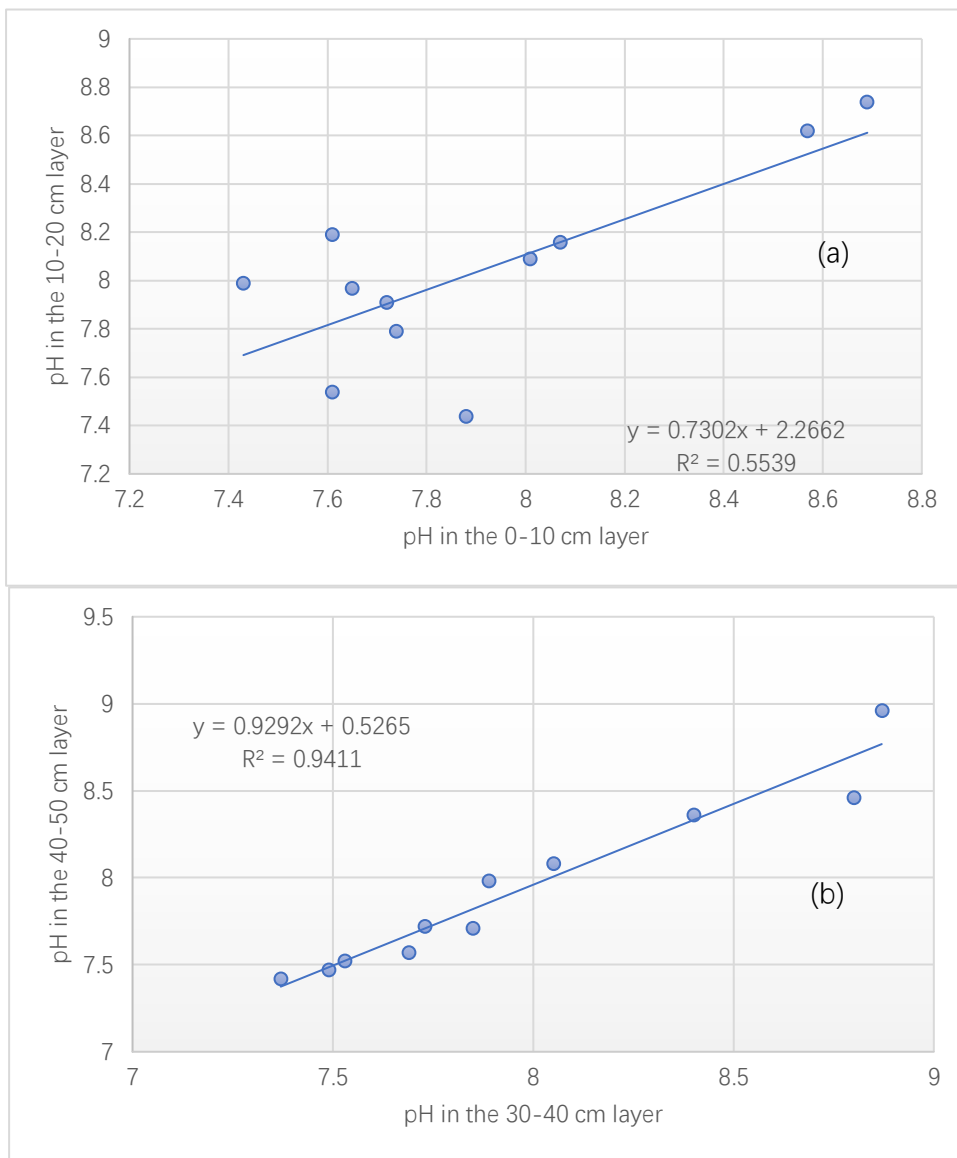


Figure 4.23 Relationship in pH between the adjacent soil layers. (a) the 0-10 cm layer vs the 10-20 cm layer, and (b) the 30-40 cm layer vs the 40-50 cm layer

The distribution patterns of pH for the different soil layers were different for the upper part of the soil profiles but were getting very similar for the lower part of the profiles. Fig. 4.23a showed the relationship of pH between the 0-10 cm layer and the 10-20 cm layer with a R² being 0.3271. However, the relationship of pH between the 30-40 cm layer and the 40-50 cm layer was very close with a R² > 0.94 being obtained (Fig. 4.23b).

4.3.3.2 Electrical conductivity (EC)

EC in the soils was highly variable amongst the investigated locations with the soil profile mean as low as 183 mS/m being recorded at Location 17 while over 5000 mS/m was detected at Location 5. No clear increasing or decreasing trend in soil EC was observed except for Soil Profile 8, which showed that EC decreased with increasing depth (Tables 4.8 and 4.9).

Table 4.8 EC (mS/m) in the investigated soils collected from northern part of the study area

Location	0-10 cm	10-20 cm	20-30 cm	30-40 cm	40-50 cm	Mean
4	2440±297	1055±106	2565±346	1805±220	1601±141	1893
5	4735±255	2700±219	6905±389	6315±113	5870±260	5305
6	1796±72	1289±72	1099±20	1826±44	1239±233	1450
7	2955±78	2875±0	3400±85	4530±92	3845±71	3521
8	2420±24	803±69	521±9	394±3	352±25	898
9	1224±35	2315±52	1954±64	2355±219	3845±134	2339
10	2125±57	2520±156	2560±20	1616±576	1123±10	1989
13	2500±161	906±78	3055±276	3165±141	3930±83	2711
15	2265±133	1716±205	1665±148	4415±170	3440±35	2700
16	655±14	280±21	336±1	339±19	307±39	383
17	153±15	352±6	166±2	168±26	150±16	198
Mean	2115	1528	2202	2448	2337	
SD	1217	947	1912	1976	1920	

The distribution patterns of EC for the different soil layers were different, particularly for the upper part of the soil profiles. Fig. 4.24a showed that the relationship of EC between the 0-10 cm layer and the 10-20 cm layer was poor (R²=0.3271). The relationship of EC between the adjacent soil layers were closer in the low part of the soil profiles, as showed in Fig. 4.24b that a R² > 0.86 was obtained.

Table 4.9 Electrical conductivity (mS/m) in the investigated soils collected from southern part of the study area

Location	0-20 cm	20-40 cm	40-60 cm	60-80 cm	80-100 cm	Mean
11	747±8	324±21	496±5	944±1	209±30	544
12	1099±29	770±41	771±90	1267±11	1478±212	1077
14	1192±40	792±56	745±23	1014±175	1396±78	1028
18	831±27	1070±71	670±78	3165±49	3495±32	1846
19	328±28	731±1	1131±62	456±35	1756±109	880
20	1423±137	1723±5	727±71	2200±71	1020±56	1419
Mean	937	902	757	1508	1559	
SD	386	468	208	995	1089	

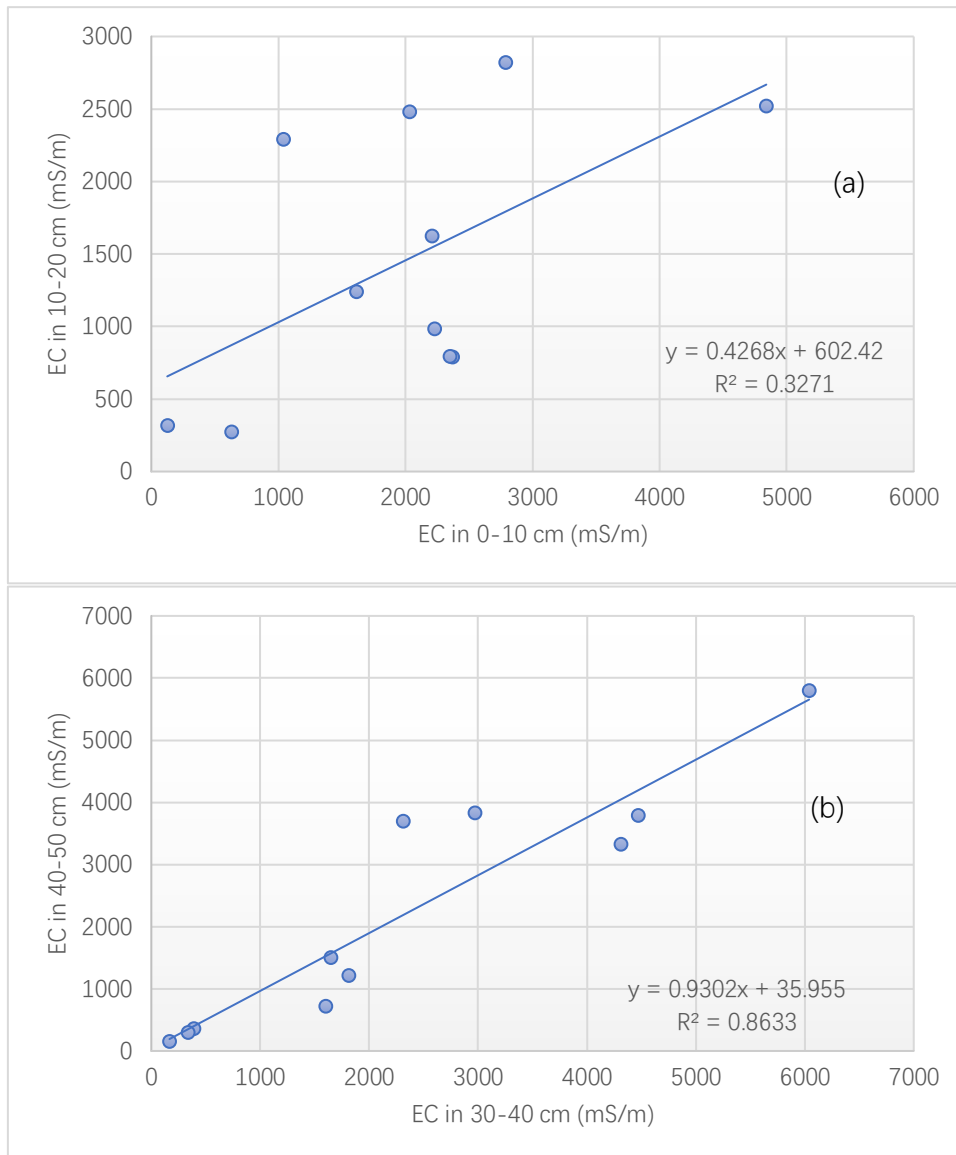


Figure 4.24 Relationship in EC between the adjacent soil layers. (a) the 0-10 cm layer vs the 10-20 cm layer, and (b) the 30-40 cm layer vs the 40-50 cm layer.

4.3.3.3 Chemical composition

The major elements detected from the two representative soil profiles (profile 10 and profile 19) included aluminium, calcium, iron, magnesium, manganese, phosphorus, potassium, silica, sodium and sulfur. The elements of potential toxicity such as arsenic, antimony and heavy metals were all at low levels (Tables 4.10 and 4.11).

Table 4.10 Chemical composition of the soil collected from Location 10

Element	0-10 cm	10-20 cm	20-30 cm	30-40 cm	40-50 cm	Mean	SD
Potassium	1400	1300	1100	780	870	1090	239
Sodium	7100	6000	7900	6900	11000	7780	1720
Aluminium	7600	8200	6500	4400	3200	5980	1900
Arsenic	5	4	6	4	3	4	1
Barium	130	38	56	24	15	53	41
Beryllium	<2	<2	<2	<2	<2	-	-
Calcium	72000	74000	96000	140000	120000	100400	26364
Cadmium	<1	<1	<1	<1	<1	-	-
Cobalt	7	7	5	3	2	5	2
Chromium	47	43	35	23	19	33	11
Copper	70	11	8	6	4	20	25
Iron	14000	14000	9200	6000	4000	9440	4076
Mercury	<1	<1	<1	<1	<1	-	-
Magnesium	12000	11000	9000	5300	3700	8200	3212
Manganese	320	280	210	120	65	199	95
Molybdenum	2	<2	<2	<2	<2	2	0
Nickel	51	49	36	22	12	34	15
Phosphorous	410	220	170	110	71	196	118
Lead	13	5	3	2	2	5	4
Antimony	4	1	1	<1	<1	2	1
Selenium	<3	<3	<3	<3	<3	-	-
Silica	950	970	760	720	720	824	112
Tin	3	2	<1	1	1	2	1
Sulfur	1000	1400	17000	69000	68000	31280	30935
Tellurium	2	1	1	<1	<1	1	0
Thallium	<1	<1	<1	<1	<1	-	-
Vanadium	49	44	35	22	19	34	12
Zinc	93	24	22	13	9	32	31

For the shallow soil profile, most of the elements showed a clear trend that the concentration decreased with increasing depth. However, calcium and sulfur exhibited a clear opposite trend that the concentration markedly increased with increasing depth. Sodium fluctuated within a range of 6000-8000 mg/kg in the top 40 cm of the soil

profile but suddenly increased to a level of 11000 mg/kg in the 40-50 cm layer. Phosphorus concentration ranged from 71 to 410 mg/kg with a mean value of 196 mg/kg (Table 4.10).

Table 4.11 Chemical composition of the soil collected from Location 19

Element	0-20 cm	20-40 cm	40-60 cm	60-80 cm	80-100 cm	Mean	SD
Potassium	1500	1400	1100	970	1300	1254	194
Sodium	960	500	610	940	270	656	264
Aluminium	9900	9700	7900	7500	11000	9200	1308
Arsenic	5	6	6	6	10	7	2
Barium	39	39	35	32	220	73	74
Beryllium	<2	<2	<2	<2	<2	-	-
Calcium	72000	81000	82000	82000	91000	81600	6020
Cadmium	<1	<1	<1	<1	<1	-	-
Cobalt	8	8	6	6	7	7	1
Chromium	50	47	39	38	52	45	6
Copper	12	12	9	9	7	10	2
Iron	16000	15000	10000	9200	13000	12640	2676
Mercury	<1	<1	<1	<1	<1	-	-
Magnesium	12000	11000	8900	8100	8200	9640	1576
Manganese	300	290	220	190	150	230	58
Molybdenum	<2	<2	<2	<2	<2	-	-
Nickel	62	55	41	37	30	45	12
Phosphorous	210	180	130	110	70	140	50
Lead	4	4	3	3	5	4	1
Antimony	1	1	<1	1	1	1	0
Selenium	<3	<3	<3	<3	<3	-	-
Silica	830	800	740	760	770	780	32
Tin	<1	<1	<1	1	1	1	0
Sulfur	800	400	400	400	300	460	174
Tellurium	1	1	1	1	<1	1	0
Thallium	<1	<1	<1	<1	<1	-	-
Vanadium	43	43	42	39	61	46	8
Zinc	25	24	17	17	22	21	3

For the representative deep soil profile, a decreasing trend down the soil profile (similar to the shallow soil profile) to a depth of at least 60 cm was observed for most of the investigated elements. However, many elements showed elevated concentration in the 80-100 cm layer. Like the shallow soil profile, the concentration of calcium increased with increasing depth but the magnitude of increase was smaller, as compared to the former. Unlike the shallow soil profile, the concentration of sulfur in the deep

soil profile was much lower, as compared to the former. The soil sulfur also showed a trend to decrease with the increasing depth rather than increase with the increasing depth, as observed in the shallow soil profile (Table 4.11).

The concentration of sulfate contain in the soils at the two selected locations was shown in Fig. 4.25. For the shallow soil profile (Profile 10), sulfate increased markedly with increasing depth, showing a trend exactly the same as the total sulfur (Fig. 4.25a). The concentration of sulfate in the deep soil profile was low, consistent with the total sulfur. However, the vertical variation was different from that for the total sulfur (Fig. 4.25b).

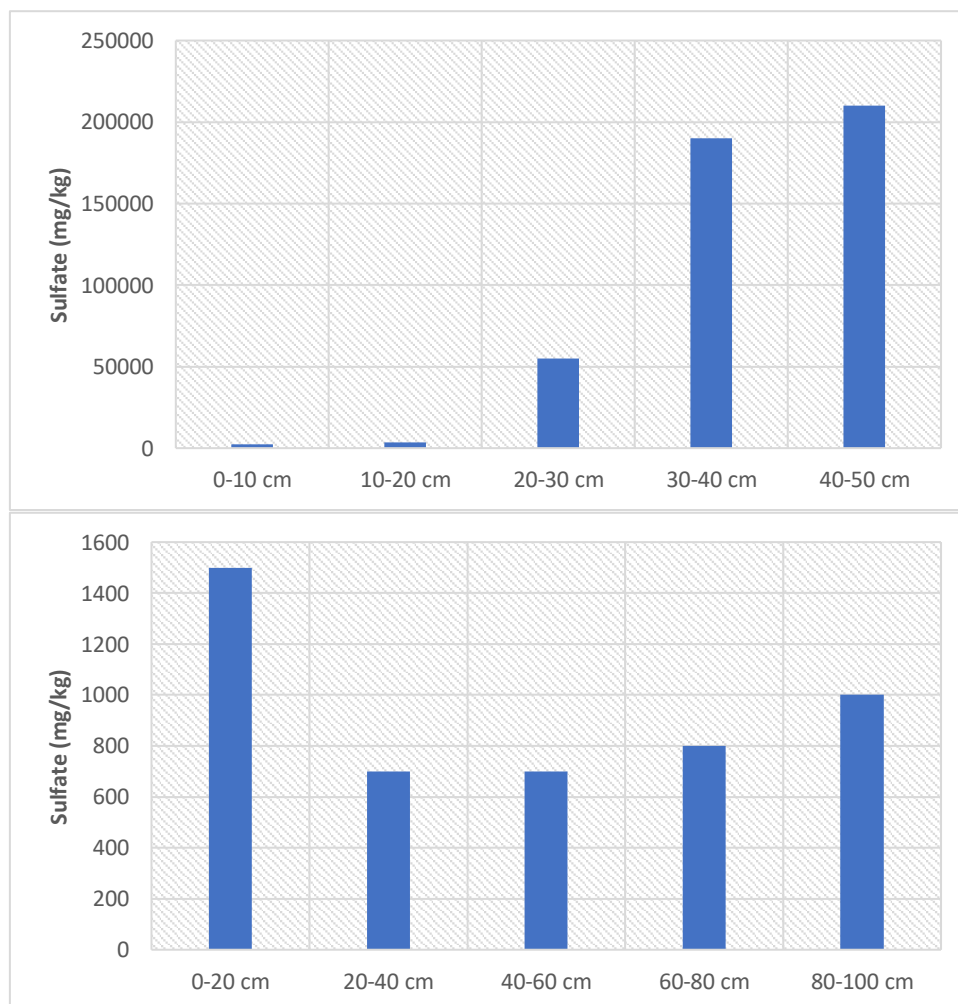


Figure 4.25 Concentration of sulfate in the two selected soil profiles. (a) Profile 10 and (b) Profile 19

4.3.3.4 Soil Particle Size Distribution

The soils consisted mainly of coarse materials with a grain diameter greater than 0.6 mm (gravels and sands). The percentage of gravels (>2mm) was over 60% for some soil layer (Figs. 4.26 and 4.27).

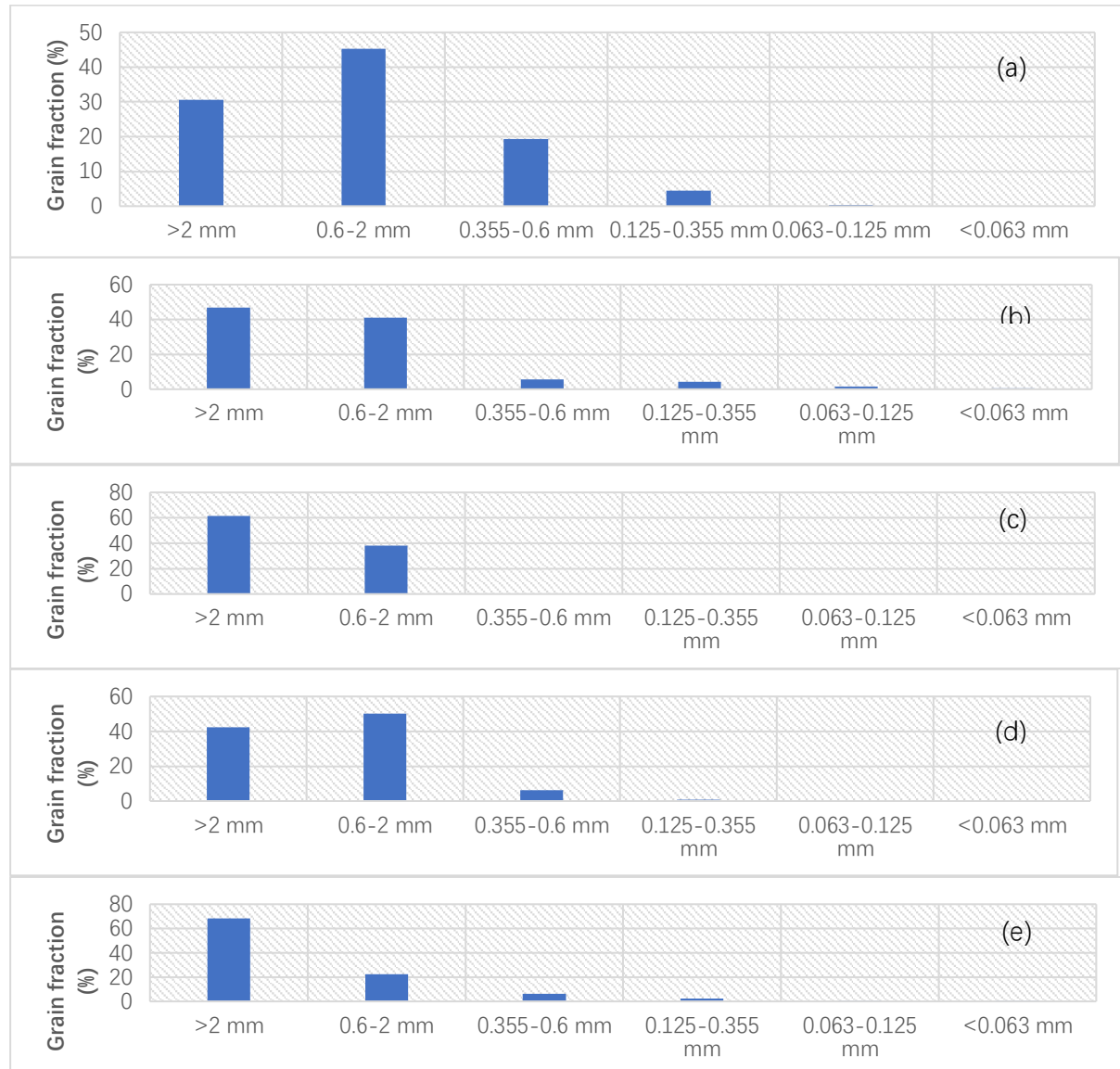


Figure 4.26 Soil grain size distribution patterns for the different soil layers in Soil Profile. (a) the 0-10 cm layer, (b) the 10-20 cm layer, (c) the 20-30 cm layer, (d) the 30-40 cm layer, and (e) the 40-50 cm layer.

Different patterns of soil particle size distribution were observed for the different soil layers. For the surface layer (0-10 cm) of the shallow soil profile (Profile 10), grain fraction 0.6-2 mm (> 45%) dominated the soil particle fractions, followed by

gravel (>2 mm) and the 0.355-0.6 mm fraction. Particle size <0.355 only accounted for less than 5%. The 30-40 cm layer showed a pattern similar to the surface soil layer. Other soil layers had the highest percentage of soil particles in the fraction >2 mm and the percentage of soil grain fractions decreased with decreasing particle size. For the 20-30 cm layer, no soil particles with a diameter <0.6 mm were detected (Fig. 4.26).

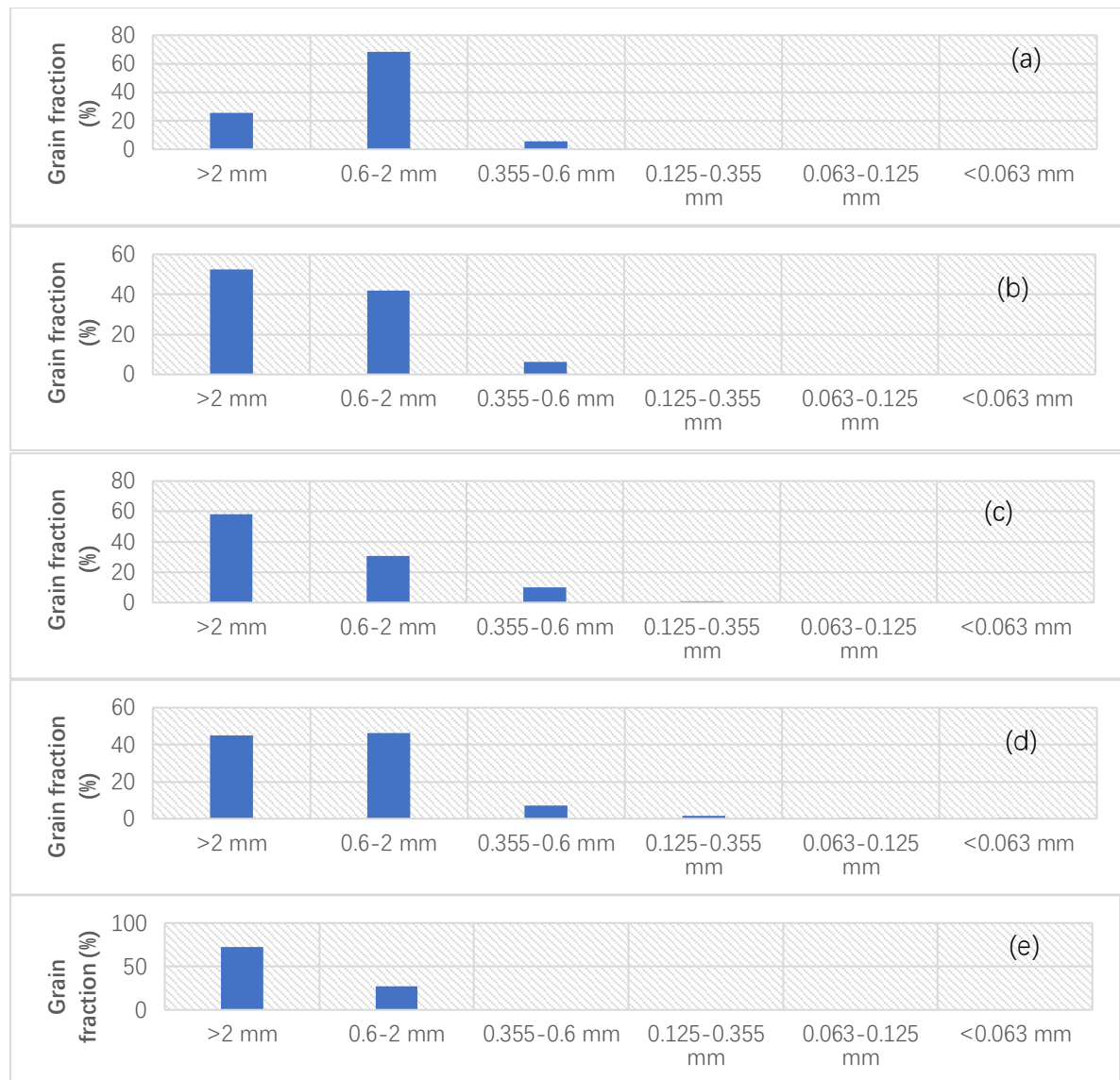


Figure 4.27 Soil grain size distribution patterns for the different soil layers in soil Profile. (a) the 0-20 cm layer, (b) the 20-40 cm layer, (c) the 40-60 cm layer, (d) the 60-80 cm layer, and (e) the 80-100 cm layer.

The deep soil profile (Profile 19) exhibited a similar pattern to the shallow soil profile except that the percentage >2 mm fraction and the 0.6-2 mm fraction in the 30-40 cm layer was very close to each other (Fig. 4.27).

4.4 Discussion

The Arabian Peninsula experienced a humid period during the early to mid-Holocene (Engel et al., 2012), followed by the late-Holocene dry period (Woronko, 2012). The soils in this region were developed from the sediments deposited under humid climate. The reworking of these sediments under desert conditions could lead to the removal of fine soil particles by winds, making the soils become coarse texture, as observed in this study. As expected, the soils also had alkaline pH, which is common in desert areas (Wiesman, 2009).

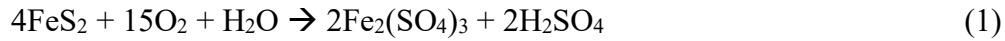
The oil lakes are located in the low-lying areas. These topographic positions acted as sink for sediments and soluble salts being brought from the surrounding highlands during the Holocene humid period. Evaporation drove the precipitation of salts. Depending on the location, the chemical composition of the soils could be very different. Table 4-12 gives a comparison of the soil chemical composition between the soil profile in the norther part (Profile 10) and the southern part (Profile 19) of the study area. It can be seen that the concentration of potassium and magnesium was very similar at the two locations. However, the concentration of sodium, calcium and sulfur was much higher in the Profile 10 than in the profile 19.

Table 4.12 A comparison of major soil properties (profile average) between profile 10 and Profile 19

Soil parameter	Profile 10	Profile 19
Potassium (mg/kg)	1090	1254
Sodium (mg/kg)	7780	656
Calcium (mg/kg)	100400	81600
Magnesium (mg/kg)	8200	9640
Sulfur (mg/kg)	31280	460
pH	7.93	8.36
EC (mS/m)	1855	844

Calcium in desert soils is usually present as chemical compounds of low water solubility such as calcium carbonates and gypsum. In Profile 10, the soil contained a substantial amount of sulfur, suggesting that gypsum was present in the soil. The molar ratio of calcium to sulfur was about 2.56, indicating over half of the calcium was associated with other ligands, most likely carbonate to form practically insoluble

calcium carbonate. In contrast, the mean concentration of sulfur in Profile 19 was very low (460 mg/kg), suggesting that gypsum might be present, if any, at a small amount. Sulfate in geological formations is derived from acid sulfate weathering e.g. oxidation of pyrite, as described by the following chemical equation:



Acid sulfate weathering generates sulfuric acid, which can react with calcium ion to form sparsely insoluble calcium sulfate (gypsum):



There was a perfect relationship between the total sulfur and sulfate-sulfur with a slope nearly 1 (Fig.4.28) for Soil profile 10, indicating that the sulfur contained in the soil was all in the form of sulfate.

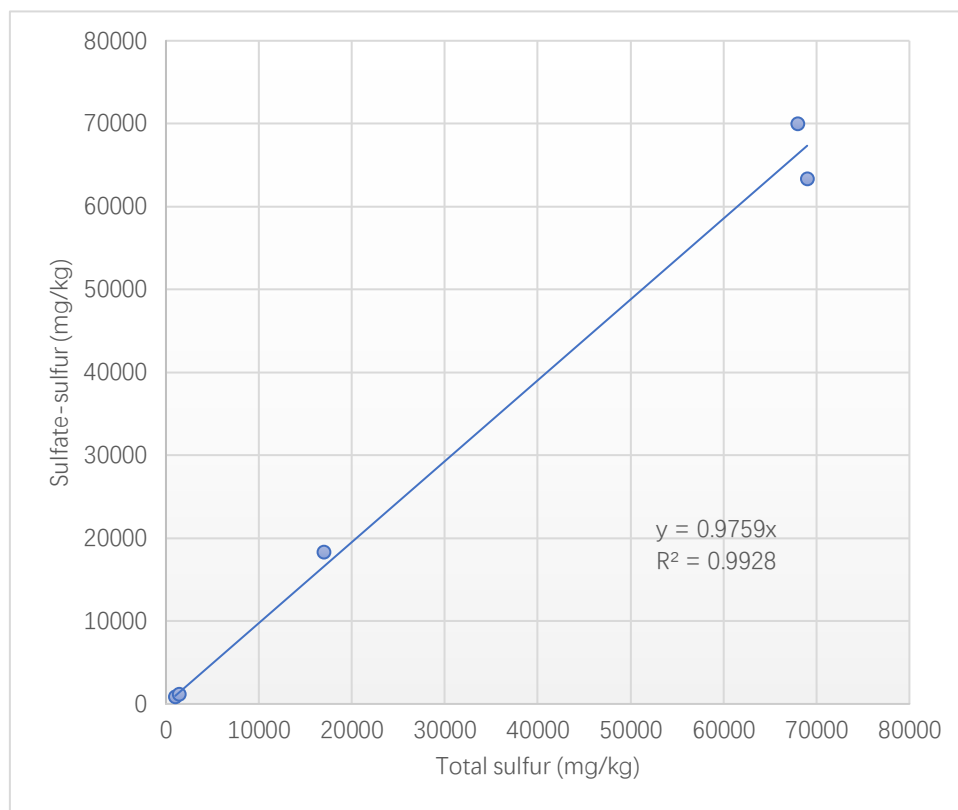


Figure 4.28 Relationship between the total sulfur and the sulfate-sulfur for profile 19

The hydrogen ion (H⁺) can consume hydroxy ion (OH⁻) and lower soil pH. This explains the relatively lower pH in Profile 10, as compared to profile 19.

Acid sulfate weathering accelerates decomposition of silicate minerals, leading

to release of soluble salts and increase electrical conductivity. This may be responsible for the observed relationship between the pH and EC in the investigated soils that soil pH is inversely related to soil EC (Fig. 4.29).

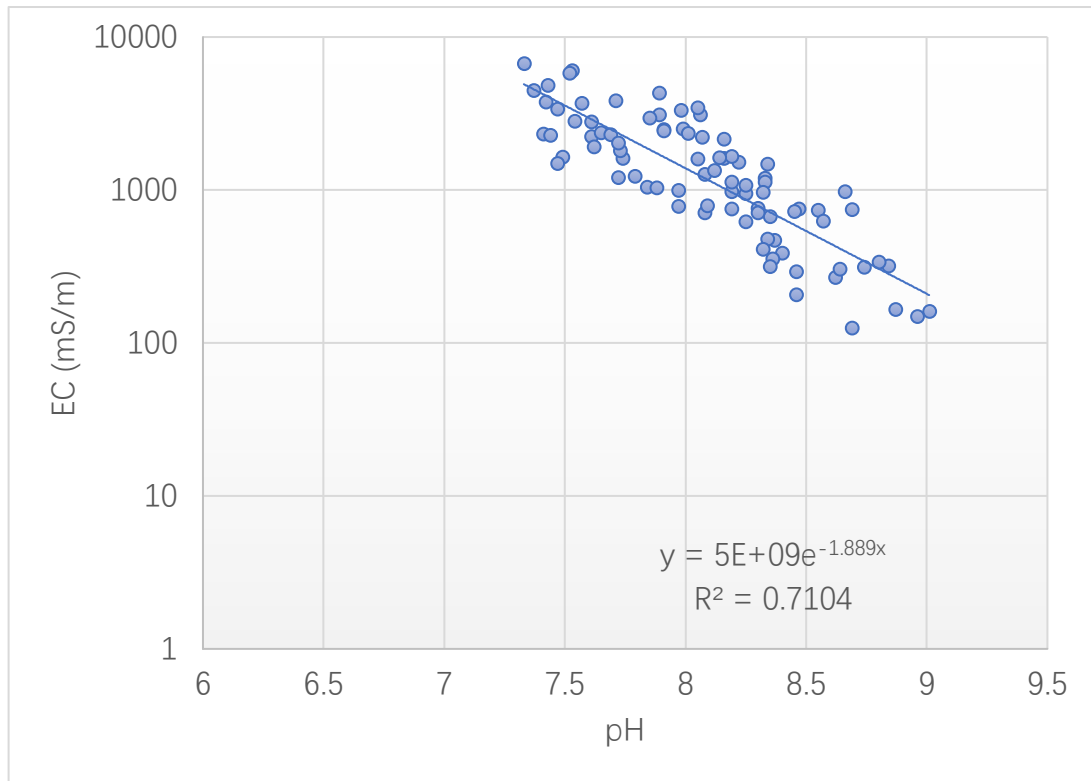


Figure 4.29 Relationship between pH and EC for the investigated soils

The absence of short-chain hydrocarbons in most of the investigated locations suggests that emission of volatile hydrocarbons dominated transport processes in the investigated area. This can be attributed to the desert climate conditions which, on one hand, favor (due to low relative humidity and high temperature) volatilization of these lighter hydrocarbon species with low vapor pressure and, on the other, disfavor their downward migration (due to a lack of rainfall). Under such conditions, the heavier component (after partitioning of the volatile portion) migrated through the soil column under the force of gravity. Because of their low mobility and large molecular size that could be easily trapped in soil pores, the downward moment of these long-chain hydrocarbons tended to be slower, as compared to the low-molecular-weight petroleum hydrocarbons. After the oil lake completely dried out, it is unlikely that any further downward migration of hydrocarbons by force of gravity will take place.

The extremely variable TPH among the different sampling location is probably attributable to the thickness of the overlying crude oil layer that was controlled by the surface elevation. Although the soils were generally of coarse texture, the connectivity of soil pores was likely to be poor due to the presence of secondary minerals such as gypsum and carbonates, which could block soil pores. This may be another reason for the impeded vertical migration of the spilled oil. The relatively deeper penetration of the downwardly moving PHCs at Locations 11, 18, 19 and 20 may be attributed by the lack of gypsum present within the soil profiles, as demonstrated from Profile 19, which favoured the infiltration of the spilled crude oil at the earlier stage. This allowed some of the short-chain PHCs being transported downwards and stored with the soil profiles, as observed at locations 11, 18, 19 and 20 in the southern part of the study area, which represents a hot spot that poses high level of environmental risk.

In-situ biodegradation is likely to be very limited due to the harsh environmental conditions encountered in the investigated area, including extreme soil temperatures, low moisture content and high salinity etc. In addition, the supply of nutrients especially nitrogen may not be sufficient to sustain the microbes that mediate the biodegradation of the petroleum hydrocarbons.

There is no evidence to show that groundwater has been contaminated in the investigated area. As mentioned above, any further downward migration of hydrocarbons by force of gravity is unlikely after the oil lake dried out. Rainwater is the only possible driver for future downward migration of the soil-borne hydrocarbons. However, since the hydrocarbons retained in the soils are almost completely composed of long-chain aliphatic hydrocarbons that have very low solubility in water and rainfall in the investigated area is rare in the predictable future, it is most unlikely that these soil-borne petroleum hydrocarbons pose any risk to groundwater in the investigated area.

Despite the high levels of TPH at many locations, the pre-dominant presence of less toxic long-chain aliphatic hydrocarbons means that the hazardousness of the contaminated soils is likely to be much lower than what was thought during development of the KERP program. The oil lake was far away from any residential areas and unlikely to be used for agricultural purposes. The most likely land uses will

be for industrial purposes because it is within the major oil field. Therefore, human exposure to the petroleum hydrocarbons will be limited to the KOC workers and the contractors who will carry out soil remediation work. Except for the locations where there were still short-chain petroleum hydrocarbons, the inhalation of volatile petroleum hydrocarbons is unlikely. The only exposure pathways will be ingestion and dermal contacts though inhalation of PHC-containing dusts may be possible.

For the small areas of contaminated hot spots such as those at Locations 11, 18, 19 and 20, inhalation of volatile petroleum hydrocarbons is likely due to the presence of xylenes, ethylbenene and toluene. However, the concentration of xylenes, ethylbenene and toluene in the soils was below the unacceptable levels for industrial/commercial uses or for excavation workers (New Zealand Ministry for Environment, 2011).

From an environmental remediation perspective, removal of the PHCs from the soils may be challenging due to the fact that long-chain PHC fractions that are resistant to either chemical or biological decomposition dominated the soil-borne PHCs, especially for biodegradation, which can also be adversely affected by the high soil salinity apart from the harsh climatic conditions such as strong solar radiation, high temperature and low moisture content. The soils contained certain level of phosphorus but they may not be bioavailable due to the immobilization by calcium to form practically insoluble calcium phosphate.

Given that the composition and quantity of hydrocarbons varies markedly from location to location within the investigated area, different strategies are required to meet the specific needs in various parts of the investigated area. For the contamination hotspots that contain high concentrations of BTEX, aromatics and PAHs, more active treatment methods should be used to remove the contaminants as soon as practical to minimize their adverse impacts on the environment and human health. For the larger area of the non-hotspots, more cost-effective passive methods should be considered to minimize the remedial costs.

Soil washing is a possible method for clean-up of hydrocarbon-contaminated soils. However, this method is unlikely to be effective for the contaminated soils

containing predominantly long-chain aliphatic hydrocarbons that are practically insoluble in water. In addition, intensive soil washing operations could enhance the volatilization of BTEX, causing air pollution and possibly harms to the operators.

The soils contained no elevated concentration of heavy metals and metalloids that could inhibit petroleum hydrocarbon-degrading microbes. The presence of phosphorus is also a beneficial factor for microbially mediated degradation of hydrocarbons. However, the high soil salinity at many locations, as indicated by high electrical conductivity, will affect microbial activities. Therefore, desalinization of these soils may be required for bioremediation of the contaminated soils.

Chemical treatment using advanced oxidation technologies may be a more cost-effective method for treating the mobile fractions of hydrocarbons. The advanced oxidation method is rapid with no release of harmful substances. It is also possible to develop in-situ oxidation method to reduce the costs associated with translocation of contaminated soils to purpose-built facilities for ex-situ treatment.

For the soils containing no or small amounts of BTEX, aromatics and PAHs, containment may be more appropriate. However, ex-situ containment such as landfilling may be only appropriate for hydrocarbon-rich sludge but not the soils with dominant presence of aliphatic hydrocarbons. Given the extremely low risk in terms of groundwater contamination by the contaminated soils, it is not necessary to remove the soils from the contaminated sites. A low-cost capping method should be sufficient to minimize human exposure to the contaminated soils.

4.5 Conclusions

The soils in the investigated oil lake area were of coarse texture and had alkaline pH. They contained large amounts of calcium compounds. Depending on the location, large amounts of gypsum might be present, causing blockage of soil pores and impeding infiltration of the spilled crude oil. The soils without significant amounts of gypsum appeared to allow better penetration of the PHCs. This also enabled storage of some short-chain PHCs within the soil profile that was absent in the other soil profiles. Overall, most of the lighter PHCs was lost due to evaporation under the desert climatic conditions. Long-chain aliphatic PHCs dominated the PHCs in the investigated oil lake area. This has implications for developing remediation strategies. The dominance of long-chain PHCs in the contaminated soils means that it will be difficult to treat these soils because the heavier PHCs are resistant to decomposition. However, long-chain PHCs are generally less toxic and intensive treatment of these PHCs may not be necessary.

Chapter 5

Geochemical Characteristics and Environmental Risk of the Crude Oil-Contaminated Soils in a Constructed Sludge Pit

5.1 Introduction

Oil sludge pits are storage facilities used for disposal of oil wastes (drilling mud and cuttings) generated from drilling oil wells (Gorlenko and Timofeeva, 2019) or collection of crude oil due to the emergency activities of drill operation (Helmy and Kardena, 2015). These facilities are usually constructed with a liner to prevent penetration of the oil into the underlying soils. Therefore, soil contamination associated with oil waste disposal in oil sludge pits may not be as severe as the uncontrolled oil lakes.

Oil sludge pits are widespread in Kuwait's major oil fields and they are sometimes overlapped with the oil lakes formed during the First Gulf War. As part of the Kuwait Oil Company's oil contamination remediation efforts, (KOC) also set up a program named as SEED to clean up the oil contaminated soils caused by its own oil production operations, including oil sludge pits. This chapter aims to characterise the contaminated soils in the oil sludge pits to provide a comparison with the unintendedly formed oil lakes.

In addition, the oil sludges overlying the contaminated soils in the oil lake investigated in Chapter 4 were not collected and therefore no characterisation work was made. This study includes detailed characterisation of the surface oil sludges for Oil Sludge Pit EPE4, Samples were taken from 16 locations, as shown in Figure 5.1 and as described in chapter 3.

5.2 Methodology

The information on the study site and the research methods used for this component are described in Chapter 3.

5.3 Results

5.3.1 Soil profile characteristics

The soils with oil contamination depth greater than 0.45 m were only found at two locations (Locations 1 and 12). Details on soil morphology for each soil profile were provided in Table 5.1. In general, a layer of dry oil sludge ranging from 0.01 to 0.09 m was found across the investigated sludge pit. This was underlain by a layer of brownish sandy soil at most of the sampling locations, followed by the uncontaminated soil at the bottom of the soil profiles.

Table 5.1 Soil profile characteristics at the 16 sampling locations.

Location	Sample Depth (m)	Material type
1	0-0.04	Black dark dry sludge
	0.04-0.14	
	0.14-0.24	
	0.24 - 0.34	Brown fine to medium sand, 2% Rocky
	0.34-0.45	
	0.450-0.455	Light brown sand
2	0.455-0.500	Clean gatch
	0-0.01	Dry Sludge, black silt
	0.01-0.07	Brownish dark soil
3	0.07-0.15	Brownish white gatch(rock above 50%)
	0-0.06	Semi solid, dark sticky sludge
	0.06-0.13	Black Wet Soil, Strong HC Odor
4	0.13-0.20	Clean gatch with small gravel
	0-0.02	Dry Sludge with interface of soil
	0.02-0.03	Soil of 1 cm below sludge, soil is dark with silt content
5	0.03-0.15	Dry white clean gatch
	0-0.02	Sludge (Dark & Dry)
	0.02-0.03	Dark Brownish contaminated sand
6	0.03-0.15	Clean hard gatch with 30% gravel
	0-0.01	Sludge (Dark & Dry, visually contaminated)
	0.01-0.06	Soil (low-med, oily odor)
	0.06-0.18	gatch

7	0-0.04	Sludge (Dark firm, salt inclusions)
	0.04-0.14	Dark Brown clayish
	0.14-0.20	gatch
8	0-0.03	Black hard dry sludge
	0.03-0.06	Contaminated sand
	0.06-0.15	White clean gatch, 15% gravel
9	0-0.09	Black thick sludge
	0.09-0.18	Oily sand, highly contaminated, medium odor
	0.18-0.25	White clean gatch
10	0-0.12	Black thick sludge
	0.12-0.17	Oily sand, HC Odor
	0.17-0.35	Clean gatch, above 10% gravel, odorless
11	0-0.01	Dry Sludge, Odor
	0.01-0.12	Medium Brown sand
	0.01-0.22	Medium Brown sand
	0.22-0.50	Coarse sand
12	0-0.07	Dry Sludge, Odor
	0.07-0.17	
	0.17-0.27	
	0.27-0.37	Dark Brown sand
	0.37-0.47	
	0.47-0.52	
	0.52-0.65	White clean gatch
13	0-0.05	Dry Sludge, Semi dry
	0.05-0.15	Dark Brown sand
	0.15-0.25	Whitish brown gatch
14	0-0.03	Black Dry Sludge
	0.03-0.07	Dark Black sand
	0.07-0.25	White gatch with gravels
15	0-0.03	Black Dry Sludge
	0.03-0.06	Dark Black sand wih gravels
	0.06-0.20	White gatch, clean with gravels
16	0-0.03	Black Dry Sludge
	0.03-0.05	Dark Black sand
	0.05-0.25	White gatch, clean with gravels

5.3.2 Characteristics of the oil sludges

5.3.2.1 Total petroleum hydrocarbon (TPH)

From Fig. 5.1, it can be seen that the TPH in the oil sludges overlying the soils was spatially variable. It ranged from 18430 to 172430 mg/kg with a mean value of 68724 mg/kg (n=16). The distribution of TPH within the investigated area is given in Figure 50b. Locations 3, 14 and 16 had TPH over 140000 mg/kg. Location 15 had the least concentration of TPH among the investigated locations. No BTEX was detected from any sludge sample.

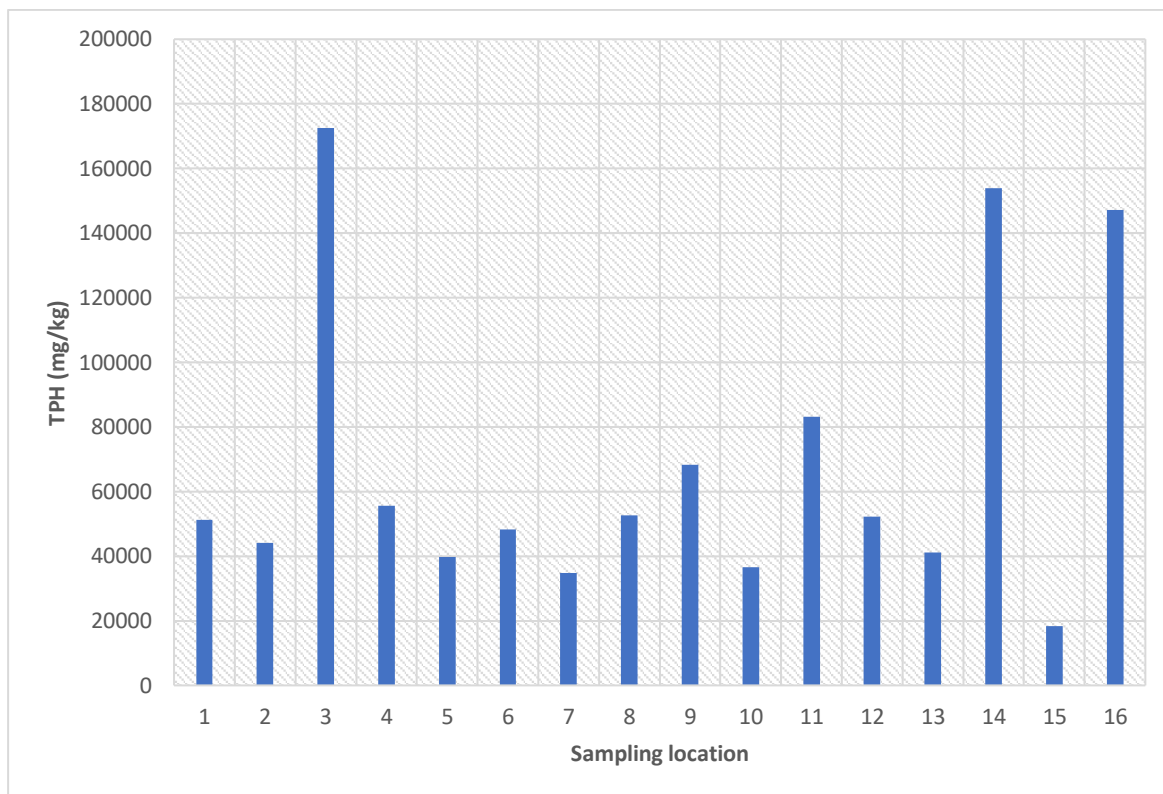


Figure 5.1 TPH in the oil sludges at the 16 sampling locations.

5.3.2.2 Aliphatic Hydrocarbons

Almost no hydrocarbons with a length of carbon chain <C16 were detected from the collected sludge samples and the predominant petroleum hydrocarbon fraction was C21-C35 (mean±SD was 45750±30108; n=16) for all the investigated samples. The distribution of total aliphatic hydrocarbon and the three major fractions are given in Table 5.2

The mean total aliphatic petroleum hydrocarbon for the 16 locations was 56260 mg/kg with a standard deviation of 39136 mg/kg. Like TPH, Locations 3, 14 and 16 had much higher concentration of aliphatic hydrocarbon, as compared to the sludges collected at other sampling locations (Fig. 5.1 and Table 5.2).

Table 5.2 Concentration (mg/kg) of aliphatic hydrocarbons in the oil sludges

Location	C16-C21	C21-C35	C35-C40	Sum
1	2400	35000	4400	41801
2	2500	31000	3000	36502
3	20000	110000	12000	142003

4	3700	36000	4100	43804
5	1400	28000	3500	32905
6	1100	33000	3600	37706
7	1200	23000	2300	26507
8	6600	33000	3500	43108
9	7200	45000	3900	56109
10	870	27000	330	28210
11	8100	56000	4800	68911
12	4500	35000	3400	42912
13	3500	27000	2800	33313
14	15000	100000	11000	126014
15	920	13000	1400	15335
16	14000	100000	11000	125016
Mean	5812	45750	4689	56260
SD	5808	30108	3481	39136

5.3.2.3 Aromatic hydrocarbons

Aromatic petroleum hydrocarbon fractions with carbon chain shorter than C12 and longer than C35 were not detected from the 16 collected sludge samples. Fraction C21-C35 dominated the aromatic hydrocarbons. Fraction C12-C16 was at a small amount or not detectable. The total aromatic hydrocarbon had a mean value of 12461 with a standard deviation of 7704 mg/kg (Table 5.3).

Again, Locations 3, 14 and 16 had much higher concentration of aromatic hydrocarbon, as compared to the sludges collected at other sampling locations (Fig. 5.1 and Table 5.3).

Table 5.3 Concentration (mg/kg) of aromatic hydrocarbons in the oil sludges

Location	C12-C16	C16-C21	C21-C35	Sum
1	110	1500	7800	9410
2	130	1100	6400	7630
3	230	6200	24000	30430
4	0	2000	9800	11800
5	0	850	6000	6850
6	0	1300	9200	10500
7	0	1100	7100	8200
8	0	2100	7500	9600
9	0	2400	9800	12200
10	0	790	7500	8290
11	0	2200	12000	14200
12	0	1600	7700	9300
13	0	1400	6400	7800
14	270	4700	23000	27970
15	0	510	2600	3110
16	180	3900	18000	22080
Mean	58	2103	10300	12461
SD	95	1559	6110	7704

5.3.2.4 Polycyclic aromatic hydrocarbons (PAHs)

Total PAH in the sludge materials was only detected in 10 out of the 16 sampling locations with a very low value (<20 mg/kg). Only three PAH species were found in the sludge samples: chrysene, pyrene and phenanthrene (Table 5.4). Chrysene is the most common PAH species with its presence at 8 out of the 16 sampling locations and Location 3 had the highest level of chrysene (10 mg/kg). Pyrene was only detected at Locations 1 and 6.

Table 5.4 Concentration (mg/kg) of PAHs in the oil sludges

Sampling location	1	3	5	6	7	8	9	11	12	13
Naphthalene	<1.0	<1.0	<1.0	<1.0	<1.0	<1.0	<1.0	<1.0	<1.0	<1.0
Acenaphthylene	<1.0	<1.0	<1.0	<1.0	<1.0	<1.0	<1.0	<1.0	<1.0	<1.0
Acenaphthene	<1.0	<1.0	<1.0	<1.0	<1.0	<1.0	<1.0	<1.0	<1.0	<1.0
Fluorene	<1.0	<1.0	<1.0	<1.0	<1.0	<1.0	<1.0	<1.0	<1.0	<1.0
Phenanthrene	<1.0	5.2	<1.0	<1.0	<1.0	2	1	<1.0	<1.0	1.2
Anthracene	<1.0	<1.0	<1.0	<1.0	<1.0	<1.0	<1.0	<1.0	<1.0	<1.0
Fluoranthene	<1.0	<1.0	<1.0	<1.0	<1.0	<1.0	<1.0	<1.0	<1.0	<1.0
Pyrene	1.7	<1.0	<1.0	1	<1.0	<1.0	<1.0	<1.0	<1.0	<1.0
Benzo(a)anthracene	<1.0	<1.0	<1.0	<1.0	<1.0	<1.0	<1.0	<1.0	<1.0	<1.0
Chrysene	<1.0	10	3.5	3.6	4.4	4.9	2.9	4.9	4.2	<1.0
Benzo(a)pyrene	<1.0	<1.0	<1.0	<1.0	<1.0	<1.0	<1.0	<1.0	<1.0	<1.0

Indeno(123-cd)pyrene	<1.0	<1.0	<1.0	<1.0	<1.0	<1.0	<1.0	<1.0	<1.0	<1.0
Dibenzo(ah)anthracene	<1.0	<1.0	<1.0	<1.0	<1.0	<1.0	<1.0	<1.0	<1.0	<1.0
Benzo(ghi)perylene	<1.0	<1.0	<1.0	<1.0	<1.0	<1.0	<1.0	<1.0	<1.0	<1.0
Benzo(b)fluoranthene	<1.0	<1.0	<1.0	<1.0	<1.0	<1.0	<1.0	<1.0	<1.0	<1.0
Benzo(k)fluoranthene	<1.0	<1.0	<1.0	<1.0	<1.0	<1.0	<1.0	<1.0	<1.0	<1.0

5.3.3 The contaminated soils

5.3.3.1 Total petroleum hydrocarbon

TPH in the soils varied horizontally and vertically. The TPH in the surface soil layer ranged from 86 to 3350 mg/kg with a mean value of 1447 mg/kg. Location 23 had the highest level of TPH while Locations 1, 4, 5, 7 and 10 had TPH less than 500 mg/kg (Fig. 5.2).

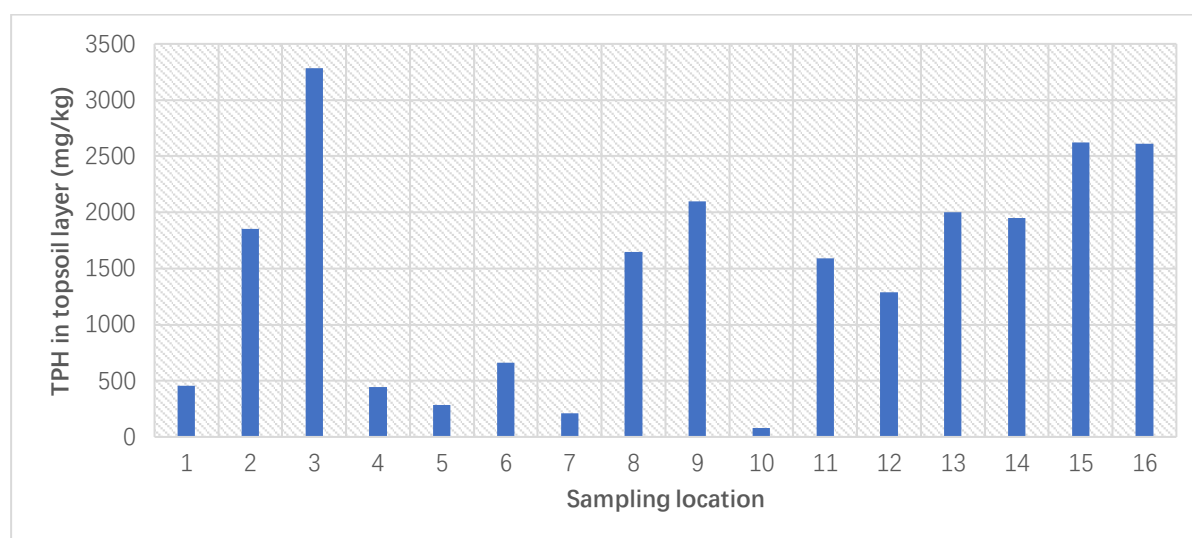


Figure 5.2 TPH in the surface soil layer for the 16 sampling locations

5.3.3.2 Distribution of aliphatic and aromatic hydrocarbon fractions

The C21-C35 fraction dominated the aliphatic hydrocarbon fraction, followed by C16-C21 fraction, C35-C40 fraction, C12-C16 fraction and C10-C12 fraction. Fractions with carbon number less than 10 were not detected (Fig. 5.3a).

For the aromatic hydrocarbons, fractions with a carbon number less than 12 and more than 35 were not detected. The concentration of the detectable aromatic petroleum hydrocarbon fractions follows the following decreasing order: C21-C35 > C16-C21 > C12-C16 (Fig. 5.3b)

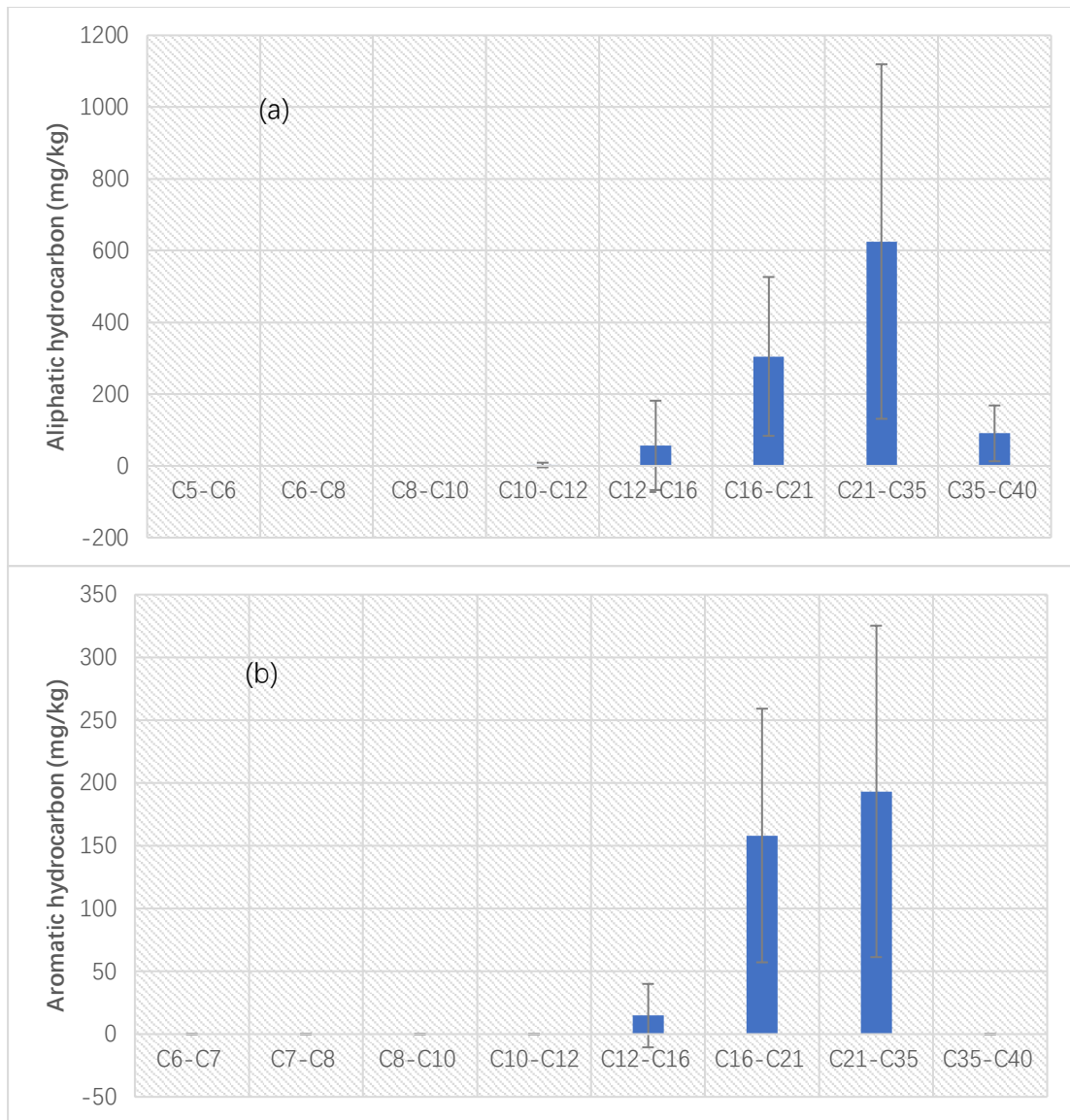


Figure 5.3 Distribution of various (a) aliphatic hydrocarbon fractions and (b) aromatic hydrocarbon fractions in the contaminated soils

5.3.3.3 Vertical variation in various hydrocarbon fractions

The two soil profiles with a contamination depth extending to about 50 cm are used to show the vertical variation in various petroleum hydrocarbon fractions (Figs. 5.4).

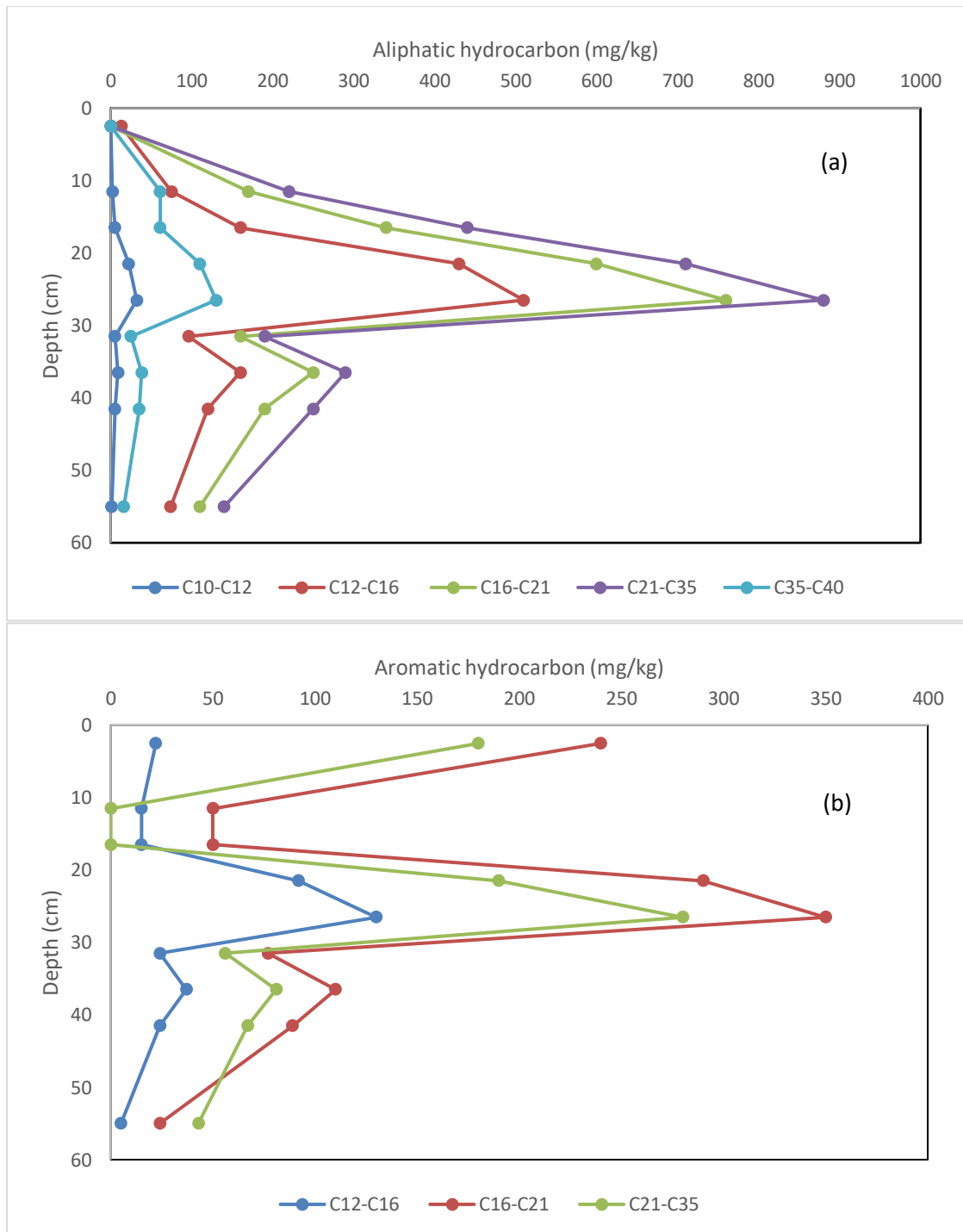


Figure 5.4 Changes in various (a) aliphatic hydrocarbon fractions and (b) aromatic hydrocarbon fractions along Soil Profile 1

For soil profile 1, the vertical variation pattern was similar for the same type of hydrocarbon fractions (i.e. either aliphatic or aromatic). However, there was difference in the vertical variation pattern between the two different types of the hydrocarbon; aliphatic hydrocarbon fractions in the surface soil layer was at very low level and increased to reach a peak at around 25 cm depth (Fig. 5.4a) while aliphatic hydrocarbon

fractions decreased from the surface to a depth at 15 cm and then increased to reach a peak at around 25 cm (Fig. 5.4b).

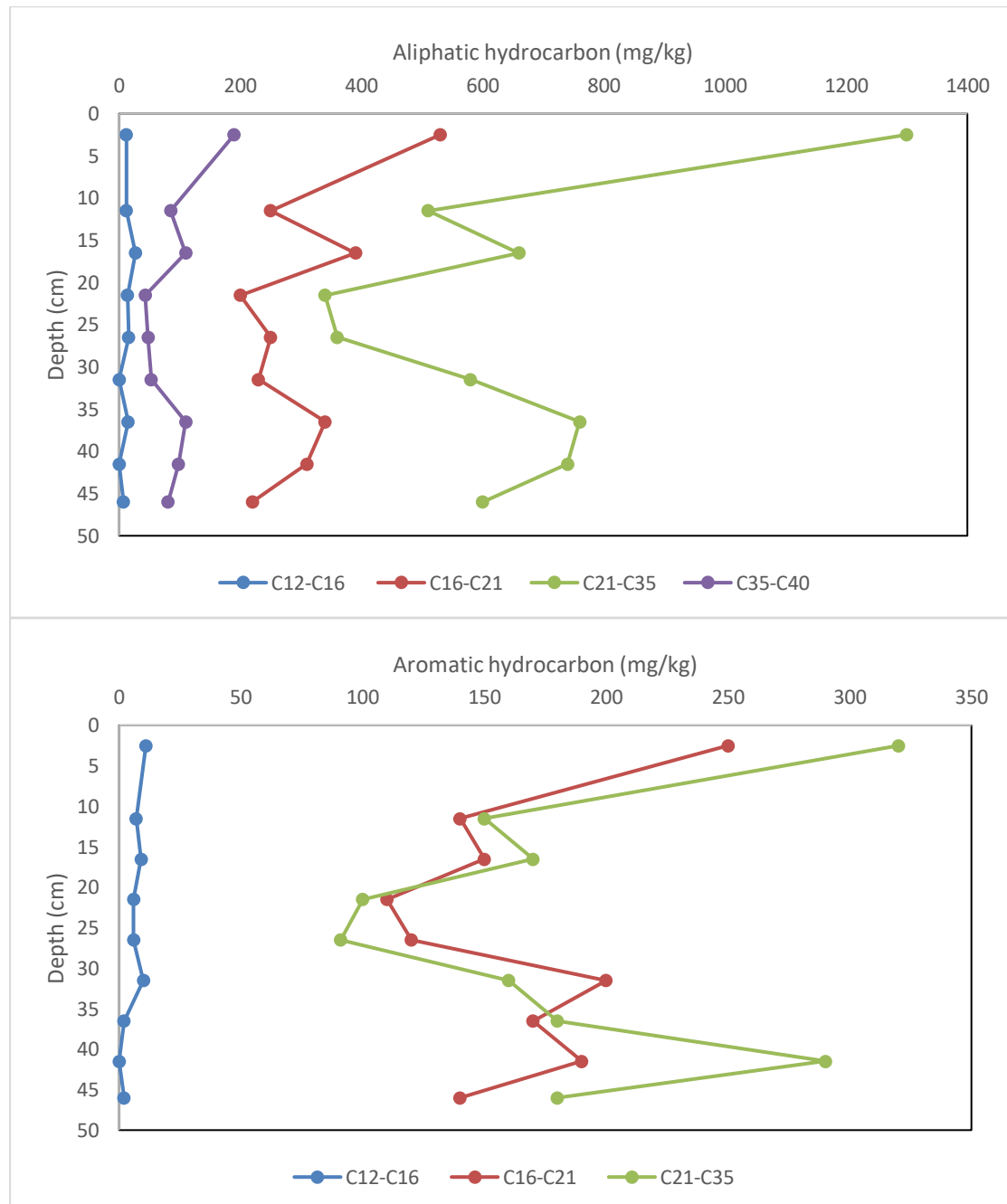


Figure 5.5 Changes in various (a) aliphatic hydrocarbon fractions and (b) aromatic hydrocarbon fractions along Soil Profile 12

For Soil profile 12, the vertical variation pattern had a certain level of similarity between the aliphatic hydrocarbon and the aromatic hydrocarbon and between different fractions for the same type of petroleum hydrocarbons (Fig. 5.5).

5.4 Discussion

In most of the sampling locations, the contamination depth was limited to less than 15 cm. Oil sludge pits are purpose-built structure to store spilled oil during oil production. A liner is usually used to minimize the penetration of oil into ground (Pazoki & Hasanidarabadi, 2017; Tanzharikov et al., 2018). The limited number of deep contamination locations was probably the result of liner failure, causing movement of oil beyond the liner (Kuwayama et al., 2015). The findings here suggest that it is important to make sure that the quality of liner is sufficiently good to avoid deep contamination of soils by the stored oil from occurring.

It is interesting to note that there was only a loose relationship in TPH between the oil sludge and the underlying surface soil layer for the 16 sampling locations (Fig. 5.6). The differential spatial distribution pattern in TPH between the surface soil layer and the overlying oil sludge may be explained by two reasons. Firstly, the TPH concentration in the sludge is determined by the amount of impurities present in the original crude oil and incorporation of sediments from atmospheric deposition driven by wind into the sludge; sludge pit received petroleum with different chemical composition from different spill events and sediments at different amount; sludge derived from drilling mud tends to contain less PHCs, as compared to that derived from spilled oil. Secondly, the concentration of TPH in soils is affected by the porosity of the soil; a high porosity tended to accommodate more penetrating oil and consequently had a higher concentration of TPH. This also explains the observed fluctuation in either the aliphatic and aromatic hydrocarbons along the soil profiles (Figs. 5.4 and 5.5).

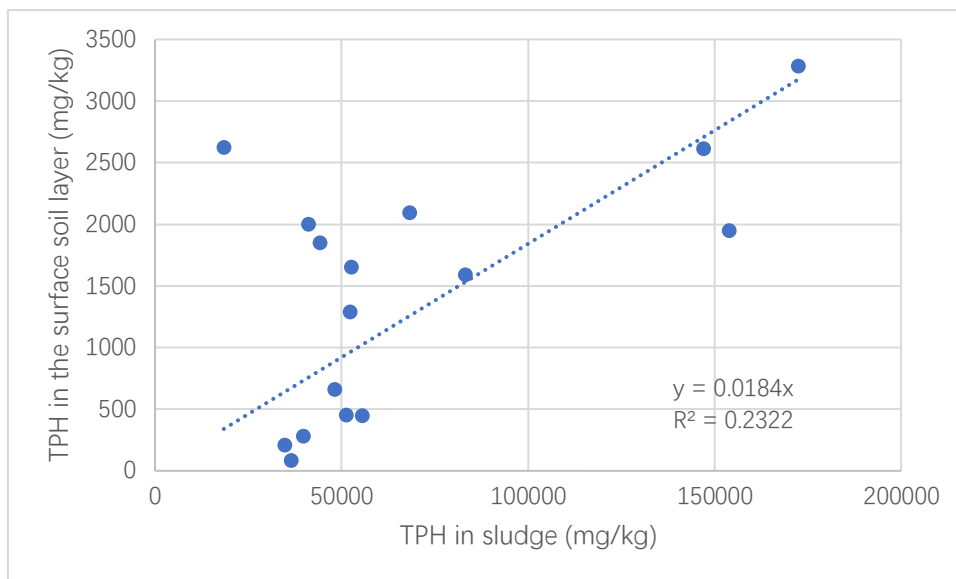


Figure 5.6 Relationship in TPH between the sludge and the underlying surface soil layer.

There was a close relationship ($R^2 = 0.9469$) between the total aliphatic hydrocarbon and the total aromatic hydrocarbon in the oil sludges (Fig. 5.7). However, the ratio of total aromatic hydrocarbon to the total aliphatic hydrocarbon was around 0.2, indicating that over 80% of the total petroleum hydrocarbon was in aliphatic forms. Park and Park (2010) determined petroleum hydrocarbon fractions in two petroleum hydrocarbon-contaminated sites and found that aliphatic fraction C8-C16 and aromatic fraction C10-C21 were the major contributors to human health risk along all the exposure routes. The pre-dominant aliphatic fraction and aromatic fraction were all C21-C35 in the investigated sludge, suggesting that the sludge is likely to pose a low risk to human health.

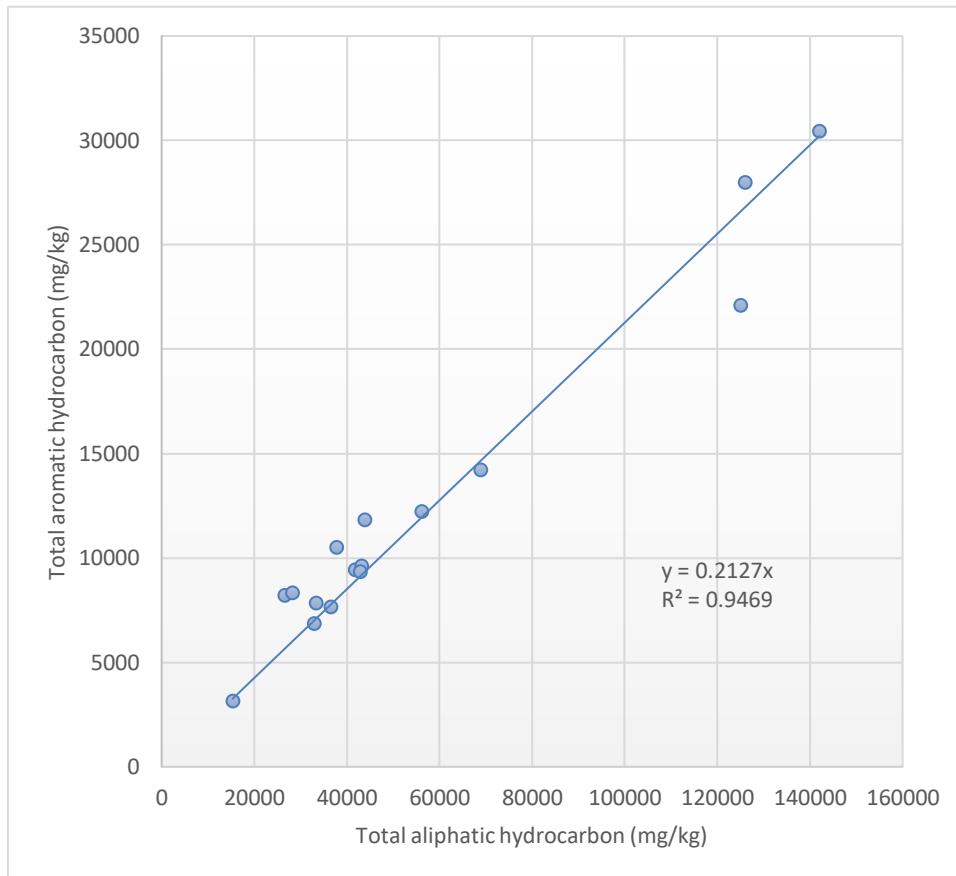


Figure 5.7 Relationship between the total aliphatic hydrocarbon and the total aromatic hydrocarbon

In general, there was no clear relationship of the same aliphatic petroleum hydrocarbon fraction between the sludge and the surface soil layer ($R^2 < 0.09$) (Fig. 5.7). This suggests that the crude oil-borne aliphatic hydrocarbons did not proportionally penetrate into the underlying soils.

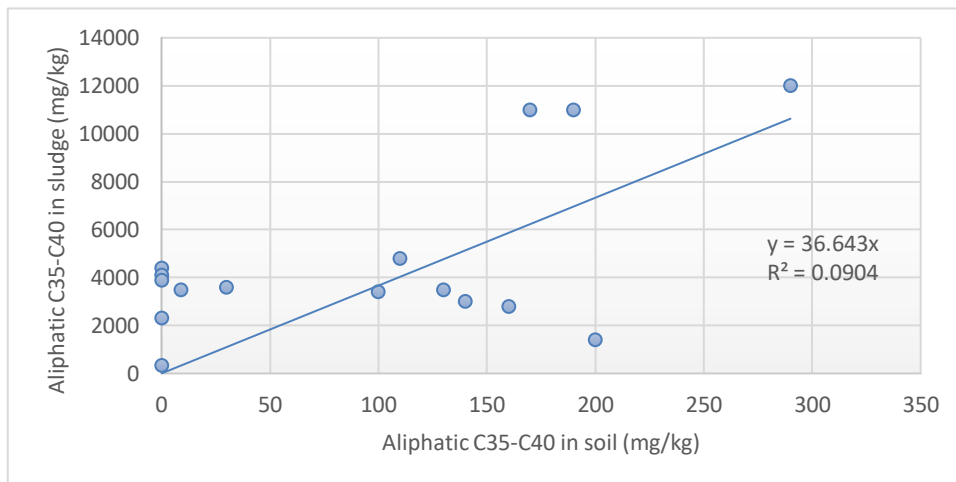
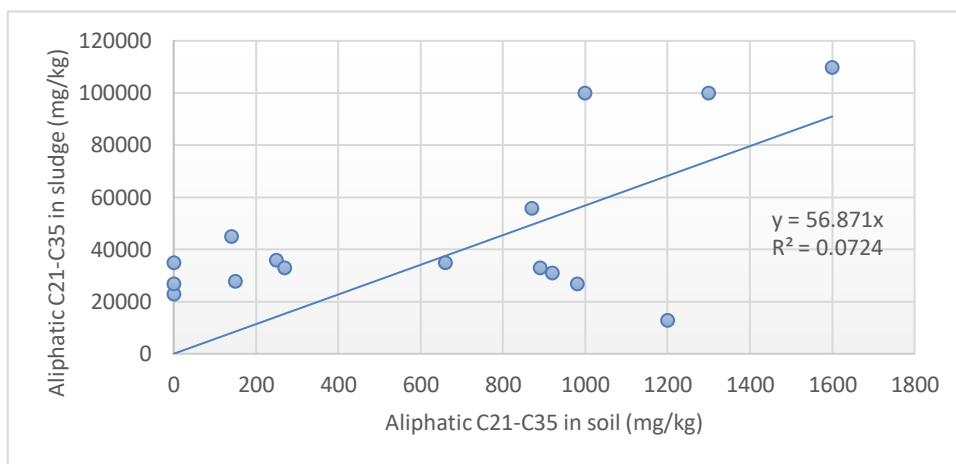
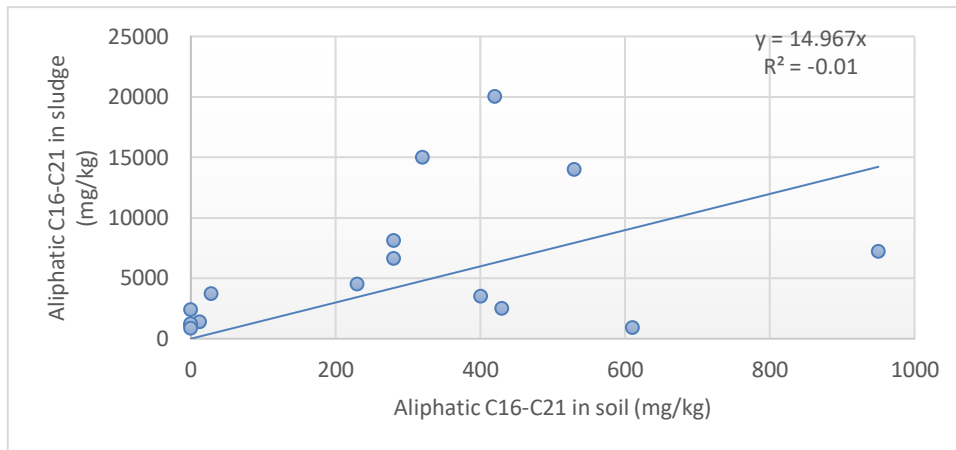


Figure 5.8 Relationship in aliphatic fraction (a) C16-C21, (b) C21-C35, and (c) C35-C40 between the sludge and the surface soil

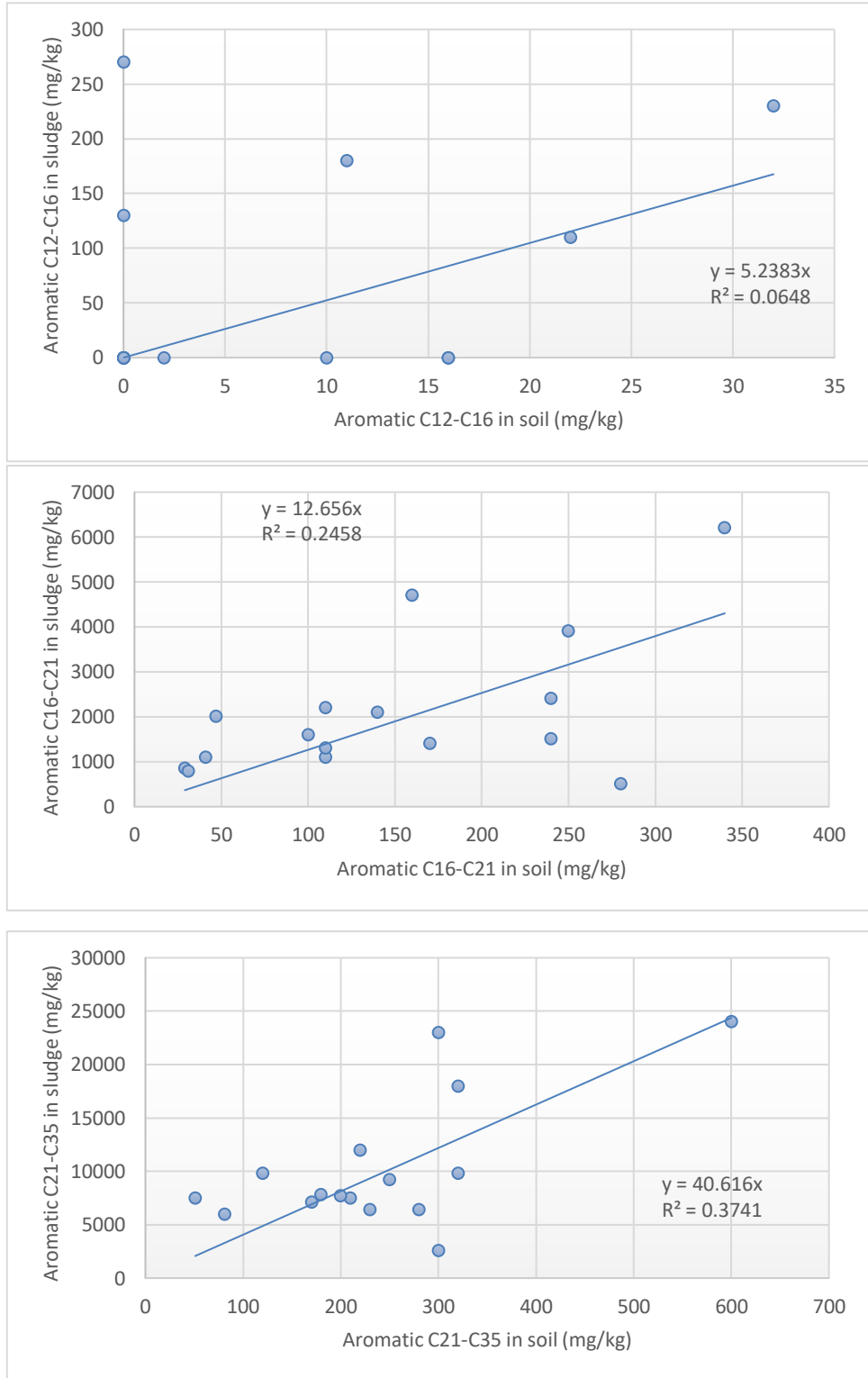


Figure 5.9 Relationship in aromatic fraction (a) C12-16, (b) C16-C21, and (c) C21-C35 between the sludge and the surface soil.

For the aromatic hydrocarbon fractions, there was a trend that R2 increased with

increasing carbon number. There was no clear relationship of the C12-C16 aromatic petroleum hydrocarbon fraction between the sludge and the surface soil layer while the R2 for the C16-C21 and C21-C35 aromatic petroleum hydrocarbon fractions was 0.2458 and 0.3741, respectively. This may be attributed to the semi-volatile nature of Fraction C12-C16 (Fig. 5.8).

The soils underlying the sludges had lower TPH, relative to those in the oil lake area, as shown in Chapter 4. This can be attributed to the soil compaction during preparation of liner for the sludge pit. This makes the environmental risk from the contaminated soils in the sludge pit lower, as compared to the contaminated soils in the oil lake area. From an environmental remediation point of view, it may be more cost-effective to use a soil capping approach to limit human contacts with the oil sludge and contaminated soils.

5.5 Conclusions

Unlike contaminated soils in the oil lake area, the contamination depth was generally very shallow due to the presence of a liner. No BTEX was detected and the concentration of TPH was generally lower, as compared to the oil lake soils. There was a close relationship between the total aliphatic hydrocarbon and the total aromatic hydrocarbon in the oil sludges. Over 80% of the total petroleum hydrocarbon in the oil sludges was in long-chain aliphatic forms. This, combined with the generally low TPH level in the underlying contaminated soils make the environmental risk from the sludges and contaminated soils relatively low. From an environmental remediation perspective, soil capping may be a more cost-effective method for minimizing the environmental impacts from the petroleum hydrocarbons in the sludge pits.

Chapter 6

3-D Model Development for Predicting Spatial Variation of Crude Oil-Contaminated Soil

6.1 Introduction

Currently soil investigation into petroleum hydrocarbon-contaminated soil in oil lake areas involves grid sampling with a high horizontal sampling density. However, vertical variation in petroleum hydrocarbon concentration along the soil profile is not sufficiently considered. This approach could lead to substantial costs due to intensive horizontal sampling on one hand and inaccurate estimation of the contaminated soil volume that need to be treated on the other hand.

Geostatistical interpolation techniques have been used to estimate the value of the investigated soil parameter in un-sampled locations by a weighted average of the nearby observations. This allows a predictive model being established to assist in soil mapping for a large area without the need to conduct intensive soil sampling, and therefore significantly reduces capital and labour inputs. Interpolation methods are widely used for 2-D soil mapping. However, until now, there have been limited applications of geostatistical interpolation techniques to 3-D mapping of soil properties.

To develop predictive models that can be used for 3-D soil mapping, a combination of 2-D interpolation with soil profile depth function is required. The accuracy of 3-D distribution of soil parameters heavily depends on the reliability of soil dataset obtained from soil survey. To obtain highly reliable datasets, soil sampling design needs to be optimized for geostatistics. This represents a major challenge for developing sensible 3-D soil mapping technologies.

There have been a few pieces of research work on 3-D mapping of soil organic carbon and soil texture. However, no systematic research work has so far been done to develop 3-D predictive models for spatial distribution of oil-contaminated soils. The spatial variation of a given soil property is determined by many factors. To optimize soil sampling design, it is important to understand the biogeochemical processes governing the soil formation. Soil contamination by petroleum hydrocarbons is a complex process. So far, most of research on petroleum hydrocarbon-contaminated soils was conducted in small areas with light petroleum hydrocarbons being the major

contaminants entering the soil systems. There has not been sufficient understanding on geochemical processes related to contamination of soils by crude oil, especially for those experiencing long-term weathering in desert areas such as the oil lakes in Kuwait. This does not allow optimization of soil sampling design for the development of reliable predictive models for 3-D mapping of various petroleum hydrocarbons with varying degrees of environmental hazardousness.

To achieve cost-effective goals for remediation of the oil-contaminated soils, it is necessary to develop innovative predictive models that can be used to guide 3-D mapping of the key soil parameters for characterization of the contaminated soils in order to inform environmental risk assessment, development of remediation strategies, and selection of appropriate soil treatment methods and technologies.

In chapters 4 and 5, the geochemical characteristics of the soils in a selected section of the Raudhatain oil lake from the KERP and a selected oil sludge pit (Sludge Pit EPE4) from the SEED were reported. In this chapter, the data collected from these two study areas, together with data provided by KOC contractor for another sludge pit (SPB1) were used to develop 3-D predictive models for mapping of the petroleum hydrocarbon distribution.

6.2 Research methods

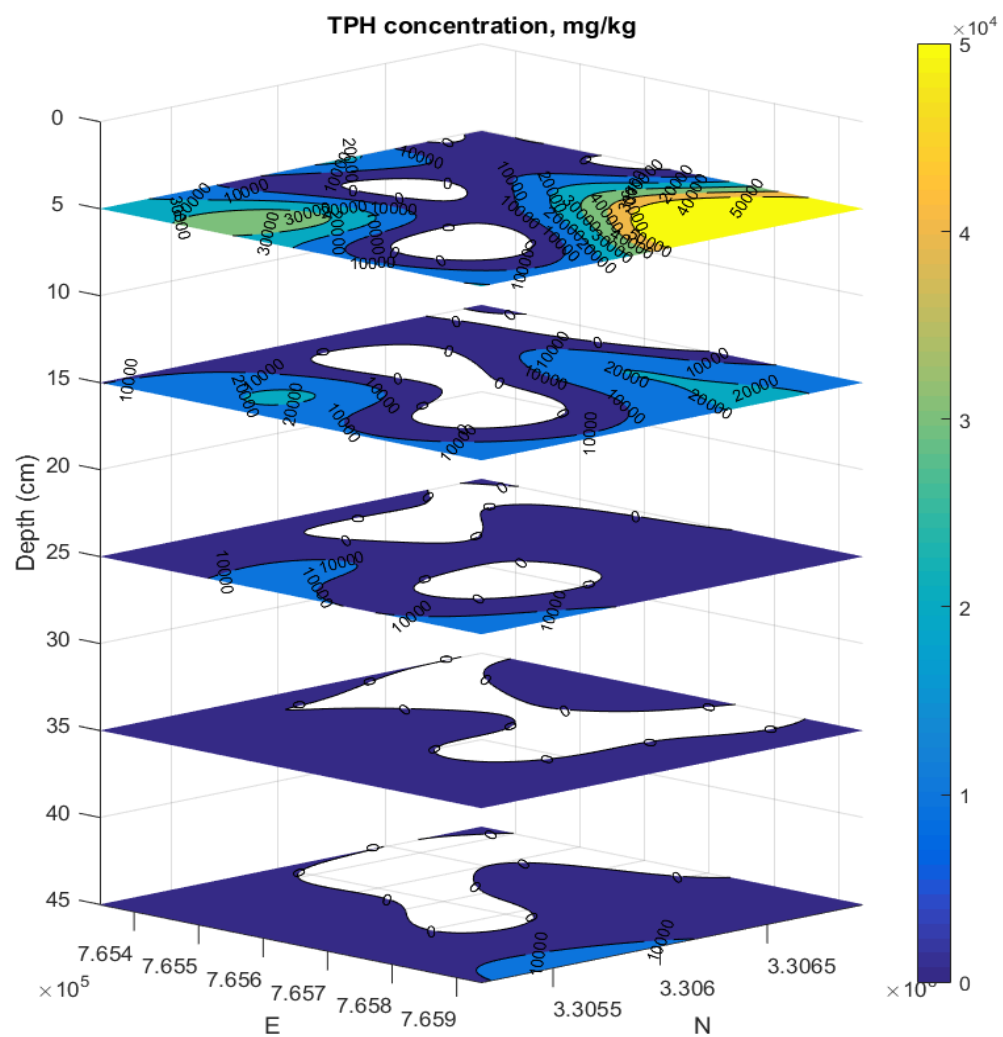
The methods used for model development and validation are provided in Chapter 3.

6.3 Data analysis and 3D mapping technology for 2-B Section of the Raudhatain Area

In this Chapter of our research the 85 soil samples that been collected from 20 locations will be analysed by using our developed 3D mapping technology and our novel sampling design and laboratory method for the 2-B Section of the Raudhatain Area.

6.3.1 Total petroleum hydrocarbon

TPH in the contaminated soil was highly variable both horizontally and vertically. The depth of contamination was limited to the top 50 cm of the soil profiles except in 4 locations (11, 18, 19 and 20) where the depth of contamination extended to about one metre from the soil surface. The soils with a TPH concentration of over 10000 mg/kg (>1%) were found at 9 out of 17 sampling locations (i.e. locations 5, 7, 10, 11, 13, 15, 18, 19 and 20) and limited to the topsoil layer (0-10 cm) except for soil profiles 11, 18, 19 and 20. The 3-D distribution of TPH within the investigated area is given in Fig. 6-1. The white colour region means that there is no contamination of the specific contaminants.



(B)

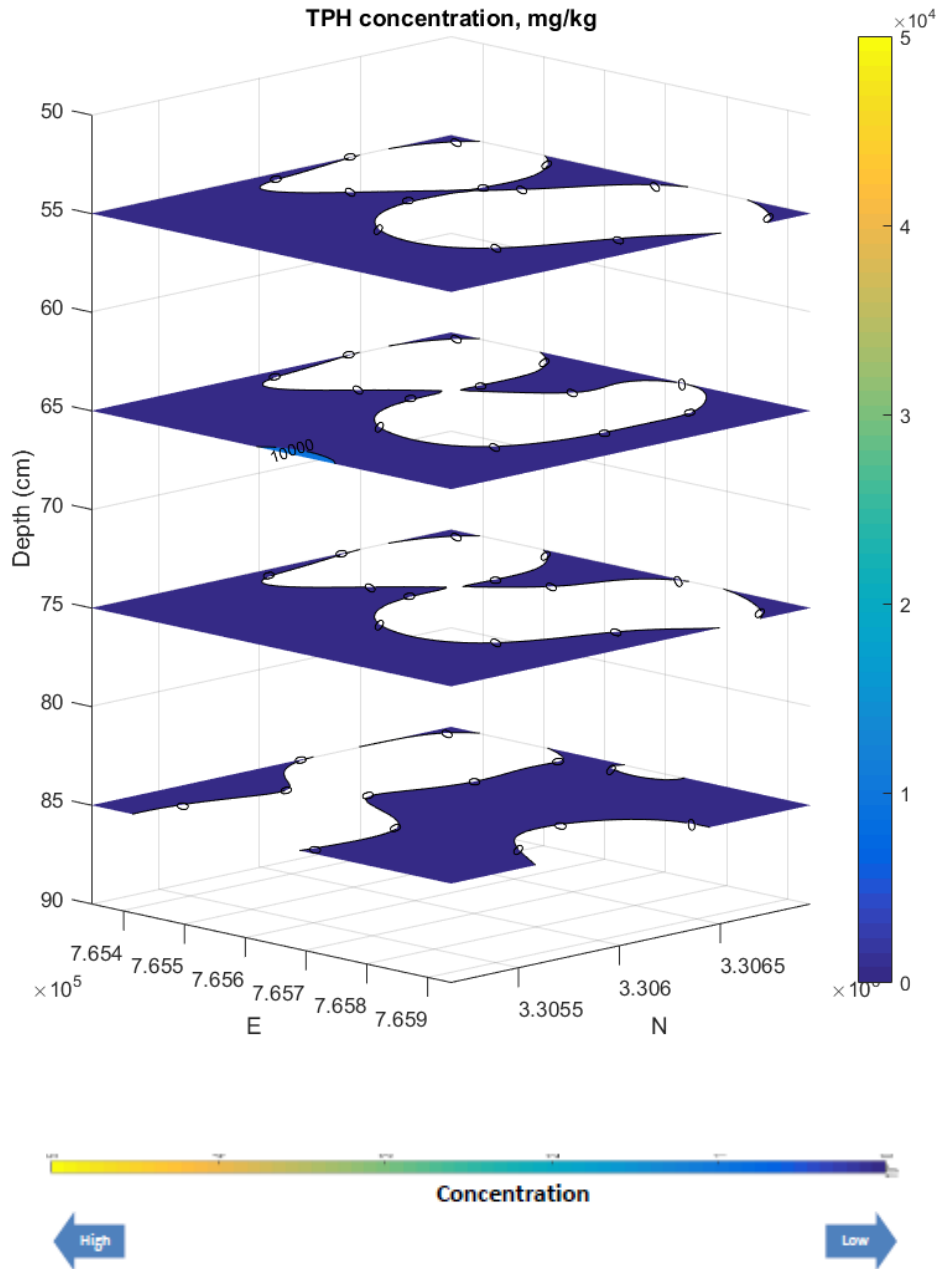
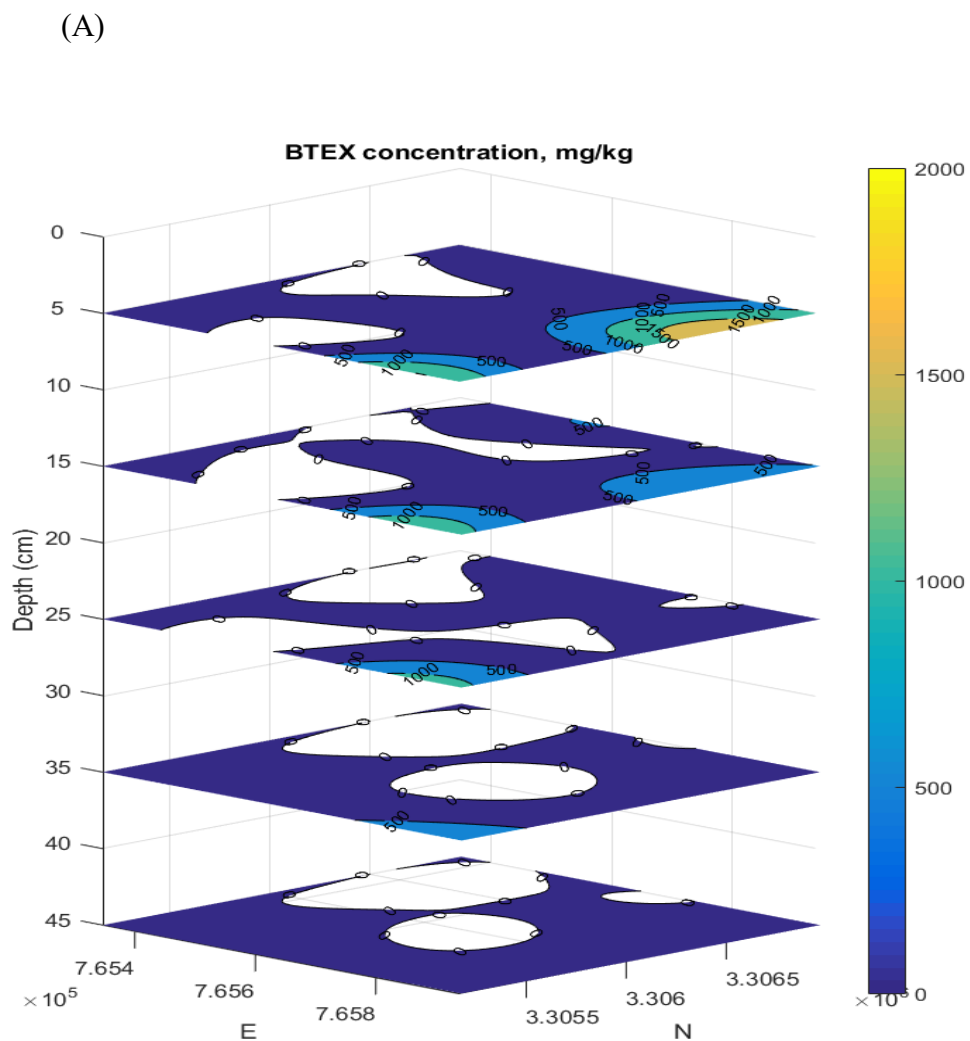


Figure 6.1 3-D distribution of TPH within the investigated area. (A) 0-50 cm consisting of 5 soil layers; 0-10, 10-20, 20-30, 30-40 and 40-50 cm, and (B) 50-90 cm consisting of 4 soil layers: 50-60, 60-70, 70-80 and 80-90cm. Change in color from blue to yellow indicates increase (horizontally and vertically) in the concentration (mg/kg) of TPH in the soils within the investigated area. The color bar is a standard way and explicitly indicates the variation of value of the parameter in Z axis.

6.3.2 BTEX

The sum of BTEX ranged from 0 to 14350 mg/kg with a mean value of 686 mg/kg. No benzene and methyl tert-butyl ether were detected in any samples collected. Xylene (o xylene and m/p xylene) dominated BTEX (83%).

BTEX varied horizontally with no or only a small amount of BTEX being detected in most of the investigated locations but a substantial amount of BEXT was present in the soils at Locations 11, 18, 19 and 20. BTEX tended to decrease with increasing depth within the soil profile, but different vertical variation patterns were observed. The 3-D distribution of BTEX within the investigated area is given in Figure 6.2.



(B)

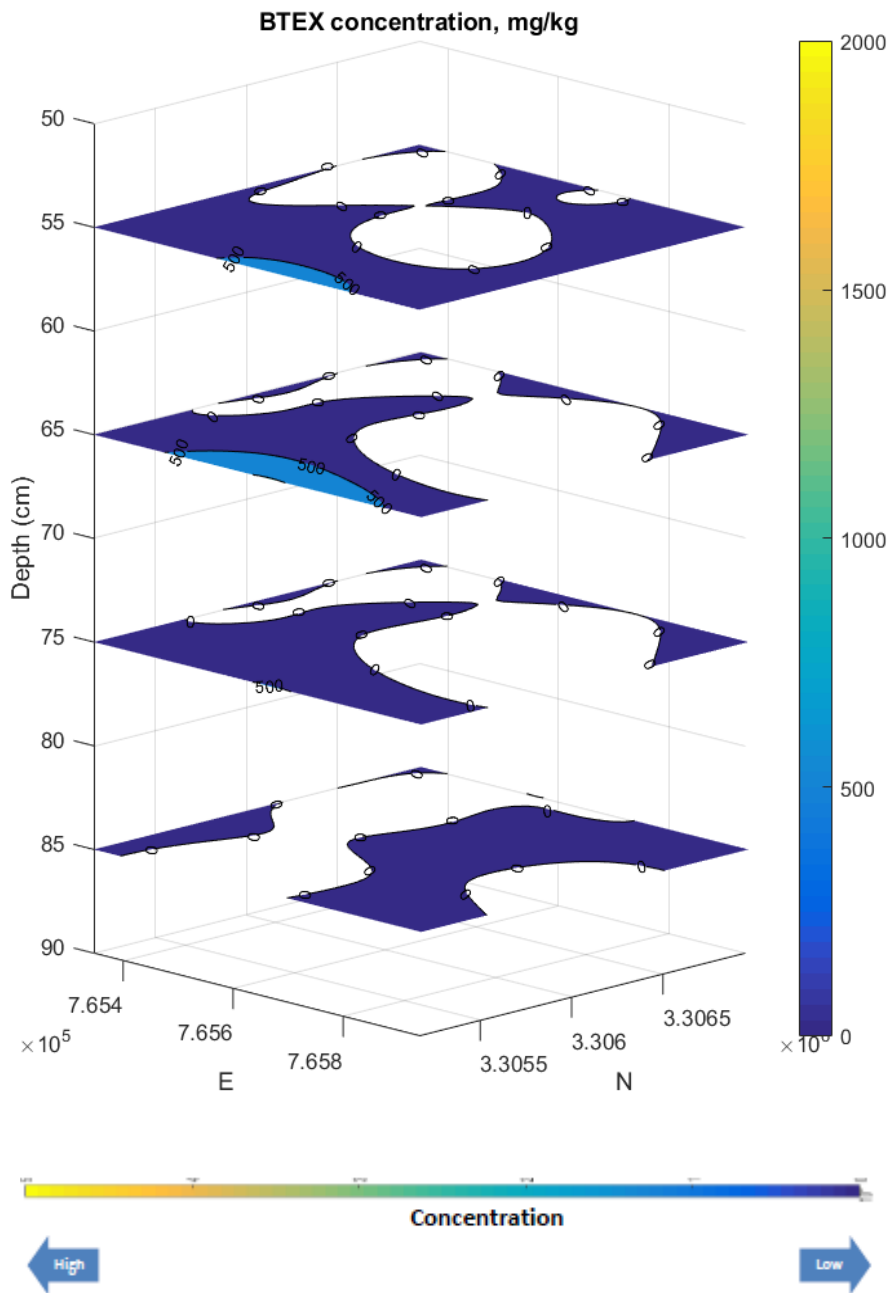
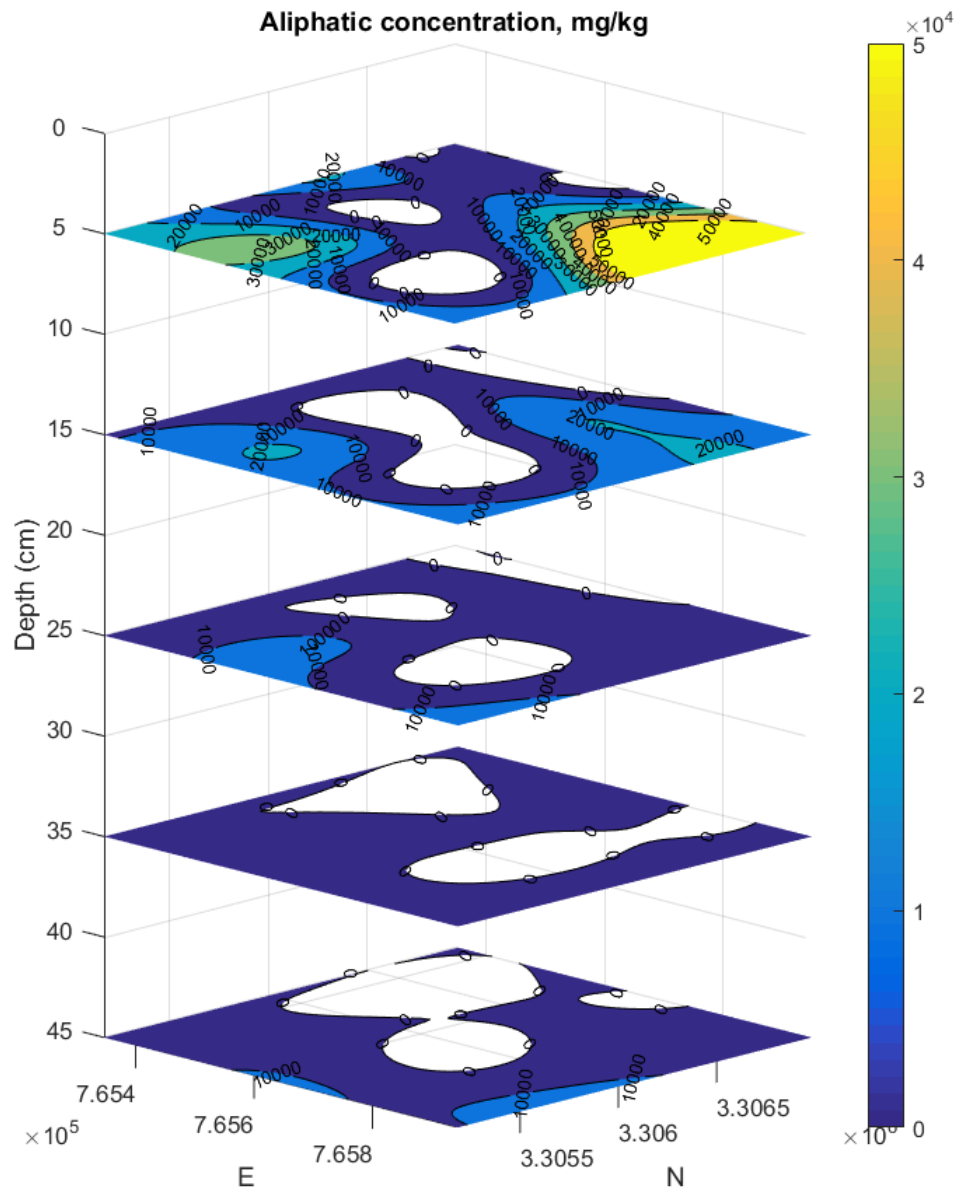


Figure 6.2 3-D distribution of BTEX within the investigated area. (A) 0-50 cm consisting of 5 soil layers; 0-10, 10-20, 20-30, 30-40 and 40-50 cm, and (B) 50-90 cm consisting of 4 soil layers: 50-60, 60-70, 70-80 and 80-90 cm. Change in color from blue to yellow indicates increase (horizontally and vertically) in the concentration (mg/kg) of BTEX in the soils within the investigated area. The color bar is a standard way and explicitly indicates the variation of value of the parameter in Z axis.

6.3.3 Aliphatic petroleum hydrocarbons

Like TPH, the sum of aliphatic hydrocarbons was highly variable both horizontally and vertically. The soils with higher concentration of aliphatic hydrocarbons were found at Locations 5, 7, 10, 11, 13, 15, 18, 19 and 20 and limited to the topsoil layer (0-10 cm) except for Soil Profiles 11, 18, 19 and 20. In most situations, Fraction C16-C35 dominated the aliphatic hydrocarbons. The 3-D distribution of aliphatics within the investigated area is given in Figure 6.3.

(A)



(B)

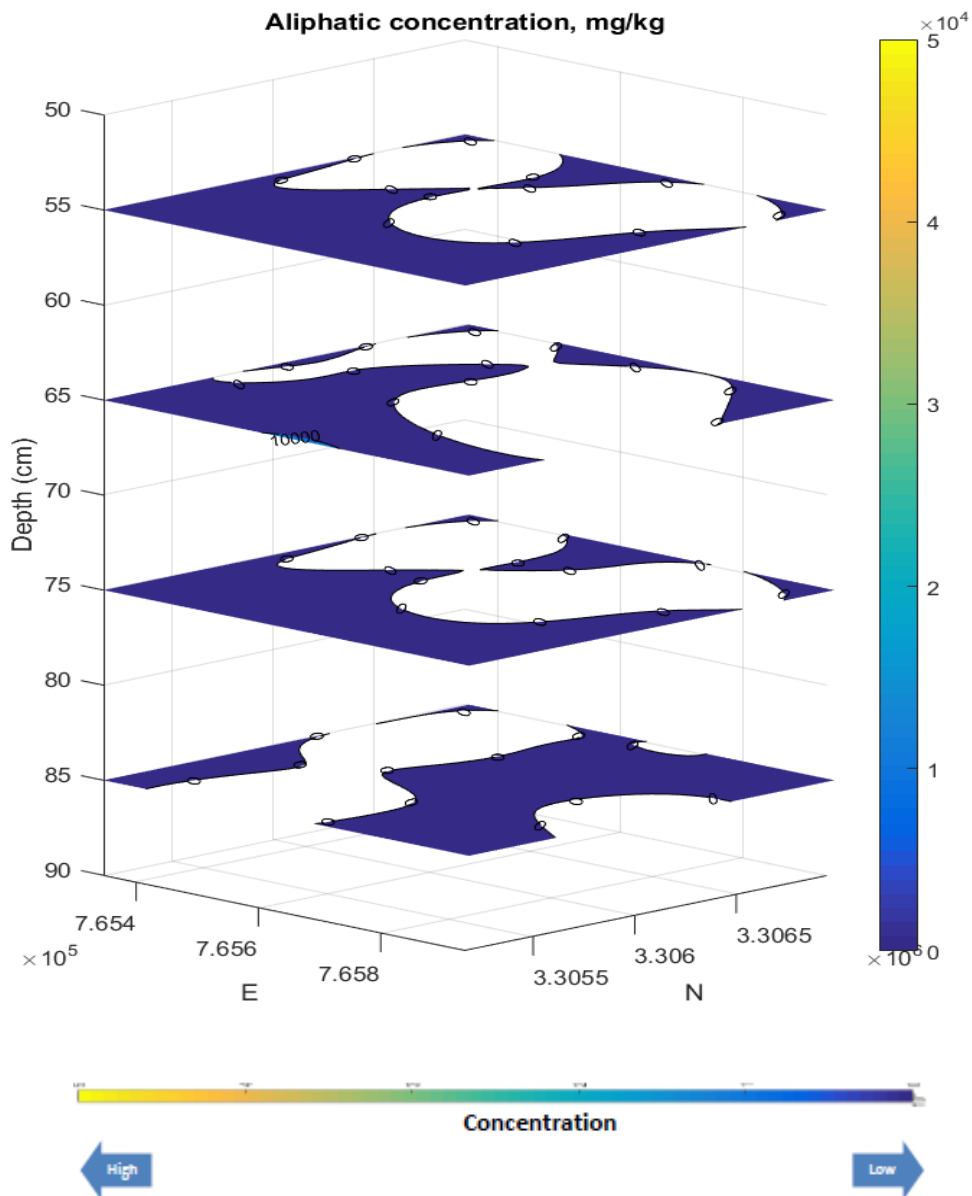
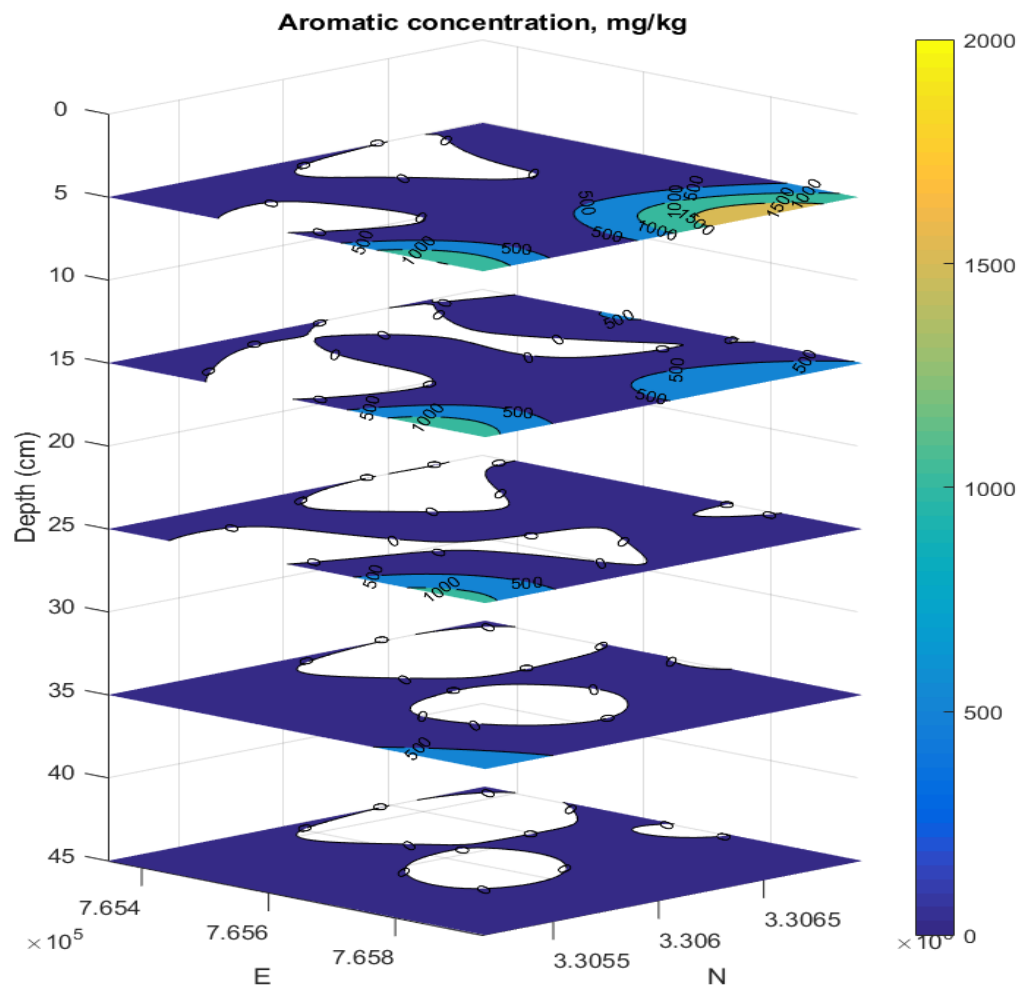


Figure 6.3 3-D distribution of Aliphatics within the investigated area. (A) 0-50 cm consisting of 5 soil layers; 0-10, 10-20, 20-30, 30-40 and 40-50 cm, and (B) 50-90 cm consisting of 4 soil layers: 50-60, 60-70, 70-80 and 80-90 cm. Change in color from blue to yellow indicates increase (horizontally and vertically) in the concentration (mg/kg) of Aliphatics in the soils within the investigated area. The color bar is a standard way and explicitly indicates the variation of value of the parameter in Z axis.

6.3.4 Aromatic petroleum hydrocarbons

No or only a small amount (<200 mg/kg) of aromatic hydrocarbons was detected in most of the investigated soil profiles except for Locations 9, 11, 18, 19 and 20. In most situations, Fraction C8- C16 dominated the aromatic hydrocarbons. The 3-D distribution of aromatics within the investigated area is given in Figure 6.4.

(A)



(B)

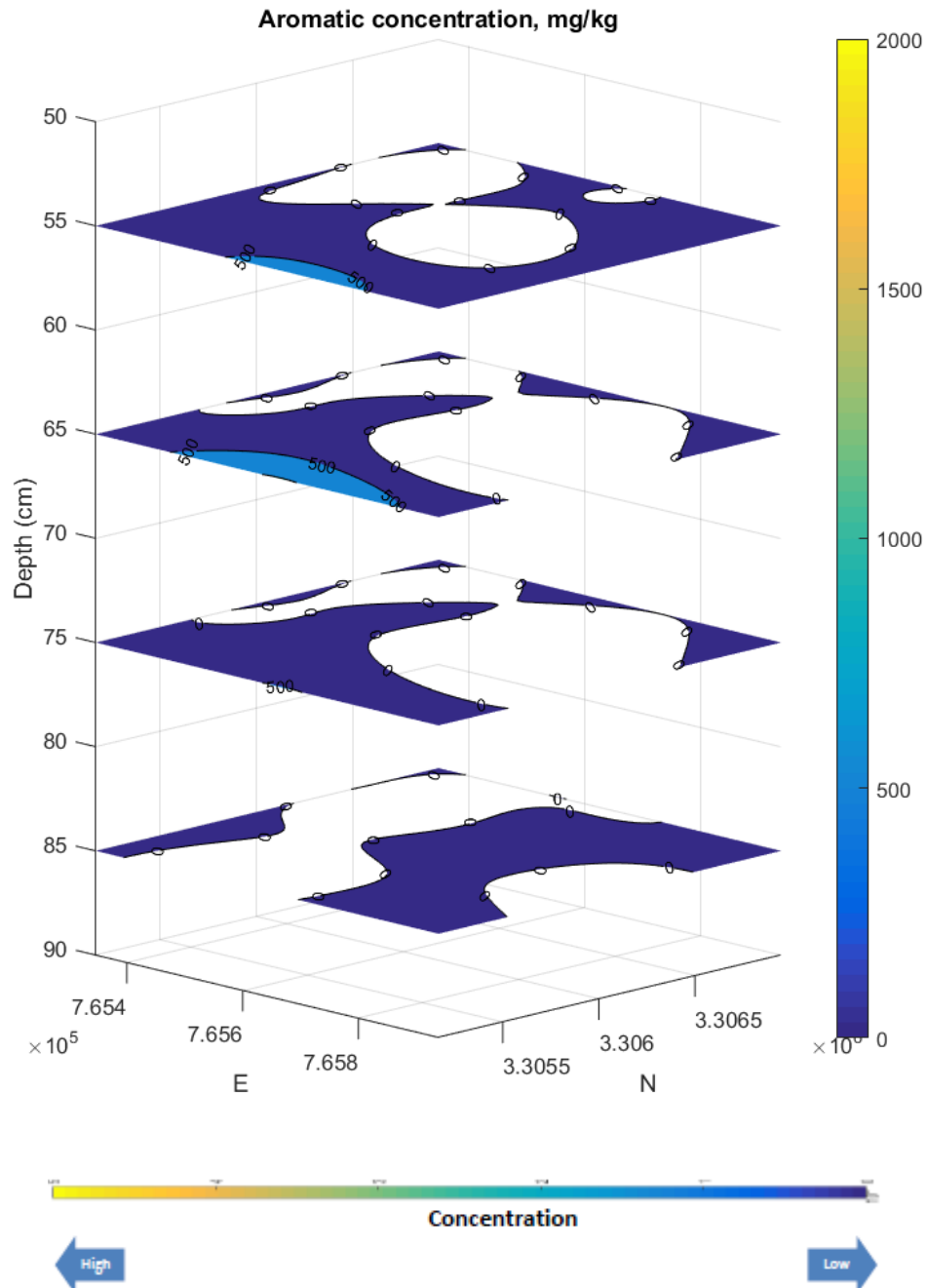


Figure 6.4 3-D distribution of aromatics within the investigated area. (A) 0-50 cm consisting of 5 soil layers; 0-10, 10-20, 20-30, 30-40 and 40-50 cm, and (B) 50-90 cm consisting of 4 soil layers: 50-60, 60-70, 70-80 and 80-90 cm. Change in color from blue to yellow indicates increase (horizontally and vertically) in the concentration (mg/kg) of Aromatics in the soils within the investigated area.

6.3.5 Polycyclic aromatic hydrocarbons

The sum of PAHs in the topsoil layer (0-10 cm) ranged from below detection limit to 16 mg/kg with a mean value of 4.7 mg/kg. No or only a small amount (<1.5 mg/kg) of total PAH was detected at locations 6, 8, 12, 15, 16 and 17 while Locations 10, 13 and 20 had a total PAH value over 12 mg/kg. Major PAH species included naphthalene, phenanthrene and anthracene. The distribution of total PAH in the surface soil layer is showed in Figure 6.5.

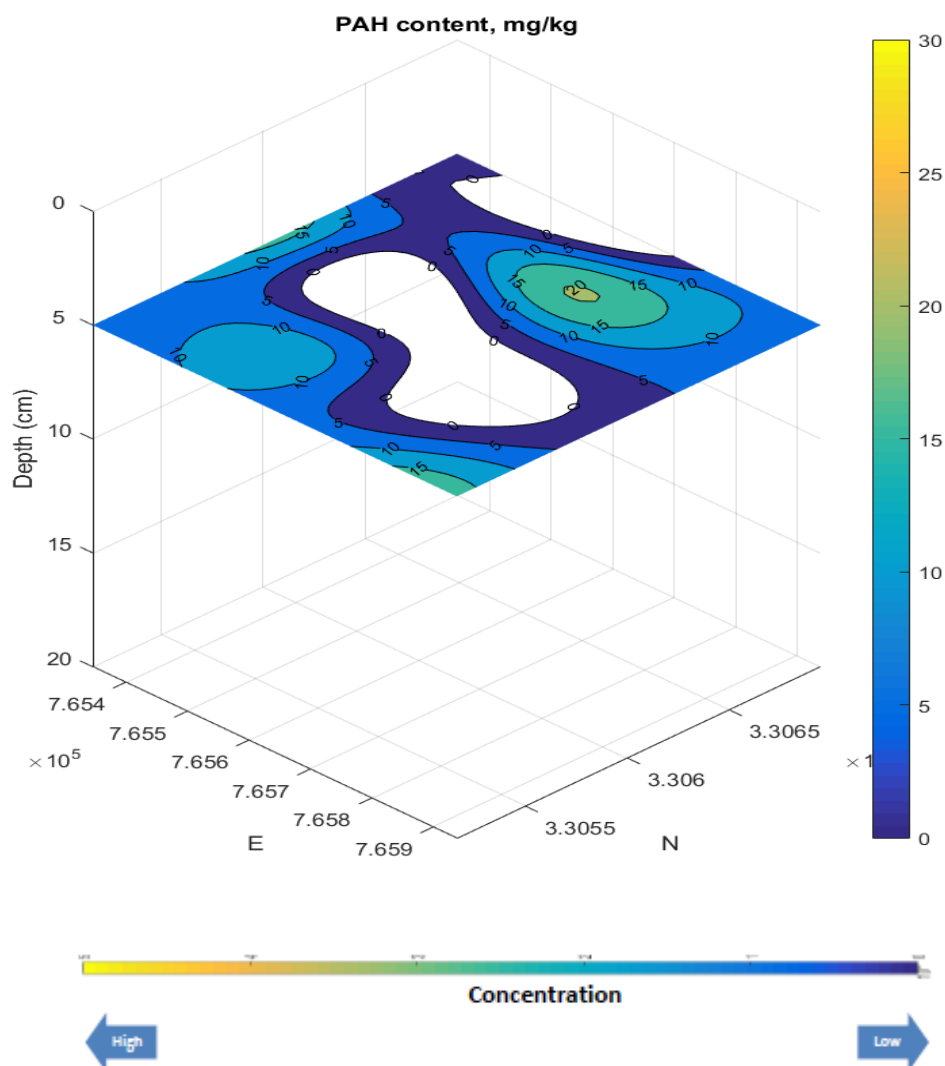


Figure 6.5 Spatial distribution of total PAH in the top 10 cm of soil within the investigated area. Change in color from blue to yellow indicates increase (horizontally and vertically) in the concentration (mg/kg) of PAH in the soils within the investigated area.

6.3.6 Estimation of Total Contaminated Soil Volume

For the 2-B Section of the Raudhatain Area, the thickness of contaminated soil (as defined by a trigger value of 10000 mg/kg (1%) for remedial action) varies from location to location. Part of the area contained no contaminated soil (<1% of TPH). The total volume of contaminated soils (>1% of TPH) is estimated to be 112,730 m³, which only accounts for 11.8% of the total soil volume from the surface to the 90 cm depth within the investigated area Figure 6.6.

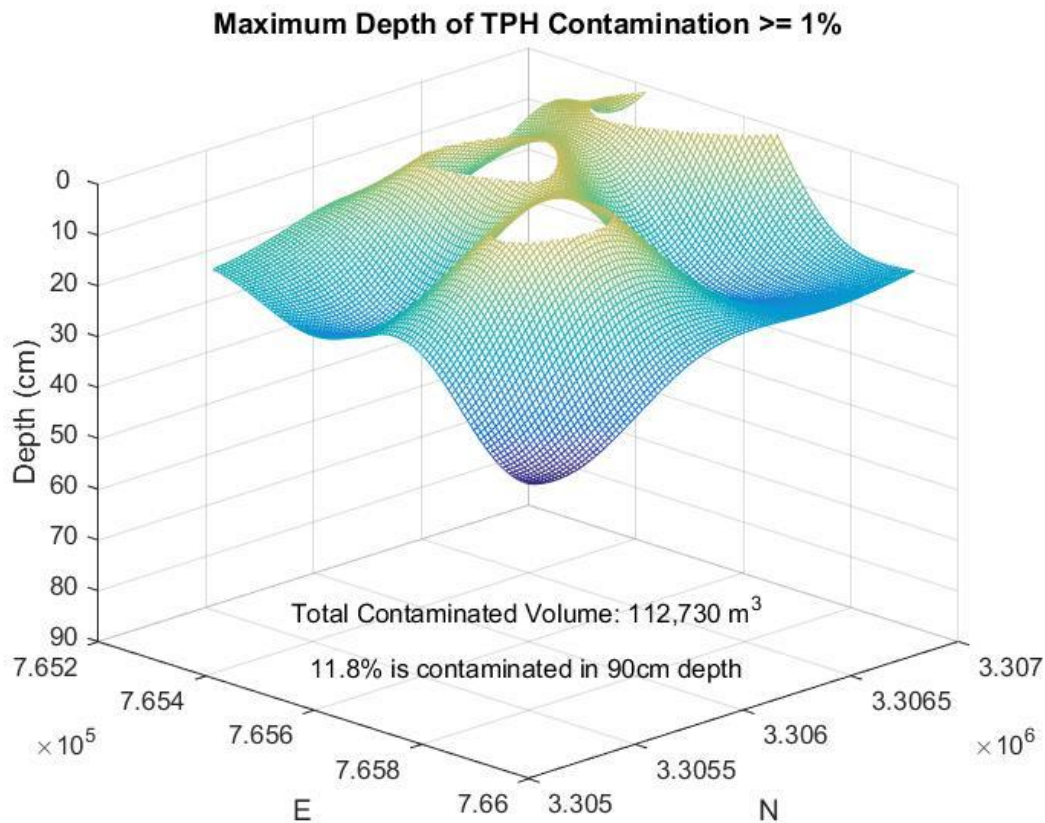


Figure 6.6 Graph showing the interface between the soil (upper part) with TPH > 10000 mg/kg (1%) and the soil (lower part) with TPH <10000 mg/kg (1%). The estimated total volume of soil above the interface is 112,730 m³, which accounts for 11.8% of the total volume of soil for the 90 cm thick soil layer in the investigated area.

6.3.7 Summary

In this case study research project several new novel methods have been developed to serve as a package with our novel 3D mapping technology. Our proposed methods which improve the cost-effectiveness of soil characterization include: (a) taking into account the vertical variation in both total petroleum hydrocarbon and various hydrocarbon species and (b) using 3-D mapping technology to establish models for spatial distribution of petroleum hydrocarbons affected soils with markedly reduced sampling density. In the next section of our research we will implement our developed 3D mapping technology for hydrocarbon contaminated sites in to our case study EPE4.

6.4 Model development for the Sludge Pit EPE4

Detailed information concerning effluent Pit EPE4 study areas and site selection was presented in Chapter 4. In this study, geostatistical interpolation techniques were used to develop site-specific predictive models for 3D mapping of TPH and various petroleum hydrocarbon fractions using the soil data directly from this investigation. Cross-validation methods were performed to minimize the number of sampling locations and sampling depths while the accuracy of prediction for the 3-D distribution of various soil parameters can be satisfactorily achieved.

6.4.1 Oil sludge

6.4.1.1 Total petroleum hydrocarbon

TPH in the sludge was spatially variable. It ranged from 18430 mg/kg to 172430 mg/kg with a mean value of 68724 mg/kg (n=16). The distribution of TPH within the investigated area is given in Figure 1. Aliphatic hydrocarbon fraction accounted for >81% of TPH and no BTEX was detected from any sludge sample. The distribution of TPH in the sludge materials within the investigated area is shown in Figure 6.7.

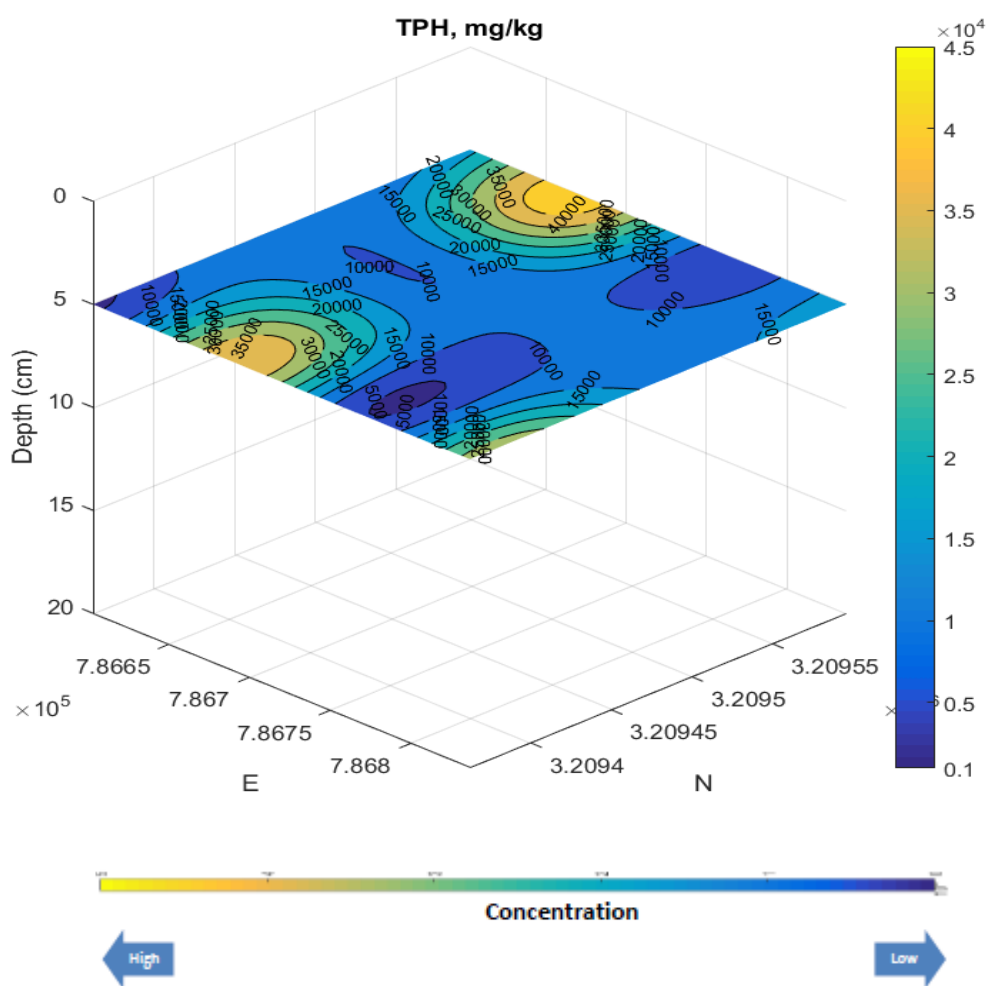


Figure 6.7 Distribution of TPH in the sludge materials within the investigated area. Change in color from blue to yellow indicates increase (horizontally and vertically) in the concentration (mg/kg) of TPH in the soils within the investigated area. The color bar is a standard way and explicitly indicates the variation of value of the parameter in Z axis.

6.4.1.2 Aliphatic hydrocarbons

Almost no hydrocarbons with a length of carbon chain > C16 were detected and the predominant hydrocarbon fraction was C21-C35. The distribution of total aliphatic hydrocarbon and the three major fractions are given in Figs. 6.8-6.9.

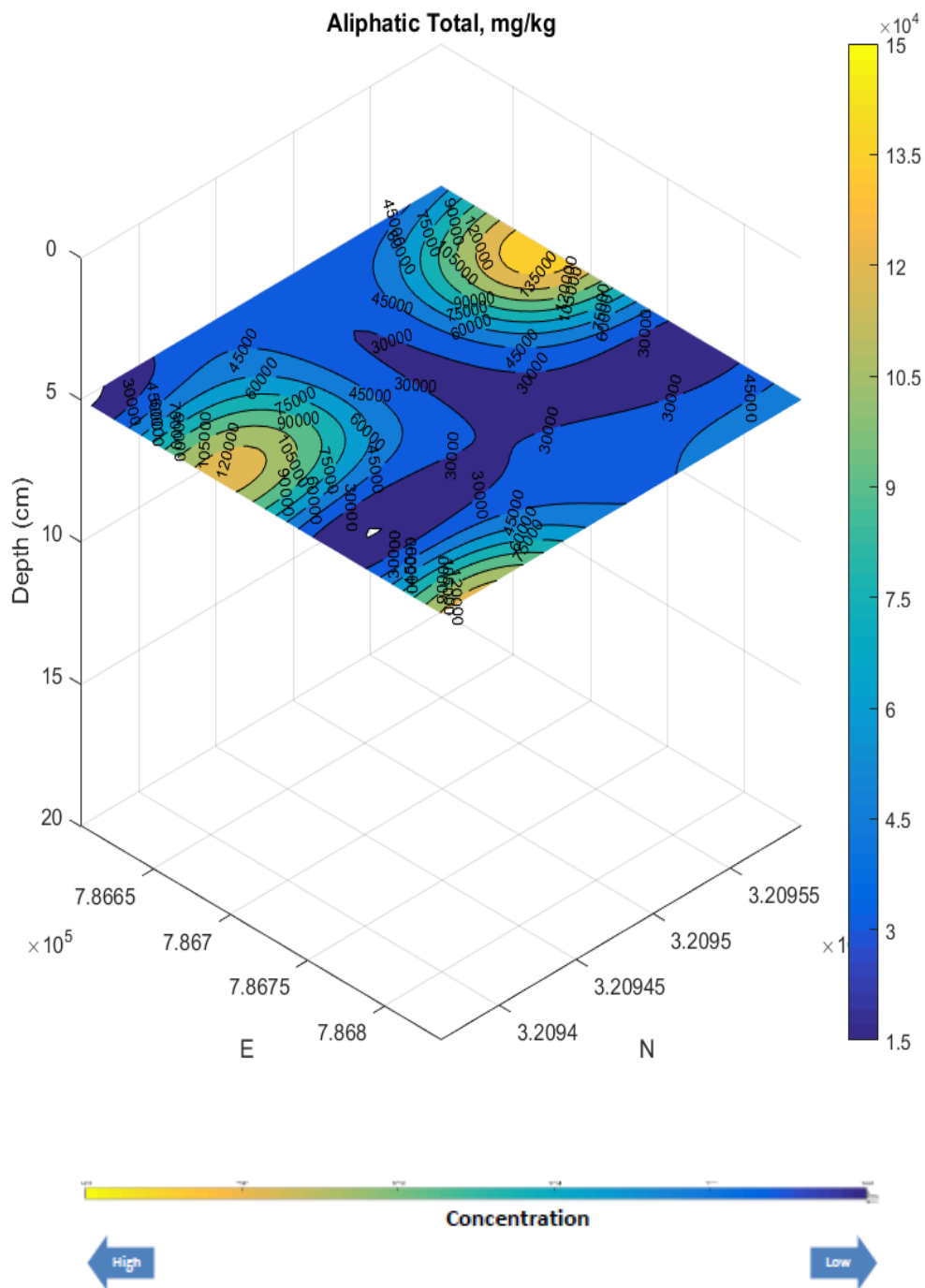


Figure 6.8 Distribution of the total aliphatic hydrocarbon in the sludge materials within the investigated area. Change in color from blue to yellow indicates increase (horizontally and vertically) in the concentration (mg/kg) of Aliphatic in the soils within the investigated area. The color bar is a standard way and explicitly indicates the variation of value of the parameter in Z axis.

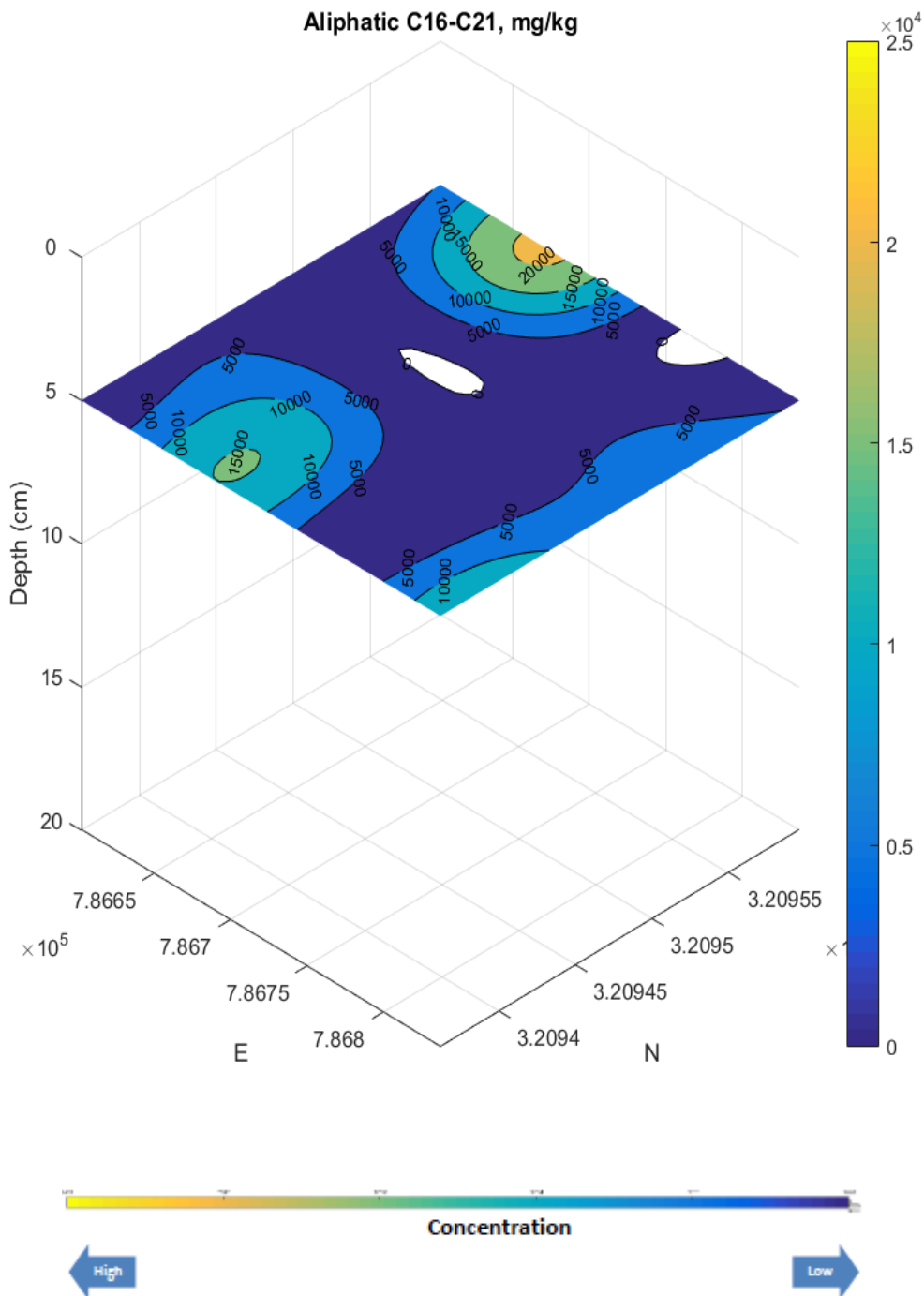


Figure 6.9 Distribution of the aliphatic hydrocarbon fraction C16-C21 in the sludge materials within the investigated area. Change in color from blue to yellow indicates increase (horizontally and vertically) in the concentration (mg/kg) of Aliphatic in the soils within the investigated area. The color bar is a standard way and explicitly indicates the variation of value of the parameter in Z axis.

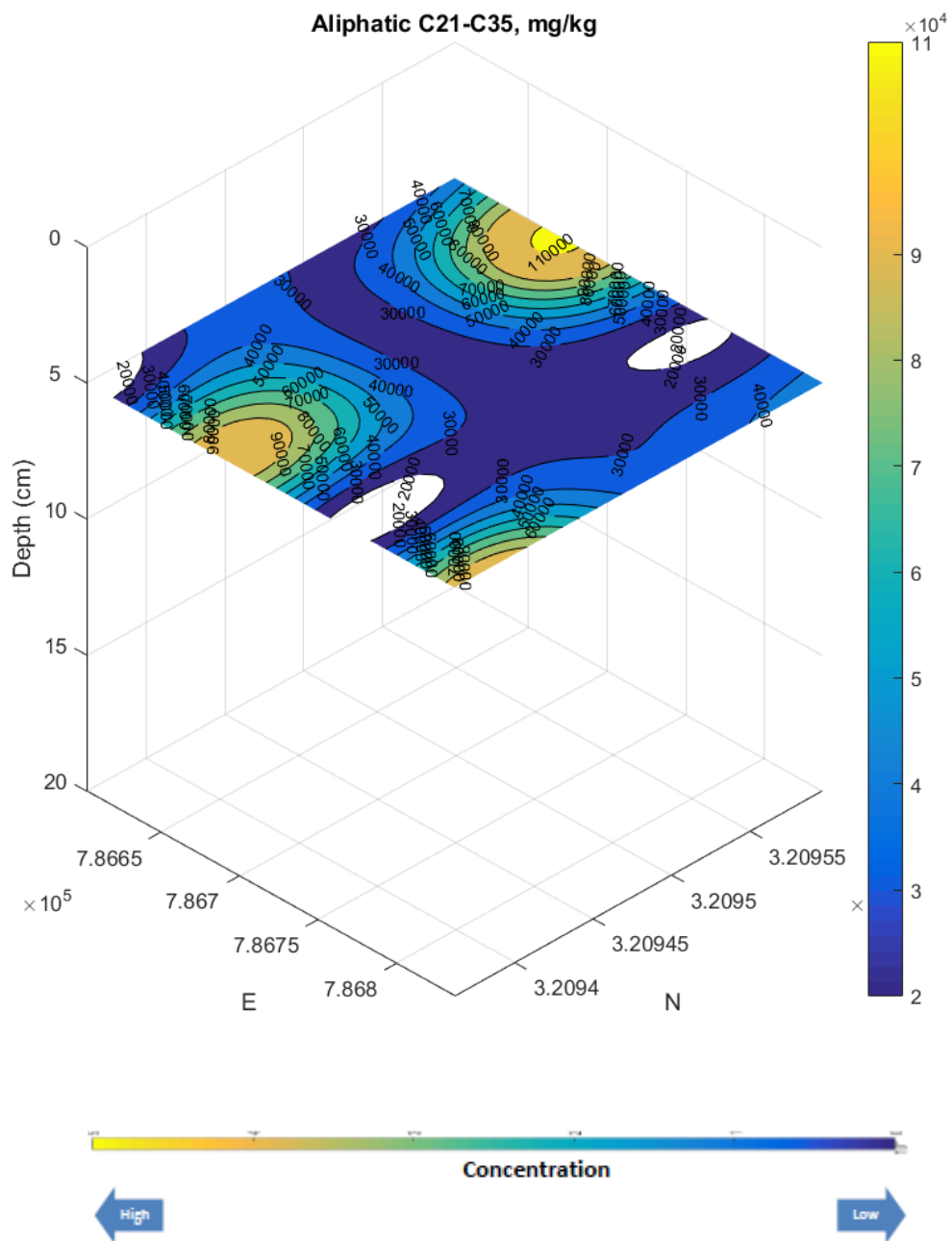


Figure 6.10 Distribution of the aliphatic hydrocarbon fraction C21-C35 in the sludge materials within the investigated area. Change in color from blue to yellow indicates increase (horizontally and vertically) in the concentration (mg/kg) of Aliphatic in the soils within the investigated area. The color bar is a standard way and explicitly indicates the variation of value of the parameter in Z axis.

6.4.1.3 Aromatic hydrocarbons

The distribution pattern of aromatic hydrocarbons was similar to that of aliphatic hydrocarbons. Fractions with carbon chain longer shorter than C12 and longer than C35 were not detected with Fraction C21-C35 dominated the aliphatic hydrocarbons (Figs. 6.12-6.13)

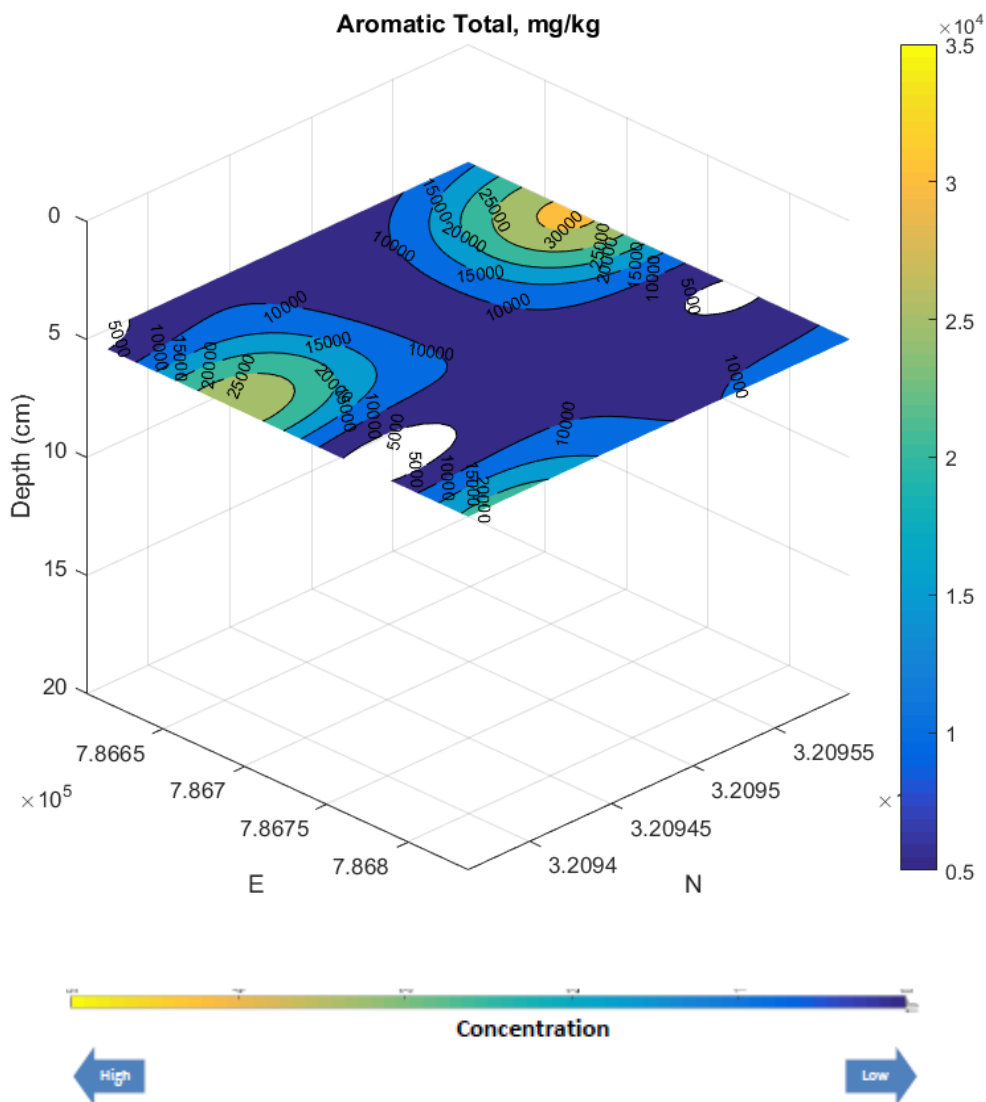


Figure 6.12 Distribution of the total aromatic hydrocarbon in the sludge materials within the investigated area. Change in color from blue to yellow indicates increase (horizontally and vertically) in the concentration (mg/kg) of aromatic in the soils within the investigated area. The color bar is a standard way and explicitly indicates the variation of value of the parameter in Z axis

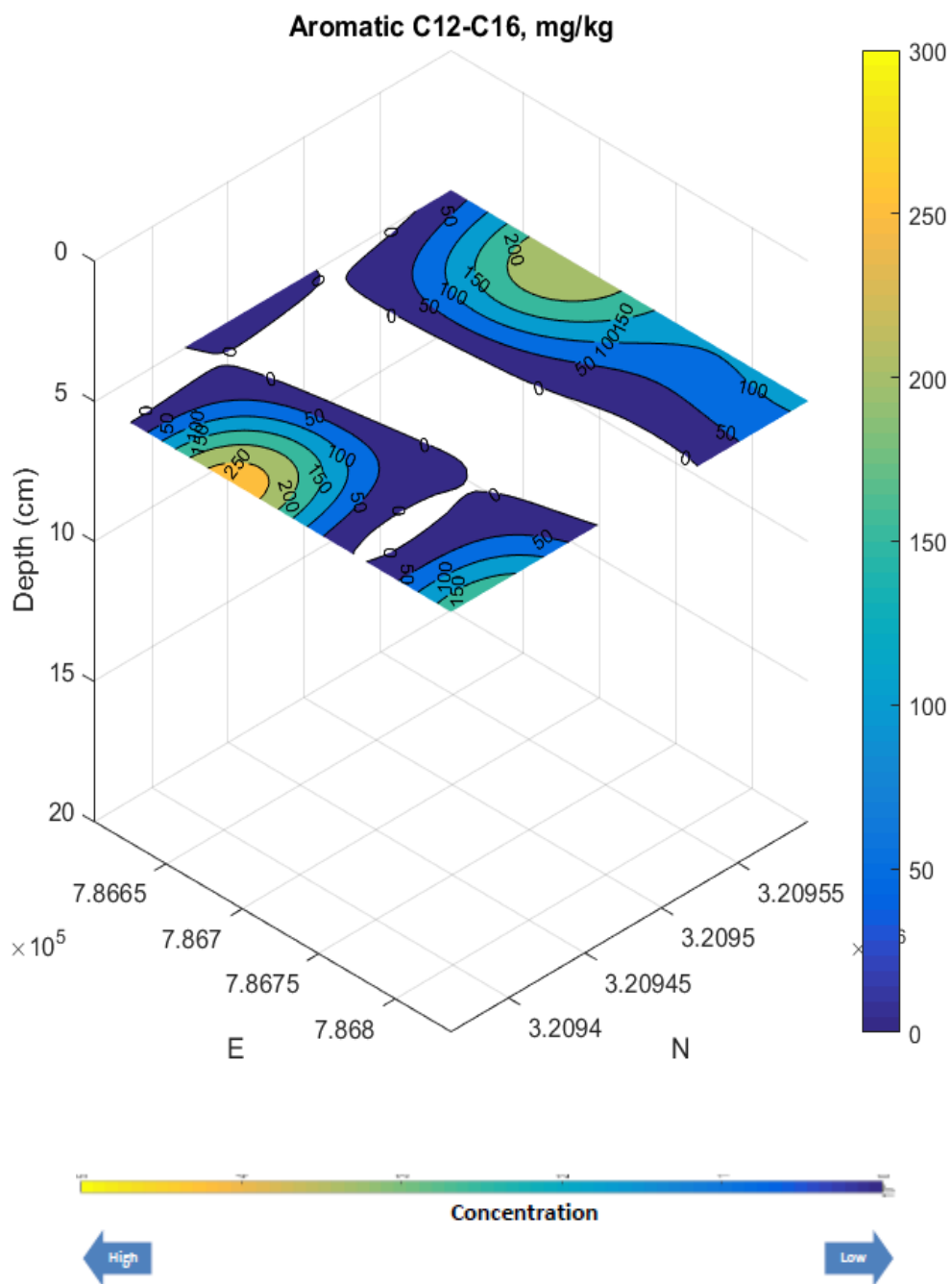


Figure 6.13 Distribution of the aromatic hydrocarbon fraction C12-C16 in the sludge materials within the investigated area. Change in color from blue to yellow indicates increase (horizontally and vertically) in the concentration (mg/kg) of aromatic in the soils within the investigated area. The color bar is a standard way and explicitly indicates the variation of value of the parameter in Z axis

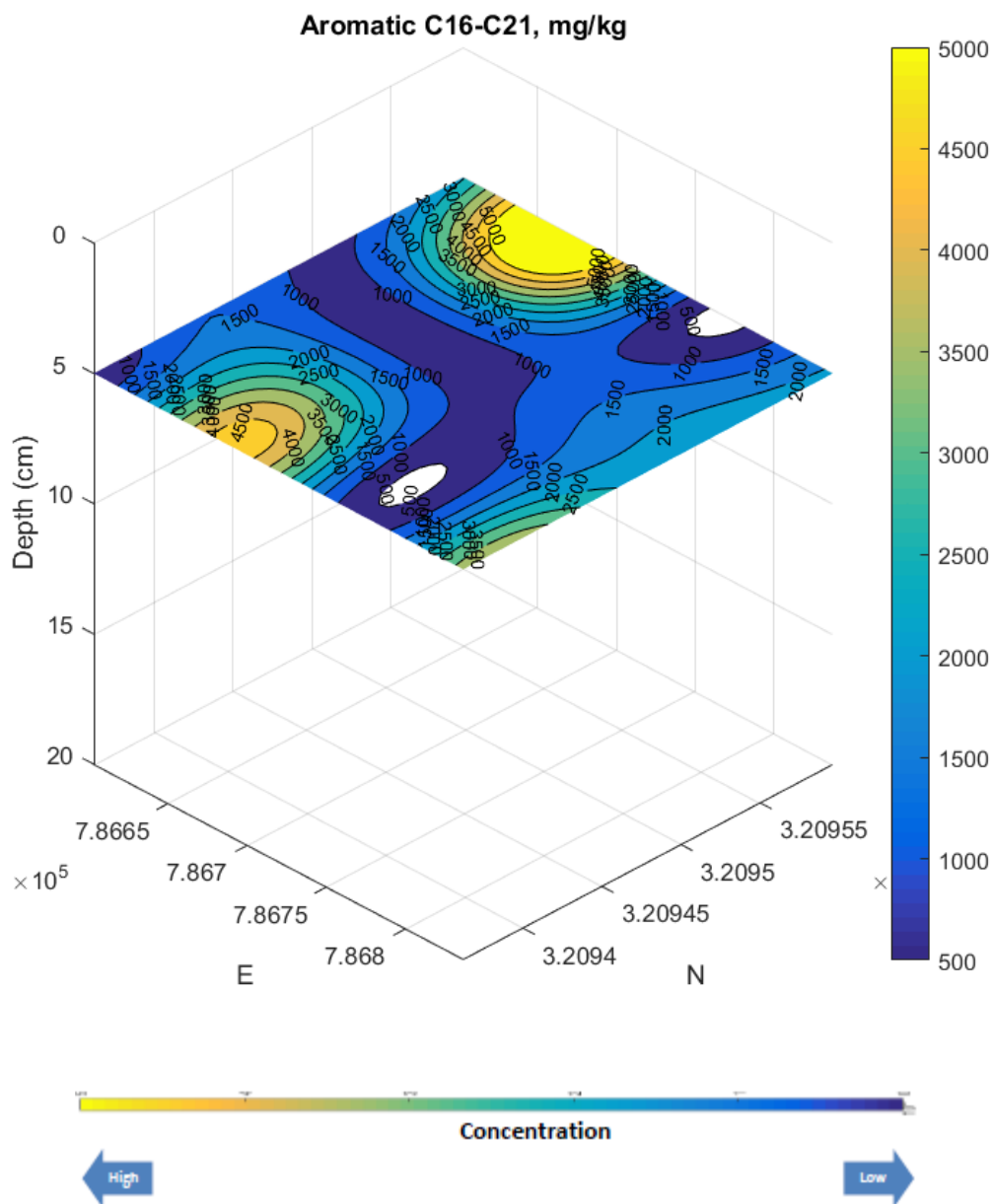


Figure 6.14 Distribution of the aromatic hydrocarbon fraction C16-C21 in the sludge materials within the investigated area. Change in color from blue to yellow indicates increase (horizontally and vertically) in the concentration (mg/kg) of aromatic in the soils within the investigated area. The color bar is a standard way and explicitly indicates the variation of value of the parameter in Z axis

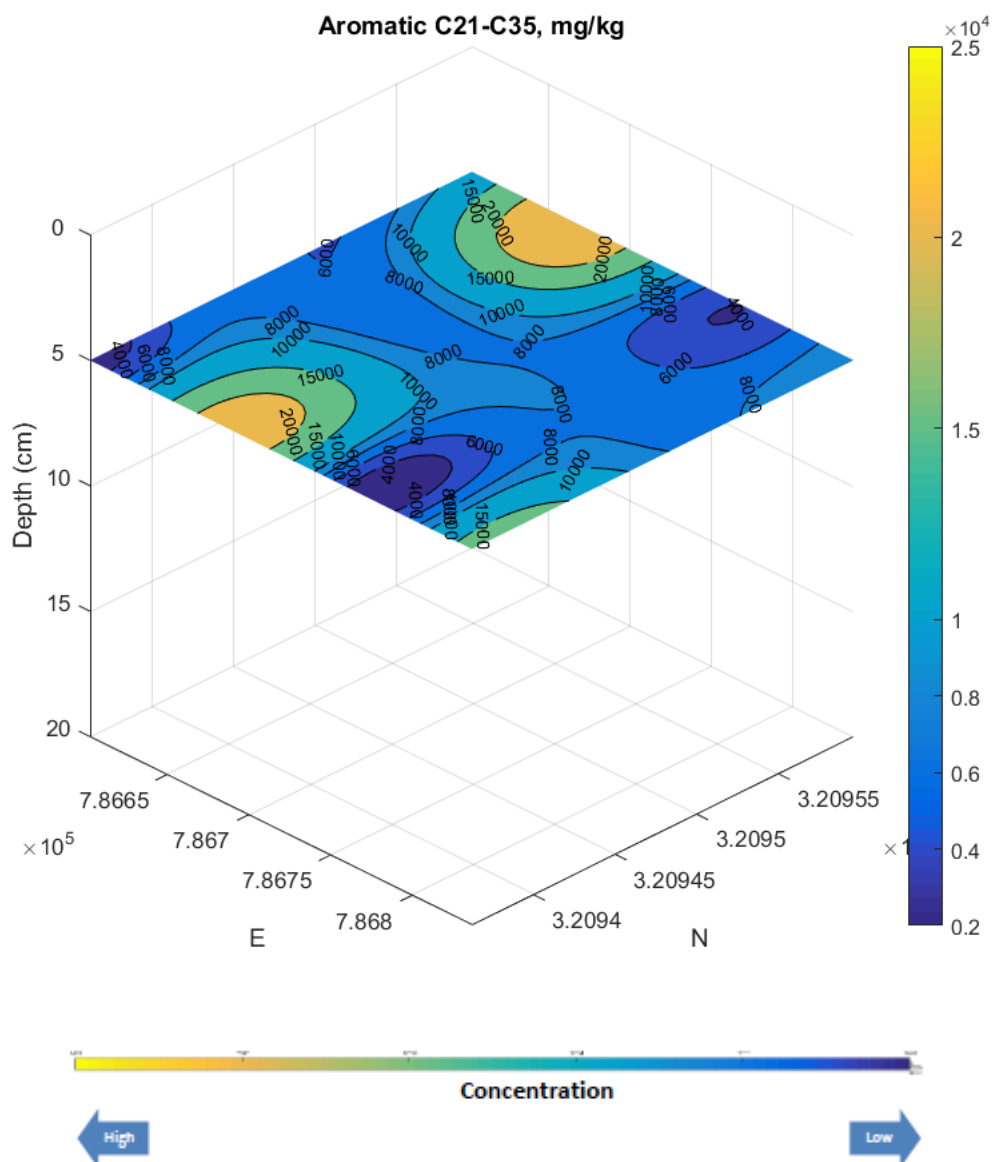


Figure 6.15 Distribution of the aromatic hydrocarbon fraction C21-C35 in the sludge materials within the investigated area. Change in color from blue to yellow indicates increase (horizontally and vertically) in the concentration (mg/kg) of aromatic in the soils within the investigated area. The color bar is a standard way and explicitly indicates the variation of value of the parameter in Z axis

6.4.1.4 Polycyclic aromatic hydrocarbons

Total PAH in the sludge materials was only detected in isolated locations with a very low value (<20 mg/kg). The distribution of total PAH is given in Fig. 6.16.

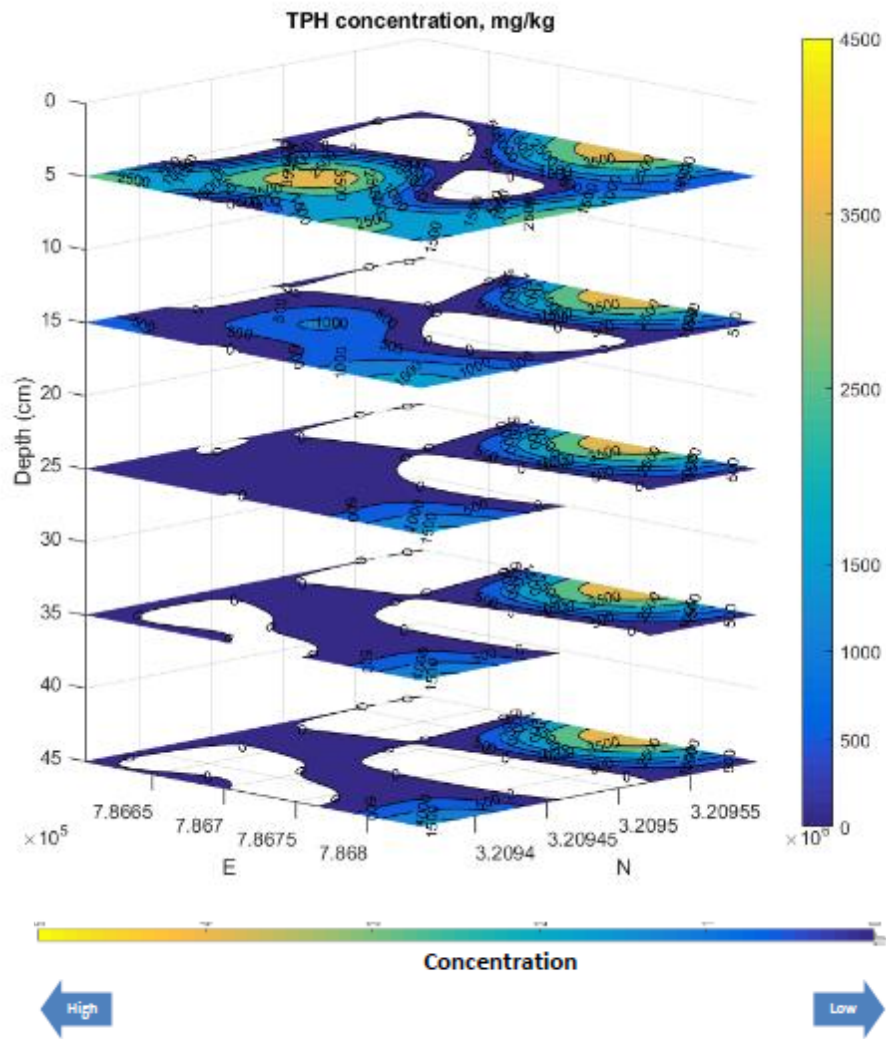


Figure 6.17 3-D distribution of TPH within the investigated area. Change in color from blue to yellow indicates increase (horizontally and vertically) in the concentration (mg/kg) of TPH in the soils within the investigated area. The color bar is a standard way and explicitly indicates the variation of value of the parameter in Z axis.

6.4.2.2 Aliphatic hydrocarbon

Like TPH, either the sum of aliphatic hydrocarbons or the sum of aromatic hydrocarbons was highly variable both horizontally and vertically. Similar to the overlying sludge materials, Fraction C16-C35 dominated both the aliphatic hydrocarbons and aromatic hydrocarbons. The 3-D distribution of the total aliphatic hydrocarbon and total aromatic hydrocarbon within the investigated area is given in Fig. 6-18 and 6-19, respectively.

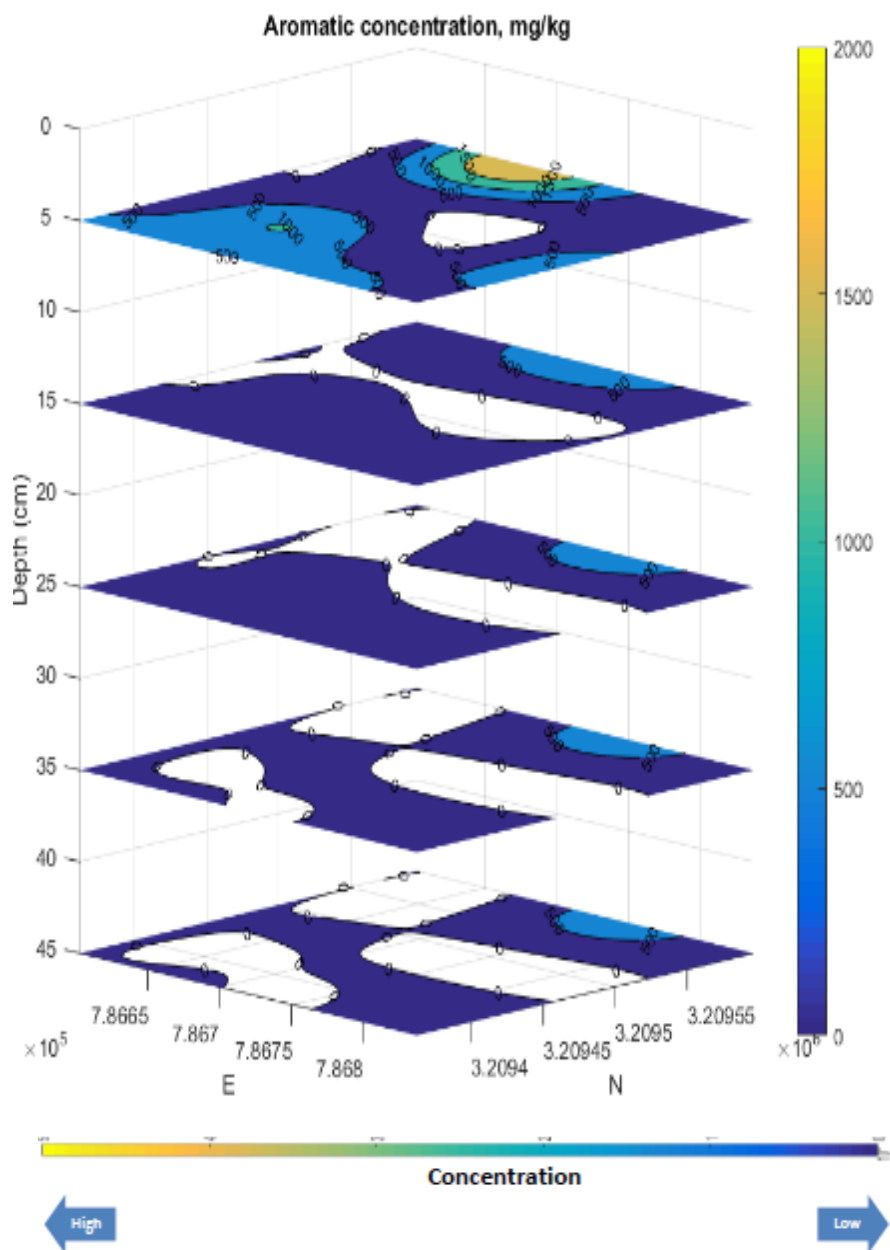


Figure 6.19 3-D distribution of aromatics within the investigated area. Change in color from blue to yellow indicates increase (horizontally and vertically) in the concentration (mg/kg) of aromatics in the soils within the investigated area. The color bar is a standard way and explicitly indicates the variation of value of the parameter in Z axis.

6.4.2.3 Polycyclic aromatic hydrocarbons

The sum of PAHs in the topsoil layer (0-10 cm) ranged from below detection limit to 15 mg/kg. Major PAH species included chrysene and phenanthrene. The

distribution of total PAH in the surface soil layer is showed in Figure 6.20.

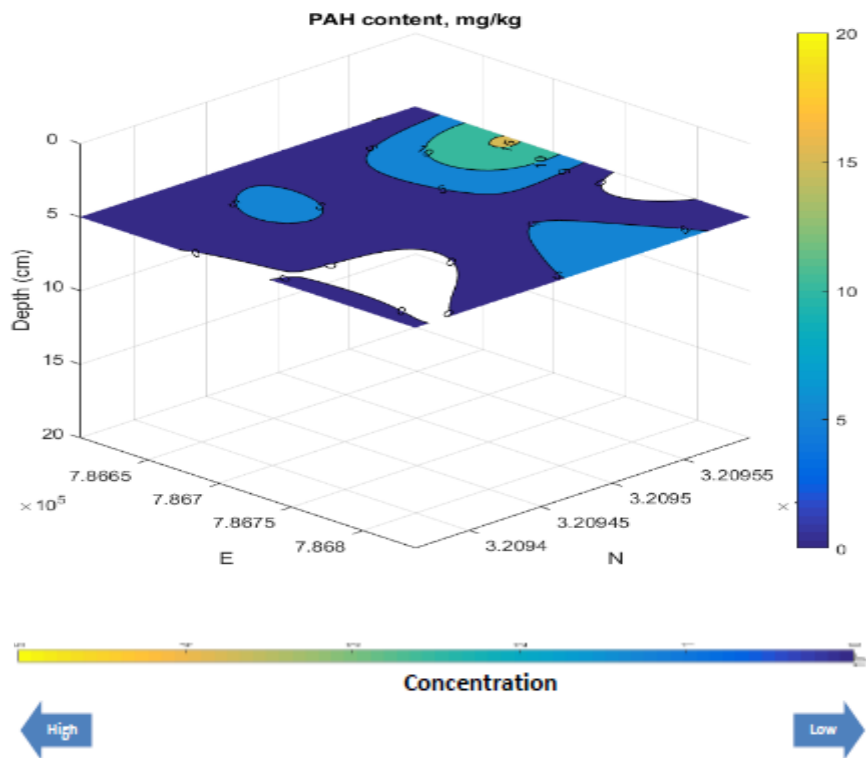


Figure 6.20 Spatial distribution of total PAH in the top 10 cm of soil within the investigated area. Change in color from blue to yellow indicates increase (horizontally and vertically) in the concentration (mg/kg) of PAH in the soils within the investigated area. The color bar is a standard way and explicitly indicates the variation of value of the parameter in Z axis.

6.4.3 Concluding Discussion

Any interpolation methods only provide reasonable prediction based on the reliability of the data provided. However, different methods certainly possess individual advantages for varied situations. IDW method gives prediction which sensitively depends on the amount of the available data or data density because the local interpolation is solely determined by its distance to the sampling points. However, Kriging provides the interpolation based on an initial trend evaluation for the sampling data obtained. In terms of the difference in fundamental principles, Kriging has been ascertained to be more practical and reliable for the project requesting for less sampling data. Regarding the cross-validation, we didn't believe that it has practical meaning for this project because all data had been noticed to have little correlation between each other. It means that any results of the a cross-validation have little general meaning and couldn't provide confidence. Consequently, only Kriging provided fundamental confidence Figure 6.21.

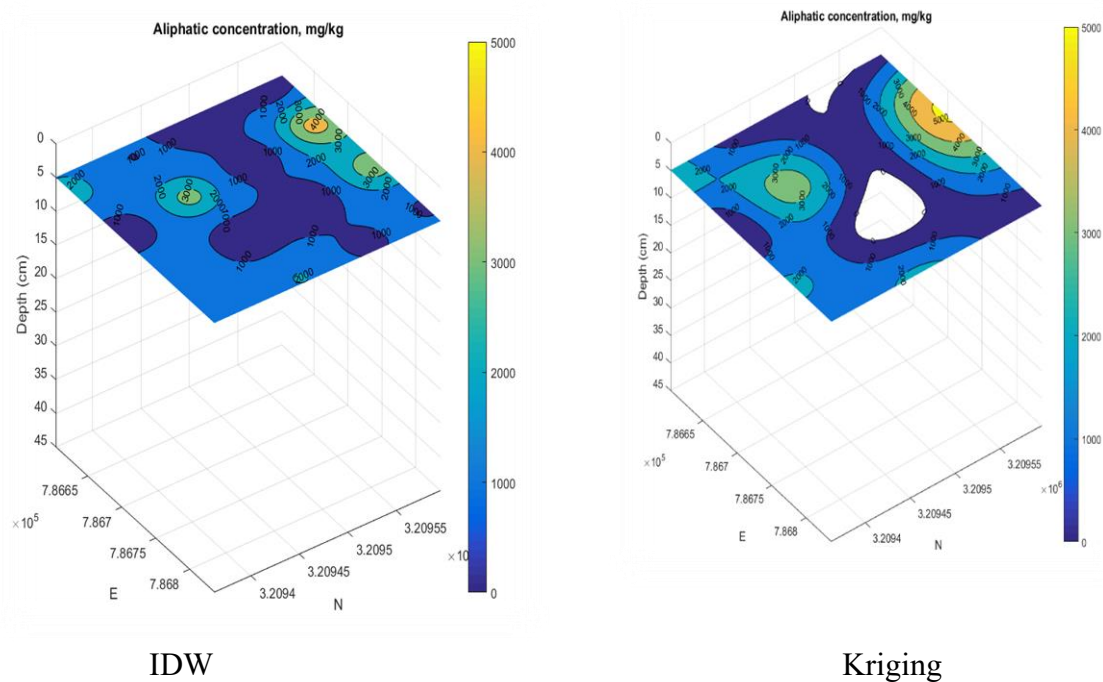
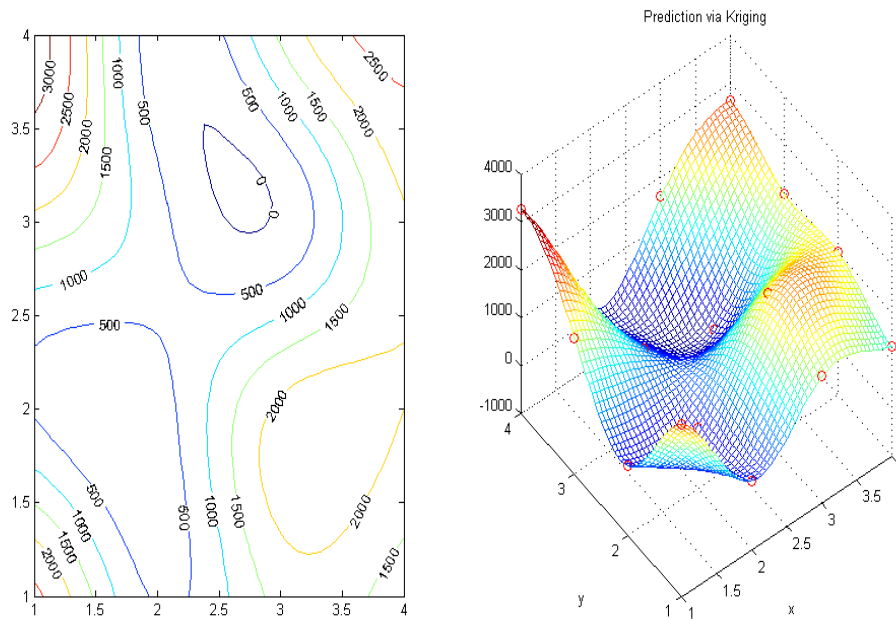


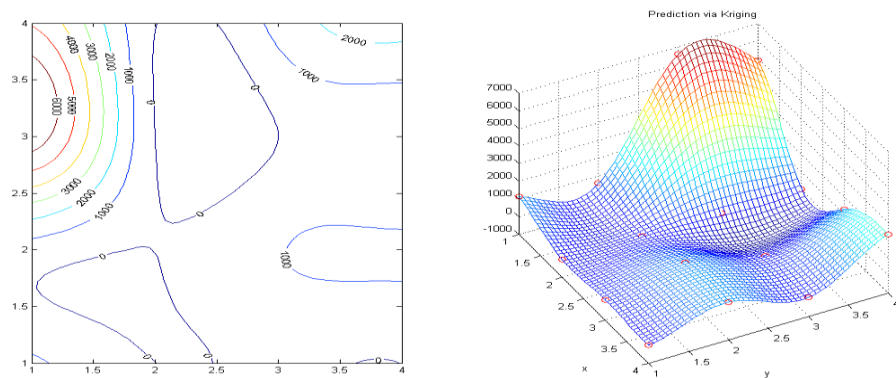
Figure 6.21 Comparison between the Kriging and IDW for one set of the observation data.

The investigation shows that both methods perform poor when extrapolating data based on the sampling points in a small region for a wide region. Kriging produced significant improvement if the random sampling points covers that whole interpolation

range, quality of Kriging is quite sensitive to the distribution of sample data as presented in Figure 6.22 below.



Level 1



Level 2

Figure 6.22 Quality of Kriging is quite sensitive to the distribution of sample data.

In the first phase of our 3D Models development for predicting spatial variation of crude Oil-Contaminated soil, we have developed inverse distance weighting interpolation code using MATLAB for project SPB1 as a first milestone achievement towards our 3D soil mapping for hydrocarbon contaminated sites. In the second phase the software tool has been further developed to implement a more advanced

interpolation method, the Kriging. To validate the developed tool and compare the performance of the Kriging and IDW modeling two theoretical mathematical functions of a single variable to evaluate the influence of the sampling number and distribution. In the third phase of our technology development we applied our sampling design, methodology and our sampling method analysis into our developed 3D mapping technology for further improvement and used cross-validation on the two pilot studies 2-B section Northern Kuwait, and Pit EPE4 southern Kuwait for further improvement, adjustment and toning.

Chapter 2 section 2.4.7.1 cross-validation, has been performed as one of the most important concepts in any type of data modeling for assessing the performance of spatial interpolation methods for 2-B Section of the Raudhatain Area Figure 6.23.

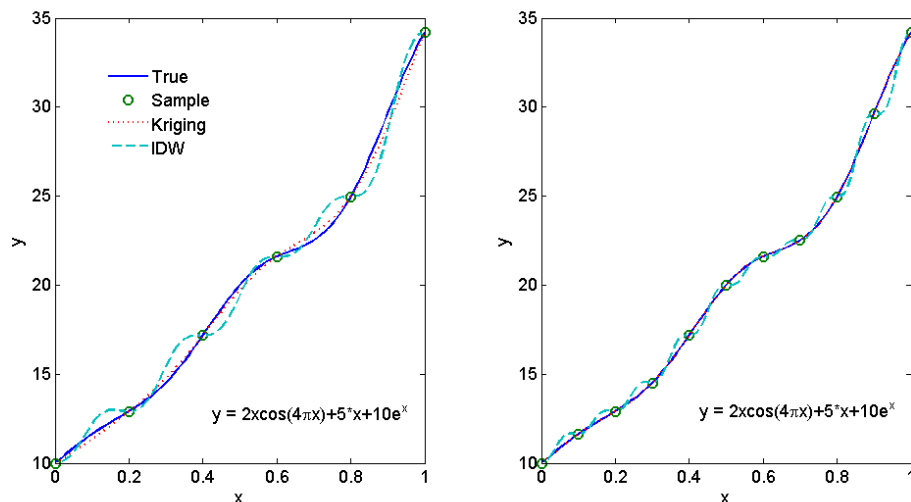


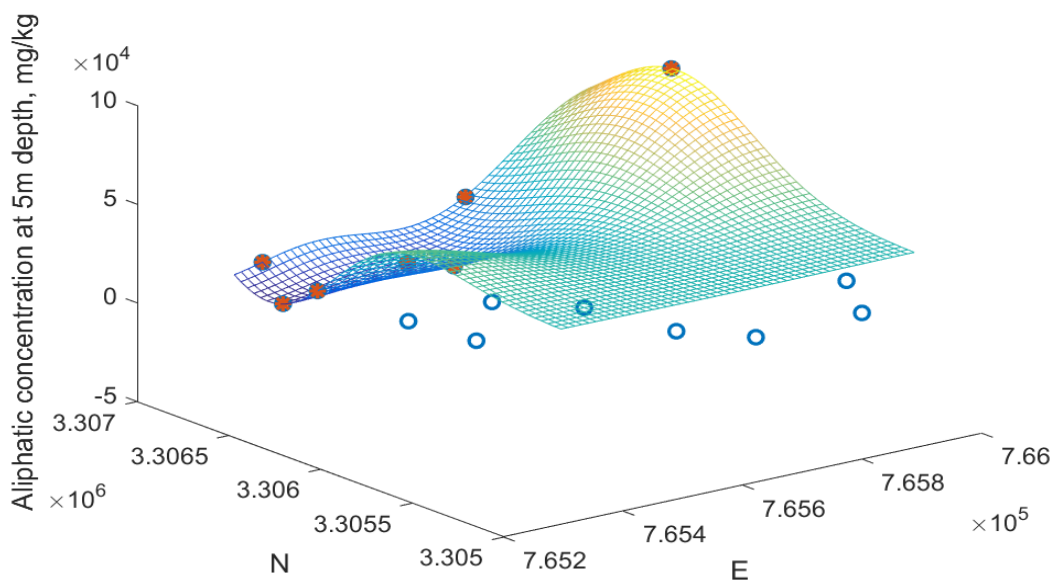
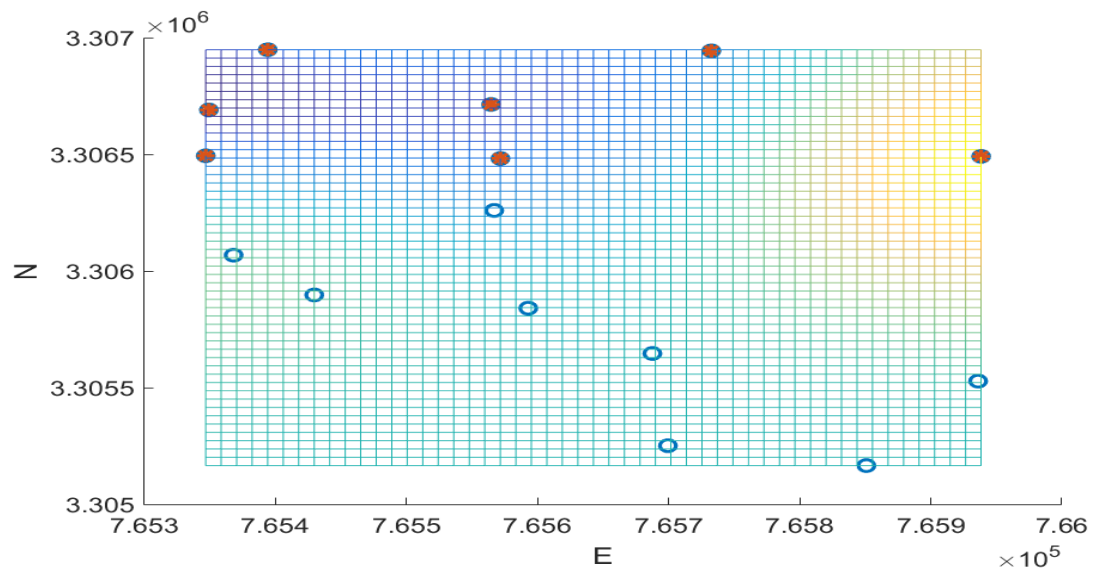
Figure 6.23 Cross-validation for assessing the performance of spatial interpolation methods for 2-B Section of the Raudhatain Area.

It has been clearly concluded from Figure 6.23 above and from the three validation tests in comparison between the Kriging and IDW prediction results for an analytical formula based on different number of sampling points that the Kriging produces better results than IDW. It can be seen that the accuracy for both methods increases with the increase of the number of sampling points. Furthermore, it can be clearly observed that Kriging has a certain advantage for the properties of a steep spatial variation, and is a more accurate method than IDW. It provides more reliable prediction for data interpolation rather than extrapolation. As a result, this study used the Kriging method and interpolation approach to characterize the soil field contamination.

The programme we developed had been tested and validated against the cases

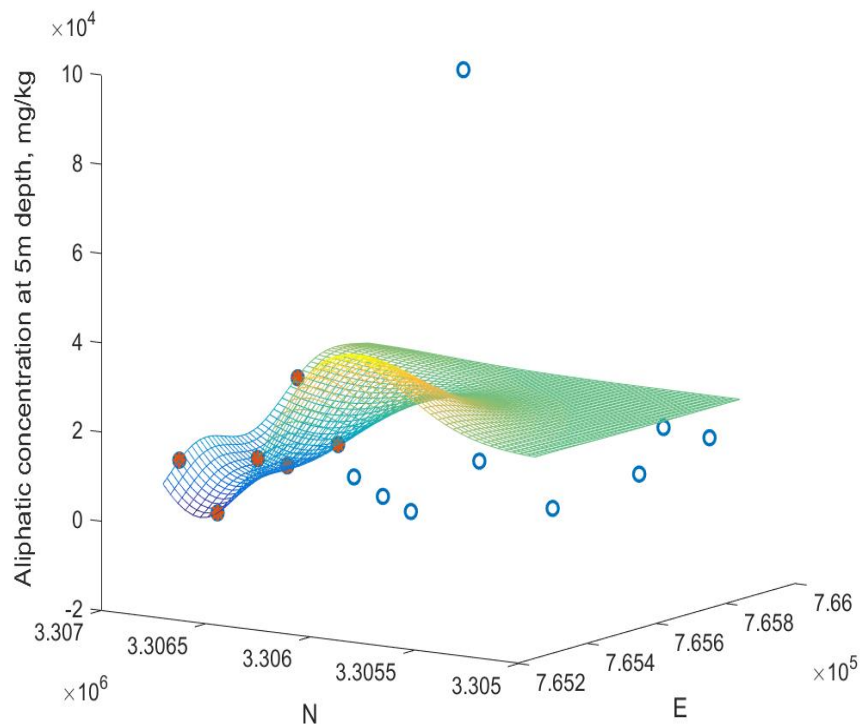
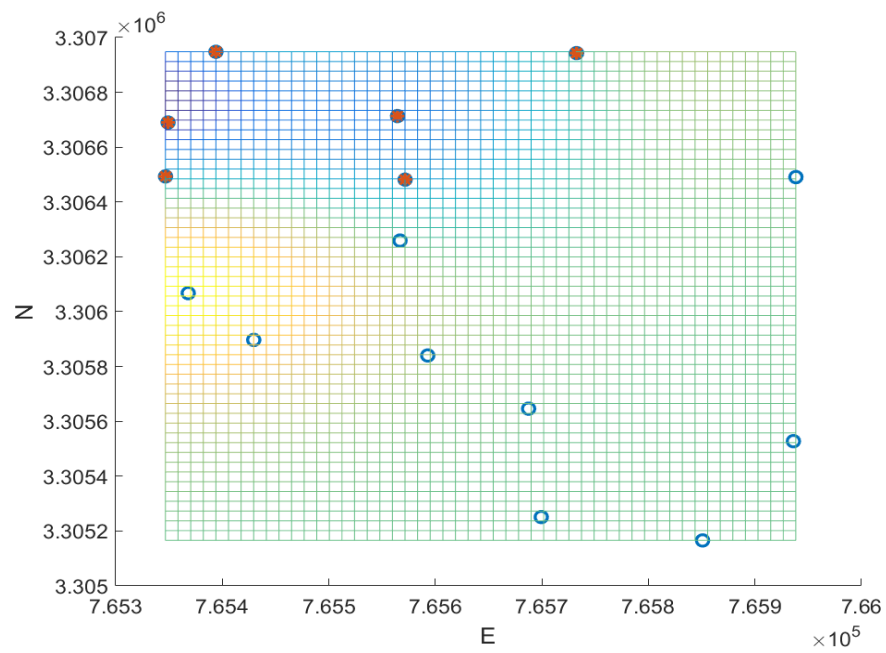
and data obtained. Both Kriging and IDW applied in this project produce prediction for the contamination profile in surface direction. For the local contamination degree in depth direction, we noticed that both Kriging and IDW performed poorly. This was seen in the provided vertical interpolation profile because they do not consider any physical mechanisms of the soil contamination process. One advantage of our novel investigation in this project was the consideration of the vertical infiltration mechanism and the corresponding vertical contamination profile modelling, which has proved to be more reasonable and accurate. Based on the predicted vertical contamination profile modelling presented and the Kriging surface mapping, the integrated prediction for the 3D profile of contamination degree can give a flexible assessment for varied information demanded.

The performance of our developed spatial interpolation methods has been assessed in section 4.7.2 by following section 2.4.7.1 cross-validation as one of the most important concepts in any type of data modeling. Furthermore, in this section we will perform chapter 2 section 2.4.7.2 Coefficient of Variation (CV) as the most selective factor. It is equally a useful statistic for comparing the degree of variation from one data series to another.



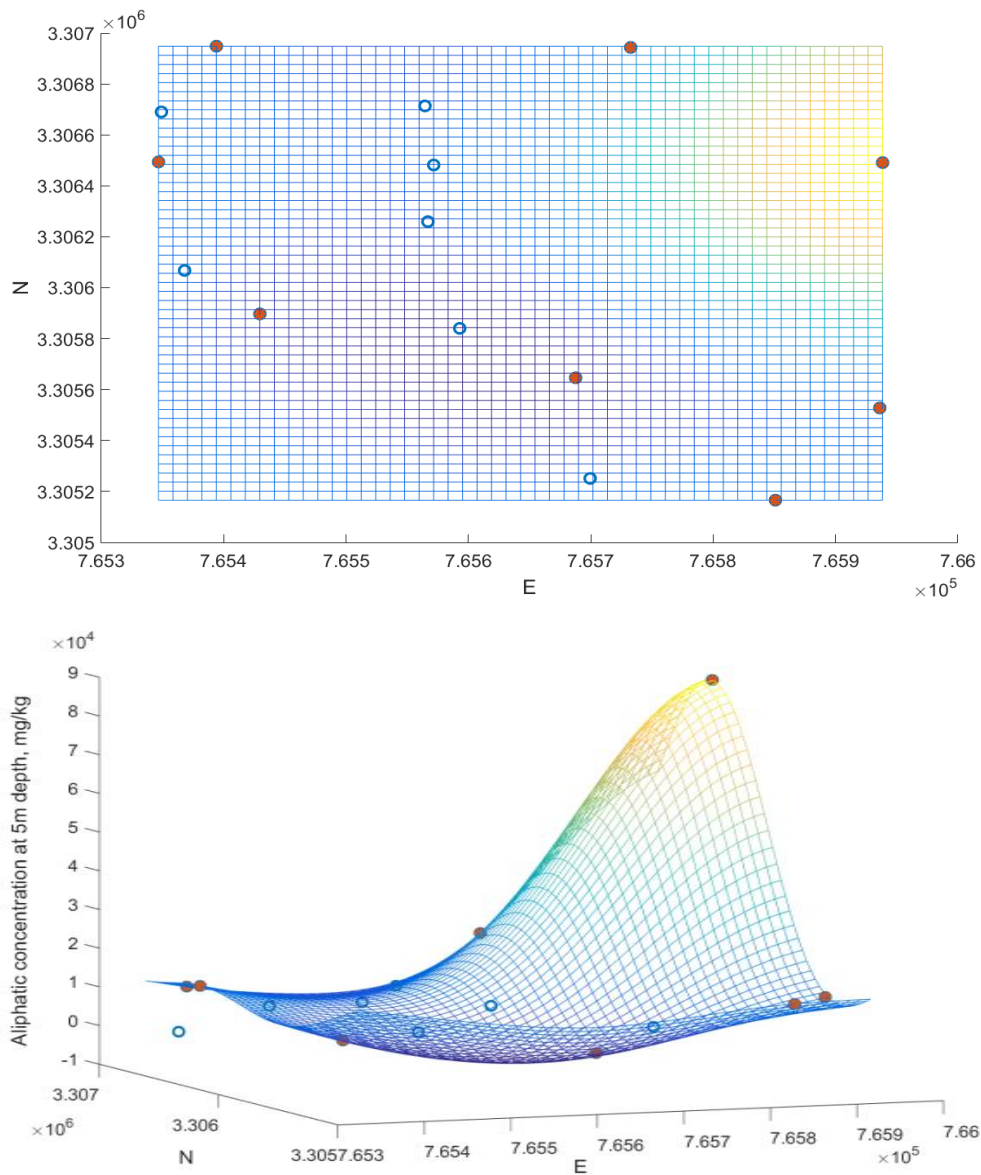
CV = 139.58%

Figure 6.24 The use of 7 samples from the 15 locations.



CV = 66.49%

Figure 6.25 The use of 6 samples from the 15 locations.



$$CV = 136.61\%$$

Figure 6.26 The use of 8 samples from the 15 locations.

The results above (Figs. 6.24-6.26) show that the prediction accuracy is not controlled by coefficient of variation of the data of samples, but depends on the location and distribution of sampling. Interpolation provides more reliable prediction than extrapolation. We can increase the accuracy by increasing the numbers of sample.

Furthermore, in our opinion the cross-validation method for assessing the performance of spatial interpolation is more reliable technique as it depends on removing one data location, then it predicts the associated data using the data at the rest of the locations, while assessing the performance by coefficient of variation relies more on total numbers of sample.

What I found was that several factors can affect the performance of the spatial interpolation methods, including sampling design, sample density, sample spatial distribution, data quality, correlation between the primary and secondary variables, and interaction among various factors. As the variation increases, the accuracy of all methods decreases. Surface type, distinct and sharp spatial changes, like changing soil types across a region, may also cause problems with the estimations--spatial correlation in samples is also essential for reliable estimation.

The sampling method that the KOC contractors use will not meet the data requirements for development of 3-D predictive models. The new sampling design, procedure, analysis and method for 3D soil mapping for hydrocarbon contaminated sites has been developed and accomplished during this research and presented. This novel sampling procedure will reduce the future required number of samples within any hydrocarbon contaminated site and dramatically reduce the cost of remediation projects. It will reduce the sampling cost which is the main cost related element in any remediation project. In addition, this analysis method, together with the doubted CWG laboratory method used for determination of various petroleum hydrocarbon fractions allows for sound evaluation of the environmental risk of any soil at any given location. This can effectively inform decision making on the selection of soil treatment methods.

For optimization of soil sampling design related to 2-B Section of the Raudhatain Area, given that only a part of the oil lake area was investigated in this study, there is relatively limited room to reduce the number of sampling locations. However, cross-validation of the predictive models suggests that the number of sampling locations in the study can be reduced from 17 to 15 with the total number of soil samples being reduced from 85 to 56. The accuracy of the 3-D distribution of various soil parameters can still be satisfactorily achieved. It is expected that when this method is applied to the whole area of the oil lake, a larger reduction in sampling locations can be achieved, thus effectively reducing costs associated with characterization of contaminated soils.

For the contamination hotspots that still contain hydrocarbon species of high toxicity, active treatment methods need to be adopted to eliminate the source of high environmental risk in a timely manner. It seems that advanced oxidation treatment is among the most appropriate methods for remediation of the contaminated soils present in the investigated area, though a pilot study is required to verify this.

For the investigated area as a whole, it is most unlikely that contamination of groundwater by the soil-borne petroleum hydrocarbons will take place under the current climatic conditions. However, human exposure to potentially toxic hydrocarbons through ingestion and inhalation is still likely. To minimize the human exposure risk, any activities causing large-scale soil disturbance, including excavation and removal of the contaminated soils for landfill disposal and ex-situ treatment operations should be avoided. A simple, low-cost capping method should be sufficient for satisfactorily preventing human exposure to toxic hydrocarbons from occurring.

From the two-pilot studies Pit EPE4 southern Kuwait, and 2-B section Northern Kuwait it has been concluded that the advantage of our developed novel 3D mapping technology includes:

- The use of geostatistical methods to develop 3-D predictive models that can be used to account for both horizontal and vertical variation in petroleum hydrocarbons. This allows much more accurate estimation of contaminated soil volume as compared to the existing simple average method used by the KOC contractors. It also enables estimation of contaminated soil volumes with different TPH levels (i.e <0.5-5%, 5-7% and >7%) or any other desired concentration ranges).
- The developed method includes the evaluation of 17 aliphatic and aromatic petroleum hydrocarbon fractions in addition to total petroleum hydrocarbon (TPH). This allows sound evaluation of the environmental risk of any soil at given location and therefore effectively informs decision making on the selection of soil treatment methods.
- The developed technologies include provision of a computer software that can be used to predict the concentration of TPH and the accuracy depth of each concentration range (i.e <0.5-5%, 5-7% and >7%) or any other desired

concentration ranges at a given location as long as the GPS information is provided. This can be used to effectively guide the on-ground excavation.

- By cross validation checking using the data from the two projects Pit EPE4 southern Kuwait, and 2-B section Northern Kuwait. The developed technology has a coefficient of variation (CV), a cross-validation similar to the international best practice for 1D, and 2-D soil prediction while our sampling density was much lower than the latter. This indicates that the developed novel technology has a high accuracy with a reduced number of soil sampling points required, as compared to the current international best practices for prediction of soil distribution.

The research findings obtained from this study allows the establishment of a standard operating procedure for evaluating the contaminated soils in the oil lake area of Kuwait (Procedure for Evaluation of Oil Lake Soils). This procedure has the following features:

Step 1: Carrying out a reconnaissance survey focusing characterization of surface soil layer (0-10 cm) only.

Step 2: Using the information obtained from above to guide selection of locations for soil profile observation and sample collection in order to minimise the number of sampling locations.

Step 3: Selecting analytical parameters that are needed for environmental risk assessment.

Step 4: Employing geostatistical interpolation techniques to establish predictive models for 3D mapping of TPH and various hydrocarbon fractions.

Step 5: Conducting an environmental risk assessment by interpreting, analysing and evaluating the data collected.

Step 6: Make recommendations for developing management/remediation strategies.

Step 7: Producing computer software that can be used to estimate the total volume of contaminated soils and guide on-ground excavation operations by providing the

contamination depth at any location within the project area.

In summary, geostatistical interpolation techniques were used and Fick's First Law was interpreted for contaminate ingress and transportation process for crude oil vertical contamination in soils. This was done to develop site-specific predictive models for 3-D mapping of TPH and various petroleum hydrocarbon fractions using the soil data. Cross-validation methods were performed to minimize the number of sampling locations and sampling depths while the accuracy of prediction for the 3-D distribution of various soil parameters. The findings suggest that it can be satisfactorily achieved using a minimum number of sampling locations and soil samples. This will effectively reduce the cost and labor input associated with characterization of contaminated soils with high quality results.

Chapter 7

Conclusions and Recommendations

7.1 Conclusions

The soils in the investigated oil lake area were of coarse texture and had alkaline pH. They contained large amounts of calcium compounds. Depending on the location, large amounts of gypsum might be present. Some locations had a high value of soil electrical conductivity, indicating a high level of soil salinity. The concentration of heavy metals was generally low.

Following nearly 3-decade weathering, most of lighter petroleum hydrocarbon species from the original spilled crude oil in the oil lake has already been emitted to atmosphere due to their low vapor pressure. Under desert climate conditions, volatilization of the light component of hydrocarbons were enhanced and downward migration of the spilled oil is limited due to a lack of rainfall. The heavier component (after partitioning of the volatile portion) of petroleum hydrocarbons migrated through the soil column under the force of gravity. However, the downward moment of these long-chain hydrocarbons tended to be slow because of their low mobility and large molecular size that could be easily trapped in soil pores. The penetration of petroleum hydrocarbons could also be impeded by the presence of gypsum and carbonates in the soils, which reduced the connectivity of soil pores. After the oil lake completely dried out, it is unlikely that any further downward migration of petroleum hydrocarbons by force of gravity will took place. Topography controls the thickness of the overlying crude oil layer, which, together with soil texture, affected the spatial variation in petroleum hydrocarbons.

In-situ biodegradation is likely to be very limited due to the harsh environmental conditions encountered in the investigated area, including extreme soil temperatures, low moisture content and high salinity etc. In addition, the supply of nutrients especially nitrogen may not be sufficient to sustain the microbes that mediate the biodegradation of the petroleum hydrocarbons.

Unlike contaminated soils in the oil lake area, the contamination depth was generally very shallow in the oil sludge pit due to the presence of a liner. No BTEX was detected and the concentration of TPH was generally lower, as compared to the oil lake soils. This can be attributed to the soil compaction, which effectively reduced soil pore space. However, liner failure occurred, resulting in penetration of the oil beyond the liner

There is no evidence to show that groundwater has been contaminated in the investigated area. Despite the high levels of TPH at many locations, long-chain aliphatic hydrocarbons dominated the petroleum hydrocarbons in both the oil sludges and the contaminated soils. BTEX were only detected at isolated locations in the oil lake area.

The pre-dominant presence of less toxic long-chain aliphatic hydrocarbons means that the hazardousness of the contaminated soils is likely to be much low. The oil lake was far away from any residential areas and unlikely to be used for agricultural purposes. The most likely land uses will be for industrial purposes because it is within the major oil field. Therefore, human exposure to the petroleum hydrocarbons will be limited to the KOC workers and the contractors who will carry out soil remediation work. Except for the locations where there were still short-chain petroleum hydrocarbons, the inhalation of volatile petroleum hydrocarbons is unlikely. The only exposure pathways will be ingestion and dermal contacts though inhalation of PHC-containing dusts may be possible.

The application of geostatistical interpolation techniques to the development of 3-D predictive models for the investigated sites suggests that this approach is appropriate for 3-D mapping of petroleum hydrocarbons in the petroleum hydrocarbon-contaminated soils, as confirmed by cross-validation methods. Number of sampling locations and sampling depths can be reduced while the accuracy of prediction for the 3-D distribution of various soil parameters can be ensured.

7.2 Implications of the research findings

The research findings obtained from this PhD work provides fundamental knowledge and practical methods that can be used to better guide the development of remediation strategies for both the KERP and SEED programs.

Since it is most unlikely that the soil-borne petroleum hydrocarbons pose any risk to groundwater in the investigated area and the hazardousness of the oil sludges and contaminated soils is likely to be much lower than what was thought during development of the KERP and SEED programs, it may be necessary to adjust the target value for soil clean-up in order to achieve cost-effective remediation goals.

From an environmental remediation perspective, removal of the PHCs from the soils may be challenging due to the fact that long-chain PHC fractions that are resistant to either chemical or biological decomposition dominated the soil-borne PHCs, especially for biodegradation, which can also be adversely affected by the high soil salinity apart from the harsh climatic conditions such as strong solar radiation, high temperature and low moisture content. The soils contained certain level of phosphorus but they may not be bioavailable due to the immobilization by calcium to form practically insoluble calcium phosphate.

Given that the composition and quantity of hydrocarbons varies markedly from location to location within the investigated area, different strategies are required to meet the specific needs in various parts of the investigated area. For the contamination hotspots that contain high concentrations of BTEX, aromatics and PAHs, more active treatment methods should be used to remove the contaminants as soon as practical to minimize their adverse impacts on the environment and human health. For the larger area of the non-hotspots, more cost-effective passive methods should be considered to minimize the remedial costs.

Soil washing is a possible method for clean-up of hydrocarbon-contaminated soils. However, this method is unlikely to be effective for the contaminated soils containing predominantly long-chain aliphatic hydrocarbons that are practically insoluble in water. In addition, intensive soil washing operations could enhance the volatilization of BTEX, causing air pollution and possibly harms to the operators.

The soils contained no elevated concentration of heavy metals and metalloids that could inhibit petroleum hydrocarbon-degrading microbes. The presence of phosphorus is also a beneficial factor for microbially mediated degradation of hydrocarbons. However, the high soil salinity at many locations, as indicated by high electrical conductivity, will affect microbial activities. Therefore, desalinization of these

soils may be required for bioremediation of the contaminated soils.

Chemical treatment using advanced oxidation technologies may be a more cost-effective method for treating the mobile fractions of hydrocarbons. The advanced oxidation method is rapid with no release of harmful substances. It is also possible to develop in-situ oxidation method to reduce the costs associated with translocation of contaminated soils to purpose-built facilities for ex-situ treatment.

For the soils containing no or small amounts of BTEX, aromatics and PAHs, containment may be more appropriate. However, ex-situ containment such as landfilling may be only appropriate for hydrocarbon-rich sludge but not the soils with dominant presence of aliphatic hydrocarbons. Given the extremely low risk in terms of groundwater contamination by the contaminated soils, it is not necessary to remove the soils from the contaminated sites. A low-cost capping method should be sufficient to minimize human exposure to the contaminated soils.

For the soil characterization prior to the soil treatments, the 3-D models developed from this study will provide a more cost-effective solution for accounting for the spatial variation in various petroleum hydrocarbon fractions with varying toxicity. The research findings obtained from this study allows the establishment of a standard operating procedure for evaluating the contaminated soils in the oil lake area of Kuwait (Procedure for Evaluation of Oil Lake Soils). This procedure has the following features:

Step 1: Carrying out a reconnaissance survey focusing characterization of surface soil layer (0-10 cm) only.

Step 2: Using the information obtained from above to guide selection of locations for soil profile observation and sample collection in order to minimise the number of sampling locations.

Step 3: Selecting analytical parameters that are needed for environmental risk assessment.

Step 4: Employing geostatistical interpolation techniques to establish predictive models for 3D mapping of TPH and various hydrocarbon fractions.

Step 5: Conducting an environmental risk assessment by interpreting, analysing and evaluating the data collected.

Step 6: Make recommendations for developing management/remediation strategies.

Step 7: Producing computer software that can be used to estimate the total volume of contaminated soils and guide on-ground excavation operations by providing the contamination depth at any location within the project area.

7.3 Limitations

The oil lake areas are exclusion zones that required strict approval for site access. Also due to insufficient funding for the field investigations, the sample collection in the two study sites was conducted as part of the projects performed by the KOC contractors. This did not allow the PhD candidate to collect the samples as what he intended to. Therefore, the sampling design did not fully meet the requirements for this specific research. This compromise, to some extent, adversely affect the quality of the data collected. For example, sludges in the oil lake area were not collected for laboratory analysis. Some important soil parameters such as organic matter content, soil bulk density, soil structure, soil permeability, soil nutrients etc. were not determined.

In the original research proposal, a third pilot study in the oil lake area of Burgan, southern Kuwait was planned upon a research contract under negotiation with the KOC Department of Research Technology. This research contract is expected to allow investigation of oil lake soils in a larger area with much better sampling design being adopted. However, the contract negotiation has taken much more time that we expected and could not been signed before the time required for thesis submission. This make it impossible to include the data to be collected from the third pilot study.

Due to insufficient funding to purchase the required computer software and time available for developing computer program writing, the originally planned computer program for estimating the total volume of contaminated soils and guide on-ground excavation operations by providing the contamination depth at any location within the project area was not completed.

7.4 Recommendations for future study

The above-mentioned research contract with the KOC Department of Research and Technology is expected to be signed in August 2019. For this new pilot study, a grid sampling scheme with more appropriate sampling density will be implemented to collect a complete set of data with more soil parameters being analyzed. This will allow improved understanding of the biogeochemical processes governing the transport and transformation of the spilled oil being obtained.

To improve the reliability of environmental risk assessment, a comprehensive site-specific conceptual model needs to be established based on up-to-date toxicity data, including conduct of ecotoxicity testing using site-relevant test organisms. It is realized that the currently available risk analysis software packages were not designed for desert areas and thus may not be suitable for being used in the Kuwait oil lake areas. To provide reliable environmental risk assessment outcomes, a site-specific human health and ecological risk analysis software needs to be developed.

References

- Adam, G., & Duncan, H.J. (1999). *Effect of diesel fuel on growth of selected plant species. Environmental Geochemistry and Health, 21(4)*, 353-357.
- Adhikari, K., Kheir, R.B., Greve, M.B. (2013). *High-Resolution 3-D Mapping of Soil Texture in Denmark. Soil science society of America Journal, 77*:860-876.
- Agbogidi, O.M., Eruotor, P.G., & Akparobi, S.O. (2007). Evaluation of crude oil contaminated soil on the mineral nutrient elements of maize (*Zea mays* L.). *Journal of Agronomy, 6(1)*: 188.
- Aguilera, F., Laffona, B., Méndez, J., & Pásaroa, E. (2019). *Review on the effects of exposure to spilled oils on human health. Journal of Applied Toxicology, 30*:291–301.
- Aislabie, J.M., Balks, M.R., & Foght, J.M. (2004). *Hydrocarbon spills on Antarctic soils: Effects and management. Environmental Science & Technology, 38(5)*: 1265–1274.
- Akinwumi, I., Diwa, D., & Obianigwe, N. (2014). *Effects of crude oil contamination on the index properties, strength and permeability of lateritic clay. International Journal of Applied Sciences and Engineering Research, 3*, 816-824.
- Al-Awadi, E., Quinn, M., & Mukhopadhyay, A. (2009). *Extent and nature of hydrocarbon occurrence in groundwater of Kuwait. Environmental Geology, 56(5)*:877–889.
- Alison, S. (2012). Review of methods to assess risk to human health from contaminated land. Multi-disciplinary specialists in Occupational and Environmental Health and Hygiene, Retrieved from <http://www.iom-world.org>.
- Alloway, B.J, Ayres, D.C. (1993). Organic Pollutants. In: Chemical Principles of Environmental Pollution. 1st edition. Chapman and Hall, India.
- Almasi, A., Jalalian, A., & Toomanian, N. (2014). *Using OK and IDW Methods for Prediction the Spatial Variability of A Horizon Depth and OM in Soils of Shahreko, Iran. Journal of Environment and Earth Science, 4*, 17-27.
- Almebayedh, H. (2014). Environmental and Economical Oil and Groundwater Recovery and Treatment Options for hydrocarbon contaminated Sites, 5th International Conference on Environmental Science and Technology (ICEST2014) Gdansk, Poland,.
- AlMebayedh, H. (2014). Remediation Technology Review and Selection Process for Hydrocarbon Contaminated Sites. SPE Annual Technical Conference and Exhibition held in Amsterdam, The Netherlands.
- Almebayedh, H. (2014). SPE Annual Technical Conference and Exhibition held in

Amsterdam, The Netherlands, "Remediation Technology Review and selection process".

Almebayedh, H., Lin, C.X., & Wang, Y. (2016). Improving Management and Technology Selection Process for Petroleum Hydrocarbon-contaminated Sites by Innovation of 3D Mapping Technology for Soil Characterization. Fourth European Conference on Sustainability, Energy & the Environment.

Almeda, R., Wambaugh, Z., Chai, C., Wang, Z., Liu, Z., & Buskey E.J. (2013). Effects of Crude Oil Exposure on Bioaccumulation of Polycyclic Aromatic Hydrocarbons and Survival of Adult and Larval Stages of Gelatinous Zooplankton. PLoS ONE 8(10): e74476.

Aqeel, M., Jamil, M., & Yusoff, I. (2014). Soil Contamination, Risk Assessment and Remediation. Environmental Risk Assessment of Soil Contamination.

Arocena, J.M., & Rutherford, P.M. (2005). *Properties of hydrocarbon- and salt-contaminated flare pit soils in northeastern British Columbia (Canada)*. Chemosphere, 60(4): 567–575.

Baker, J. M. (1970). *The effects of oils on plants*. Environmental Pollution, 1(1), 27-44.

Barbara, W., Woronko, B. (2012). *Late-holocene dust accumulation within the ancient town of marea (coastal zone of the south mediterranean sea, n egypt)*. Quaternary International. 266, 17, 4-13.

Bennett, P.C., Siegel, D.E., & Baedeker, M.J. (1993). *Crude oil in a shallow sand and gravel aquifer-I. Hydrogeology and inorganic geochemistry*. Applied Geochemistry, 8(6): 529-549.

Beyke, G., & Fleming, D. (2005). In situ thermal remediation of DNAPL and LNAPL using electrical resistance heating. Remediation, 15, 5-22.

Bhunia, G.S., Kumar, P., & Maiti, S.R. (2016). *Comparison of GIS-based interpolation methods for spatial distribution of soil organic carbon (SOC)*. Journal of the Saudi Society of Agricultural Sciences.

Bhunia, G.S., Shit, P.K., & Maiti, R. (2016). *Comparison of gis-based interpolation methods for spatial distribution of soil organic carbon (soc)*. Journal of the Saudi Society of Agricultural Sciences, S1658077X15300825.

Biological and Chemical Research. (2015). Kuwait Environmental Remediation Program (KERP), Remediation Demonstration Strategy. Science Signpost Publishing, 289-296.

Biological and Chemical Research. (2015). Remediation Demonstration Strategy Dhari Al-Gharabally, Aisha-Al-Barood Kuwait Oil Company, Soil Remediation Group, PO Box 9758, ahmadi 61008, Ahmadi, Kuwait, 289-296.

Bowen, H., & John, M. (1966). Trace elements in biochemistry. Academic Press.

Brassington, K.J., Hough, R.L., Paton, G.I., Semple, K.T., Risdon, G.C., & Crossley, J.

- (2007). *Weathered hydrocarbon wastes: a risk management primer*. Critical Reviews in Environmental Science and Technology, 37(3), 199-232.
- Brian, W. (2000). reports. Vast lakes of oil, contaminated water reserves and increasing cases of asthma are the legacies of the Gulf war, For Kuwait, *The guardian*.
- Brost, E.J. & DeVaul, G.E. (2000). Non-aqueous phase liquid (NAPL) mobility limits in soil. API Soil and Groundwater Research Bulletin.
- Browning, K.A. (1991). Allam RJ. *Environmental effects from burning oil wells in Kuwait*. Nature, 351, 363-367.
- Brum, D.M., Cassella, R.J., & Pereira Netto, A.D. (2008). *Multivariate optimization of a liquid–liquid extraction of the EPA-PAHs from natural contaminated waters prior to determination by liquid chromatography with fluorescence detection*. Talanta, 74(5), 1392–1399.
- Bundy, J.G., Paton, G.I., & Campbell, C.D. (2002). *Microbial communities in different soil types do not converge after diesel contamination*. Journal of Applied Microbiology, 92, 276-288.
- Canadian Council of Ministers of the Environment. (2008) . Canada-wide Standards for Petroleum Hydrocarbons (PHC) in Soil. CCME, Winnipeg , Retrieved from https://www.ccme.ca/en/resources/contaminated_site_management/phc_cws_in_soil.html.
- Cappello, S., Gabriella, G., & Vivia, B. (2004). *Crude oil-induced structural shift of coastal bacterial communities of rod bay and characterization of cultured cold-adapted hydrocarbonoclastic bacteria*. FEMS Microbiology Ecology, 49, 419–432.
- Chaîneau, C.H., Morel, J.L., & Oudot, J. (1997). *Phytotoxicity and Plant Uptake of Fuel Oil Hydrocarbons*. Journal of Environment Quality, 26(6), 1478-1483.
- Charles, P., Ian, G., Pepper, L., Charles, P., Terry, G., & Gentry, J. (2015). Environmental Microbiology (Third Edition), Academic Press, (pp. 565-579).
- Charman, P.E.V., & Murphy, B.W. (1998). Soils: their properties and management, Oxford University Press, Melbourne.
- Chartres, N., Bero, L.A., & Norris, S. L. (2019). *A review of methods used for hazard identification and risk assessment of environmental hazards*. Environment International, 123, 231-239.
- Chen, C., Hu, K., & Li, H. (2015). *Three-Dimensional Mapping of Soil Organic Carbon by Combining Kriging Method with Profile Depth Function*. PLoS ONE, 10(6), e0129038.
- Chen, C.S., Hseu, Y.C., & Liang, S.H. (2008). *Assessment of genotoxicity of methyl-tert-butyl ether, benzene, toluene, ethylbenzene, and xylene to human lymphocytes using comet assay*. Journal of Hazardous Materials, 153(1-2), 351-356.

- Chen, S., & Guo, J. (2016). Geomatics, Natural hazards and risk, 1947-5713.
- Chen, Z., Huang, G.H., & Chakma, A. (1998). *Integrated environmental risk assessment for petroleum-contaminated sites — a north American case study*. Water Science and Technology, 38(4-5), 131-138.
- Christos, G., Karydas, I., & Ioannis, Z. (2009) Evaluation of spatial interpolation techniques for mapping agricultural topsoil properties in crete. EARSel eProceedings, 8, 26-39.
- Coleman, H.J., Shelton, E.M., Nichols, D.T., & Thompson, C.J. (1978). Analysis of 800 Crude Oils from United States Oilfields. Report BETC/RI-78/14. Department of Energy, Bartlesville, OK.
- Daniel, V. (2014). Fundamental of air pollution (Fifth Edition), Academic Press, Pages 215-246.
- Das, K., & Mukherjee, A. K. (2007). *Crude petroleum-oil biodegradation efficiency of bacillus subtilis and pseudomonas aeruginosa strains isolated from a petroleum-oil contaminated soil from north-east india*. Bioresource Technology, 98(7), 1339-1345.
- David M, B., Matthijs, B., Richard, G., James, D., Peter, J., & Boogaard. (2017). *Heavy hydrocarbon fate and transport in the environment*. *Quarterly Journal of Engineering Geology and Hydrogeology*, 50(3): 333-346.
- Davis, D. D. (2016). *Bioremediation of hydrocarbon contaminated soils and drill cuttings using composting with agricultural wastes* (Doctoral dissertation, Newcastle University).
- Davis, J.B., Farmer, V.E., Kreider, R.E., Straub, A.E., & Reese, K.M. (1972). The Migration of Petroleum Products in Soil and Groundwater: Principles and Countermeasures. American Petroleum Institute, Report, 4149.
- De Blas, M., Navazo, M., Alonso, L., Durana, N., & Iza, J. (2011). *Automatic on-line monitoring of atmospheric volatile organic compounds: Gas chromatography–mass spectrometry and gas chromatography–flame ionization detection as complementary systems*. Science of The Total Environment, 409(24), 5459–5469.
- Dhari, A.G., & Aisha. A.B. (2015). Kuwait Environmental Remediation Program (KERP), Remediation Demonstration Strategy, Biological and Chemical Research, (pp.289-296).
- Dorn, P. B., Vipond, T. E., Salanitro, J. P., & Wisniewski, H.L. (1998). *Assessment of the acute toxicity of crude oils in soils using earthworms, microtox®, and plants*. Chemosphere, 37(5), 845-860.
- Doughty, C. E., Roman, J., Faurby, S., Wolf, A., Haque, A., Bakker, E. S., ... & Svenning, J. C. (2016). Global nutrient transport in a world of giants. *Proceedings of the National Academy of Sciences*, 113(4), 868-873.

Drešković, N., & Đug, S. (2012). Application of the Inverse Distance Weighting and Kriging methods of the Spatial Interpolation on the mapping the Annual Amount of Precipitation in Bosnia and Herzegovina, International Environmental Modelling and Software Society (iEMSs) 2012 International Congress on Environmental Modelling and Software Managing Resources of a Limited Planet, Sixth Biennial Meeting, Leipzig, Germany R. Seppelt, A.A. Voinov, S. Lange, D. Bankamp (Eds.)

Dunn, R. E., Madden, R. H., Kohn, M. J., Schmitz, M. D., Strömberg, C. A., Carlini, A. A., ... & Crowley, J. (2013). *A new chronology for middle Eocene–early Miocene South American land mammal ages. Bulletin*, 125(3-4), 539-555.

Edwan Kardena, Q. H. (2015). *Petroleum Oil and Gas Industry Waste Treatment; Common Practice in Indonesia*. *Journal of Petroleum & Environmental Biotechnology*, 06(05).

Ekundayo, E., Obuekwe, O. (2000). *Effects of an oil spill on soil physico-chemical properties of a spill site in a typic udipsamment of the Niger delta basin of Nigeria*. *Environmental Monitoring and Assessment*, 60(2): 235-249.

Engel, M., Helmut, B., Pint, A., Wellbrock, K., Ginau, A., & Voss, P. (2012). *The early holocene humid period in nw saudi arabia – sediments, microfossils and palaeo-hydrological modelling*. *Quaternary International*, 266, 131-141.

Environmental Legislation and Human Health – Guidance for Assessing Risk. (2007). Scotland & Northern Ireland Forum for Environmental Research (SNIFFER) , Retrieved from <https://www.sepa.org.uk/media/28984/assessment-of-environmental-legislative-and-associated-guidance-requirements-for-protection-of-human-health>.

Environmental Protection Agency. (2002). Federal Remediation Technologies Roundtable (FRTR), Javed Iqbal, Spatial Variability Analysis of Soil Physical Properties of Alluvial Soils, Soil Science Society of America.

Eugene, B. (2009). Spatial Interpolation: A Brief Introduction, Retrieved from <http://www.bisolutions.us/A-Brief-Introduction-to-Spatial-Interpolation.php>.

Fabio Veronesi. (2012). 3D Advance mapping of soil properties, School of Applied Sciences, Cranfield university.

Fabio, VeronesiM, Ron, Corstanje., & Thomas, Mayr. (2012). *Mapping soil compaction in 3D with depth functions*. *Soil and Tillage Research*, 124, 111-118.

Figure 2-6 Soil texture triangle based on USDA particle-size classification (after U.S. Soil Conservation Service.)

Fingas, M.F. (1997). *Studies on the evaporation of crude oil and petroleum products: I. the relationship between evaporation rate and time*. *Journal of Hazardous Material*, 56, 227-236.

FRTR. (1993). *Remediation Technologies Screening Matrix and reference Guide, Version 4.0, Journal of Soil Contamination*, 2014, 2(2).

Gerba, C.P. (2004). Risk Assessment and Environmental Regulations. In *Environmental*

Monitoring and Characterization (pp. 377-392).

Ghobakhlou, A., Zandi, S., & Sallis, P. (2011). Development of Environmental Monitoring System with Wireless Sensor Networks. Geoinformatics Research Centre, Auckland University of Technology, Auckland, New Zealand. the International Congress on Modelling and Simulation, Perth, Australia, 12-16.

Gina, L., Sari, Y.T., & Ni, M. (2019). *Bioremediation of Petroleum Hydrocarbons in Crude Oil Contaminated Soil from Wonocolo Public Oilfields using Aerobic Composting with Yard Waste and Rumen Residue Amendments*. *Journal of Sustainable Development of Energy, Water and Environment Systems*, 7(3),482-492.

GIS Resources. (2015). Types of Interpolation Methods, Retrieved from <http://www.gisresources.com/types-interpolation-methods>.

Gorlenko, N.V., & Timofeeva, S.S. (2019). Assessment of environmental damage from oil sludge to land resources in the Irkutsk region. IOP Conf. Ser.: Earth Environ. Sci.

Gotway, C.A., Ferguson, R.B., & Hergert, G.W. (1996). *Comparison of kriging and inverse distance methods for mapping soil parameters*. *Soil Science Society of America Journal*, 60,1237-1247.

Greer, C.W., Whyte, L.G., & Niederberger, T.D. (2010) Microbial Communities in Hydrocarbon-Contaminated Temperate, Tropical, Alpine, and Polar Soils. In: Timmis K.N. (eds) *Handbook of Hydrocarbon and Lipid Microbiology*. Springer, Berlin, Heidelberg

Guidance on the Management of Contaminated Land and Groundwater at EPA Licensed Sites. (2013). Retrieved from <https://www.epa.ie/pubs/advice/waste/contaminatedland/contaminatedl>.

Gustafson, J.B., Tell, J.G., & Orem, D. (1997). Total Petroleum Hydrocarbon Criteria Working Group. Selection of Representative TPH Fractions Based on Fate and Transport Considerations (pp. 128-135).

Hamad A.M. (2014). International Conference on Environmental Science and Technology: Environmental and Economical Oil and Groundwater Recovery and Treatment Options for hydrocarbon contaminated Sites, Kuwait Oil Company.

Hamad, A., Lin, C.X., Yu, Wang., Muthanna, A., & Meshari, A. (2017). 3D Mapping Technology for Soil Characterization of Kuwait Hydrocarbon Contaminated Sites. Proceedings of the 3rd World Congress on New Technologies (NewTech'17) Rome, Italy – June 6 – 8, Paper No. ICEPR 173.

Hanna, S.H.S., & Weaver, R.W. (2002). *Earthworm survival in oil contaminated soil*. *Plant and Soil*, 240(1), 127-132.

Harrak, R.E., Calull, M., Marcé, R.M., & Borrull, F. (1996). *Determination of polycyclic aromatic hydrocarbons in water by solid-phase extraction membranes*. *International Journal of Environmental Analytical Chemistry*, 64(1), 47-57.

- Hentati, O., Lachhab, R., Ayadi, M., & Ksibi, M. (2013). *Toxicity assessment for petroleum-contaminated soil using terrestrial invertebrates and plant bioassays*. *Environmental Monitoring and Assessment*, 185(4), 2989-2998.
- Hosseini, E., Gallichand, J., & Marcotte, D. (1994). *Theoretical and experimental performance of spatial interpolation methods for soil salinity analysis*. *Trans ASAE*, 37, 1799-1807.
- Huguenot, D., Mousset, E., Van Hullebusch, E.D., & Oturan, M.A. (2015). *Combination of surfactant enhanced soil washing and electro-fenton process for the treatment of soils contaminated by petroleum hydrocarbons*. *J Environ Manag*, 153:40-47.
- Hutcheson, M.S., Pedersen, D., Anastas, N.D., Fitzgerald, J., & Silverman, D. (1996). *Beyond tph: health-based evaluation of petroleum hydrocarbon exposures*. *Regulatory Toxicology & Pharmacology*, 24(1), 85-101.
- Ijimdiya., & Stephen, T. (2011). *Effect of oil contamination on particle size distribution and plasticity characteristics of lateritic soil*. *Advanced Materials Research*, 367, 19-25.
- Incardona, J.P., Collier, T.K., & Scholz, N.L. (2004). *Defects in cardiac function precede morphological abnormalities in fish embryos exposed to polycyclic aromatic hydrocarbons*. *Toxicology and Applied Pharmacology*, 196(2), 191-205.
- Iqbal, J., Thomasson, J.A., & Jenkins, J.N. (2005). *Spatial Variability Analysis of Soil Physical Properties of Alluvial Soils*. *Soil Science Society of America Journal*, 69(4), 1338-1350.
- Ishaque, A.B., Aighewi, I.T., Response, D., Sven, E.J., & Brian, D. (2008). *Encyclopedia of Ecology*, Academic Press, 2008, Pages 957-967.
- Iyyanki, V., Muralikrishna, V.M., & Chapter, E. (2017). *Environmental Risk Assessment, Environmental Management*, Butterworth-Heinemann, Pages 135-152.
- Jørgensen, K.S., Puustinen, J., & Suortti, A. (2000). *Bioremediation of petroleum hydrocarbon-contaminated soil by composting in biopiles*. *Environmental Pollution*, 107, 245-254.
- Keller, K.M., & Simmons, C.S. (2005). *The influence of selected liquid and soil properties on the propagation of spills over flat permeable surface*. Pacific Northwest National Laboratory, Washington, Report, PNNL-15058.
- Keshavarzi, A., & Sarmadian, F. (2012). *Mapping of spatial distribution of soil salinity and alkalinity in a semi-arid region*. *Annals of Warsaw University of Life Sciences – SGGW Land Reclamation*, 44 (1), 3-14.
- Keshavarzi, A., & Sarmadian, F. (2012). *Mapping of Spatial Distribution of Soil Salinity and Alkalinity in a Semi-arid Region*. Department of Soil Science Engineering, University of Tehran. *Annals of Warsaw University of Life Sciences -SGGW Land Reclamation*. 44 (1), 3-14.

- Khamehchiyan, M., Charkhabi, A.H., & Tajik, M. (2007). *Effects of crude oil contamination on geotechnical properties of clayey and sandy soils*. *Engineering Geology*, 89(3-4), 220-229.
- Khan, F.I., Husain, T., & Hejazi, R. (2004). An overview and analysis of site remediation technologies. *J Environ Manage* 71:95–122PubMedCrossRefGoogle Scholar.
- Khan, M. A. I., Biswas, B., Smith, E., Mahmud, S. A., Hasan, N. A., & Khan, M.A.W. (2018). *Microbial diversity changes with rhizosphere and hydrocarbons in contrasting soils*. *Ecotoxicology and Environmental Safety*, 156, 434-442.
- Kheirmand, M., Barkhordari, A., Mosaddegh, MH., & Farajzadegan, Z. (2014). Determination of benzene, toluene, ethyl benzene and xylene in administration room's air of hospitals using solid phase micro extraction/gas chromatography/flame ionization detector.
- King, R.B., Long, G.M., & Sheldon, J.K. (1998). *Practical environmental bioremediation: the field guide*. CRC Press/Lewis Publishers, Boca RatonGoogle Scholar.
- Kostecki, P., Morrison, R., & Dragun, J. (2005). Hydrocarbons. 217. In: Daniel Hillel (Editor-in-Chief), *Encyclopedia of soils in the environment*, Academic Press, 2200 pp.
- Kravchenko, A.N., & Bullock, D.G. (1999). *A comparative study of interpolation methods for mapping soil properties*. *Agronomy Journal*, 91,393-400.
- Kravchenko, A.N., & Bullock, D.G. (1999). *A comparative study of interpolation methods for mapping soil properties*. *Agronomy Journal*, 91, 393-400.
- Kumar, S., Meena, H., Chakraborty, S., & Meikap, B.C. (2018). *International Journal of Mining Science and Technology Application of response surface methodology (RSM) for optimization of leaching parameters for ash*.
- Kuppusamy, S., Maddela, N. R., Megharaj, M., & Venkateswarlu, K. (2019). *Total Petroleum Hydrocarbons: Environmental Fate, Toxicity, and Remediation*. Springer.
- Kuwayama, Y., Roeshot., S.S., Krupnick, A., & Richardson, N.D. (2015). *Risks and Mitigation Options for On-Site Storage of Wastewater from Shale Gas and Tight Oil Development* (December 17, 2015). Resources for the Future Discussion Paper 15-53. Retrieved from <http://dx.doi.org/10.2139/ssrn.2738725>.
- Lacoste, M., Minasny, B., Mcbratney, A., Michot, D., Viaud, Valérie., & Walter, C. (2014). *High resolution 3d mapping of soil organic carbon in a heterogeneous agricultural landscape*. *Geoderma*, 213, 296-311.
- Lacoste, M., Minasny, B., Mcbratney, A., Michot, D., Viaud, Valérie., & Walter, C. (2014). *High resolution 3d mapping of soil organic carbon in a heterogeneous agricultural landscape*. *Geoderma*, 213, 296-311.
- Lacoste, M., Minasny, B., Mcbratney, A., Michot, D., Viaud, Valérie., & Walter, C.

- (2014). *High resolution 3d mapping of soil organic carbon in a heterogeneous agricultural landscape. Geoderma*, 213, 296-311.
- Law, R.J., & Biscaya, J.L. (1994). *Polycyclic aromatic hydrocarbons (PAHs)—problems and progress in sampling, analysis and interpretation. Marine Pollution Bulletin*, 29: 235–241.
- Leeper, G.W., & Uren, N.C. (1993). *Soil science: An introduction*, Melbourne University Press, Melbourne.
- Lill, L. (2018). *Healing Mother Earth: A Vedic Perspective*. Xlibris Corporation.
- Mackay, D. (1987). Formation and stability of water in oil emulsions. Environment Canada Manuscript Reports, EE-93, Ottawa, Ontario, 97-99.
- Madadian, E., Gitipour, S., Amiri, L., Alimohammadi, M., & Saatloo, J. (2014). *The application of soil washing for treatment of polycyclic aromatic hydrocarbons contaminated soil: a case study in a petrochemical complex. Environmental Progress & Sustainable Energy*, 33(1), 107-113.
- María, B., & Monterroso, C. (2014). *Phytotoxicity of fuel to crop plants: influence of soil properties, fuel type, and plant tolerance. Toxicological & Environmental Chemistry Reviews*, 96(8), 1162-1173.
- Marshall, T.J., & Holmes, J.W. (1979). *Soil Physics*, Cambridge University Press.
- Massachusetts Department of Environmental Protection. (2003). Updated Petroleum Hydrocarbon Fraction Toxicity Values for the VPH/EPH/APH Methodology. Office of Research and Standards, Massachusetts Department of Environmental Protection, Boston, MA, Retrieved from http://www.state.ma.us/dep/bwsc/vph_eph.htm.
- Massachusetts Department of Environmental Protection. (1994). Interim Final Petroleum Report: Development of Health-Based Alternative to the Total Petroleum Hydrocarbon (TPH) Parameter. Bureau of Waste Site Clean-up, Boston, MA, Retrieved from http://www.state.ma.us/dep/bwsc/vph_eph.htm.
- Massachusetts Department of Environmental Protection. (1994). Interim Final Petroleum Report: Development of Health-Based Alternative to the Total Petroleum Hydrocarbon (TPH) Parameter. Bureau of Waste Site Cleanup, Boston, MA, Retrieved from http://www.state.ma.us/dep/bwsc/vph_eph.htm.
- Massachusetts Department of Environmental Protection. (1996). Issues Paper: Implementation of the VPH/EPH Approach. Public Comment Draft. Bureau of Waste Site Clean-up, Boston, MA, Retrieved from http://www.state.ma.us/dep/bwsc/vph_eph.htm.
- Massachusetts Department of Environmental Protection. (1997). Characterizing Risks Posed by Petroleum Contaminated Sites: Implementation of the MADEP VPH/EPH Approach. Public Comment Draft. Bureau of Waste Site Clean-up, Boston, MA, Retrieved from http://www.state.ma.us/dep/bwsc/vph_eph.htm.

Massachusetts Department of Environmental Protection. (2001). Characterizing Risks Posed by Petroleum Contaminated Sites: Implementation of the MADEP VPH/EPH Approach. Final Draft. June 2001. Bureau of Waste Site Clean-up, Boston, MA, Retrieved from http://www.state.ma.us/dep/bwsc/vph_eph.htm.

Massachusetts Department of Environmental Protection. (2002). Characterizing Risks Posed by Petroleum Contaminated Sites: Implementation of the MADEP VPH/EPH Approach. Final Policy. October 31, 2002. Bureau of Waste Site Clean-up, Boston, MA, Retrieved from http://www.state.ma.us/dep/bwsc/vph_eph.htm.

McMillen, S.J., Rhodes, I.A., Nakles, D.V., & Sweeney, R.E. (2001). Application of the Total Petroleum Hydrocarbon Criteria Working Group (TPHCWG) methodology to crude oils and gas condensates. In: McMillen, S.J. (ed.) Risk-Based Decision-Making for Assessing Petroleum Impacts at Exploration and Production Sites. Department of Energy and the Petroleum Environmental Research Forum, Tulsa, OK, 58–76.

McNeill, J. R., & Vrtis, G. (Eds.). (2017). *Mining North America: an environmental history since 1522*. Univ of California Press.

Megharaj, M., Singleton, I., McClure, N.C., & Naidu, R. (2000). *Influence of petroleum hydrocarbon contamination on microalgae and microbial activities in a long-term contaminated soil*. *Archives of Environmental Contamination & Toxicology*, 38(4), 439-445.

Mehdi, H., & Simone, C. (2013). Crude Oil Biodegradation in the Marine Environments, Biodegradation - Engineering and Technology, Rolando Chamy and Francisca Rosenkranz, IntechOpen.

Milton, D.I. (1967). "Geology of the Arabian Peninsula, Kuwait." Washington, D.C.: United States Government Printing Office, Reston, Va.: Geological Survey Professional Paper 560-D.

Mueller, T.G., Pusuluri, N.B., Mathias, K.K., Cornelius, P.L., Barnhisel, R.I., & Shearer, S.A. (2004). *Map quality for ordinary kriging and inverse distance weighted interpolation*. *Soil Science Society of America Journal*, 68(6), 2042-2046.

Muhammad, A.K., Bhabananda, B., Euan, S., Ravi, N., & Mallavarapu, M. *Toxicity assessment of fresh and weathered petroleum hydrocarbons in contaminated soil- a review*, Chemosphere, Volume 212, 2018, Pages 755-767.

Mullins, O. C. (2007). *Rebuttal to comment by professors herod, kandiyoti, and bartle on "molecular size and weight of asphaltene and asphaltene solubility fractions from coals, crude oils and bitumen"*. *Fuel*, 86(1-2), 309-312.

National Academies of Sciences. (2003). Contamination of groundwater in a much quick manner.

National Research Council. (2002). Oil in the Sea III: Inputs, Fates and Effects. National Academy of Sciences Washington DC.

New Zealand Ministry for the Environment. (2011). Guidelines for Assessing and

Managing Petroleum Hydrocarbon Contaminated Sites in New Zealand (Revised Version), Tier 1 soil acceptance criteria.

Oluremi, Johnson., Adewuyi, A.P., & Sanni, A. (2015). COMPACTION CHARACTERISTICS OF OIL CONTAMINATED RESIDUAL SOIL. *Journal of Engineering and Technology*. 6. 75 - 87.

Omran, E.S.E. (2012). *Improving the Prediction Accuracy of Soil Mapping through Geostatistics. Soil and Water Department, Faculty of Agriculture, Suez Canal University, Ismailia, Egypt. International Journal of Geosciences*. 3, 574-590.

Osuji, L.C., & Nwoye, I. (2007). *An appraisal of the impact of petroleum hydrocarbons on soil fertility: the Owaza experience. African Journal of Agricultural Research* 2(7): 318 – 324.

Panabek, T., Ayfer, E., Zhangyl, A., Ulbosyn, S., & Nurzhamal, E. (2018). *The technology of preparation of the oil sludge pit with polymerorganic screen for oil waste. ARPN Journal of Engineering and Applied Sciences*.

Pazoki, M., & Hasanidarabadi, B. (2017). *Management of toxic and hazardous contents of oil sludge in siri island. Global Journal of Environmental Science and Management*. 3(1), 33-42.

Pinholt, Y., Struwe, S., & Kjoller, A. (1979). "Microbial changes during oil decomposition in soil," *Holarctic Ecology*, vol. 2, (pp. 195–200).

Poonian, C. (2003). The effects of the 1991 Gulf War on the marine and coastal environment of the Arabian Gulf: Impact, recovery and future prospects, MSc Aquatic Resource Management, King's College, London.

Potter, T.L., & Simmons K.E. (1998). *Composition of Petroleum Mixtures, Volume 2 of the TPH Criteria Working Group Series*.

Principles for Evaluating the Human Health Risks from Petroleum Hydrocarbons in Soils. (2003). Environment Agency, Rio House, Waterside Drive, Aztec West, Almondsbury, BRISTOL, BS32 4UD, Retrieved from [http:// www.environment-agency.gov.uk](http://www.environment-agency.gov.uk).

Rahman, Z.A., Hamzah, U., & Ahmad, N. (2010). *Abstract: geotechnical characteristics of oil-contaminated granitic and metasedimentary soils. Asian Journal of Applied Sciences*, 3(4), 237-249.

Rahman. (2010). *Influence of oil contamination on geotechnical properties of basaltic residual soil. American Journal of Applied Sciences*, 7(7), 954-961.

Ramadass, K., Megharaj, M., Venkateswarlu, K., & Naidu, R. (2015). *Ecological implications of motor oil pollution: earthworm survival and soil health. Soil Biology & Biochemistry*, 85, 72-81.

Rasheed, Z.N., Ahmed, F.R., & Jassim, H.M. Effect of crude oil products on the geotechnical properties of soil WIT Transactions on Ecology and The Environment, Vol 186, © 2014 WIT Press.

- Rehman, H., Abduljawwad, S.N. & Akram, T. (2007). *Geotechnical behavior of oil-contaminated fine-grained soils*. *Electronic Journal of Geotechnical Engineering*, 12, 1-12.
- Reynoso-Cuevas, L., Gallegos-Martínez, M.E., Cruz-Sosa, F., & Gutiérrez-Rojas, M. (2008). *In vitro evaluation of germination and growth of five plant species on medium supplemented with hydrocarbons associated with contaminated soils*. *Bioresource Technology*, 99(14), 6379-6385.
- Robinson, T. P., & Metternicht, G. (2006). *Testing the performance of spatial interpolation techniques for mapping soil properties*. *Computers and Electronics in Agriculture*, 50(2), 97-108.
- Robinson, T. P., & Metternicht, G. (2006). *Testing the performance of spatial interpolation techniques for mapping soil properties*. *Computers and Electronics in Agriculture*, 50(2), 97-108.
- Roosbehani, N., & Saadat, B.A. (2014). *The most recent research in oily sludge remediation process*. *Am J Oil Chem Technol*, 2:340–348.
- Saiz, E., Movilla, J., Yebra, L., Barata, C., & Calbet, A. (2009). *Lethal and sublethal effects of naphthalene and 1,2-dimethylnaphthalene on naupliar and adult stages of the marine cyclopoid copepod *Oithona davisae**. *Environmental Pollution*, 157(4), 1219–1226.
- Salanitro, J.P., Dorn, P.B., Huesemann, M. H., Moore, K.O., Rhodes, I.A., & Rice Jackson, L.M. (1997). *Crude oil hydrocarbon bioremediation and soil ecotoxicity assessment*. *Environmental Science & Technology*, 31(6), 1769-1776.
- Saterbak, A., Toy, R.J., Wong, D.C., McMMain, B.J., Williams, M.P., Dorn, P.B., Brzuzy, L.P., Chai, E.Y., Salanitro, J.P. (1999). *Ecotoxicological and analytical assessment of hydrocarbon-contaminated soils and application to ecological risk assessment*. *Environmental Toxicology and Chemistry*, 18(7), 1591-1607.
- Shin, E., & Das, B. (2000). *Some physical properties of unsaturated oil-contaminated sand*. *Geotechnical Special Publication*, 142-152.
- Singh, S., Srivastava, R., & John, S. (2008). *Settlement characteristics of clayey soils contaminated with petroleum hydrocarbons*. *Soil & Sediment Contamination*, 17, 290-300.
- Soil Protection Law. (2015). Retrieved from <https://www.umweltbundesamt.de/en/topics/soil-agriculture/soil-protection/soil-protection-law>.
- Soil Sampling for Environmental Contaminants. (2004). International Atomic Energy Agency, Vienna, Austria.
- Spickett, J., Katscherian, D., & Goh, Y. M. (2012). *A new approach to criteria for health risk assessment*. *Environmental Impact Assessment Review*, 32(1), 118–122.
- STATE OF KUWAIT Environment Public Authority. (2012). *Kuwait's Initial National*

Communications under the United Nations Framework Convention on Climate Change.

Statistics of petroleum hydrocarbon-contaminated soils within the State of Kuwait (2011). Kuwait Environment Public Authority.

Steliga, T., Jakubowicz, P., & Kapusta, P. (2015). *Changes in toxicity during treatment of wastewater from oil plant contaminated with petroleum hydrocarbons*. *Journal of Chemical Technology & Biotechnology*, 90(8), 1408-1418.

Stephenson, G.L. (2000). CCME Canada-wide Standards for Petroleum Hydrocarbons: Assessment of Motor Gasoline and Surrogate Toxicity Data for Derivation of SQGs. ESG International for Alberta, Environmental Protection, Edmonton, Alberta, pp. 30.

Tang, J., Wang, M., Wang, F., Sun, Q., & Zhou, Q. (2011). *Eco-toxicity of petroleum hydrocarbon contaminated soil*. *Journal of Environmental Sciences*, 23(5), 845-851.

Teefy, D.A. (1997). *Remediation technologies screening matrix and reference guide: version iii*. *Remediation Journal*, 8(1), 115-121.

Tenkouano, G. T. (2017). *Paleolimnological Reconstruction of the Environmental Impact of the Deloro Industrial Site on Moira Lake (Ontario)* (Doctoral dissertation).

The Contaminated Land Exposure Assessment Model. (2002). Technical Basis and Algorithms. R & D Publication CLR 10. DEFRA and Environment Agency, Retrieved from <http://interspill.org/previous-events>.

TPHCWG (Total Petroleum Hydrocarbon Criteria Working Group). 1997a. Volume 3. Selection of Representative TPH Fractions Based on Fate and Transport Considerations. Amherst Scientific Publishers, Amherst, MA. Available at <http://www.aehs.com/publications/catalog/contents/tph.htm>

TPHCWG. 1997b. Development of Fraction Specific Reference Doses (RfDs) and Reference Concentrations (RfCs) for Total Petroleum Hydrocarbons (TPH). Volume 4. Amherst Scientific Publishers, Amherst, MA.

TPHCWG. 1998a. Analysis of Petroleum Hydrocarbons in Environmental Media. Volume 1. Amherst Scientific Publishers, Amherst, MA.

TPHCWG. 1998b. Composition of Petroleum Mixtures. Volume 2. Amherst Scientific Publishers, Amherst, MA.

TPHCWG. 1999. Human Health Risk-Based Evaluation of Petroleum Release Sites: Implementing the Working Group Approach. Volume 5. Amherst Scientific Publishers, Amherst, MA.

Turcryniewicz, L., & Robinson, N. (2008). Review of current international approaches to total petroleum hydrocarbon assessment, CRC for Contamination Assessment and Remediation.

Uhler, R.M., Healey, E.M., McCarthy, K.J., Uhler, A.D., & Stout, S.A. (2003). *Molecular Fingerprinting of Gasoline by a Modified EPA 8260 Gas*

Chromatography-Mass Spectrometry Method. International Journal of Environmental Analytical Chemistry, 83(1), 1–20.

USEPA. 1996, Method 8015B, Revision 2, “Non halogenated Volatile Organics Using GC/FID”, SW-846, 3rd Edition.

US EPA Method 8015B, Revision 2, December 1996 “Non halogenated Volatile Organics Using GC/FID”, SW-846, 3rd Edition. TNRCC Method 1006 “Characterisation of C6 to C35 Petroleum Hydrocarbons in Environmental Samples”.

US EPA Method 8260, Revision B, Volatile Organic Compounds by Gas Chromatography-Mass Spectrometry (GC/MS).

US EPA Method 8260, Revision B, Volatile Organic Compounds by Gas Chromatography-Mass Spectrometry (GC/MS). Analysis of Petroleum Hydrocarbons in Environmental Media, Total Petroleum Hydrocarbon Working Group Series, Volume 1, March 1998.

USEPA (1979b). EPA Method 413.1

USEPA (1979c). EPA Method 413.2

USEPA (1979a). EPA Method 418.1

Environmental Sciences Division. (1993). Use of Gross Parameters for Assessment of Hydrocarbon Contamination of Soils in Alberta, Oxford, UK.

Voysey, P., Jewell, K., Stringer, M., Martyn, B., & Mike S. (2002). In Woodhead Publishing Series in Food Science, Technology and Nutrition, Microbiological Risk Assessment in Food Processing, Woodhead Publishing, 2002, (pp.127-154).

Wang, Y., Feng, J., Lin, Q., & Xianguo, L.Y. (2013). *Effects of crude oil contamination on soil physical and chemical properties in momoge wetland of china*. Chinese Geographical Science, 23(6), 708-715.

Wei, Q.F., Mather, R.R., & Fotheringham, A.M. (2003). *Characterization of water-in-crude oil emulsions in oil spill response*. *Journal of Environmental Sciences*, 15 (4), 506-509.

Weisman, W. (1998). Analysis of Petroleum Hydrocarbons in Environmental Media. Amherst Scientific Publishers, MA.

William, B. (2017). Human Health and Ecological Risk Analysis, Soil and Environmental Chemistry (Second Edition), Academic Press, 2017, (pp.491-533).

Williams, S.D., Ladd, D.E., & Farmer, J.J. (2015). Fate and transport of petroleum hydrocarbons in soil and ground water at Big South Fork National River and Recreation Area, Tennessee and Kentucky, 2002-2003: U.S. Geological Survey Scientific Investigations Report.

Wittcoff., Harold, A., Reuben., & Bryan, G. (1996). *Industrial Organic Chemicals*. New York: John Wiley.

Xueling, Y., Bojie, F., Lü, Y., Feixiang, S., Shuai, W., & Min, L. (2013). Comparison of four spatial interpolation methods for estimating soil moisture in a complex terrain catchment. *PLoS ONE*, 8(1), e54660.

Y. Pinholt, S. Struwe, and A. Kjoller, "Microbial changes during oil decomposition in soil," *Holarctic Ecology*, vol. 2, pp. 195–200, 1979.

Yasrebi, J., Saffari, M., Fathi, H., Karimian, N., Moazallahi, M., & Gazni, R. (2012). *Evaluation and comparison of ordinary kriging and inverse distance weighting methods for prediction of spatial variability of some soil chemical parameters. Research Journal of Biological Sciences*, 4(1), 385-394.

Yihdego, Y., & Al-Weshah, R. A. (2016). *Gulf war contamination assessment for optimal monitoring and remediation cost-benefit analysis, Kuwait. Environmental Earth Sciences*, 75(18), 1234.

Z. N. Rasheed, F. R. Ahmed & H. M. Jassim. Effect of crude oil products on the geotechnical properties of soil *WIT Transactions on Ecology and The Environment*, Vol 186, © 2014 WIT Press

Zandi, S., Ghobakhlou, A., & Sallis, P. (2011). *Development of Environmental Monitoring System with Wireless Sensor Networks*. Geoinformatics Research Centre, Auckland University of Technology, Auckland, New Zealand. the International Congress on Modelling and Simulation, Perth, Australia.

Zeev Wiesman, 2009, Chapter 3 - Key characteristics of the desert environment. *Desert Olive Oil Cultivation, Advanced Biotechnologies*, 31-53

Appendix1

ANALYTICAL METHOD STATEMENTS

Method statements for TPH CWG by GC/FID and GC/MS (Headspace) are presented on Appendix 2 (SALLTD, 2016);

3.6.1 METHOD STATEMENT VOC TARGETS BY HEADSPACE GC / MS. BTEX, MTBE AND TPH ALI/ARO C5-C10 –

The performance of this method is validated in accordance with internationally recognised procedures (SALLTD, 2016).

This procedure describes the determination of volatile organic compounds (VOC) in soils and waters by headspace gas chromatography mass spectrometry (GC / MS).

This method is also suitable for the determination of mercaptans, heptane and methyl acetate.

Note: The determination of mercaptans, heptane and methyl acetate are not UKAS accredited.

3.6.1.1 PRINCIPLE

The sample is heated and shaken vigorously. This carries the volatile components into the headspace of the extraction vessels. A volume of the headspace is sampled and passed onto the head of gas chromatography (GC) column which separates the different components. The eluent from the GC column passes into the ion source of a mass spectrometer, which, records mass spectra continually at a regular interval and with unit mass resolution.

A series of aqueous standards are analyzed by this method and the data are used for reference and calibration. Deuterated internal standards are added to all samples, spikes and blanks prior to analysis.

In instances where a compound is not present in the calibration material, a tentative identification and result is produced based upon a comparison of the mass spectra obtained with those found in the NIST mass spectral databases. Such tentative results are subject to confirmation by the analyst.

Samples are stored in a refrigerator (5 +/- 4 °C) prior to and following analysis.

3.6.1.2 SOIL SAMPLES

0.1 to 10 g aliquots are spiked with the internal standards, immersed in 10 ml of deionised water and then analysed.

3.6.1.3 WATER SAMPLES

A 1 to 10 ml aliquot is removed directly from the sample vessel, spiked with the internal standards, then analysed.

3.6.1.4 PERFORMANCE CHARACTERISTICS

3.6.1.5 SUBSTANCES DETERMINED

A range of volatile hydrophobic organic compounds, ranging in boiling points from circa -10 °C to 200 °C. Standard target suites include chlorinated solvents, 'BTEX' and other priority pollutants.

3.6.1.6 RANGE OF APPLICATION

- 1 to 2000 ug / L, ug / kg (compound dependent)
- Mercaptans 25 to 300 mg / L

3.6.1.7 LIMIT OF DETECTION SOILS

- Typically 5 ug / kg for VOC 624 suite
- Typically 1 ug / kg for BTEX
- Methyl Acetate 100 ug / kg
- Heptane 20 ug / kg

3.6.1.8 WATERS

- Typically 1 ug / L
- Mercaptans 0.1 – 5 mg / L (compound dependent)
- Methyl Acetate 100 ug / L
- Heptane 20 ug / L

3.6.1.9 VALIDATION

Initial method validation was conducted via the analysis of 6 x 2 replicate spike samples prepared and analysed independently, along with a three-point calibration, method blanks and independent QC samples. The precision, bias and uncertainty for each analyte was determined from the data acquired and found to be as follows for all analytes:

- Precision: < 5 %
- Bias: < 8 %
- Uncertainty: < +/- 5 %

Ongoing method performance is monitored via analytical quality control charts.

3.6.1.10 ANALYTICAL QUALITY CONTROL

Analytical quality control is maintained by a number of measures:

- Multi-point calibration with authentic standards (with defined minimum performance characteristics).
- Analysis of control samples within each analytical batch, such as independent standards, matrix spikes or reference materials.
- Analysis of reagent / method blanks within each analytical batch.
- Ongoing quality assured by the use of control charts in conjunction with warning and action limits for the QC sample data.
- Participation in external proficiency testing and inter laboratory schemes such as LGC Standards CONTEST and AQUACHECK.

3.6.2 METHOD STATEMENT TOTAL PETROLEUM HYDROCARBONS TPH ALI/ARO C10-C35 –

The performance of this method is validated in accordance with internationally recognized procedures (SALLTD, 2016);

This method describes the determination and speciation of Total Petroleum Hydrocarbon (TPH) in soils / sediments, waters and charcoal tubes by GC / FID.

3.6.2.1 PRINCIPLE

The TPH is extracted into an appropriate solvent and analysed by capillary gas chromatography with flame ionisation detection. Quantitation is performed against an external standard (diesel standard). Speciation is performed by comparison of the chromatograms obtained to those from a set of standards which contain straight chain aliphatic hydrocarbons, ranging from C₁₀ to C₂₈. The results are expressed as carbon number ranges.

3.6.2.2 SOIL SAMPLES

10 g of sample (as received) is extracted with dichloromethane. Impurities are removed from the extract with sodium sulphate and silica. They are reduced in volume and analysed by GC / FID.

3.6.2.3 WATER SAMPLES

250 ml homogenised sample extracted with dichloromethane. Impurities are removed from the extract with sodium sulphate and silica, they are reduced in volume and analysed by GC / FID.

Where lower limits of detection are required, a 1 L aliquot is extracted in the same manner.

3.6.2.4 CHARCOAL TUBES

The whole sample is extracted with carbon disulphide and analysed by GC / FID.

3.6.2.5 ALIPHATIC AROMATIC SPLITS

Samples requiring aliphatic / aromatic banding are prepared in the normal manner for the matrix. The aliphatic and aromatic fractions are separated using solid - phase extraction techniques.

3.6.2.6 ADDITIONAL CLEAN UP

Where, due to matrix effects, it is considered necessary to perform additional clean up for the sample extracts, the following procedure is followed:

Test samples are extracted as normal. The extract is filtered into a clean round bottom flask as per the SAL SOP. Ca. 10 – 15 g of acid silica is added to the flask and the extract mixed on a rotary evaporator with no heat for 30 minutes to ensure adequate mixing. The extract is filtered reduced in volume for analysis by GC / FID.

3.6.2.7 PERFORMANCE CHARACTERISTICS SUBSTANCES DETERMINED

For the purposes of this method TPH is defined as all hydrocarbons extractable by the method within the carbon range from circa C₈ to circa C₃₅. This range is appropriate for the determination of contamination caused by products such as diesel, fuel, heating and lubricating oils, paraffin / kerosene and white spirit. This method is **not** suitable for the analysis of gasoline range organic compounds.

3.6.2.8 RANGE OF APPLICATION

- Soils 1 to 1000 mg / kg
- Waters 0.10 to 100 mg / L
- Large volume waters 0.01 to 100 mg / L
- Tubes 10 to 10,000 ug / tube

3.6.2.9 LIMIT OF DETECTION

- Soils 1 mg / kg
- Waters 0.10 mg / L
- Large volume waters 0.01 mg / L
- Tubes 10 ug / tube

3.6.2.10 ANALYTICAL QUALITY CONTROL

Analytical quality control is maintained by a number of measures (SALLTD,2016) :

- Multi-point calibration with authentic standards (with defined minimum performance characteristics).
- Analysis of control samples within each analytical batch, such as independent standards, matrix spikes or reference materials.
- Analysis of reagent / method blanks within each analytical batch.
- Ongoing quality assured by the use of control charts in conjunction with warning and action limits for the QC sample data.
- Participation in external proficiency testing and inter-laboratory schemes such as LGC standards CONTEST and AQUACHECK.

Element analysis of soil by ICP-OES after aqua regia digestion

1+/- 0.01g of dried and ground (to pass 425uM sieve) soil is weighed into a 50ml Environmental express Digtube. 10mls of concentrated Hydrochloric and 3.5mls of Nitric acid are added to the sample via dispenser
Samples are digested in Aqua Regia at 110°C +/-5 °C for 90-100minutes in a digiblock (Hotblock).

Samples are made up to a volume of 50mls using deionised water.

Samples are analysed on an Agilent 5110 ICP-OES running ICP Expert software.

Instrumentation uses the following wavelengths to analyse for metal concentrations in the samples.

Element	Wavelength (nm)
Al	396.152
As	188.98

Ba	233.527
Be	249.473
Bi	223.061
Ca	315.887
Cd	228.802
Co	230.786
Cr	267.716
Cu	217.895
Fe	259.940
Hg	184.887
K	766.491
Li	610.365
Mg	279.078
Mn	259.373
Mo	202.032
Na	589.592
Ni	231.604
P	213.618
Pb	220.353
S	181.972
Element	Wavelength (nm)
Sb	206.834
Se	196.026

Sn	189.925
Sr	346.445
Ti	334.941
Tl	190.794
V	311.070
Zn	213.857

TPH C10-40

The GC would have been a Varian 3900 GC-FID using Varian Star software. The column was a 15m select mineral oil with a 0.32mm ID and a 0.1um phase thickness. Stationary phase is a polysiloxane based mixture.

The temperature profile was: initial temp of 45°C, hold for 1.5 minutes then ramp at 40°C/min up to 320°C hold for 2.6 minutes. Instrument ran under constant flow 1.4ml/min conditions splitless. Helium carrier gas. Inlet temperature of 250°C. Injection pressure pulse 10psi for 0.5minutes

BTEX and TPH C5-10 by headspace GC-MS

The GC-MS was an Agilent 7890A GC coupled to an Agilent 5975C MSD using a Gerstel headspace autosampler using Agilent Chemstation E.01.00 software. The column was a 30m DB-624 with a 0.32mm ID and a 1.8um film thickness. Stationary phase was 6% Cyanopropylphenyl/94% dimethyl polysiloxane.

The temperature profile was: initial temp 60°C held for 2 minutes then ramp at 20°C/min up to 280°C then hold for 1 minute. System ran in constant flow mode with a 60:1 split. Autosampler was set to agitate for 15 minutes at 60°C. Helium carrier gas, inlet temperature of 250°C

MSD was operated in scan mode between 40 and 450 Da and set to high resolution.

EPA 16 PAH by GC-MS

The GC-MS was an Agilent 6890N GC attached to an Agilent 5973 MSD using Chemstation D.02.02 software. The column was a 30m HP-5MS with a 0.25mm ID

and a 0.25um film thickness. Stationary phase was 5% Diphenyl/95% dimethyl polysiloxane.

Temperature profile was: initial temp 50°C hold for 5 minutes then ramp at 20°C/min to 310°C then hold for 3 minutes. System ran ramped flow with a hold at 1ml/min for 18 min then ramp to 1.5ml/min and hold for 3 mins. 25:1 split injection. Inlet temperature of 280°C, helium carrier gas.

MSD was operated in SIM mode. Dwell time of 50m/s utilising SIM grouping. Ions monitored for PAH's were:

Internal standards

The use of *s to denote which internal standard is used with which analyte

d8 naphthalene* - m/z 136
d10 acenaphthene** - m/z 164
d10 phenanthrene*** - m/z 188
d12 chrysene**** - m/z 240
d12 perylene***** - m/z 264
d14 dibenz(ah)anthracene***** - m/z 292

Analytes

Naphthalene* - m/z 128
Acenaphthylene* - m/z 152
Acenaphthene** - m/z 153
fluorine** - m/z 166
Phenanthrene*** - m/z 178
Anthracene*** - m/z 178
Fluoranthene*** - m/z 202
Pyrene*** - m/z 202
Chrysene**** - m/z 228
benzo(a)anthracene**** - m/z 228
benzo(b)fluoranthene**** - m/z 252
benzo(k)fluoranthene**** - m/z 252
benzo(a)pyrene***** - m/z 252
indeno(123cd)pyrene***** - m/z 276
dibenz(ah)anthracene***** - m/z 278
benzo(ghi)perylene***** - m/z 278
coronene***** - m/z 300

